Targeting the Terminal Pathway in Complement – Driven Disease.

Wioleta Milena Zelek

A thesis submitted to Cardiff University in candidature for the degree of Doctor of Philosophy.

September 2019

Choose a job you love, and you will never have to work a day in your life.

- *Confucius*

ACKNOWLEDGEMENTS;

I would like to express my deepest thanks to the following people:

- My primary supervisor Professor Paul Morgan for taking me on a journey of Complement, for his encouragement, direction and much appreciated motivating discussions throughout my PhD, all the inspiring quotes such as;
  "it's only impossible until someone does it"
  "an expert is someone who knows almost everything about almost nothing"
  "…you answered one question, now there are two more to ask"
  "choose your battles!"
- My PhD co-supervisor Professor Philip Taylor, for his inspiring comments.
- Professor Claire Harris for her much valued advice, and extensive expertise during the SPR analysis, for her encouragement and ongoing support.
- My PhD Annual Review panel for valuable feedback during the course of this study.
- Collaborators for providing crucial reagents for this project; F. Hoffmann-La Roche Ltd., Complement Pharma, GSK, David Kavanagh and Brigitta Stockinger.
- Grant Funders; Welsh Government and Life Science Research Network in Wales (LSRN) for supporting this work, LSRN Translational Support Fund for sequencing the antibodies developed and Systems Immunity Research Institute for funds to visit Monash University.
- Travel award funders (British Society of Immunology and WM Thomas Fund) and conference organisers (Complement UK, ICW, EMCHD, BSI and I&I) for all the opportunities to present my data.
- My industrial supervisors in particular Ms Nikki Robinson from BBI Group for the provided training that have accustomed me to laboratory SOPs; the Senior Scientist job helped me develop skills essential for success of this project.
- My MSc supervisors; Professor J. Zaleski and B. Zarychta and teachers; Kusykowie and Swiechowie for their enormous support, especially Jadwiga who has been my great inspiration for many years.
- Dr Michelle Dunstone and Dr Brad Spicer for hosting me at Monash University, introduction to cryo-EM and providing a friendly and enjoyable environment whilst on placement.
- Complement Biology Group members for interesting presentations and helpful discussions over this work.
- My family and friends for their love, encouragement and continues support, a special thanks to my sisters for all the uplifting moments and for putting up with my science talk. I dedicate this Thesis to Marian, memory of you shall never pass away.

It has been a pleasure and a great opportunity to be a part of the BPM Group, I have enjoyed my PhD, and the experience and knowledge I have gained will take me forward into my future complement adventures.

Published papers during this PhD

1. Zelek, W. M., Xie, L., Morgan, B. P., & Harris, C. L. (2019). Compendium of current complement therapeutics. *Molecular Immunology*, 114, 341–352. https://doi.org/10.1016/j.molimm.2019.07.030
2. Zelek, W. M., Taylor, P. R., & Morgan, B. P. (2019). Development and characterization of novel anti-C5 monoclonal antibodies capable of inhibiting complement in multiple species. *Immunology*, 157(4), 283–295. https://doi.org/10.1111/imm.13083
3. Zelek, W. M., Harris, C. L., & Morgan, B. P. (2018). Extracting the barbs from complement assays: Identification and optimisation of a safe substitute for traditional buffers. *Immunobiology*, 223(12), 744–749. https://doi.org/10.1016/j.imbio.2018.07.016
4. Zelek, W. M., Stott, M., Walters, D., Harris, C. L., & Morgan, B. P. (2018). Characterizing a pH-switch anti-C5 antibody as a tool for human and mouse complement C5 purification and cross-species inhibition of classical and reactive lysis. *Immunology*, 155(3), 396–403. https://doi.org/10.1111/imm.12982
5. Kopczynska, M., Zelek, W. M., Vespa, S., Touchard, S., Wardle, M., Loveless, S., Morgan, B. P. (2018). Complement system biomarkers in epilepsy. *Seizure,* 60, 1–7. https://doi.org/10.1016/j.seizure.2018.05.016
6. Zelek, W. M., Watkins, L. M., Howell, O. W., Evans, R., Loveless, S., Robertson, N. P., Morgan, B. P. (2019). Measurement of soluble CD59 in CSF in demyelinating disease: Evidence for an intrathecal source of soluble CD59. *Multiple Sclerosis*, 25(4), 523–531. https://doi.org/10.1177/1352458518758927
7. *Kopczynska, M., *Zelek, W., Touchard, S., Gaughran, F., Di Forti, M., Mondelli, V., Morgan, B. P. (2019). Complement system biomarkers in first episode psychosis. *Schizophrenia Research*, 204, 16–22. https://doi.org/10.1016/j.schres.2017.12.012 (*equal first author)
8. Boshra, H., Zelek, W. M., Hughes, T. R., Rodriguez de Cordoba, S., & Morgan, B. P. (2018). Absence of CD59 in Guinea Pigs: Analysis of the Cavia porcellus Genome Suggests the Evolution of a CD59 Pseudogene. *Journal of Immunology*, 200(1), 327–335. https://doi.org/10.4049/jimmunol.1701238

Papers in press;

1. Zelek, W. M., Fathalla, D., Morgan, A., Touchard S., Loveless S., Tallantyre E., Robertson N.R., Morgan B. P. Cerebrospinal Fluid Complement System Biomarkers in Demyelinating Disease. (Manuscript submitted to *Multiple Sclerosis*, in revision).

LIST OF ABBREVIATIONS

AAV Anti-neutrophil cytoplasmic antibody (ANCA)-associated vasculitis
AChR Acetylcholine Receptor
AD Alzheimer's disease
AKI Acute kidney injury
AMD Age-related macular degeneration
AMR Antibody-mediated rejection
APS Antiphospholipid syndrome
AP Alternative pathway
APB Alternative pathway buffer
aHUS Atypical haemolytic uremic syndrome
BSA Bovine serum albumin
βME Beta mercaptoethanol
Ca2+ Calcium ion
C3aR C3a receptor
C5aR C5a receptor
C3G C3 glomerulopathy
CFD Complement fixing diluent
COPD Chronic obstructive pulmonary disease
CR1 Complement receptor 1
CVF Cobra Venom Factor
CV Column Volumes
CSF Cerebrospinal fluid
DAF Delay accelerating factor
DDD Dense deposit disease
DGF Delayed graft function
DMSO Dimethyl Sulphoxide
DNA Deoxyribose Nucleic Acid
DSA Donor specific antibody
ECL Enhanced chemiluminescence
ECM Extracellular matrix
EDTA Ethylene diamine tetra-acetic acid
EGF Epidermal Growth factor
EGTA Ethylene glycol-bis (ß-aminoethyl
ether) tetra-acetic acid VIII
EAMG Experimental autoimmune myasthenia gravis
ELISA Enzyme linked immunosorbent assay
FACS Fluorescence activated cell sorter
Fab Fragment antigen binding
FB Factor B
FD Factor D
FH Factor H
FITC Fluorescein Isothiocyanate
GA Geographic atrophy
GBS Guillain-Barré syndrome
gMG Generalized myasthenia gravis
GPI Glycosylphosphatidylinositol
HAE Hereditary angioedema
HBS HEPES buffered saline
HS Hidradenitis suppurativa
HU Huntington's Disease
IgAN IgA nephropathy
IgG Immunoglobulin G
IgM Immunoglobulin M
I/R Ischemia/reperfusion
K+ Potassium ion
KO Knockout
KT Kidney transplant
MN Membranous nephropathy
MS Multiple sclerosis
mAb Monoclonal antibody
MAC Membrane attack complex
MASP Mannose associated serine protease
MBL Mannose Binding Lectin
MCP Membrane co-factor protein
Mg2+ Magnesium ion
MW Molecular weight
Na+ Sodium ion
NMO Neuromyelitis optica spectrum disorder
NMR Nuclear magnetic resonance
OmCI Ornithodoros moubata complement inhibitor
PAGE Polyacrylamide gel electrophoresis
PBS Phosphate buffered saline
PG Pyoderma Gangrenosum
PD Parkinson's Disease
PNH Paroxysmal nocturnal hemoglobinuria
RA/OA Rheumatoid arthritis/Osteoarthritis
RA Rheumatoid Arthritis
RaCI Rhipicephalus appendiculatus complement inhibotor
RBC Red blood cell
RL Reactive lysis
RPE Retinal pigment epithelium
SCR Short consensus repeat
SDS Sodium Dodecyl Sulphate
SEM Standard error of the mean
SIRS Systemic inflammatory response Syndrome
SLE Systemic lupus erythematosus
sMAC Soluble MAC
SNP Single nucleotide polymorphism
SPR Surface Plasmon Resonance
TCC Terminal complement components
TED Thioester domain
TMA Thrombotic microangiopathy
TRIS Tris (Hydroxymethyl) methylamine
UV Ultra Violet
wAIHA Warm type autoimmune hemolytic anemia
wAMD Wet AMD
WT Wild type

LIST OF FIGURES

LIST OF TABLES

SUMMARY

Objectives; In the last decade there has been an explosion of interest in inhibiting complement for therapy of disease; the principle target has been complement component C5, activation of which generates the pro-inflammatory and cytotoxic products C5a and the membrane attack complex. The anti-C5 monoclonal antibody Eculizumab is a blockbuster drug, currently only approved for two ultra-rare diseases. There is abundant evidence that complement, and specifically the membrane attack complex, is involved in more common diseases for example in age related macular degeneration, myasthenia gravis and neurological disorders like neuromyelitis optica spectrum disorder and multiple sclerosis. Hence, there is an urgent need to develop better, cheaper drugs targeting membrane attack complex. Here I describe novel monoclonal antibodies targeting membrane attack complex downstream of C5 that are efficient inhibitors of its formation in humans and rodents.

Methods; A large panel of anti-membrane attack complex monoclonals was generated from spleens of terminal pathway deficient mice hyperimmunised with human or rat C5b6 and/or C5b67. Antibody clones were screened using immunochemical and novel functional (haemolytic) assays to identify those with binding and blocking activities. Biophysical methods, including surface plasmon resonance were used to characterise monoclonal antibodies of interest, and selected antibodies were tested in rodents to characterise pharmacokinetics and therapeutic capacity in complement-mediated disease models.

Results; Several function inhibitory anti-membrane attack complex antibodies were identified and characterised in terms of binding to membrane attack complex intermediates and cross-species lytic inhibitory capacity in comparison to current therapeutic anti-C5 monoclonal antibody. Blocking antibody selected include three against C5, two against C6 and five against C7; these efficiently inhibited lysis by human, rat, or mouse serum *in vitro* and were further characterised for binding specificity and affinity by enzyme linked immunosorbent assay, western blot and surface plasmone resonance, confirming strong and stable binding. One antibody has so far been tested in vivo; administration of this antibody intraperitoneally in rats efficiently inhibited serum lytic activity and blocked the disease and protected muscle endplates from destruction in a rat model of myasthenia gravis.

Conclusions; I report novel blocking antibodies that target membrane attack complex formation at different stages of the pathway to efficiently inhibit complement terminal pathway across species (human, rat and mouse). Rodents treated with selected antibody were protected in a complement-driven disease model. These antibodies offer an alternative to C5 targeting for membrane attack complex-driven pathologies in animal models and man and add new data on membrane attack complex assembly and function.

Table of Contents

CHAPTER 3; GENERATION AND CHARACTERISATION OF THE KEY REAGENTS

CHAPTER 1; Introduction

1.1 The complement system

Complement was discovered in the 19th century when Hans Buchner showed that immune serum contained a heat-labile "factor" or "principle" capable of killing bacteria. In 1896 Jules Bordet demonstrated that the “principle” had two components: one that was heat stable and present only in immune serum and another that loses killing capacity after heating the serum but could be replaced using fresh non-immune serum (Sim *et al* 2016). In the late 1890s Paul Ehrlich introduced the term "complement" for the heat-sensitive component in serum because it “complemented” the capacity of the “immune body” (or antibody) present in immune serum to kill bacteria. In the 1940s and 1950s, the haemolysis assay utilising sheep erythrocytes was used by Mayer and colleagues to unravel the reaction sequence. In the middle part of the 20th century, the various complement proteins were identified and assembled into the complement pathways by Nilsson, Muller-Eberhard and co-workers (Nesargikar *et al* 2012). The ancient origin and evolutionary conservation of complement shows its importance in immune processes in the body.

Complement compromises a network of proteins circulating in plasma and on cells, interacting together to provide defence against infection and efficient debris removal coordinated by the activation products generated when the system is triggered. Because of Its complexity and destructive character, complement is tightly regulated by an array of fluid-phase and membrane regulators (Morgan *et al* 2003; Harris 2018; Ricklin *et al* 2018).

The homeostatic role of complement is to be alert and ready to respond promptly to pathogen or other invader. When this homeostatic balance is interrupted, uncontrolled activation occurs that can result in self-cell/tissue damage. As a consequence, complement contributes to pathology in many diseases where inflammation is a driver. Examples of these include paroxysmal nocturnal haemoglobinuria (PNH) and atypical haemolytic uremic syndrome (aHUS). These two rare complement driven-diseases are caused by complement gene mutations or polymorphisms, but in many more common diseases, such as myasthenia gravis (MG), Alzheimer’s disease (AD) or age-related macular degeneration (AMD), complement dysregulation exacerbates/perpetuates pathology (Morgan and Harris 2015; 2017; 2018; Hakoyban *et al* 2016; Hu *et al* 2016, Carpanini *et al* 2019). In aHUS and PNH the membrane attack complex (MAC) causes cell damage and drives inflammation. Blocking MAC assembly with the anti-C5 monoclonal antibody (mAb) Eculizumab prevents these effects and transforms patient outcomes, but it is one of the most expensive drugs in the world with the cost of the treatment ~$600k per patient per year (Morgan and Harris 2015). The price of the therapy and the imperative to use anti-complement drugs in more common diseases provokes an urgent need for development of more affordable and

effective therapeutics to inhibit MAC. (Morgan and Harris 2015; 2018, Harris 2018; Carpanini *et al* 2019; Zelek *et al* 2019).

Three complement activation pathways; classical (CP), lectin (LP) and alternative pathway (AP), converge on a common terminal pathway (TP). The CP and LP are composed of the same components except for the factor responsible for the initial activation (Morgan 2003). The CP is triggered by C1 binding to antigen-antibody complexes resulting in activation of the C1r/C1s enzymes in the C1 complex. The LP is dependent on recognition of specific carbohydrate moieties such as mannan located on the surface of the microorganism; recognition in the LP is mediated by mannose-binding lectin (MBL) or ficolins instead of the C1 complex. The binding of MBL to mannose residues on the pathogen surface activates the MBL-associated serine proteases, MASP-1, and MASP-2 (Morgan and Harris. 2015; Heja *et al* 2012). Ficolins are homologous to MBL and function via MASPs in a similar way, but recognise other surface carbohydrates (Endo *et al* 2012, Garred *et al* 2016).
The AP, better thought of as the common amplification loop (AL), is activated whenever C3b is generated in the activation pathways and is perhaps also continuously activated at a low level as a result of spontaneous C3 hydrolysis, termed “tickover”.
All three activation pathways lead to the formation of homologous variants of a C3-cleaving protease, the C3 convertase (C4b2a for classical and lectin; C3bBb for alternative); this cleaves C3 to form C3a and C3b. C3b association with the C3 convertase generates the C5 convertase (C4b2a3b in classical and lectin; C3bBbC3b in alternative) that cleaves C5 to form C5a and C5b, the latter initiating the formation of the TP that culminates in formation of MAC or the soluble terminal complement complex (TCC) (Morgan and Harris 2015; Harris 2018; Ricklin *et at* 2018) (Fig. 1.1).

1.1.1 The classical pathway (CP)

The CP of complement was the first to be discovered when investigating the lytic properties of serum; complement dependent lysis of erythrocytes was dependent on erythrocyte sensitisation with antibody. The CP is activated by binding of the C1 complex to the Fc region of IgG or IgM antibody: the CP can also be directly activated by many pathogens, including gram negative bacteria and some viruses, and by damaged cells (Loss 1982; Cooper *et al* 1976; Ebenbichler *et al* 1991). The CP protects against infection but also recognises and clears immune complexes and apoptotic cells (Fishelson *et al* 2001) and plays a major role in organ rejection in transplantation (Dalmasso 1992). All activators of the CP bind multiple heads of the C1q domain, inducing conformational changes that activate the catalytic subunits in the enzyme tetramer C1s-C1r-C1r-C1s.

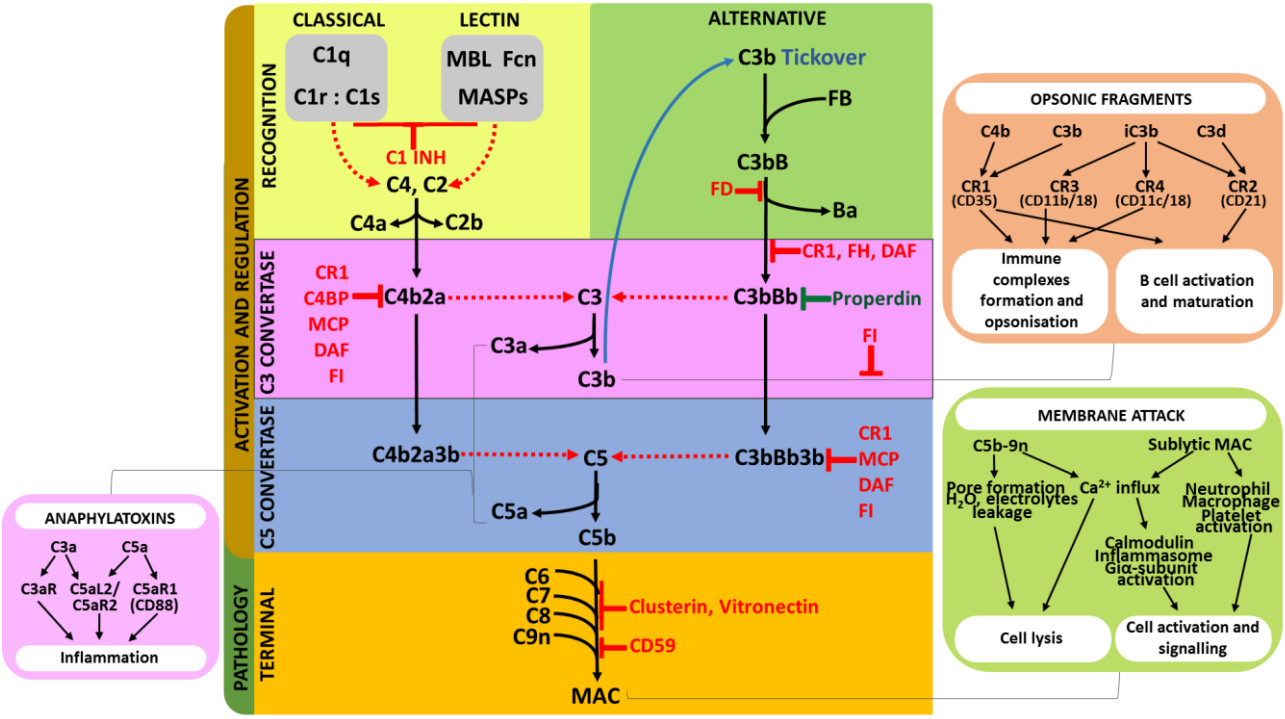

Figure 1.1 *Cascade of complement activation pathways; classical, lectin and alternative, leading to MAC generation. The enzymatic cleavages are represented by dotted red arrows and show the responsible enzymes alongside. Negative regulators are highlighted in red, positive regulators in green. Complement effectors (opsonic fragment, anaphylatoxins and membrane attack) are shown in boxes.*

The tetramer interacts in a Ca^{2+}-dependent manner with each of the six triple helical collagen-like stems projecting from each globular head of C1q (Gregory *et al* 2003). The autolytic activation of proenzyme C1r leads to conversion of proenzyme C1s. Activated C1s cleaves specifically first C4 into C4a and C4b and then C2 into C2a and C2b, but only when C2 is in complex with C4b (Polley et al. 1967; 1968), to generate the CP C3 convertase C4b2a (Nagasawa *et al* 1977, Sharp *et al* 2017). When C4 is cleaved, an internal thioester is exposed covalently linking C4b to amino or hydroxyl groups present on pathogen surfaces, thus localising the convertase to the surface (Dodds *et al* 1996). This surface binding mechanism also applies to the C3b opsonin (Sim *et al* 1981).

C1 function is strictly regulated by C1 inhibitor (C1INH), a serine protease inhibitor that inhibits by forming stoichiometric complexes with active C1r and C1s, removing them from the C1 complex (He *et al* 1998; Ziccardi 1986).

1.1.2 The lectin pathway (LP)

The LP is the "newest" complement activation pathway, discovered in the 1980s (Ikeda *et al* 1987) following isolation of mannose-binding lectin (MBL) (Presanis *et al* 2003). MBL activates complement when bound to cell surfaces (Ikeda *et al* 1987). In CP, C1q is the only recognition protein, whereas LP includes several families of recognition proteins: ficolins (Ficolin-1, 2 or 3) and collectins (collectin-10 or 11) in addition to MBL (Holmskov *et al* 2003; Garred *et al* 2016). MBL is a trimer of polypeptide chains that each comprise four domains; 1. N-terminal cysteine-rich region (21- amino acid (aa) long) responsible for oligomerization by formation of the disulfide bonds; 2. Collagen-like domain (59-aa) consisting of 20 tandem repeats of Glycine-Xaa-Yaa that account for the stalk of the molecule; 3. Neck region (30-aa) that assembles into triple alpha-helical hydrophobic coiled-coil structures, which is crucial for initiating the oligomerization; 4. C-terminal carbohydrate recognition domain (CRD, 188-aa) (Garred *et al* 2016; Dong *et al*, 2007). The MBL polypeptide chain is ~25.5 kDa (Larsen *et al* 2004; Teillet *et al* 2005); in serum it exists predominantly as trimers and tetramers; higher (pentamers, hexamers) and lower (monomers, dimers) forms are less common (Mogues *et al* 1996; Garred *et al* 2003). MBL, collectins and ficolins all use the same serine proteases (MASPs) to activate the complement system (Mogues *et al* 1996; Matshshita *et al* 2000; Ma *et al* 2013). MASP-1 activates MASP-2 (Kerr *et al* 2008; Heja *et al* 2012; Degn *et al* 2013) similar to the C1r/s interaction in CP. The LP is also regulated by C1INH (Takahashi *et al* 2010). Recent studies showed that MASP-1 activates MASP-3, which cleaves pro-factor D, essential in AP activation (Oroszlan *et al* 2016).

1.1.3 The amplification loop (AL) of the AP

The AP was first propounded in the 1950s by Louis Pillemer following his discovery of properdin the now well-known positive regulator of the AP (Nesargikar *et al* 2012; Pillmer *et al* 1954). The AP is better defined as an amplification loop (AL) as it provides stable and continuous amplification of complement activation initiated by any of the activation pathways; I will use the terms interchangeably. C3b generated in the activation pathways (or hydrolysed C3 in some circumstances), either covalently bound to a surface or in the fluid phase, binds factor B (FB, a structural homolog of C2) in the presence of Mg^{2+} (Forneris *et al* 2010), causing conformational change that allows cleavage at a single site by the plasma serine protease factor D (FD) into Bb and Ba (Milder *et al* 2007). FD is locked in an inactive resting state that becomes unlocked upon interaction with C3b (Jing *et al* 1998). The Ba fragment is released and the enzymatically active Bb fragment remains attached to C3b forming the AP convertase C3bBb. Bb in the C3bBb complex cleaves C3 to generate more C3b that can bind FB and feed the AL (Jongerius *et al* 2009). C3bBb convertase is stabilised by binding of properdin which protects C3b from degradation by the regulatory

proteins factor I (FI) and factor H (FH) and inhibits dissociation of C3b and Bb hence prolonging the half-life of the C3 convertase (Alcorlo *et al* 2013; Fearon 1975; Hourcade 2006). Uncontrolled activation of the AL, seen in individuals deficient in FH or FI, leads to total consumption of C3.

1.1.4 The terminal pathway (TP)/ membrane attack complex (MAC)

The final enzymatic step in the complement cascade involves cleavage of C5, a close homolog of C3 and C4 that lacks an internal thioester so cannot covalently bind surfaces. C5 is cleaved by the CP/LP and AP C5 convertases (C4b2aC3b and C3bBbC3b). The extra C3b molecule captures C5 which allows C5 to be cleaved into C5a and C5b by C2a or Bb enzymes in the complex. The small biologically active fragment C5a anaphylatoxin is released and the larger cleavage product C5b remains associated with the enzyme complex; generation of C5b is the first step in the TP. C5b sequentially binds the plasma proteins C6 and C7, generating C5b67 complex that undergoes conformational change enabling its release from the convertase and exposing a hydrophobic membrane binding site. The C5b67 complex through its hydrophobic surface tightly binds membrane and sequentially recruits C8 and C9 to create the MAC. The complete transmembrane pore contains one molecule each of C5b, C6, C7 and C8 and 18 copies of C9 that are recruited sequentially and rapidly polymerise to form the lytic pore through which metabolites and small proteins leak out of the cell and water into the cell due to osmotic pressure leading eventually to lytic cell death (Morgan and Harris 2015; Ricklin *et al* 2018; Morgan *et al* 2016; Menny *et al* 2018; Heesterbeek *et al* 2019) (Fig.1.2).

1.2 Complement regulation

The potentially self-destructive nature of complement requires rigid control. Complement regulation is important to direct actions against invaders but also to protect self-cells. Dysregulation of complement is a component of many diseases, including autoimmune conditions. Many of the complement cascade intermediate products are short-lived, for instance the thioester groups in nascent C4b and C3b are inactivated by hydrolysis instantly upon exposure, limiting their capacity to bind surfaces. The enzyme complexes of the activation pathways decay very fast after formation; the active C5b67 complex exists for only a fraction of a second on plasma before being bound by the chaperone inhibitors clusterin and S-protein (Preissner *et al* 1985; Morgan *et al* 2017; Parsons *et al* 2019). Apart from this endogenous control, natural regulators are present at each step of the pathway, dictating efficient control of auto-activation and self-amplification of the system (Table 1.1).

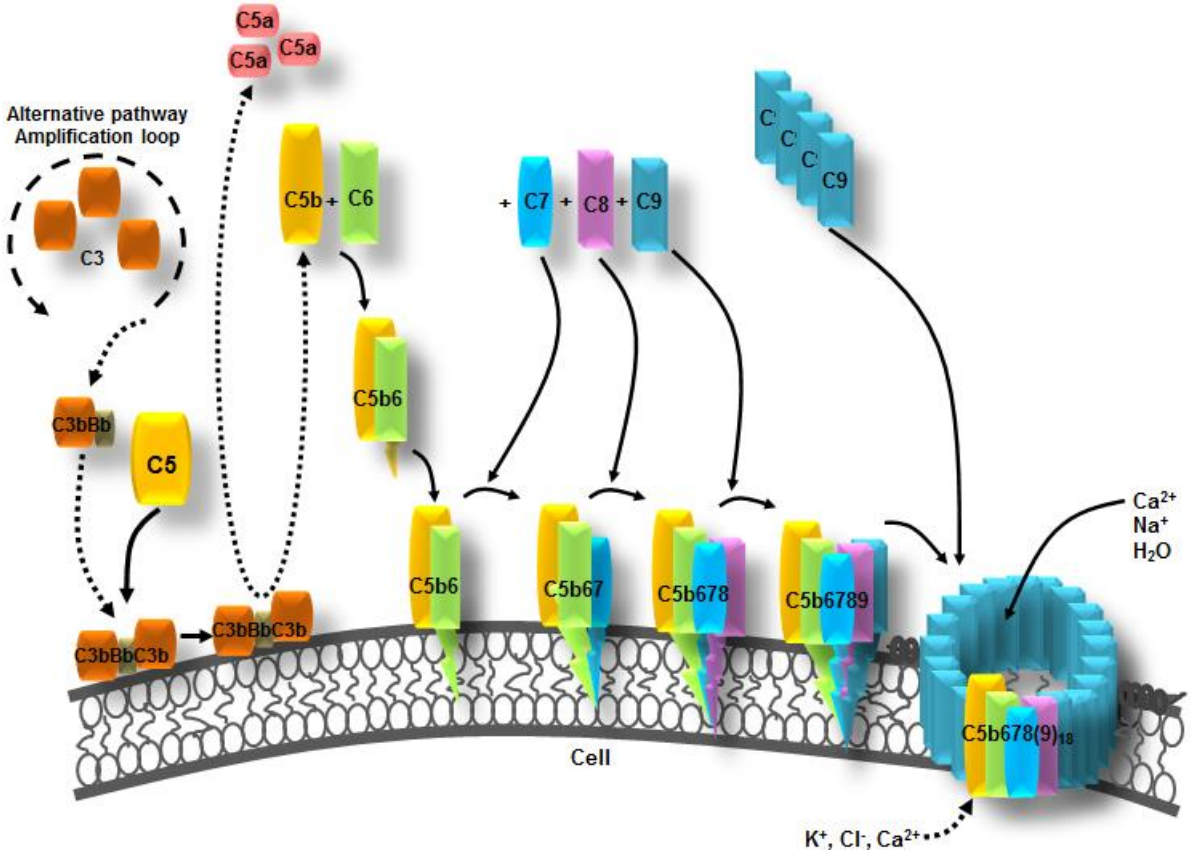

Figure 1.2 *Schematic of MAC formation showing sequential complement TP component binding to form the lytic pore.*

	REGULATOR	CONTROLED PROTEIN
PLASMA	C1 Inhibitor	C1qsrrs, MASPs
	Factor H	C3bBb, C3b, iC3b
	Factor I	C4b, C3b, iC3b
	C4BP	C4b2a, C4b
	S Protein	C5b67
	Clusterin	C5b67
	Carboxypeptidase N	C3a, C4a, C5a
MEMBRANE	CR1 (CD35)	C4b2a, C4b, C3bBb, C3b, iC3b
	DAF (CD55)	C4b2a, C3bBb
	MCP (CD46)	C4b, C3b
	CD59	C5b678, C5b6789n, C8, C9

Table 1.1 *Complement pathway regulators and their corresponding regulated components.*

1.2.1 Regulation of classical and lectin pathway activation

The activated C1 (C1qr2s2) complexes are regulated by C1INH, a plasma serpin inhibitor, by strong, irreversible binding to the activated C1s and C1r sub-units of C1 which results in their dissociation from C1q thereby inactivating C1 (Patston *et al* 1991; Garcia *et al* 2016). MBL-MASP complexes are inhibited in the same manner by stripping off the MASPs.

C1INH (MW = 110 kDa) plays major roles in the regulation of the initial stages of complement activation, but it is also the major regulator of the kinin-kallikrein system responsible for autacoid production. Hereditary angioedema (HAE) is a disease caused by C1INH deficiency; patients suffer soft tissue swelling, including mucosal swelling that may lead to life threatening conditions (Gower *et al* 2011). In these patients even a minor trauma or stress can trigger complement and kinin system activation in the tissue resulting in an inflammatory attack. Treatment with plasma derived or recombinant C1INH (Ruconest, Berinert, Cinryze) restores full control over the systems.

1.2.2 Regulation of amplification loop (AL)

The AL C3 and C5 convertases are controlled by regulators circulating in plasma; FH, C4b binding protein (C4BP) and FI, and on membranes; CD46, CD55, complement receptor 1 (CR1, CD35) (Zipfel and Skerka 2009).

Both C3 convertases; C4b2a and C3bBb, are unstable and undergo rapid spontaneous decay. FI is a key regulator that, in the presence of cofactors (FH, MCP, CR1, C4BP), cleaves C3b and C4b to their inactive forms (iC3b and iC4b) (Lambris *et al* 1996; Nishida *et al* 2006). FI cleaves C3b into iC3b and C3f; the C3f fragment is released into the circulation while iC3b remains bound to the membrane but cannot recruit FB to form convertase (Alcorio *et al* 2011). CR1 is the only co-factor mediating further FI cleavage of iC3b into C3c, which is released into the circulation, and C3dg, which remains anchored to the membrane (Furtado *et al* 2008). C3dg is a ligand for complement receptor 2 (CR2) that takes part in regulation of B cell activation (Dempsey *et al* 1996; Lyubchenko *et al* 2005; Kremlitzka *et al* 2016). The cofactors; CR1, MCP and C4BP also support FI cleavage of C4b into inactive forms, iC4b and C4d, which inhibits further formation of C4b2a complexes (Masaki *et al* 1992).

FH is plasma glycoprotein (~300µg/ml, MW = 155 kDa) that binds negatively charged carbohydrates. (Meri and Pangburn 1990; 1990). FH displays both decay-accelerating and cofactor activities for the AP C3 convertase (Wu et al. 2009). FH has several functional sites; the N-terminal four short consensus repeats (SCRs) disturb formation and stability of the convertases, the C-terminal two SCRs are responsible for binding surfaces and self/ non-self-discrimination. Mutations in FH C-terminus have been linked to aHUS. (Warwicker *et al* 1998; Buddles *et al* 2000; Richards *et al* 2001; Perez-Caballero *et al* 2001; Caprioli *et*

al 2001; Hyvärinen *et al* 2016; Goicoechea de Jorge *et al* 2018). Three sites in FH play roles in recognition of polyanions and another three are known to interact with various regions of C3b. Binding at one site modulates interactions at other sites and it has been postulated that each of the 20 SCR modules of FH, by its distinct flexibility and structure, contributes to biological function (Meri and Pangburn 1990). Transmission electron microscopy (TEM) indicated that FH is a monomeric protein that adopts an extended bead on a string conformation (Sim and DiScipio 1982; Hannan *et al* 2016). SCR 20 is a key player in surface recognition, the site of many aHUS-associated mutations (Caprioli *et al* 2001; Perkins and Goodship 2002; Aslam and Perkins 2001). Deficiencies in FH are very rare and, cause loss of control of the AL and complete consumption of C3; as a consequence, patients suffer severe, recurrent bacterial infections (Grumach and Kirschfink 2014). A number of disease-associated single nucleotide polymorphisms (SNP) in FH are reported, including 1277 T>C that encodes a single amino acid change, Y402H, and is a strong genetic risk factor for AMD. The polymorphism has no direct impact on the interaction of FH with C3bBb, but may affect its interaction with C reactive protein (CRP), sulphated glycosaminoglycans (GAGs) and other cell surface proteins, impacting FH binding to surfaces (Hageman *et al* 2005). Autoantibodies to FH are found in some patients with aHUS and also sometimes in rheumatoid arthritis (RA) and systemic lupus erythematosus (SLE) (Foltyn-Zadura *et al* 2012; Jiang *et al* 2016).

CD46 (membrane cofactor protein, MCP) and CD55 (decay accelerating factor, DAF) interact together to prevent opsonisation and self-cells damage by controlling the C3/C5 convertase enzymes (Morgan and Meri 1994; Morgan and Harris 1999; Brodbeck *et al* 2000). CD55 accelerates the natural decay of the enzyme complex to release C3b or C4b. CD46 binds to the surface of these proteins and acts as a cofactor for its irreversible proteolytic inactivation by FI, preventing further convertase formation. Both CD46 and CD55 are assembled from similar functional domains; SCRs found in many complement regulatory proteins and responsible for binding to C3b and C4b (Reid and Day 1989).

CD46 is a type one transmembrane glycoprotein made up of 4 SCR modules, a linker region, transmembrane region and cytoplasmic tail, expressed by most nucleated cells (Liszewski *et al* 1996; Wang *et al* 2017). CD46 plays an important role in innate and adaptive responses; its ubiquity has made it an attractive target for many invaders, including measles virus (Dorig *et al* 1993; Naniche *et al* 1993; Sajjadi *et al* 2019), human herpesvirus (Santoro *et al* 1999; Charvet *et al* 2018), cytomegalovirus (Stein *et al* 2019), group B adenoviruses (Gaggar *et al* 2003; Segerman *et al* 2003; Cho *et al* 2016) and Neisseria, the latter with evidence that CD46 may play a role in enabling the organism to breach the blood brain barrier (BBB) in meningitis. (Jonsson *et al* 2003; Kim *et al* 2019). Similarly, to FH, SNP in

MCP (notably that encoding the amino acid change S206P) are associated with aHUS (Richards *et al* 2003).

CD55 is formed of four SCR modules with specific biological functions a heavily glycosylated linker and a GPI anchor (Nicholson-Weller and Wang 1994; Medof *et al* 1984; Kinoshita *et al* 2018). Domain deletion and mutagenesis studies (Kuttner-Kondo *et al* 2001; Brodbeck *et al* 1996; Williams *et al* 2003) demonstrated that SCRs 2 and 3 modulate CP convertase whereas SCRs 2, 3 and 4 are required to regulate the AL. CD55 is expressed at high copy number on the surface of most cells exposed to complement (Medof *et al* 1984; Nicholson-Weller *et al* 1985; Kinoshita *et al* 1985; Flückiger *et al* 2018), preventing amplification of complement on these cells. Because of its broad expression, many pathogens take advantage of cell surface CD55 to progress invasion by cellular attachment (Hamann *et al* 1996; 1998; Lea 2002, Ward *et al* 1998; Lindahl *et al* 2000), including enteroviruses (Bergelson *et al* 1994; 1995) and Escherichia coli (Le Bouguenec *et al* 2001; Nowicki *et al* 1993; 2013).

1.2.3 Regulation of anaphylatoxins: C3a and C5a

Carboxypeptidase N (CPN) is a zinc metalloprotease that cleaves C-terminal arginine (Arg) and Lysine (Lys) residues of plasma peptides including kinins and complement anaphylatoxins C3a, C5a (Matthews *et al* 2004). C5a/C3a cleavage by CPN generates the less effective desArg-C5a/desArg-C3a (Campbell *et al* 2001; Zarbock *et al* 1988). The interactions of C5a and C3a with their respective receptors (C5a receptor (C5aR; CD88); C3a receptor (C3aR)) respectively, are mediated by their C-terminus residues Arg74 and Lys68 (Lambris and Holers 2000) (Mollison *et al* 1989; Kawai *et al* 1992) and loss of these terminal residues severely reduces binding. Indeed, the C-terminal tail of C5a has been used to design small molecule antagonists for C5aR binding. (Ember *et al* 1992; Kawai *et al* 1991; Konteatis *et al* 1994). C5a is one of the most pro-inflammatory products of the complement cascade; therefore, it is a good target for development of anti-inflammatory drugs. Both C5a and C3a induce leukocyte chemotaxis, trigger release of leukocyte granule-associated enzymes and vasoactive mediators, increase vascular permeability and cell adhesion, induce smooth muscle contraction and stimulate the release of specific cytokines by myeloid, endothelial and epithelial cells and astrocytes (Lambris and Holers 2000). Both C5a and C3a are implicated in Inflammasome activation. C3a is needed for LPS-triggered NLRP3 Inflammasome activation in human macrophages and dendritic cells (Asgari *et al* 2013), while C5a takes part in inflammasome activation by cholesterol crystals (implicated in atherosclerosis) (Samstad *et al* 2014). This study demonstrated that cholesterol crystal induced inflammation in atherosclerosis requires complement activation and may be regulated with anti-complement agents.

Over recent years it was shown that roles of C5a and C3a extend beyond inflammatory responses (Mastellos and Lambris 2002). Both anaphylatoxins are key players in developmental and morphogenetic processes, including haematopoiesis, reproduction, liver regeneration, apoptosis, and central nervous system (CNS) development (Girardi *et al* 2003; van Beck *et al* 2001; Farkas *et al* 1998; Reca *et al.*2003; Strey *et al* 2003). A number of pathological conditions are associated with excessive production of C5a and/or C3a, including adult respiratory distress syndrome, asthma, septic shock, RA, inflammatory bowel disease, psoriasis, pemphigoid, and AD (Hammerschmidt *et al* 1980; Humbles *et al* 2000; Czermak *et al* 1999; Moxley and Ruddy *et al* 1985; Woodruff *et al* 2002; Ahrenstedt *et al* 1990; Mukherjee *et al* 2000; Mrowietz *et al* 2001; Chen *et al* 2001, Camparini *et al* 2019; Zheng *et al* 2019).

1.2.4 Regulation of terminal pathway/ MAC

The terminal pathway (TP) comprises five components; C5b, C6, C7, C8 and C9 that individually behave as hydrophilic plasma proteins but when combined in the context of cell membranes form the amphiphilic MAC complex. Release of the C5b67 complex from the convertase provides the first point of regulation of MAC assembly. First, the complex spontaneously decays within a fraction of second due to the unstable nature of its membrane binding site (Preissner *et al* 1985; Morgan *et al* 2017); second, the complex is inhibited by plasma proteins that bind C5b67 and prevent its association with membrane (S-protein, Clusterin) (Tsuruta *et al* 1990). Together, these events reduce the efficiency of C5b67 deposition on the cell surface and hence MAC formation; C8 association with C5b67 complex in the fluid phase also prevents assembly of MAC on the membrane (Nemerow *et al* 1979). The fluid-phase C5b67 complex, while bound to S-protein and/or clusterin, can still interact with C8 and C9 to form sC5b-9, also known as TCC (Ware and Kolb 1981; Ware *et al* 1981; Preisner *et al* 1989). Conformational changes in C9 occur exposing neo-epitopes identical to those exposed in MAC, however the structure does not physically resemble the MAC. TCC is a good biomarker of complement activation and has therefore found application in many in vitro studies on inflammatory diseases (Falk *et al* 1983; Mollnes *et al* 1984; Prohászka *et al* 2016; Morgan *et al.* 2019).

If the trimolecular C5b67 complex attaches to the lipid bilayer of the cell, it binds strongly and recruitment of C8 further aids stability by promoting insertion of the complex into the membrane, C9 binding and its rapid polymerisation. As many as 18 molecules of C9 can bind in each complex, although only one or two are sufficient to create a functional pore (Podack *et al* 1984). Recruitment and insertion of C9 promotes major structural rearrangements in the complex that disrupt the membrane and create space for the next copies of C9 sequentially recruited. Polymerisation of C9 generates the large pore visible

in electron microscopy of lysed cells (Podack *et al* 1982; Morgan *et al* 2017). Recent advances in cryo-electron microscopy (cryo-EM) have defined MAC structure precisely, demonstrating an asymmetric pore of “split-washer” appearance (Fig. 1.4): the function of the “split-washer” in MAC remains debatable (Parsons *et al* 2019; Bubeck *et al* 2018; Morgan *et al* 2017).

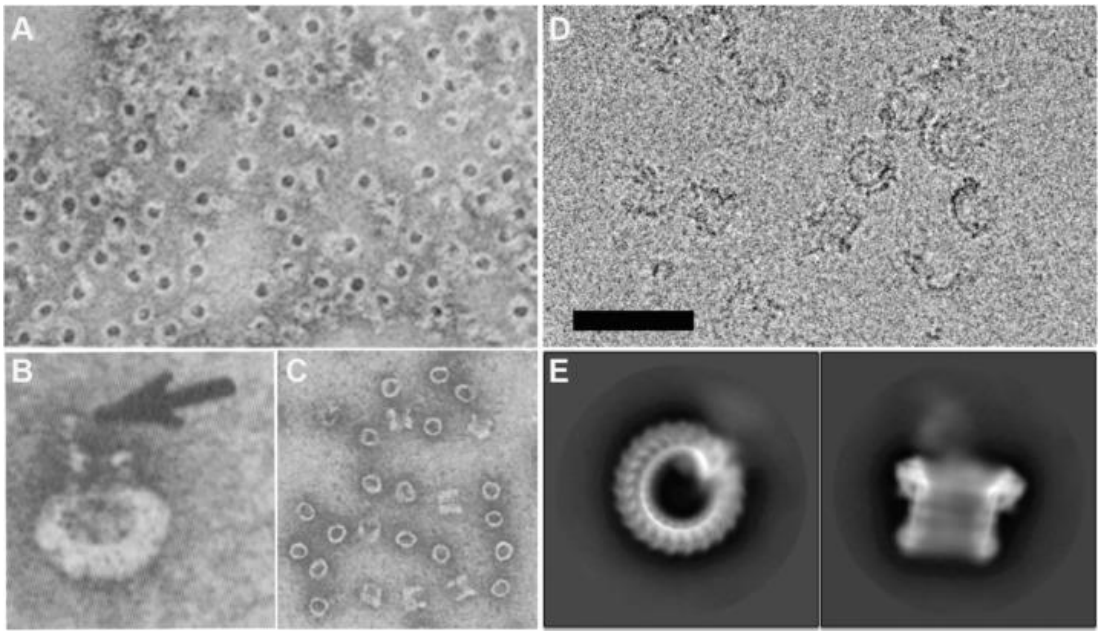

Figure 1.3 *MAC visualisation using past and current techniques.* ***A – C****: early negatively stained pictures of MAC and its in vitro analogue poly-C9 captured with electron microscopy.* ***A.*** *MAC complexes assembled on rabbit erythrocytes,* ***B.*** *MAC formed on liposomes.* ***C.*** *Poly-C9; top and side view.* ***D – F.*** *Recent images of MAC by more advanced technologies.* ***D.*** *Cryo-EM image of detergent-solubilised MAC complexes (scale bar 50nm).* ***E.*** *Top and side views of 2D structure of detergent-solubilised MAC (Morgan et al 2017).*

A recent study of MAC assembly on bacterial model membranes demonstrated that the initial insertion of C9 together with its binding to C5b-8 is the choke point in pore formation. Interestingly, this rate-limiting step coincides with CD59 binding to prevent MAC assembly (Parson *et al* 2019; Bubeck *et al* 2018; Hamilton *et al* 1990; Farkas *et al* 2002; Lehto and Meri 1993). Cryo-EM demonstrated that the β-barrel pore of the MAC is formed when helical bundles in the MAC-Perforin (MACPF) domains of the component proteins transform into transmembrane amphipathic β-hairpins (TMH-1 and TMH-2) that unravel and insert into the membrane (Menny *et al* 2019; Dudkina *et al* 2016; Rosado *et al* 2007; Shatursky *et al* 1999) (Fig. 1.4). This results in release of TMH2 and conformational changes in HTH (helix turn helix) region that expose the elongated face of the inserted C9, allowing the next C9 molecule to bind and unfold to grow the pore. A C9 mutant with TMH1 immobilised by a

disulphide lock was able to bind C5b-8 but unfolding and hence MAC assembly was prohibited, suggesting a possible therapeutic potential of the mutant (Spicer *et al* 2018).

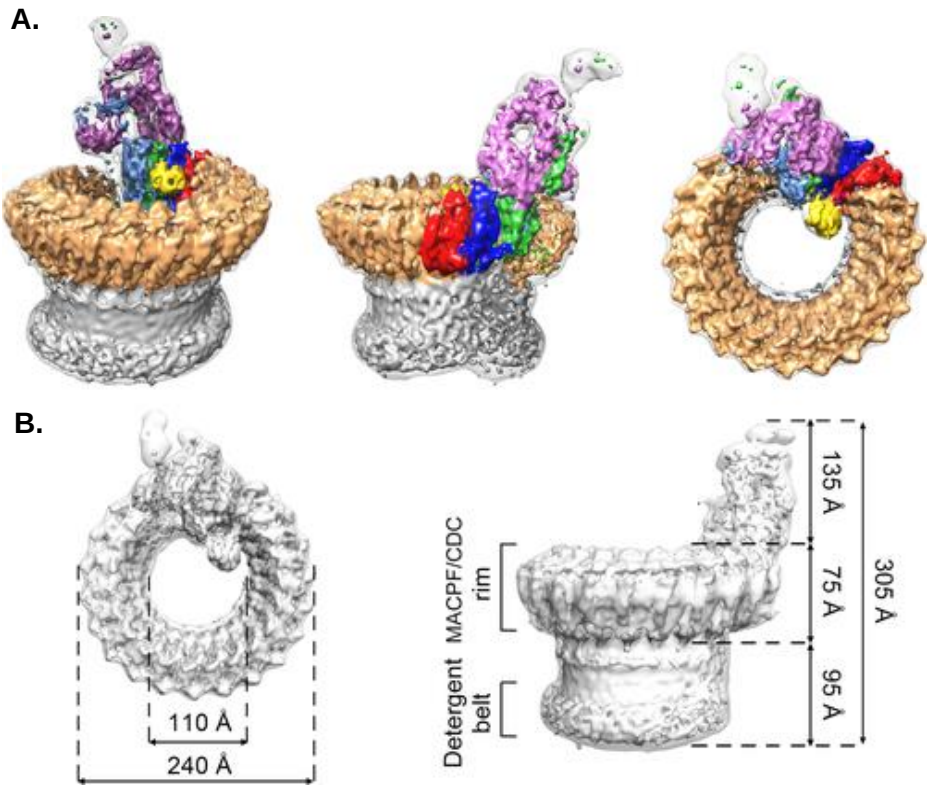

Figure 1.4 *Cryo-EM structure of MAC. A. Three views of the MAC, individual proteins highlighted in different colours; C5b (magenta), C6 (light blue), C7 (green), C8α (red), C8β (dark blue), C8γ (yellow), C9 (orange). The contiguous MAC β-barrel and detergent belt are in grey. B. Top and side views of the structure with dimensions indicated. Adapted from Serena et al 2016.*

The recent cryo-EM and flickr spectroscopy studies on MAC formation on lipid bilayers show that MAC is a flexible pore. The membrane rupture mechanism involves C6 and C7 binding to the outer leaflet that reduces the energy of membrane bending. This allows C8 and C9 to insert into the bilayer, increasing membrane rigidity. C5b6 here acts as a platform directing the β-barrel formation supported by C9 glycan scaffold. This mechanism shows precisely how MAC destroys pathogens and facilitates cell activation but also gives an insight how cells recover from MAC attack (Menny *et al* 2018).

Assembly of MAC on the membrane is regulated by CD59, a small glycosylphosphatidylinositol (GPI) anchored protein that patrols the cell surface to block forming complexes. CD59 binds the forming complex and prevents the completion of the

MAC pore (Lehto *et al* 1997; Rooney *et al* 1993; Morgan *et al* 2016). CD59 was first described in late 1980s as a broadly expressed 18 – 20 kDa membrane protein extracted from erythrocytes that inhibited MAC mediated lysis of the targeted cells (Holguin *et al* 1989; Okada *et al* 1989; Sugita *et al* 1988). Nowadays the structure of CD59 (MW = 18 – 25 kDa, depending on the tissue/ cell source), including the glycosyl phosphatidylinositol (GPI) anchor is well defined. (Ratnoff *et al* 2008). The glycosylation of CD59 comprises a single large, complex N-linked carbohydrate group at Asn18 which accounts for between 4 and 6 kDa of the molecular mass, and variable amounts of O-glycosylation (Wheeler *et al* 2002; Ninomyia *et al* 1992). Removal of the N-glycosylation site by mutation of Asn18 in a recombinant soluble form of CD59 increased 7-fold complement inhibitory activity (Suzuki *et al* 1996) (Fig. 1.5).

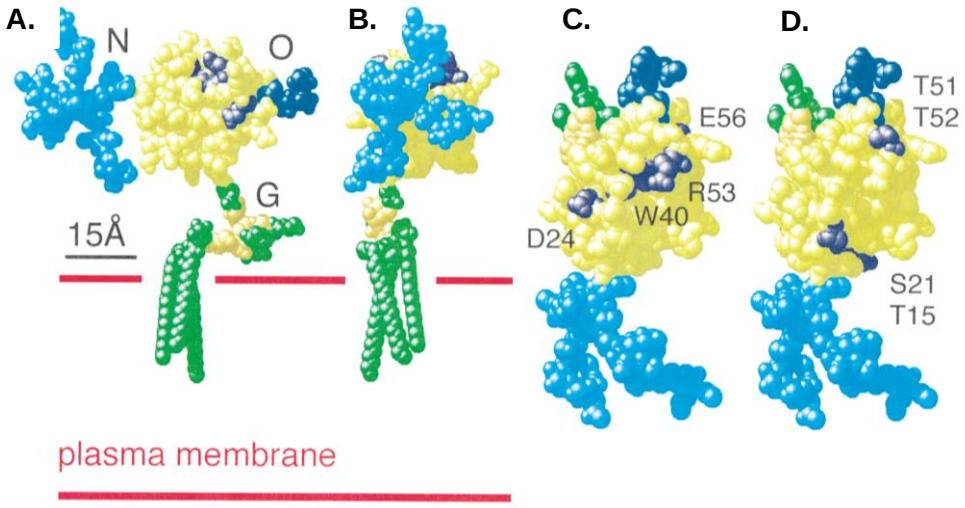

Figure 1.5 *Structure of native anchored CD59. Above the membrane is the protein core and O, N – glycans. The GPI anchor (G) is inserted into the membrane,* ***A, B.*** *The two orthogonal views of the model drawn in space-filling format.* ***C, D.*** *Top views (Rudd et al 1997).*

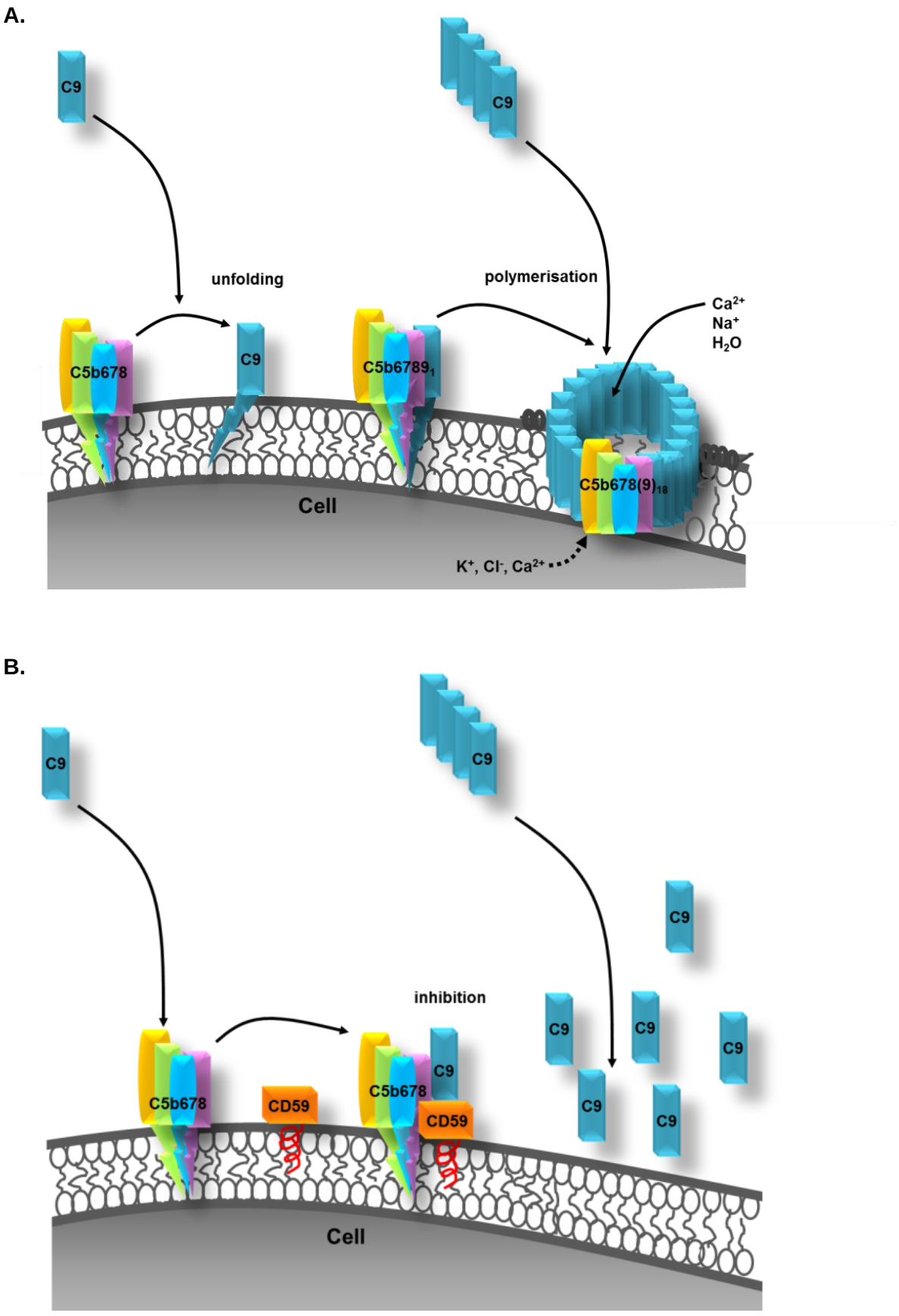

Figure 1.6 *Inhibition mechanism of MAC formation by CD59.* ***A.*** *MAC assembly in the absence of CD59: C9 unfolds and binds to C5b-8 complex allowing deep insert of the*

complex into the membrane, recruitment of additional C9 molecules and rapid C9 polymerisation to form MAC resulting in membrane disruption. ***B.*** *CD59, moving in the plane membrane, encounters and binds C5b-8 complex, the first C9 molecule binds the complex, but the C9 unfolding and insertion into the membrane is inhibited by the steric hindrance of the bound CD59. As a consequence, C9 polymerisation does not occur, MAC is not formed, and membrane is not damaged.*

Structural studies to determine the MAC inhibition site demonstrated that CD59 does not interact with any of the individual MAC proteins or intermediates upstream of C5b-8 complex but shows strong affinity for the C5b-8 complex, restricting incorporation and polymerisation of C9. (Rollins and Sims 1990; Meri *et al* 1990). CD59 binds to the C8α chain and the carboxy-terminal b domain of C9 (Lehto *et al* 1997). Further studies showed that introduction of CD59 after the first insertion of C9 into the C5b-8 complex stops the subsequent recruitment of C9 molecules (Fig. 1.6).

The demonstration that CD59 was absent from the affected erythrocytes in PNH, a consequence of defective GPI anchor formation, provided an explanation for the lytic susceptibility of these cells (Parker *et al* 2008; Holguin *et al* 1989; Yamashina *et al* 1990). The GPI anchor facilitates CD59 mobility in the membrane, but also may be involved in signalling; cross-linking of CD59 on human neutrophils caused increased intracellular Ca^{2+} concentration and oxidase activation (Morgan *et al* 1993). Other suggested functions of CD59 include stimulation of cytokine release and cell proliferation in T cells (Korty *et al* 1991; Okada *et al* 1989), neutrophil activation (Morgan *et al* 1993), cell adhesion and activation through CD2 (Deckert *et al* 1992; Hahn *et al* 1992). Some tumour cells overexpress CD59 which may promote tumour cell growth and survival (Fishelson *et al* 2003; Fonsatti *et al* 2000). CD59 can be shed from the cell membrane and released into the circulation in a soluble form (sCD59) that can be detected in various body fluids including urine, milk, serum, plasma and cerebrospinal fluid (Hakulinen and Meri 1995; Vakeva *et al* 2000; Meri *et al* 1996; Zelek *et al* 2019). Elevated levels of sCD59 have been found in acute myocardial infarction, diabetes and lung allograft dysfunction (Hakulinen and Meri 1995; Vakeva *et al* 2000; Budding *et al* 2016) and has been suggested as a disease biomarker. In vitro assays showed that sCD59 is an efficient inhibitor of MAC formation (Sugita and Masuho 1994); indeed, in a wet AMD model, local administration of sCD59 reduced choroidal neovascularisation (Bora *et al* 2007).

1.2.5 Role of sub-lytic MAC in immune responses

The main purpose of MAC is lytic killing of pathogens. The assembly of the pore on homologous nucleated cells does not always cause lysis; sub-lytic MAC has a number of

effects beginning with Ca^{2+} influx through the pore that in turn triggers Ca^{2+} store release that dramatically increases intracellular Ca^{2+} from low nM to µM levels within seconds (Morgan 1989). The generated Ca^{2+} binds multiple proteins within the cell, for example calmodulin which activates downstream calmodulin-dependent kinases to modulate many processes in the cells. Ca^{2+} is likely the primary mediator of sub-lytic MAC effects in nucleated cells; however, MAC may regulate cyclic AMP (cAMP) generation by direct interaction with the Giα-subunit of G-protein-coupled receptors, although the precise mechanism is unknown. MAC downstream signalling pathways have been identified for different cell types, tissues, and complement sources, with PI3kinase, AKt/FOX01, and ERK1 pathways emerging from multiple studies (Qiu *et al* 2012; Ren *et al* 2008; Fosbrink *et al* 2006). MAC-mediated activation of cyclic dependent kinases 2 and 4 (CDKs) resulted in cell activation and proliferation (Tegla *et al* 2011), while activation of apoptotic pathways via phosphorylation of Bad (BCP-2 associated death receptor) and caspase activation has been described (Cudrici *et al* 2006; Fishelson *et al* 2001; Lusthaus *et al* 2018).

Inflammatory effects of sub-lytic MAC on various cell types have been reported. Studies on neutrophils, macrophages and T-cells have reported that sub-lytic MAC induced secretion of inflammatory cytokines (Chauhan and Moore 2011). Retinal epithelial cells challenged with non-lytic MAC released IL-6, MCP-1, and VEGF (Lueck *et al* 2011). MAC-induced platelet activation released microparticles and triggered surface modifications to enhance stickiness. (Martel *et al* 2011). Sub-lytic MAC triggered assembly and activation of NLRP3 inflammasome in lung epithelial cells resulting in a dramatic increase of IL-1β secretion (Triantafilou *et al* 2013). Inflammasome activation was also seen on murine dendritic cells with resultant synthesis of IL-1β and IL-18 (Laudusi *et al* 2013). Taken together, these findings suggest that drugs targeting IL-1β could be effective in MAC-driven pathologies.

1.2.6 Complement receptors

Complement activation and its effects require receptors on target cells. In the CP, multiple C1q receptors are defined, binding to the globular head (gC1qR) or collagenous tail (cC1qR) regions of C1q (Peerschke *et al* 1994; Hosszu *et al* 2010; McGreal and Gasque 2002; Zhang *et al* 2018). Their role is yet to be clearly defined, although they likely have an opsonic effect in debris removal (McGreal and Gasque 2002). Several receptors for C3 activation products play key role in processing of opsonised molecules and pathogens. Complement receptor 1 (CR1, CD35) associates with C3b and C4b. CR2 (CD21) interacts with C3b breakdown products iC3b and C3d. CR3 (CD11b, CD18) and CR4 (CD11c, CD18) bind iC3b and are involved in removal of the opsonized particles. C3a binds two receptors; C3aR and C5L2, both are present on myeloid cells. It has also been postulated that C5L2

is a decoy receptor for C5a rather than having a functional role (Sacks *et al* 2010; Cain and Monk 2002; Okinada *et al* 2003). Table 1.2 summarises the membrane bound complement receptors.

	RECEPTOR	ASSOCIATED PROTEIN
MEMBRANE	gC1qR	C1q
	cC1qR	C1q
	CR1 (CD35)	C3b, C4b
	CR2 (CD21)	iC3b, C3d
	CR3 (CD11b, CD18)	iC3b
	CR4 (CD11c, CD18)	iC3b
	C3aR	C3adesArg, C3a
	C5aR1 (CD88)	C5adesArg, C5a
	C5L2 (C5aR2)	C3adesArg, C5adesArg, C3a, C5a

Table 1.2 *Summary of membrane bound complement receptors and their interacting complement protein.*

1.3 Complement roles in health and disease

1.3.1 Antibacterial activities of complement

The main role of complement in human health is to protect from bacterial infections, this can be facilitated in three ways. First, opsonisation of bacteria with C3b/ iC3b that are bound by phagocyte receptors. Second, the anaphylatoxins C3a and C5a attract phagocytes to the infection site and cause cell activation. Third, direct lytic killing of gram-negative bacteria (Neisseria; N. meningitidis, N. gonorrhoeae) by MAC. As a consequence, complement deficiencies predispose to infections with multiple bacterial species as described in section 1.3.5.

1.3.2 Immune complex clearance

Immune complexes (ICs) are formed by antibody binding to a specific antigen. Because of antibody divalency, aggregates form and ICs grow. Deposition of large aggregations of ICs in tissue blood vessels causes pathology. The complement system efficiently controls ICs via opsonisation. Decoration of ICs with C3b/ iC3b restricts antibody access to the antigen and thus inhibits further growth and promotes their engulfment. C3b on ICs binds to CR1 (cofactor of FI) expressed on erythrocytes, thus removing free ICs from the plasma. Cleavage of CR1-bound C3b to iC3b by FI releases the IC that can then re-bind through a

different C3b on the ICs to repeat the cycle. This dynamic binding permits the efficient uptake of ICs by fixed tissue macrophages that express CR3 which binds iC3b on the IC, triggering phagocytic elimination (Lindorfer *et al* 2001).

1.3.3 Priming adaptive immunity

Complement is also implicated in humoral immune responses, triggering B cell activation and maturation into antibody-secreting plasma cells. C3d on the opsonised target antigen binds to CR2 (CD21) on the B cell which reduces the threshold for B cell activation and increases the final signal (Fearon 1998; Fearon *et al* 2000). CR2 also plays roles in uptake of opsonised ICs from lymphatics and transport to follicular dendritic cells (FDCs) and B cells in the lymphoid follicles. Complement has also been implicated in T cell regulation, notably with involvement of CD46 and C3 activation products emerging in adaptive immunity (Carroll and Isenman 2012; Kemper *et al* 2005; Heeger and Kemper 2012).

1.3.4 Involvement in lipid metabolism

Rather little is known about complement roles in lipid metabolism. FD (the key enzyme of the AL) is identical to Adipsin, a serine protease discovered independently, implicated in lipid metabolism and produced only in adipose tissue; further, acylation stimulating protein (ASP) a product of adipsin activities responsible for augmentation of glucose transport, was shown to be identical to C3adesArg (Cianflone *et al* 1989; Sniderman and Cianflone 1994). The adipsin-ASP pathway appears to play an important role in lipid handling in adipose tissue. Studies on adipocytes have shown that they are the main source of FD (adipsin), but also produce the key AL proteins C3 and FB. Local AL activation generates ASP (C3desArg) that then interacts with C5L2R to drive triglyceride synthesis in adipocytes (McLaren and Cianflone 2008).

1.3.5 Lessons from Complement deficiencies

Deficiencies of each of the complement proteins, regulators and receptors deficiencies have been reported, some of which can lead to life-threatening conditions; these provide natural experiments that highlight the homeostatic roles of complement (Morgan and Walport, 1991; Grumach and Kirschfink 2014; van den Broek *et al* 2019). Complement deficiencies are caused by mutations restricting synthesis or function of the protein. The most obvious consequences of complement deficiencies are increased susceptibility to infection and IC diseases. In CP deficiencies, IC-mediated pathologies predominate; frequency and severity is highest in individuals deficient in any component of the C1 complex who usually present with SLE-like symptoms in childhood (van Schaarenburg *et al* 2016). C4 deficiency is also strongly associated with SLE-like disease while the least severe deficiency in CP is of C2;

often without any disease manifestation. MBL deficiency is very common in Caucasians (5% of population) and in general harmless with no symptoms (Heitzender *et al* 2012). C3, the most abundant complement protein in plasma, generates most of the important activation products. Patients with C3 deficiency suffer frequent and serious bacterial infections often resulting in death in infancy. Deficiencies of AL components FD and FB are rare with increased risk of bacterial infections. Individuals deficient in any of the TP components (C5 – C9) are prone to Gram-negative bacterial infections, notably with Neisseria. Patients with C5 deficiency cannot make either MAC or C5a which increases significantly their risk of infections compared with other TP deficiencies (Skattum *et al* 2011). In the Japanese population C9 deficiency is very common (1 in 1000 of the population) (Grumach and Kirschfink 2014). Although the majority of the complement component deficiencies can be treated with immunisation and prophylactic use of antibiotics, early diagnosis is crucial.

Dysregulation of complement can also be a result of deficiencies in complement regulators. C1INH is the major regulator of CP ad LP and the kinin system responsible for production of the inflammatory mediator bradykinin. Individuals deficient in C1INH present with soft tissue swelling, a disease known as hereditary angioedema (HAE) (Cicardi and Zamichelli 2010). The recurrent episodes of severe tissue swelling are localized or wide spread affecting mainly the limbs, face, intestinal tract, and airway. Patients with HAE are usually heterozygous deficient for C1INH. Small insults such as stress or minor injury trigger low complement and kinin system activation that in healthy individual is regulated by C1INH, but in HAE C1INH is rapidly consumed, hence control of the systems is lost resulting in a burst of tissue inflammation and swelling (Zeerleder and Levi 2016). C1INH deficiency is one of the most common complement deficiencies with a frequency of 1:10000 in Caucasians (Lumry *et al* 2013).

FI and FH deficiencies are very rare and lead to dysregulation of AL with complete consumption of C3. These deficiencies have the same outcome as C3 deficiency; severe and frequent bacterial infections (Roumenina *et al* 2011).
Complement regulators (CD55 and CD59) attach to membrane via GPI anchor and defects in synthesis of GPI anchor result in loss of the regulator expression which clinically manifests in PNH characterised by haemolytic crises, anaemia and thrombosis. PNH erythrocytes are extremely sensitive to lysis due to the lack of the membrane regulators, unlike most cells, erythrocytes do not express CD46 (Roumenina *et al* 2011; Hall *et al* 2002; Morgan and Harris 1999).

Complement receptors are widely distributed on cells and tissue playing a role in mediating biological responses; however, apart from CD11b deficiency in Leukocyte Adhesion Syndrome (Mazzone *et al* 1995) no other deficiencies are associated with disease.

1.3.6 Complement mutations and polymorphisms

Each individual has a unique, inherited set of common polymorphisms in genes encoding complement proteins and regulators that impact the balance between complement activation and regulation and defines the "Complotype" (Harris et al 2012). The inheritance of more active variants of AL components C3 and FB, or less active variants of AL regulators FH, FI, MCP dictates AL activity and impacts inflammatory state and disease risk. Mutations and polymorphisms can also cause dysregulation of complement by reducing or enhancing expression levels of complement proteins. These changes in function or levels of complement proteins may impact risk of disease. As an example, aHUS is a disease caused by polymorphism and mutations in complement genes, most commonly FH, where changes in the C-terminus impact capacity of FH to bind membranes to protect from complement mediated damage (Le Quintrec *et al* 2010). aHUS can also be caused by mutations in C3 or FB genes which accelerate C3 convertase generation leading to AL dysregulation, and common polymorphisms in FH and CD46 increase risk of aHUS development. Common polymorphisms in FH also play important roles in AMD; notably, the FH Y402H polymorphism which enhances disease risk up to 6-fold (Donoso *et al* 2006; Thakkinstian *et al* 2006). Polymorphisms in C3, FB, FI and factor H related proteins (FHRs) have all been associated with complement dysregulation contributing to inflammation (Heurich *et al* 2011).

1.4 Complement in specific diseases

As described above, complement is essential for elimination of immune complexes and recognition and killing of bacteria through opsonisation and promotion of phagocytosis. However, dysregulated complement activation leads to disease. Complement involvement in disease may be either as the primary trigger of the pathology or as a contributor to the downstream inflammation and tissue damage. The list of inflammatory and autoimmune diseases in which complement is implicated is very long (Ricklin *et al* 2018; Zelek *et al* 2019) (Fig. 1.7). The role of complement in conditions such as RA and SLE has been known for decades (Schur and Austen 1968). Recently it was demonstrated that complement is involved in eye diseases such as AMD and glaucoma, and in multiple CNS diseases including AD, NMO, multiple sclerosis (MS), Parkinson's disease (PD), and Huntington's disease (HD) (Morgan *et al* 2019). Here I will focus on these new findings, but also briefly summarise evidence of complement involvement in renal, vascular and other diseases.

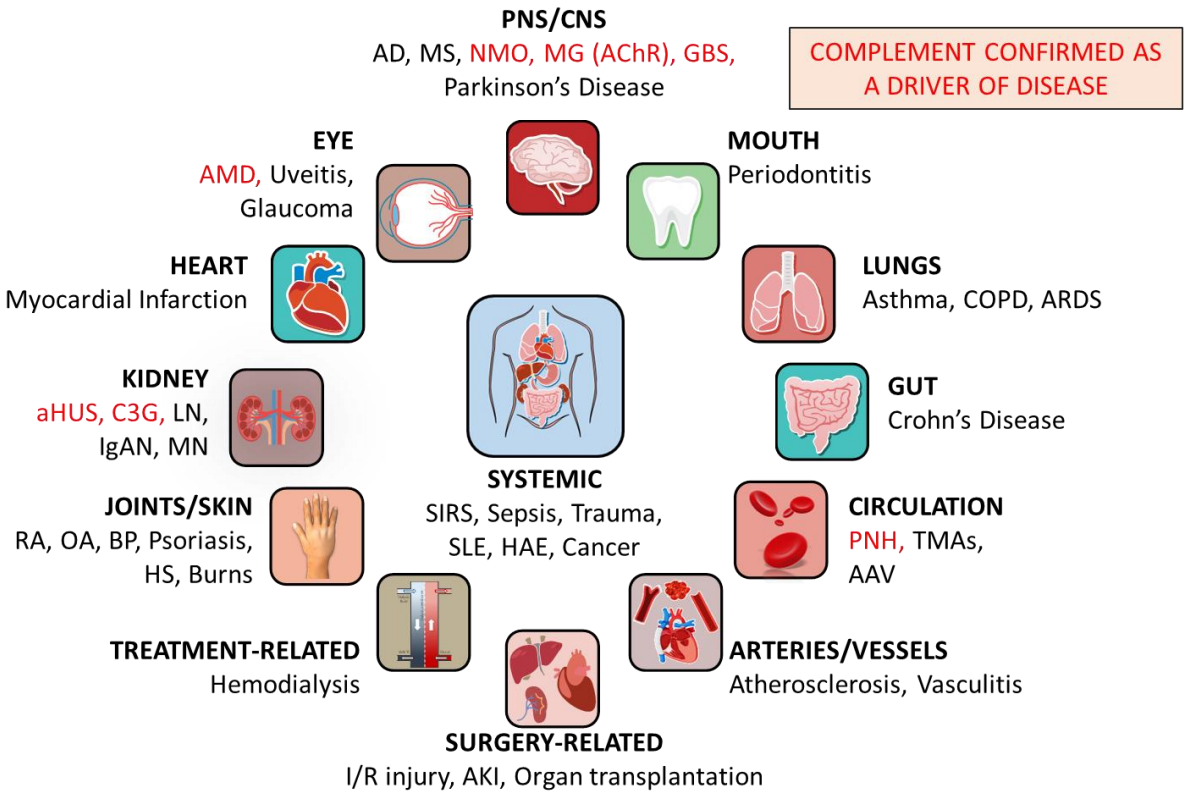

Figure 1.7 *Complement implication in various diseases; In red complement-driven diseases; PNH, aHUS, C3G, AMD, NMO, MG, GBS. In black other diseases in which complement is implicated. Cartoons are from presentermedia.com.* (Zelek *et al* 2019).

1.4.1 Complement in renal diseases

The kidney is highly susceptible to complement mediated damage. In recent years it has been recognised that C3 glomerulopathy (C3G) and aHUS are predominantly driven by complement AL dysregulation (Lambris *et al* 2018; Thurman 2015). aHUS is characterised by thrombocytopenia, microangiopathic haemolytic anaemia and acute kidney injury (Sethi and Farvenza 2014) and caused by mutations and polymorphisms in genes encoding complement proteins, mainly FH, but also FI, MCP, that increase risk of complement dysregulation. Over-activation of the AL at the cell membrane leads to downstream activation, kidney endothelial cell dysfunction, swelling and damage (Kavanagh and Goodship 2010; Rodriguez de Cordoba *et al* 2014). The pathology is driven by the two most pro-inflammatory products of the complement cascade C5a and MAC, although genetic variants in the coagulation system may also be contributory (Kavanagh and Goodship 2011). Early treatment with Eculizumab prevents progression to end-stage renal failure (Wong *et al* 2013). Eculizumab blocks cleavage of C5 and it is unclear whether its effects

are a consequence of blocking MAC and/or C5a; therefore, drug targeting only MAC (downstream of C5) or only C5a would help to define this.

C3G is another ultra-rare renal disease caused by AL dysregulation (Pickering *et al* 2013; Latropoulos *et al* 2018). In contrast to aHUS, complement dysregulation is systemic rather than local (Martinez-Barricarte *et al* 2010). C3 activation products deposit at the renal glomerular basement membrane (GBM). As in aHUS, polymorphisms and mutations in genes encoding complement activating and regulating proteins are strongly associated with the diseases. Autoantibodies termed nephritic factors (NeF) specifically contribute to the disease in many cases (Latropoulos *et al* 2018; Servais *et al* 2012); these associate mainly with neoepitopes on C3 or C5 convertases but binding to FH, FB and C3b has also been reported (Paixao-Cavalcante *et al* 2012; Skerka *et al* 2009). Precisely how NeF cause C3 activation (locally or in the fluid phase) is unclear. Patients with C3G are treated with immunosuppressants or plasma exchange, but these do not prevent end-stage renal failure. To date, Eculizumab administration has shown contradictory results in different small studies, suggesting a need for larger studies and perhaps a personalised approach to treatment (Zuber *et al* 2012).

In IgA Nephropathy (IgAN) ICs containing abnormally glycosylated IgA antibody deposit in the kidney and activate complement (Daha and van Kooten *et al* 2016). MBL levels are increased in glomeruli and C4d deposition is a marker of the disease (Espinosa *et al* 2014). A MASP2 inhibitory mAb (OMS721, Omeros, in clinical phase 3) shows promising results in IgAN. Individuals deficient in FH related proteins 1 and 3 (FHR1, 3) were protected from the disease (Gharavi *et al* 2011), implicating the AL in the disease. FHRs interfere with FH-mediated AL regulation (Goicoechea *et al* 2013; Rodriguez de Cordoba *et al* 2014). Similarly, in SLE, ICs deposit in the kidney and activate complement, leading to renal cell damage and thrombotic microangiopathy (TMA) (Yu *et al* 2017). The mechanism by which complement causes pathology in the disease is unclear, but the over activation of complement leads to consumption of C3 and C4 which drives inflammation and tissue damage. Immunoglobulin, C1q and C3 deposits are found in GBM and mesangium with proliferative glomerulonephritis and/or membranous nephropathy-type appearance (Bomback *et al* 2016).

Complement plays a crucial role in renal transplant rejection. Ischemia/reperfusion (I/R) injury and delayed graft function in the donor kidney places the graft at high risk of acute kidney injury (AKI). Complement is implicated in ischaemic graft rejection with C3 fragment deposition in the tubular basement membrane and increasing evidence of AL and TP

involvement in the pathology (Thurman *et al* 2005, McCullough *et al* 2013). Risk of organ rejection post-transplant is also dependent on donor specific antibodies (DSA). At the extreme, HLA/ABO-incompatible transplants are at very high risk of antibody-mediated allograft rejection (AMR) with hyperactivation of complement and rapid tissue necrosis (Stegall *et al* 2012). The perfect donor–recipient match eliminates the risk; however anti-complement drugs may permit non-perfect combinations and improve the supply of donor organs by allowing the organ to accommodate and survive despite the mismatch (Fiane *et al* 1999).

1.4.2 Complement in eye diseases

AMD is the most common cause of blindness in the developed world, affecting ~1.5% of the population over 40 years old in the US, and 15% of white women (of European-descent) aged over 80 (Friedman *et al* 2004); It is also the best know eye disease in which complement is implicated. Complement is present and regulated in the healthy eye (Bora *et al* 1993; Sohn *et al* 2000). In AMD, aggregates of proteins and lipids (drusen) decorated with complement proteins (Mullins *et al* 2000) accumulate within the Bruch's membrane causing separation of retinal pigment epithelium (RPE) from the choroid (Mohlin *et al* 2017), thus interfering with retinal function. A common polymorphism in FH, Y402H, is strongly associated with increased risk of AMD (Nan *et al* 2011). In dry AMD (geographic atrophy (GA)), the RPE is severely damaged and scarred. In wet AMD, choroidal blood vessels proliferate and leak causing retinal oedema, dysfunction and scarring. There is a long list of anti-complement agents in development for AMD treatment (Harris 2018), yet none is yet approved by FDA. Dry AMD is managed with the anti-VEGF (vascular endothelial growth factor) mAb ranibizumab but a significant proportion of patients do not respond (Ferrara *et al* 2006).

Uveitis, inflammation of the uveal tract of the eye can cause permanent blindness. Complement-driven inflammation is implemented in the disease. Inhibition of C5 with monoclonal antibody (BB5.1) in a mouse model reduced inflammation (Copland *et al* 2010). Anti-properdin (CLG561) and anti-C5 (LFG36, Novartis) mAbs are in clinical trials for treatment of this and other eye diseases (Volz and Pauly *et al* 2015; Kassa *et al* 2019).

1.4.3 Complement in vascular diseases

Complement mediated damage may not be tissue specific but instead target the vasculature or blood components throughout the body.

ANCA (anti-neutrophil cytoplasmic antibody)-associated vasculitis (AAV) is driven by AL dysregulation and C5a generation. C5a-induced neutrophil activation cause degranulation

and increased endothelial adhesiveness; in turn, granule-derived myeloperoxidase (MPO) and MPO autoantibodies activate complement generating more C5a that binds C5aR1 on neutrophils, completing the destructive inflammation cycle (Noone *et al* 2018; Jennette *et al* 2013). Agents targeting C5a-mediated damage in AAV are in development with Avacopan (small molecule C5aR1 antagonist by Chemocentryx) showing promising results and progressing to phase 3 clinical trials (Chen *et al* 2017; Jayne *et al* 2017).

PNH presents with haemolytic anaemia, thrombosis, smooth muscle dystonias, and, in late stages of the disease, bone marrow failure. The disease is caused by rare somatic mutations in the gene encoding PIGA (phosphatidylinositol N-acetylglucosaminyltransferase subunit A) in hematopoietic stem cells; this prevents biosynthesis of GPI anchors responsible for protein-membrane interaction (Takeda *et al* 1993; Hill *et al* 2017). The complement regulators CD55 and CD59 are GPI anchored proteins; loss of these regulators on blood cells in PNH enhances susceptibility to complement-mediated membrane damage and intravascular haemolysis (Hill *et al* 2017). Eculizumab (the first complement inhibitory drug approved by FDA) prevents this damage by blocking activation of C5 and hence MAC formation; however, Eculizumab does not stop opsonisation and accumulation on erythrocytes of C3 opsonic fragments (C3b, iC3b, C3dg) may drive extravascular haemolysis of erythrocytes (Ristano *et al* 2009; Liz *et al* 2015). Breakthrough haemolysis can occur as a result of insufficient inhibition of C5; small amounts of free C5 lead to MAC formation on the primed erythrocytes and potentially catastrophic lysis (Harder *et al* 2017). This highlights the importance of considering inhibitors of MAC downstream of C5 as will be discussed later.

Autoimmune haemolytic anaemia (AIHA) is mediated by CP activation by anti-erythrocyte autoantibodies leading to haemolysis. There are two major types of AIHA, termed warm and cold depending on the temperature at which the auto-antibodies bind erythrocytes. AIHA is currently tackled by immunosuppressants that reduce autoantibody production. Antibody against CD20 (rituximab) is effective in 70 – 80% of cases (Barcellini 2015). Anti-complement approaches are under consideration.

1.4.4 Complement in neurological disorders

GWAS, epidemiological studies, pathological analyses and biomarker measurements in plasma and cerebrospinal fluid (CSF) show that complement is implicated in many CNS disorders (Morgan *et al* 2019).

Complement-mediated damage to the neuromuscular junction (NMJ) is a key mechanism of pathology in myasthenia gravis (MG). In MG, autoantibodies destroy the acetylcholine receptors (AChR) at the NMJ, preventing the muscle from contracting (Zelek *et al* 2019; Chamberlain-Banou *et al* 2006). C3 opsonic fragments and MAC are detected at motor endplates both in patients and in animals with experimental autoimmune MG (EAMG) (Kausner *et al* 2019). The most severe form of the human disease includes paralysis of the face and throat muscles and is termed generalised MG (gMG). Complement involvement in MG has been known for nearly half century (Sahashi *et al* 1978), and recently this was brought back into the spotlight by FDA approval for the use of Eculizumab for therapy of gMG (Morgan *et al* 2019). Following the success of Eculizumab, C5 remains a favourite target in the complement drug development field. Zilucoplan (an anti-C5 peptide developed by RaPharma) is in Phase 2 clinical trials for gMG.

Dementia encompasses a wide range of disorders including AD, PD, dementia with lewy bodies and vascular dementia. AD affects ~50 million people worldwide and it is the commonest cause of dementia (60 – 80%). AD is a complex and progressive neurodegenerative disease; symptoms develop gradually from mild forgetfulness to severe mental impairment over the course of years. There is emerging evidence that complement is implicated in AD. GWAS studies associated genes encoding clusterin and CR1 with risk of AD (Lambert *et al* 2009; 2013; Karch and Goate 2013). Levels of complement proteins and activation products in plasma and CSF effectively differentiate AD from controls and predict risk of progression (Hakoyban *et al* 2016; Morgan *et al* 2017; Hu *et a.* 2016). Post-mortem analyses of AD brain provide solid evidence of CP activation with C1q, C3 and C4 deposits detected around and in amyloid plaques (Veerhuis *et al* 1995; Rogers *et al* 1992; Ishii and Hega 1984). TP proteins co-localised with amyloid beta (Aβ) in neurofibrillary tangles and neuropil threads (Rogers *et al* 1992). In vitro studies show that Aβ plaques activate the CP (Rogers *et al* 1992; Bradt *et al* 1998). In mouse models, administration of C5aR1 antagonist (PMX205) significantly reduced Aβ and tau deposits, downregulated glia and improves cognition (Fonseca *et al* 2009), while a C1q-blocking mAb (ANX-M1/ANX005, Annexon Biosciences) injected into the brain reduced synapse loss and complement mediated damage (Hong *et al* 2016). Although the evidence suggests that complement drives pathology in AD, inhibition of complement may have adverse consequences by reducing clearance of plaques (Wyss-Coray *et al* 2002). The AD animal models can cause confusion because they mimic rare inherited early-onset AD rather than common late-onset disease and usually display only one type of pathology. Another factor that needs to be considered when studying roles of complement in brain diseases is age, because it is clear from human and mouse studies that brain expression of complement proteins changes

significantly with age (Zhou *et al* 2008; Stephan *et al* 2013). Investigation of complement in brain remains challenging.

PD is a neurological disorder presenting with tremor, stiff and inflexible muscles with cognitive decline as a later feature. The pathological hallmark is the presence of aggregates of lewy bodies (LBs) that contain more than 70 different types of molecules, among which α-synuclein is predominant (Wakabayashi *et al* 2007). The pathology is associated with α-synuclein splice variants that can activate complement (Klegeris and McGeer 2007). Immunocytochemical studies showed iC3b and C9 deposited in LBs (Loeffler *et al* 2006). The C3/FH ratio in CSF differentiated disease group from the controls while C3/Aβ42 and FH/Aβ42 ratios showed positive correlation with PD severity (Wang *et al* 2011). Modelling PD in rodents is challenging, none of the available models mimic disease precisely (Antony *et al* 2011). A recent study using a toxin-induced model implicated CR3 in pathology; CR3 knockout mice were protected from neuronal loss and motor dysfunction (Hou *et al* 2018).

Huntington's disease (HD) is a dominantly inherited disorder that causes neurodegeneration with onset usually in adult life. HD symptoms include movement dysfunction, cognitive and psychiatric disability. The cause of the disorder is expansion of CAG repeat in the first exon of the Huntingtin (HHT) gene that translates into a polyglutamine tract at the N-terminus of the protein. This causes defects in protein folding; aggregates of HHT protein accumulate in striatum and cortex, causing neuronal death (Mangiarini *et al* 1996; Graveland *et al* 1985). Complement proteins C1q, C3 and C4, iC3b and TCC were co-localised with neurons, astrocytes and myelin sheaths in the HD caudate and striatum (Singhrao *et al* 1999; Hodges *et al* 2006). Expression of multiple complement proteins was upregulated in HD striatum and levels of clusterin, C7 and C9 were increased in HD plasma and correlated with disease severity (Dalrymple *et al* 2007). As for PD, contradictory results are found depending on the animal model used; however, intrathecal delivery of a C5aR antagonist (PMX53 or PMX205) in a rat HD model showed promising results with reduced weight loss, restored motor abilities and reduced lesion number and volume (Woodruff *et al* 2006).

Multiple sclerosis (MS) is a chronic, autoimmune, degenerative disease of the CNS. The symptoms include problems with movement, balance and vision. Current therapies seek to suppress the production of autoantibodies, although the nature and precise targets of the autoantibodies in MS are unclear. Complement has been implicated in MS as demonstrated by biomarkers studies in plasma and CSF (Hakoyban *et al* 2017; Zelek *et al* 2016; Tatomir *et al* 2017; Aeinehband *et al* 2015). In MS plasma, increased C4a levels correlate with the

disease activity (Ingram *et al* 2010). Complement deposits are present in the CNS in MS and NMO; immunostaining of disrupted myelin in MS lesions showed deposits of C3, C3d, FB, C1q, C3b, iC3b, C4d and TCC (Barnett *et al* 2009; Ingram *et al* 2014). Deposition of C3 on microglial clusters in chronic MS has been reported (Michailidou *et al* 2017). My recent study on demyelinating disease showed that CD59 is synthesised locally in choroid plexus (Zelek *et al* 2019). Animal models confirm complement pathology in MS and NMO (Rosenling *et al* 2012; Wren *et al* 1989; Gharibi *et al* 2019; Yao *et al* 2016); however, no studies on anti-complement drugs have yet been conducted. Neuromyelitis Optica Spectrum Disorder (NMO) is an autoimmune demyelinating disease with overlapping symptoms with MS, but the demyelination affects predominantly the optic nerves and spinal cord and the autoantibodies in most cases are directed against the water channel aquaporin 4 (AQP4-Ab) and are highly specific for NMO (Papadopoulos *et al* 2014; Hinson *et al* 2007; Lennon *et al* 2004; 2005; Mader *et al* 2011). Evidence for complement involvement comes from measurement of complement plasma and CSF biomarkers; these not only aid diagnosis but also differentiate MS and NMO with over 80% accuracy (Ingram *et al* 2009; 2010; Compston *et al* 1986). Complement therapy has been successful for NMO; treatment with Eculizumab (in phase 3 clinical trials) significantly reduced relapses compared to placebo group (3% versus 43%) (Pittock *et al* 2019; Kuroda and Fujihara 2019). Eculizumab has been recently approved for NMO treatement (https://news.alexion.com/press-release/product-news/alexion-receives-fda-approval-soliris-eculizumab-treatment-adults-neuromy). Early studies showed safety of C1INH in add-on therapy in NMO patients presenting with acute transverse myelitis and optic neuritis (Levy and Mealy 2014).

Guillain-Barré syndrome (GBS) is an autoimmune disease in which autoantibodies to gangliosides such as GM1 disrupt nodal voltage-gated sodium (Nav) channel clusters in peripheral motor nerve fibres leading to acute limb weakness (Suzuki *et al* 2007). GBS symptoms progress rapidly, causing disability within a few days, ~10% of patients die of pneumonia, cardiac or thromboembolic complications. GBS spontaneously stabilises within 2 – 3 weeks with a complete recovery in a variable proportion of patients within 6 months (GBS Group 1985). Histology on human post-mortem GBS brain showed C3d and TCC deposition on Schwann cells (Hafer-Macko *et al* 1996; Griffin *et al* 1996). CSF levels of C3a and of C5a were significantly elevated in GBS patients compared to controls (Hartung *et al* 1987); MBL2 genotype and serum MBL concentrations were associated with the development and severity of GBS (van Doorn *et al* 2006). Recent studies showed that administration of Eculizumab alongside the standard IVIg treatment in GBS patients is safe; however, effectiveness of the treatment is yet to be confirmed (Yamaguchi *et al* 2018; Misawa *et al* 2018; Davidson *et al* 2017). In an animal model of GBS, treatment with

monoclonal anti-C1q antibody reduced axonal injury and improved respiratory function (McGonigal *et al* 2016).

1.6 Evolution of complement drugs.

The role of complement inhibition as a therapy for disease has been explored for many years; cobra venom factor (CVF) was the first anti-complement agent used over 50 years ago in man and experimental animals, but was not pursued mainly because of the high immunogenicity (Linton and Morgan 1999; Morgan and Harris 2015). Other limitations were restricted accessibility and generation of C5a in high concentrations during the initial treatment that led to accumulation of neutrophils in lungs and other organs (Till *et al* 1982). Attempts were made to overcome the immunogenicity issue by generation of recombinant humanised CVF (rhCVF), successfully used in a few pre-clinical models, including AMD and ischemia reperfusion injury (Vogel *et al* 2014). rhCVF showed low immunogenicity and could be produced in large quantities; however, concerns over the complete depletion of complement and toxicity remained.

Plasma-derived C1INH was first used in therapy of HAE in the mid-1980s and continues to be used as emergency (and more recently prophylactic) therapy for this single condition (Carugati *et al* 2001). Its use in other conditions has been restricted to a handful of small studies, none of which have progressed to the clinic.

The first recombinant complement inhibitor was a soluble recombinant form of CR1 (sCR1; TP10), first described in 1990 (Weisman *et al* 1990). Although this molecule provided a wealth of data from animal studies, its translation to humans was disappointing with failure in early trials coupled with the cost and complexity of the molecule contributing to its slow progress.

Many more years passed by until Eculizumab became the first complement inhibitory drug approved by FDA, initially for treatment of PNH in 2007 (Mastellos *et al* 2018; Mandala *el al* 2013; Brodsky *et al* 2008) and two years later for aHUS (Wong and Kavanagh 2013; Wong 2018). Eculizumab was, for many years, restricted to these two ultra-rare complement driven diseases, but in many more common diseases complement dysregulation exacerbates/perpetuates pathology. The recent approval of Eculizumab for gMG and NMO treatment shows the potential for anti-complement therapy to benefit in more common diseases. Ravulizumab is the new improved version of Eculizumab with half-life prolongation technology for treatment of PNH and aHUS (McKeage. 2019). Despite the long history of anti-complement therapeutics and many drugs being in development, C1INH (marketed as Berinert, Cinryze, Ruconest and used for HAE) and the anti-C5 mAb (Eculizumab/ Ravulizumab) remain the only two agents approved by FDA. The lack of availability of other drugs and niche markets for those that are available dictates the high cost of the anti-complement therapies (Fig. 1.8).

The toolbox of current therapeutics in development contains various agents; biologics, small molecules including peptides, and RNA constructs. Antagonist of C5a receptor (Avacopan) is now reaching the late stages of clinical development, in phase 3 studies for ANCA vasculitis. Animals with spinal cord injury (SCI) treated with Avacopan showed rapid, short-term improvement in functional recovery (Brennan *et al* 2015). Of course, the effect of a particular drug will be dependent on the impact of the complement cascade in that disease and the pathways targeted. Drugs that target the activation pathways and/or TP will reduce generation of active products and thus have profound anti-inflammatory effects; the negative consequences – increased risk of infection or immune complex disease – will also depend on the target. Choice of route of administration is also increasing, currently including IV, topical, SC and recently, oral application. Improvements of the existing gold standard drug Eculizumab through the introduction of recycling technology yielded Ravulizumab, effective at half the dose of the parent drug and recently approved for PNH treatment (Connell 2019). Fig. 1.9 summarises the current anti-complement drug landscape.

Figure 1.8 *Timeline of complement drug development illustrating the accelerating pace of anti-complement drug entry into phase 2. Drugs which have been approved by the FDA are indicated above the timeline. Approved drugs that have entered phase 2 for a new indication are shown below the line in green. Other drugs are coloured according to their modality. The dates are indicative of the year that recruitment started (as defined by the clinical trial registry). Trials which have terminated are not indicated if the drug remains in development for other indications. The timeline indicates first entry of that drug into a phase 2 clinical study, unless otherwise indicated in above Fig. 1.8 in Notes.*

Figure 1.9 *Anti-complement drugs currently in clinical development. The rings indicate the different phases of clinical development, with 'approved' in the centre. Only drugs currently in clinical development are shown and the most advanced stage of development for any indication is shown; trials posted but not yet recruiting are included. Colouring and shape indicate modality and route of administration; this is only indicated for phase 1 and beyond. (Zelek et al 2019).*

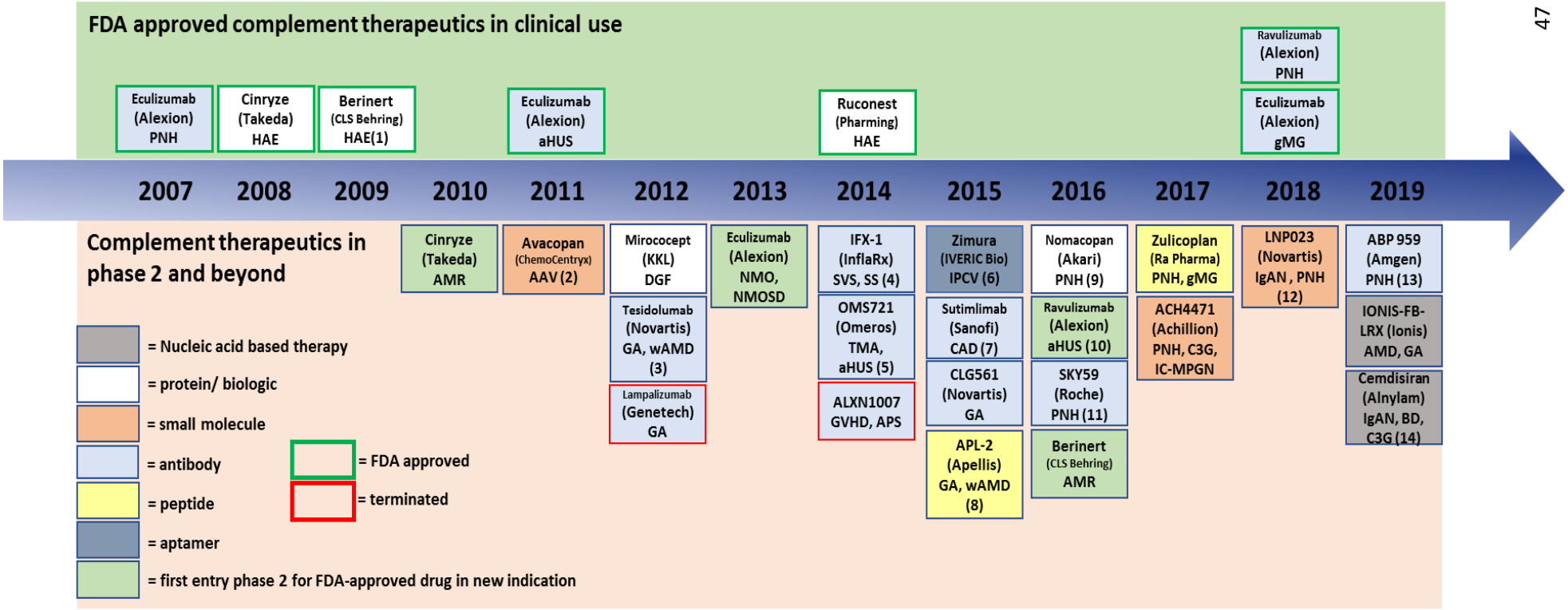

Notes, including year of phase 2 entry for additional indications:

1. Berinert (C1inh) was approved for therapy of acute HAE in Europe and other countries in 1980s.
2. Avacopan (CCX168); additional phase 2 entry: 2015, IgAN; 2017, C3G; 2018, HS.
3. Tesidolumab (LFG316); additional phase 2 entry : 2012, Uveitis; 2015, PNH; 2015, GA (combination with CLG561).
4. IFX-1; additional phase 2 entry : 2016, SIRS, CS, HS; 2018, GPA, MPA.
5. OMS721; additional phase 2 entry: 2016, IgAN, LN. MN, C3G.
6. Zimura (ARC1905); indicated above is phase 2 entry combination with anti-VEGF; additional phase 2 entry : 2016, GA; 2017, wAMD (combination with Lucentis); 2018, STGD1.
7. Sutimlimab (TNT009, BIVV009), phase 3 entry indicated
8. APL-2; additional phase 2 entry : 2017, CAD, wAIHA; 2018, PNH (phase 1b 2015); 2018, IgAN, LN, MN, C3G, DDD.
9. Nomacopan (Coversin, rVA576); additional phase 2 entry : 2017, aHUS; 2018, BP; 2018, Ph1/2 AKC.
10. Ravulizumab (ALXV1210, Ultomoris); indicated is phase 3 entry for aHUS; additional phase 2 entry: 2019, gMG.
11. SKY59 (RO7112689) entered phase 1/2 for PNH in 2016
12. LNP023; additional phase 2 entry : 2019, C3G.
13. ABP 959 (eculizumab biosimilar), indicated is phase 3 entry.
14. Cemdisiran entered phase 1/2 for PNH in 2015, no longer in development for that disease.

Figure 1.8

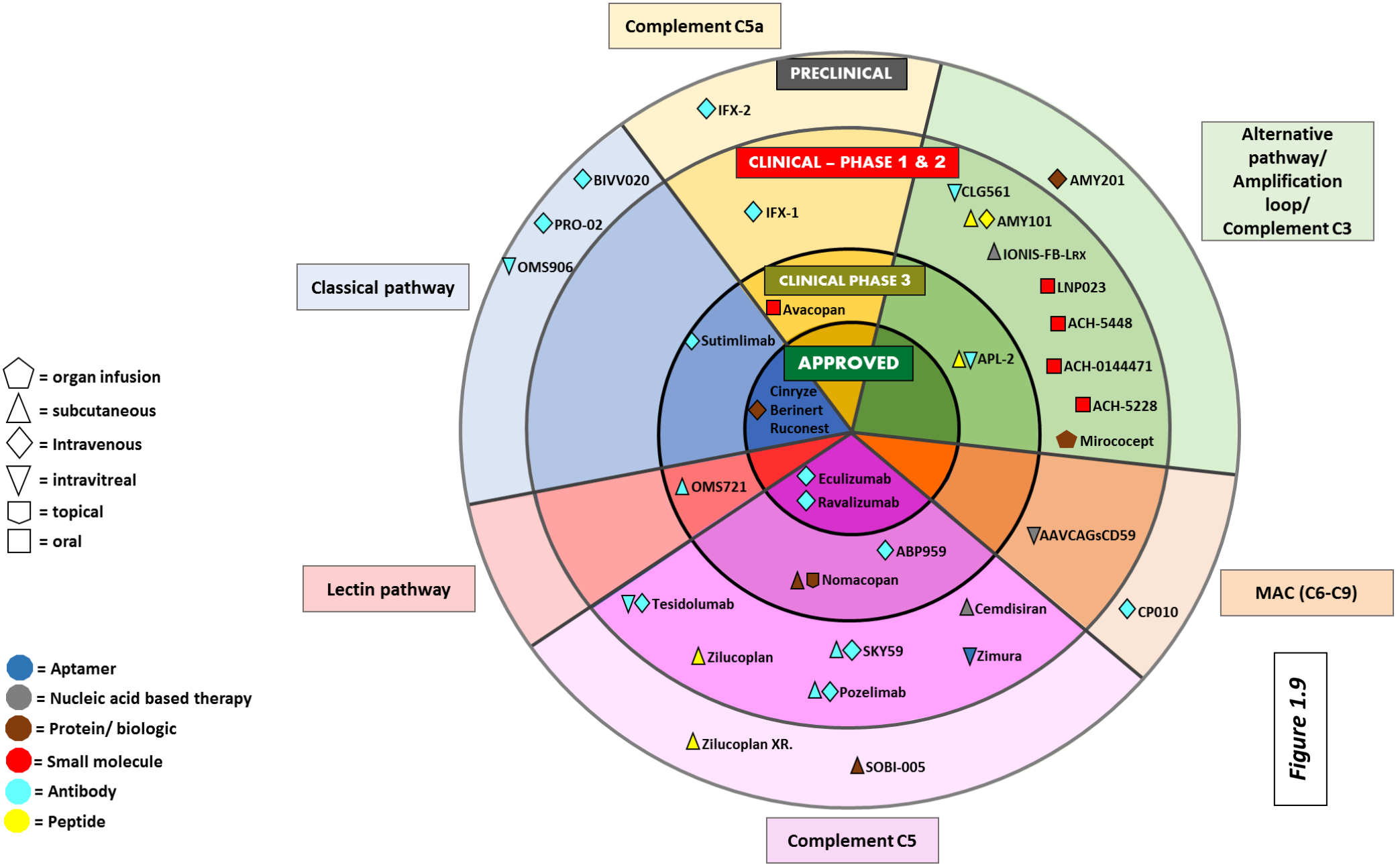
Complement C5a
PRECLINICAL
IFX-2
CLINICAL – PHASE 1 & 2
IFX-1
CLINICAL PHASE 3
Avacopan
APPROVED
Cinryze
Berinert
Ruconest
Alternative pathway/ Amplification loop/ Complement C3
AMY201
CLG561
AMY101
IONIS-FB-LRx
LNP023
ACH-5448
ACH-0144471
ACH-5228
Mirococept
APL-2
Classical pathway
BIVV020
PRO-02
OMS906
Sutimlimab
Lectin pathway
OMS721
Eculizumab
Ravalizumab
ABP959
Nomacopan
Tesidolumab
Zilucoplan
SKY59
Pozelimab
Zilucoplan XR.
SOBI-005
Cemdisiran
Zimura
MAC (C6-C9)
AAVCAGsCD59
CP010
Complement C5
= organ infusion
= subcutaneous
= Intravenous
= intravitreal
= topical
= oral
= Aptamer
= Nucleic acid based therapy
= Protein/ biologic
= Small molecule
= Antibody
= Peptide

Figure 1.9

1.6 Aims of the thesis; MAC inhibition beyond C5: targeting TP proteins and complexes

- To deliver a panel of novel monoclonal antibodies (mAbs) that inhibit TP proteins and generation of MAC intermediates as potential therapeutics that offer a new approach to inhibiting complement without preventing the potential benefits of the C5a/C5aR axis.

- To test the candidate mAbs ex vivo to confirm their TP protein binding and blocking activities and in vivo to explore pharmacokinetics, half-life and therapeutic impact, the latter in an acute animal model of a complement-driven human disease (experimental autoimmune myasthenia gravis (EAMG)).

Research Impact:

Novel approaches to terminal pathway inhibition will identify new drug candidates(s) and facilitate the evolution of anti-complement therapies from ultra-rare to common diseases with resultant impact on human health. The mAb have the potential to be safer, more effective, easier to administer, and cheaper than current anti–complement drugs.

CHAPTER 2; MATERIALS AND METHODS

2.1 Materials

All chemicals, except where stated, were obtained from either Fisher Scientific UK (Loughborough, Leicestershire, UK) or Sigma Aldrich (Gillingham, Dorset, UK) and were of analytical grade

2.2 Commercial and in house labelled antibodies

The labelled mAb were used for ELISA, WB or Flow Cytometry. The commercial labelled mAb are summarised in below Table 2.1.

Antibody	**Conjugate**	**Use**	**Catalogue number**
Donkey anti-Mouse IgG (H+L) (minimal cross reaction to Bovine, Chicken, Goat, Guinea Pig, Syrian Hamster, Horse, Human, Rabbit, Rat and Sheep).	Horseradish Peroxidase (HRP)	ELISA/ Western blot	715-035-151
Rabbit anti-Goat IgG (H+L) (minimal cross reaction to Human)	HRP	ELISA/ Western blot	305-035-045
Goat anti- Rabbit IgG (H+L) (minimal cross reaction to Bovine, Chicken, Goat, Guinea Pig, Syrian Hamster, Horse, Human, Mouse, Rat and Sheep).	HRP	ELISA/ Western blot	711-035-152
$F(ab')_2$ Fragment Donkey Anti-Mouse IgG (H+L) (minimal cross reaction to Bovine, Chicken, Goat, Guinea Pig, Syrian Hamster, Horse, Human, Rabbit, Rat and Sheep).	Fluorescein (FITC)	Flow cytometry (FACS)	715-096-150

Table 2.1 *Secondary antibodies used (Jackson ImmunoResearch Laboratories, Ely, UK).*

2.2.1 In house HRP antibody labelling using EZ-Link Plus Activated Peroxidase kit

Lyophilized EZ-Link Plus Activated Peroxidase (1mg; Thermofisher, Pierce, #31489) was reconstituted in 1ml of the antibody at 1mg/ml diluted in PBS incubated for two hours at room temperature (RT), 10 µl of cyanoborohydride added, incubated for 20 minutes at RT,

20µl of quench buffer added, incubated for 20 minutes at RT. The labelled antibody was stored in 50µl aliquots at -20°C.

2.2.2 In house Biotin antibody labelling using EZ-Link Sulfo-NHS-LC-Biotin kit

Antibody (2mg in 1ml) was dialysed overnight into PBS (as described in section 2.3). EZ-Link Sulfo-NHS-LC-Biotin, No-Weigh™ Format (Thermofisher, Pierce, # 21327) 1mg (1vial) was reconstituted in 180µl of ddH_2O; 30µl of the prepared Biotin reagent was added immediately to the dialysed antibody and incubated for 2 hours at RT with mixing in the dark. Excess biotin was removed by extensive dialysis against PBS at 4°C in dark, and labelled antibody stored in 50ul aliquots at 4°C in the dark.

2.3 Dialysis of proteins to exchange buffers

Dialysis tubing (Medicell International Ltd., London, UK) with a 12-14 kDa (used for proteins bigger than 30kDa) or 3 kDa (for proteins below 30 kDa) molecular weight cut off was soaked in dialysis buffer for ~5 minutes. The tubing was then tied securely at one end and about half-filled with the protein-containing solution to be dialysed. Air was expelled from the tubing prior to sealing by tying the other end. The tubing was placed in a large beaker filled with dialysis buffer (1000-fold the sample volume) and stirred overnight at 4°C.

2.4 Concentrating proteins

Proteins were concentrated using Vivaspin sample concentrators (GE Healthcare, Amersham Place, Little Chalfont, UK) of appropriate cut-off size (either 30 kDa or 100 kDa). The concentrators were washed with 200µl of deionised water prior to use. The protein-containing solution was placed in the tubes and concentrated via centrifugation (2000rpm, 4°C). This forced the fluid through the filter membrane while proteins of molecular mass greater than the cut-off were retained and concentrated. After use the concentrators were washed in deionised water and stored at 4°C. Concentrators were reused for the same proteins only.

2.5 Determination of protein concentration by absorbance at 280nm (A280) on NanoDrop

The approximate concentration of purified protein samples was determined by measuring the absorbance of the solution at 280 nm (A280) using NanoDrop (Labtech International Model; ND1000). A blank reading was taken as a reference using 2µl of the buffer that the protein was stored in; 2µl of the stock was then used to take the absorbance measurement.

The protein concentration of the sample was calculated according to Beer-Lambert's Law: Protein Concentration (mg/ml) = A280/ protein extinction coefficient.

2.6 BCA Protein Assay

For accurate measurement of protein concentration, the BCA assay was used. The BCA working reagent was made up by mixing 50 parts Reagent MA, 48 parts Reagent MB together with 2 parts Reagent MC and used on the day. A dilution series of BSA standard (1 – 2000µg/ml) and samples was prepared in PBS. Standard, blank (diluent only) or test sample (25µl) was added into wells of a 96-well maxisorp plate and 25µl of BCA working reagent added into each well. The plate was sealed and incubated for 30 minutes at 37°C. The absorbance of the wells was measured at 570nm on a Tecan plate reader (Labtech International, Model; Infinite F50). A standard curve was plotted and the concentrations of the test samples calculated using GraphPad Prism 5.

2.7 Sodium Dodecyl Sulphate-Polyacrylamide Gel Electrophoresis (SDS-PAGE)

SDS–polyacrylamide gel electrophoresis (SDS-PAGE) was used to characterise proteins of interest. The Invitrogen Mini Tank Gel running apparatus was used. The buffers, acrylamide stacking (upper) and resolving (lower) gel were prepared according to the formulas in Table 2.2. Proteins (~2µg) were prepared for loading by diluting 1:5 in either non-reducing (NR) or reducing (R) loading buffer and incubation at 100°C for 5 minutes. Complex protein mixtures such as serum were run at 1: 100 dilution. Molecular weight markers (PageRuler Plus; 26619, Thermofisher) were loaded onto each gel for accurate determination of protein size. The gels were run at 100V for 45 minutes, until the dye-front had reached the bottom of the gel. Electrophoresed proteins were then either visualised by staining the gel with Quick Coomassie Blue stain (Generon, # GEN-QC-STAIN-1L) or subjected to Western Blot (WB).

2.8 Coomassie blue staining and drying of electrophoresed gels

The detection limit of this technique was ~2µg of protein in a band on an SDS gel. Following gel electrophoresis, the gels were immediately immersed in Quick Coomassie Blue stain for 10 minutes on a rocker-table at RT, stain was removed, gels rinsed with deionised water for ~10 minutes until the protein bands were clearly visible and the background reduced. Following the transfer of proteins from gels to nitrocellulose (section 2.11), these gels were also stained and de-stained, to confirm the transfer had been successful.

Buffer	Composition
NR loading buffer	0.1 M Tris, 10% w/v glycerol, 2% w/v SDS, bromophenol blue, pH 6.8.
R loading buffer	NR loading buffer + 0.625% w/v 3-mercaptoethanol.
Stacking buffer (SB)	0.5 M Tris, 0.4% SDS, pH 6.8
5% Stacking gel	0.6ml SB, 0.3ml 40% Acrylamide/Bis, 1.6ml ddH2O, 0.025ml 10% Ammonium persulphate, 0.0025ml TEMED
Resolving buffer (RB)	1.5 M Tris, 0.4% SDS, pH 8.8
7.5% Resolving gel	1.875ml RB, 1.4ml 40% Acrylamide/Bis, 4.1ml ddH2O, 0.075ml 10% Ammonium persulphate, 0.0075ml TEMED
Running buffer	50 mM MES, 50 mM Tris Base, 0.1% w/v SDS, 1 mM EDTA, pH 7.3.
Gel drying buffer	4% w/v glycerol, 20% v/v methanol
Sample dilution buffer (PBS)	8.2mM Na_2HP0_4, 1.5mM KH_2P0_4, 137mM NaCl, pH 7.4.

Table 2.2 *SDS-PAGE buffers*

For a permanent record, the stained gels were equilibrated for 1 minute in gel drying buffer and sandwiched between two sheets of acetate gel drying film (Promega, #PR-V7131) pre-soaked in gel drying buffer and stretched within a gel drying frame overnight at RT.

2.9 Western Blotting (WB)

Western blot analysis was used to identify specific proteins from complex mixtures and to characterise monoclonal antibodies (mAbs). WB buffers were prepared as described in Table 2.3. Following SDS-PAGE, the gel was immediately equilibrated in transfer buffer for 5 minutes, placed on a sheet of nitrocellulose and further sandwiched between two sheets of filter paper, all of which had been pre-soaked in transfer buffer. The blotting apparatus was assembled according to the manufacturer's instructions with the gel to the anode side and the nitrocellulose to the cathode. The proteins were then transferred onto the nitrocellulose at 100V for 45 minutes at room temperature, in a tank filled with cooled transfer buffer. After this, the nitrocellulose blots were blocked for 1 hour in blocking buffer at RT with constant mixing. The blots were rinsed with wash buffer and incubated with antibody raised against the antigen of interest (primary antibody), typically diluted to 1 µg/ml (monoclonal) or 5 µg/ml (polyclonal) in blocking buffer on a roller and incubated for 1 hour at room temperature or overnight at 4°C with constant mixing. The blots were washed in wash buffer five times for five minutes each at RT with constant mixing. HRP-conjugated

secondary antibody diluted 1/1000 -1/10,000 (depending on the agent) in blocking buffer was incubated with the blots for 1 hour at room temperature with constant mixing. The blots were washed five times as described above. Bands were detected with ECL and visualised by autoradiography.

Buffer	**Composition**
Transfer buffer	25mM Tris, 191mM Glycine, 20% v/v Methanol in deionised water.
Blocking buffer	5% Bovine Serum Albumin (BSA), 0.05% Tween 20, Phosphate Buffered Saline (PBS; 8.2mM Na_2HP0_4, 1.5mM KH_2P0_4, 137mM NaCl, pH 7.4)
Wash buffer	PBS, 0.05% Tween 20

Table 2.3 *WB buffers.*

2.10 Dot Blotting (DB)

DB was used to identify terminal pathway proteins in gel filtration (GF) fractions containing MAC complexes. The same buffers were used as for WB. Fractions (5µl) were spotted onto nitrocellulose membrane, allowed to dry 15 minutes at 37°C, blocked with blocking buffer for 30 minutes, washed 3 times for 5 minutes with wash buffer, incubated with primary antibody diluted in blocking buffer (Goat anti-C5 or anti-C7, CompTech) for 30 minutes at 37°C, washed 3 times, incubated with secondary antibody rabbit anti-goat-HRP 1 in 5000 dilution in blocking buffer for another 30 minutes at 37°C. After a further 5 washes, blots were developed with ECL and visualised by autoradiography.

2.11 Enzyme linked immunosorbent assay (ELISA)

Various ELISAs, developed in house, were used during this work. Maxisorp 96 well plates (Fisher Scientific, product code; 442404) were used unless stated otherwise. In direct ELISA, protein was diluted to final concentration of 0.5 - 5 µg/ml in coating buffer (Table 2.4). All incubations, apart from sample, were for 30 minutes; sample was incubated for 1 hour. All incubations were at 37°C. One wash in PBS/tween (300µl/well) used after blocking, and two washes after all other incubations using an automated plate washer (Model; Wellwash Versa, 5165010, ThermoScientific). All protein dilutions were made in dilution buffer (50µl per well).

Buffer	Composition
Coating buffer	0.1 M $NaHC0_3/Na_2C0_3$, pH 9.6.
Wash buffer (WB)	PBS, 0.05% Tween 20
Blocking buffer	WB containing 2% w/v BSA
Dilution buffer	WB containing 1% w/v BSA
Developing solution	1 orthophenylenediamine (OPD) tablet (Sigma Aldrich) in 20ml supplied buffer in the kit.
Stop solution	10% H_2SO_4 in deionised water.

Table 2.4 *ELISA buffers*.

2.11.1 Screening for anti-complement mAb by direct ELISA

Sera from immunised mice or supernatants from individual fusion wells were screened by an ELISA adapted for the purpose. Maxisorp 96 well plates were coated with 0.5µg/ml protein (50µl per well) in ELISA coating buffer, incubated 1h at 37°C or overnight at 4°C. Coating solution was removed and plates blocked with blocking buffer (100µl per well; 30 minutes at 37°C). The blocking agent was removed, plates washed once and 50µl of test sample (tissue culture supernatant) was added to each well, incubated for 1h at 37°C. Plates were washed twice, peroxidase conjugated anti-mouse IgG (H & L chains, Jackson ImmunoResearch, product code; 715-035-151) diluted 1 in 1000 in ELISA dilution buffer was placed in each wells (50µl per well), incubated 30 minutes at 37°C. The plate was washed twice and the assay developed with ELISA developing solution (50µl per well). Colour development was stopped with stop solution (50µl per well) when the positive control had developed sufficiently so that it was highly positive and the negative control had not developed, usually within 5 minutes. The absorbance of each well was measured at 492 nm. Cells from wells with the greatest colour development were taken forward.

2.11.2 Detection of proteins by sandwich ELISA

To determine whether different mAb bind the same epitope sandwich ELISA was used. Maxisorp 96 well plates were coated with 2 -5µg/ml mAb (50µl per well) in ELISA coating buffer, incubated 1h at 37°C or overnight at 4°C. Coating solution was removed, plates blocked with blocking buffer (100µl per well; 30 minutes at 37°C). The blocking agent was removed, plates washed once and 50µl of serial dilutions of protein standard or sample were added to wells, incubated for 1h at 37°C. Plates were washed three times, and 2-5µg/ml detection mAb added (50µl per well), incubated 1h at 37°C, washed twice, then secondary peroxidase conjugated anti-mouse IgG (H & L chains, Jackson ImmunoResearch, product code; 715-035-151) or anti-Goat or Rabbit IgG (Jackson

ImmunoResearch, product code; 305-035-045 or 711-035-152 respectively) added as appropriate at 1:1000 in ELISA dilution buffer (50µl per well), incubated 30 minutes at 37°C. The plate was washed twice and the assay developed with ELISA developing solution (50µl per well). When detection mAb directly labelled with HRP were used no secondary antibody was required. Colour development was stopped with stop solution (50µl per well) when the positive control had developed sufficiently so that it was highly positive and the negative control had not developed, usually within 5 minutes. The absorbance of each well was measured at 492 nm. Cells from wells with the greatest colour development were taken forward.

2.12 Serum preparation

Blood was collected into glass containers, allowed to coagulate for 1 hour at RT and then placed for 1 hour on ice prior to centrifugation at 3000 rpm for 30 minutes at 4°C; supernatant (serum) was collected, 0.2µm filtered and (if not immediately used for purification) stored in aliquots at -80°C.

2.13 Plasma preparation

Blood was collected into EDTA pre-coated tubes, spun at 3000 rpm for 30 minutes at 4°C, supernatant (plasma) collected and 0.2µm filtered. If not directly used for purification, plasma was aliquoted and stored at -80°C.

2.14 Animals

All animals used were adults and obtained from breeding colonies in the Biomedical Services Unit (JBIOS), at Cardiff University. To generate mAb against proteins (C6, C7) and complexes (C5b6, C5b67) wild type (WT), C6-deficient or C7-deficient mice were used. The C7-deficient mouse colony was established during this project (section 5.3.1); WT mice were used to generate the first anti-C7 mAb. Deficient or WT mice were also used a source of macrophages for these fusions.

2.14.1 Preparation of mouse peritoneal macrophages

Mice were sacrificed using a Schedule 1 method and washed with 70% ethanol. Cold RPMI medium (10ml) was injected into the peritoneal cavity using a 21-gauge needle, vigorously flushed several times to dissociate peritoneal macrophages, then the medium, containing resident macrophages, was slowly withdrawn. The macrophages were pelleted by centrifugation at 1500 rpm, for 5 minutes, re-suspended in the appropriate culture medium for addition to hybridoma cultures. Typically, the peritoneal washout of one mouse would yield enough macrophages for 50 ml feeder medium – enough for ten 96-well plates.

2.15 Tissue culture

All tissue culture reagents, except where stated, were from Gibco, Invitrogen Corporation (Paisley, UK). Tissue culture was performed under sterile conditions using sterile tissue culture plates and flasks (Nunc). Cells were maintained in 5% CO_2 95% O_2 in a humidified chamber at 37°C. Medium was pre-warmed to 37°C prior to administering to cells, except where stated.

2.15.1 Tissue culture cells and media

RPMI-1640 supplemented with 3A (1% penicillin, 1% streptomycin, 2mM L-glutamine, 1mM sodium pyruvate) and 0.001% β-mercaptoethanol (BME) was used as cell culture medium. Depending upon the cell type being cultured different amounts of heat-inactivated foetal bovine serum (FBS) were added. Details of the FBS content and other additions to the cell culture medium are in Table 2.5.

2.15.2 General maintenance of cell lines

The general maintenance included feeding and splitting cells to allow them to expand. Media used are stated in the above table. The newly selected hybridoma cells were cultured in 96-well plates and then sequentially expanded into 24 well plates, T25 and T75 flasks. Integra flasks (Integra Biosciences, Generon, CeLLine 1000 DC-90005) were used to produce large quantities of the antibody.

Media	Composition	Use
Basic medium	RPMI 1640 Medium	Mouse macrophages / spleen harvest.
F15 medium	Basic medium supplemented with 15% w/v FBS plus additives (3A, BME)	Myeloma-SP2, hybridoma cell line culturing, thawing cells.
HAT-F15 medium	F15 medium supplemented with 0.1 mM hypoxanthine, 0.4 µM aminopterin and 16 µM thymidine.	Fusion to remove unfused myeloma cells.
HT-F15 medium	F-15 medium supplemented with 0.1 mM hypoxanthine and 16 µM thymidine.	As above.
Low IgG (F10; High density hybridoma medium)	Basic medium supplemented with 10% Ultra-low bovine immunoglobulin FBS, 3A, BME,	Hybridoma cell line culturing (scale up)
Bulk Hybridoma medium	RPMI 1640 Medium, supplemented with 3A, BME	Hybridoma cell line culturing (scale up in Integra flasks).
Freezing medium	10% w/v DMSO (Sigma) in FBS	Freezing cells.

Table 2.5 *Tissue culture media**.***

2.15.3 Seeding and maintenance of Integra flasks

Integra flasks were used for large scale production of antibody. These bioreactors utilize innovative membrane technology to separate the cell cultivation area from the medium chamber. Cells and cellular-secreted products with a MWCO of >10 kDa are retained within the inner chamber while the upper semi-permeable membrane allows continuous nutrient diffusion and waste elimination. The lower membrane provides direct oxygenation and ensures optimum gas exchange. These flasks are capable of yielding antibody concentrations of up to 1-2 mg/ml in harvested medium and can be harvested (~25ml) at one-week intervals once established. To set up the culture, 1000ml bulk hybridoma medium was placed in the upper chamber (green cap) to equilibrate the membrane. Then the cell compartment (white cap, lower chamber) was inoculated with at least 1.5 x 10^6 viable cells in 15ml warm high density F10-low IgG medium avoiding introduction of air bubbles. The flask neck and cell compartment were wiped with 100% ethanol, sealed and

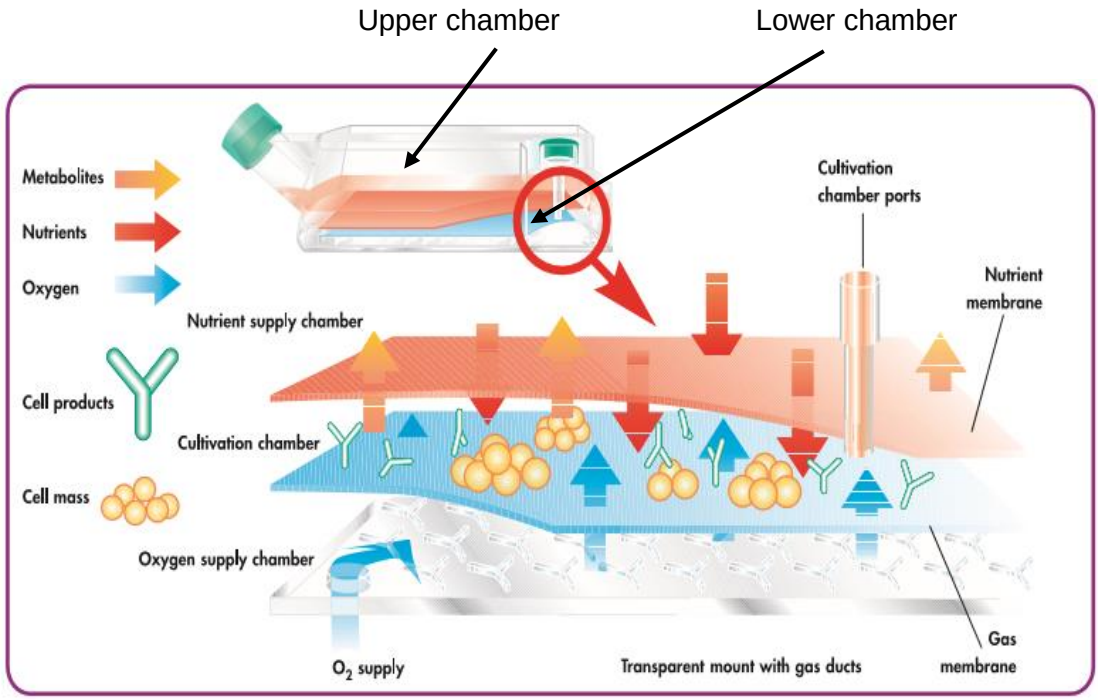

Figure 2.1 *Structure diagram of Integra flask adapted from; http://www.argos-tech.com/celline-bioreactors.html.*

incubated at 37°C, 5% CO_2 for fourteen days. The medium from both compartments was changed on day ten following inoculation (25ml harvest) and then every seven days. When harvesting from the cell compartment, cells were reseeded by mixing 5ml of the harvested cells with 25ml fresh high density hybridoma medium before re-inoculation. The collected 25ml harvest from the cell compartment was centrifuged at 3000 rpm for 10 minutes at 4°C, 0.2µm filtered, spiked with 0.01% w/v NaN_3 and kept sterile at 4°C ready for antibody purification. The bulk hybridoma medium was discarded and replaced with fresh.

2.15.4 Freezing hybridoma cells

Cells were detached from the flask surface by agitation. The suspended cells were pelleted by centrifugation at 1500 rpm for 5 minutes and supernatant discarded. The pellet from one 80 cm^2 flask was resuspended in 1 ml freezing medium and placed in seven cryovials (Greiner, # CLS430488). The cells were then slowly frozen in a freezing container (Nalgene), which is designed to decrease in temperature by 1°C per minute when placed in a -80°C freezer. After approximately 24 hours at -80°C, the frozen cells were transferred to liquid nitrogen for long-term storage.

2.15.5 Thawing hybridoma cells

Cells were thawed rapidly by transferring to a 37°C water bath. The thawed cells were immediately resuspended in F15 medium and centrifuged at 1500 rpm for 5 minutes. Pelleted cells were resuspended in 5 ml F15 media and plated out in T25 flasks. If necessary, freshly harvested mouse peritoneal macrophages were added to the culture medium to act as feeder cells. To obtain high expressing cells, the hybridoma cells were cloned out into 96 well plates pre-seeded with macrophages. The cloning was performed as stated below.

2.15.6 Cloning of hybridoma cell line

In order to isolate high expressing hybridomas, cells were cloned out by limiting dilution in 96-well plates. Cells were harvested from original wells or flasks and resuspended to 1000 cells/ml in medium. Cell suspension (5µl; app 5 cells) was added to medium-containing wells in the top row of a 96 well plate. The cells were then diluted down the plate into medium containing wells at a 1:5 serial dilution in order to ensure an average of less than 1 cell per well in lower rows. After approximately two weeks in culture, the wells were visually examined for the presence of clones and supernatant from the wells was screened by ELISA and haemolysis assay. Cells from the lower row wells where the supernatant had the highest signal in the ELISA and/or showed inhibition of classical pathway haemolysis were taken on and expanded.

2.16 Monoclonal antibody production

The immunisation protocol was as follows: the primary immunisation, administered by subcutaneous (SC) injection, comprised 20 – 50µg of the protein of interest in filtered PBS, emulsified with an equal volume of complete Freund's adjuvant (CFA) in a total volume of ~0.25ml per mouse. Four weeks after the first immunisation, the animals were boosted SC with 20 – 50µg antigen in PBS emulsified with incomplete Freund's adjuvant (IFA) (volume as above). In some cases, this boost was repeated after 7 days. Seven days after the last boost, mice were tail-bled, serum prepared (as described in section 2.15.2) and tested for the presence and titre of the specific antibodies by ELISA (according to protocol in section 2.11.1). The mouse with the highest antibody titre was boosted by intraperitoneal (IP) injection with approximately 50µg antigen, diluted in PBS, 48 hours prior to sacrifice.

2.16.1 Generation of hybridoma cell lines

Once the animal with highest antibody titre against the target protein had been identified, the next step was to select and immortalise those plasma cells secreting specific mAbs. The

animal was Schedule 1 sacrificed, the spleen harvested aseptically, taken to a tissue culture hood and repeatedly perfused with cold (4°C) RPMI 1640 medium using a 10ml syringe and a 19-gauge needle to release spleen cells. The released cells were washed in RPMI 1640 medium at 4°C. Myeloma cells (SP2) growing in log phase were harvested and washed once in cold RPMI 1640 media. Spleen cells were mixed with the myeloma cells at a ratio of 2:1, washed once in RPMI 1640 medium at 37°C and pelleted. The supernatant was completely removed, leaving a dry pellet, which was loosened by gentle agitation. Fusion was induced by the gradual addition of 1 ml PEG-1500 (37^{o}C) dropwise to the cells over 1 minute with gentle agitation. The fused cells were left to rest for 30 seconds and then 50 ml pre-warmed (37°C) RPMI 1640 was slowly added. The cells were washed by centrifugation and re-suspended in 50ml pre-warmed to 37°C HAT-F15 medium and aliquoted 50µl/well into ten 96-well plates, each well containing 50µl mouse peritoneal macrophages in the same medium to act as feeder cells. The HAT-F15 medium is used to select for hybrid cells as the unfused spleen cells die spontaneously and the SP2 cells cannot survive in HAT. The selection happens via functional complementation of two different (parental) metabolic defects to ensure survival of the hybrid cells. HAT (hypoxanthine, aminopterin, thymidine) prevents growth of cells unless 'rescued' by fusion with spleen cells which are source of HGPRT (hypoxanthine-guanine phosphoribosyltransferase), missing in the SP2 cell line (Harlow and Lane 1988). Approximately 10-14 days post-fusion, visible clones were present in the majority of wells and were ready for screening for the presence of specific antibodies by ELISA (as described in section 2.11.1). Positive wells were re-cloned by limiting dilution into HT-F15 medium in order to obtain mAb-secreting cell lines (HT is HAT medium without aminopterin) (Harlow and Lane 1988). The process of screening and re-cloning was repeated twice to obtain clonal mAb secreting hybridoma cells. After the 3rd re-cloning, clones that were strongly positive in ELISA were expanded into 24 well plates. At this stage cells were frozen down as stock and the rest were expanded further into T25, and then T75 tissue culture flasks and maintained in F15 medium. Gradually, the amount of FBS was reduced and finally cells were cultured in Low-IgG-F10. Once a week, the medium was collected and replaced with fresh medium. The collected medium was centrifuged at 3000 rpm for 15 minutes at 4°C to remove cell debris, NaN_3 (0.01% (w/v)) added and the supernatant stored at 4°C until the antibody was purified.

2.17 Haemolysis assays

Various haemolytic assays for assessment of CP or AP activity were used to identify functional blocking activity of developed mAbs on complement cell lysis. RL assay was used to identify the inhibitory mechanism of the mAb.

Animal blood used in the assays was harvested in house or purchased from TCS Biosciences (TCS Biosciences Ltd., Claydon, Buckinghamshire, UK). All sera used were freshly prepared in house.

For all haemolysis assays % Lysis was calculated by measuring released haemoglobin spectrophotometrically and calculated as follow; % lysis = [(A_{405} sample – A_{405} background lysis control) / (A_{405} maximum lysis control – A_{405} background lysis control)] x 100%. A measurement of the serum complement haemolytic activity was obtained by plotting the calculated % lysis against serum dilution and the dilution of serum at which ~80% haemolysis occurred was determined using GraphPad Prism 5 software.

Relevant controls were included in each assay; the maximum lysis control wells contained 100µl 0.1% Tween 20 in deionised water and 50µl erythrocytes (E). The background lysis control wells contained 100µl HBS and 50µl E.

2.17.1 Antibody-sensitisation of sheep erythrocytes

To prepare a 2% stock solution of antibody-sensitised sheep E (ShEA), 1ml of sheep blood in Alsever's solution was diluted in 20ml HBS (Zelek *et al* 2018) and washed three times with HBS by centrifugation at 2000 rpm for 5 minutes at 4°C. Packed E (400µl) were resuspended in 10 ml pre-warmed HBS and 10ml of pre-warmed HBS containing Amboceptor (rabbit anti-sheep E antibody, Simens, Criunn, # ORLC25) diluted 1 in 2000 was added to the sheep E suspension, mixed and incubated for 30 minutes at 37°C in a shaking water bath. The resultant ShEA were washed three times in HBS and resuspended in a final volume of 20 ml HBS and stored at 4°C for up to one week.

2.17.2 Titration of serum

Doubling dilutions of serum were made in 50µl HBS (final volume) in a round-bottomed 96 microtitre plate, to which a further 50µl each of HBS and 50µl of 2% E of an appropriate species, with or without antibody sensitisation were added. The plate was incubated at 37°C for 30 minutes before being centrifuged at 2000 rpm for 5 minutes at 4°C to pellet the cells. Supernatant from each well (100µl) was transferred to a flat-bottom 96 well microtitre plate and the release of haemoglobin into the supernatant was measured spectrophotometrically at A_{405}nm.

2.17.3 High-throughput CP haemolysis assay for mAb clones screening

NHS titration was carried out first (as described above) to determine the dilution of serum that induced ~80% haemolysis (usually ~2.5%). To determine the appropriate dilution of clone supernatant for the assay, fresh F15 medium was titrated in the assay. The maximum non-inhibitory dilution of medium dictated the dilution of clone supernatant used for

screening. Culture supernatants from individual wells at appropriate dilutions in HBS were added into a U-welled microtitre plate (50 µl/well), NHS dilutions (50 µl/well) and 2% ShEA (50µl) added. Plates were incubated for 30 minutes at 37°C, centrifuged at 2000rpm for 3 minutes at 4°C, the supernatant from each well (100µl) transferred to a flat-bottom 96 microtitre plate and the release of haemoglobin into the supernatant measured at A_{405}nm.

2.17.4 Testing mAb for complement inhibition by CP haemolysis assay

A serial dilution series of each test mAb (usually 100–0 µg/ml) was prepared in HBS and aliquoted in triplicate into a 96-well round-bottomed plate (50 µl /well), then serum dilutions (50 µl /well) added, selected in preliminary experiments to give near-complete haemolysis in the CP assay in the absence of test mAb (section 2.17.2). Dose was dependent on species, typically 2.5% for NHS, rat and guinea pig serum, 25% for rabbit and male mouse serum (the latter using the double-sensitized cells as described below). ShEA (2%; 50 µl /well) were added, plates incubated at 37°for 30 min, centrifuged at 2000rpm, 4°C for 3 minutes and haemoglobin in the supernatant measured by absorbance at A_{405}nm.

2.17.5 Testing mAb for human complement inhibition by AP haemolysis assay

To prepare a 2% stock suspension of rabbit E (RabE), 1ml of rabbit blood in Alsever's was diluted to 20ml in AP buffer (APB; HBS containing 5 mM EGTA and 3 mM $MgCl_2$) and washed three times by centrifugation at 2000 rpm for 5 minutes at 4°C. Packed E (400µl) were removed and re-suspended in a final volume of 20 ml APB and stored at 4°C for up to one week. Serial dilutions of mAb (usually 100 – 0 µg/ml) were made into APB (50µl/ well) in a 96-well round bottom plate, NHS (50µl/ well, concentration determined as described in section 2.17.2) was added followed by 50µl of 2% RabE. The plate was incubated at 37°C for 30 minutes. Maximum lysis and background lysis controls were included as above. The plate was centrifuged at 2000 rpm for 3 minutes at 4°C, the supernatant from each well (100µl) transferred to a flat-bottom 96 microtitre plate and the release of haemoglobin into the supernatant measured at A_{405}nm. % lysis was calculated as above.

2.17.6 Determination of mechanism of mAb complement inhibition by reactive lysis

To prepare a 2% stock solution of guinea pig E (GpE), 0.25ml of guinea pig blood in Alsever's was diluted in 5ml HBS and washed three times with HBS by centrifugation at 2000 rpm for 5 minutes at 4°C. Packed E (100µl) were removed and re-suspended in a final volume of 5 ml HBS and stored at 4°C for up to one week. GpE in HBS were incubated sequentially with purified in house C5b6, C7, C8 and C9 (section 3.2.1), each 10 minutes at 37°C, at doses titrated to give ~75-90% haemolysis in the absence of inhibitor. The

concentrations (per well) of the purified components used were as follow; C5b6; 45ng/ml, C7; 184ng/ml, C8; 168ng/ml, C9; 383ng/ml. Molarities in nM; C5b6, 0.16; C7, 1.99; C8, 1.11; C9, 5.39 (Ratios: 1: 13: 10: 34). Serial dilutions (in triplicate) of the mAb were made into HBS and added to the wells at different stages of MAC formation to determine the inhibition. Test and control mAb were added either prior to addition of C5b6, prior to addition of C7, or prior to addition of C8/C9 and incubated for 30 minutes at 37°C. Plates were centrifuged at 2000rpm for 3 minutes at 4°C, supernatants removed to a flat-welled microtitre plate, absorbances measured spectrophometrically (A_{405}nm) and % lysis calculated as above.

2.17.7 Testing mAb for mouse complement inhibition by CP haemolysis assay

For measurement of mouse serum haemolytic activity, ShEA (prepared as described in section 2.17.1) were additionally sensitized with mouse anti-rabbit IgG (Invitrogen, Carlbad, CA; #3123) to generate efficient activation of mouse complement. The antibody was added at a final concentration of 25µg/ml to ShEA at 2% in HBS, cells were incubated for 30 minutes at 37°C in shaking water bath and then washed 3 times in HBS. A serial dilution series of each test mAb (usually 100–0 µg/ml) was prepared in HBS and aliquoted in triplicate into a 96-well round-bottomed plate (50 µl /well), then normal male mouse serum (NMS) dilution (50 µl /well, dilution selected as above; section 2.17.2) and 2% double-sensitised ShEA added (50 µl /well). Plates were incubated at 37°C for 30 min, centrifuged at 2000rpm for 3 minutes at 4°C, haemoglobin in the supernatant measured by absorbance at A_{405}nm and % lysis calculated as above.

2.17.8 High-throughput CP haemolysis assay for testing individual mouse terminal pathway component lytic activity

This method was developed because of the difficulties of obtaining enough serum from mouse test bleeds for analysis; the method obviates the need for large amounts of mouse serum for testing the impact of blocking mAb. NHS depleted of the specific protein (the target for the test mAb) is the source of the rest of the complement proteins; the target protein is reconstituted from added mouse serum. NHS depleted of specific terminal pathway proteins (10%) was added in triplicate into a 96-well round-bottomed plate (50 µl /well), followed by 50µl/well of 2.5% mouse serum with or without various doses of the blocking mAb, and finally 2% ShEA. Plates were incubated at 37°C for 30 minutes, centrifuged at 2000rpm for 3 minutes at 4°C, and haemoglobin in the supernatant was measured by absorbance at A_{405}nm. % lysis was calculated as above.

2.17.9 Reconstitution of deficient/ depleted sera with functional protein

The assay was used to identify fractions containing functionally active terminal pathway proteins (C5, C6, C7, C8 or C9) during purification or to determine the minimum concentration of the protein required for complement mediated haemolysis. To test the lytic activity the purified protein was added back to the relevant depleted serum at physiological levels. Doubling dilutions (50 µl; 10 – 0%) of the restored functionally active serum, depleted serum or normal serum were prepared in HBS in a round bottom microwell plate (50µl/ well), 50 µl 2% ShEA and 50 µl HBS were added, incubated for 30 minutes at 37°C. Plates were centrifuged, supernatants removed to a flat-welled microtitre plate and absorbance measured spectrophometrically (A_{405}nm). % lysis was calculated.

To identify functional protein containing column fractions, 5 µl test sample was mixed with 50 µl depleted serum diluted to 10% in HBS followed by 50 µl 2% ShEA and 50 µl HBS in 96 microtitre U-shape wells plate. The plate was incubated for 30 minutes at 37°C, centrifuged, supernatants removed to a flat-welled microtitre plate and absorbances measured at A_{405}nm.

To determine the minimum amount of protein required for complement mediated haemolysis, serial dilutions of the protein (usually 10 – 0 µg/ml; 50 µl/well in triplicate in round-bottomed 96 well plates) were made, the relevant depleted serum added (10%; 50 µl/well), followed by 50 µl of ShEA. The plate was incubated for 30 minutes at 37°C, centrifuged, supernatants removed to a flat-welled microtitre plate and absorbance measured at A_{405}nm.

This chapter describes general methods and materials used in this project. In chapter 3 I will describe specific methods to obtain key reagents.

CHAPTER 3; GENERATION AND CHARACTERISATION OF THE KEY REAGENTS

3.1 Introduction

To understand precisely the mechanisms and function of complement, purified proteins are needed. All terminal pathway proteins are present in human plasma at ~50 – 100µg/ml.

In order to meet aims of the thesis several key reagents (human or animal) were required, these included terminal pathway components C5, C6, C7, C8 and C9, and complexes C5b6, C5b67, C5b-8 and sC5b-9 purified to homogeneity. This chapter describes the purification techniques developed for generation of these reagents.

All proteins were purified using immunoaffinity methods; immunoaffinity chromatography is one of the most powerful procedures to separate proteins based on the specific and reversible interaction between target protein and a specific antibody against that protein coupled to a chromatographic matrix. It is the only isolation technique that enables single-step purification of proteins from complex mixtures; the target protein binds the immobilised antibody while the unbound proteins and other contaminants are washed away. The reversible binding allows removal of the target protein usually by altering the pH or ionic strength of the buffer to disrupt the antibody-antigen binding (Burgess and Deutscher 2009). One-step isolation of the target protein from a complex mixture (serum or plasma here) is a great advantage over classical purification methods that are time-consuming, difficult and inefficient.

After the immunoaffinity purification, a “polishing” step can be applied to remove aggregates or residual contaminants using gel filtration (GF) or ion exchange chromatography (IEC). Among the chromatographic methods GF is unique in that fractionation is based solely on size of the protein, this is an advantage for fragile proteins that can become damaged by binding to a chromatographic support matrix, but also means that proteins of similar size will not be well separated. In this event IEC can be used instead where proteins are separated based on charge difference. The target protein is applied in a buffer selected to ensure that its charge is appropriate to bind the oppositely charged chromatographic medium and the protein is eluted either by increasing the salt concentration or changing the pH; the protein is concentrated during binding and collected in a purified, concentrated form.

C5, a critical reagent for this work, presented unique difficulties; the first C5 purification method, published over fifty years ago, required multiple precipitation and chromatography steps, taking many days and generating poorly active protein in low yield (Nilsson and Mueller-Eberhard 1965). Over time the method improved with reduced time to produce C5, however it still involved harsh procedures yielding poorly active C5 (Tack *et al* 1979; All *et*

al 1982; DiScipio and Sweeney 1994). The main issue was denaturation of C5 by precipitation and pH shifts, and binding of denatured C5 to C6, resulting in low yields of active C5 (Dessauer and Rother 1983; Chakravartis *et al* 1988). Later immunoaffinity methods using monoclonal antibodies presented much better C5 recovery (~50%) (Giles *et al* 2015); however, elution of the protein at extremes of pH compromised the C5 activity despite rapid pH neutralisation on elution. In this chapter I will describe a novel immunoaffinity purification method to obtain fully functional C5 in a single step with a purification yield of 98% by using a unique pH-switch antibody mAb, RO7112689 (C5i mAb, SKY59, Crovalimab, RG6107) immobilised on Sepharose. This mAb strongly binds C5 at pH7.4 but loses binding affinity below pH6 (Fukuzawa *et al* 2017).

The overall aim of this chapter is to describe reliable purification methods to obtain high quantities of homogenous terminal pathway proteins and complexes. This work has been provoked by limited or no commercial availability of good quality complements proteins (for instance C5b67 and C5b-8 are not commercially available), and high costs and variable quality of the reagents that can be sourced commercially.

3.2 Specific methods

3.2.1 Affinity purification of complement terminal pathway proteins

Human proteins were purified from normal human serum (NHS) or plasma extracted from blood kindly donated by co-workers. Animal proteins were obtained from in house prepared or commercially sourced sera. Serum or plasma was processed as described in section 2.12 and 2.13.

Because of complement protein sensitivity to temperature, all terminal pathway proteins and complexes were purified at 4°C.

3.2.1.1 Purification system

Proteins were purified using the HPLC AKTA Purification System; GE Healthcare, Model; 29018291-AD AKTA system PMvr, S/N; 1396885 or AKTA Pure 01, #WIN-QET7M352MJ, S/N; 2351541 used interchangeably.

3.2.1.2 Affinity columns preparation

HiTrap NHS activated Sepharose High Performance columns (1 or 5 ml) were used for coupling of ligands (mAb) containing primary amines according to the manufacturer's protocol (Table 3.1; GE Healthcare, HiTrap NHS-Activated HP, #17-0716-01, #17-0717-

01). Briefly, ligand (mAb; ~5mg for 1ml column and ~25mg for 5ml column) was concentrated to 5-10mg/ml using Vivaspin concentrators with 100kDa cut off membrane, then dialysed overnight at 4°C into coupling buffer (0.2M $NaHCO_3$, 0.5M NaCl, pH 8.3). Six column volumes (CV) of ice-cold 1mM HCl was injected over the NHS HiTrap column to wash out the isopropanol used to preserve active esters during storage. The concentrated mAb in coupling buffer was injected immediately into the column and incubated at ambient temperature for one hour. After coupling, residual free antibody was eluted and collected to measure unbound protein to enable coupling efficiency to be calculated (usually >95%). The column was washed with coupling buffer (3 CV) then with elution buffer Residual active esters were deactivated by washing the column with three cycles of six CV of buffer A (0.5M ethanolamine, 0.5M NaCl, pH 8.3) followed by six CV of buffer B (0.1M sodium acetate, 0.5M NaCl, pH 4). After the first cycle, the column was incubated in buffer A for 30 minutes at room temperature and then the wash continued. The mAb column was stored in PBS, 0.01% NaN_3 at 4°C. Before use the column was equilibrated with elution buffer followed by run buffer to ensure any unbound protein is removed.

Purified protein	**Immobilised protein**	**Source**
Human C5	RO7112689	Roche
Human C6	22D1, 8E1	In house
Human C7	F10	In house
Human C8	D5, E2	In house
Human C9	B7, 26	In house
Rat C5	OmCI, 4G2	In house
Rat C7	H05-40	GSK
Mouse C5	RO7112689, OmCI	Roche, In house
Mouse C7	73D1	In house

Table 3.1 *Antibodies/Proteins used for terminal pathway component purification.*

3.2.1.3 Purification protocol

Serum or plasma was passed over the column which was then washed with 20 CV of run buffer (Table 3.2), and the bound protein eluted with 5ml elution buffer, collecting 1ml fractions into tubes containing 100µl neutralisation buffer. Flow rate was 1 – 2 ml/minute. The column was re-equilibrated immediately by flushing with 5 CV storage buffer and stored at 4°C. Peak fractions were assessed for protein content by their absorbance at 280nm (NanoDrop as described). The protein concentration of the peak fractions were calculated using Beer-Lambert's Law: Protein Concentration (mg/ml) = A_{280}/ protein extinction

coefficient (EA; C5 and C5b6 = 1.03, C6 = 1.08, C7 = 1.04, C8 = 1.49, C9 = 0.988). The peak fractions were pooled and dialysed overnight at 4°C into run buffer without NaN_3 and concentrated further if necessary with Vivaspin concentrators to a final concentration of >1mg/ml, confirmed by BCA assay. C5, C6, C7 and C9 were stored frozen in aliquots at -80°C, while C8 and the terminal complexes were spiked with 20% glycerol and stored in aliquots at -20°C to enhance protein stability.

Buffer	**Composition**
Run buffer	0.01M HEPES, 0.5M NaCl, 135nM $CaCl_2$, 1mM $MgCl_2$, 0.001% w/v NaN_3, pH 7.4
Elution buffer	0.1M Glycine-HCl, pH 2.5
Neutralisation Buffer	0.1M HEPES, 0.5M NaCl, pH9
Column storage buffer	PBS, 0.001% w/v NaN_3

Table 3.2 *Affinity purification buffers.*

3.2.2 Purification of fully active, endotoxin free C5 protein using RO7112689

A novel C5 purification method has been developed to generate intact fully functional C5 in sterile conditions. All precautions described below were implemented to produce large quantities of endotoxin free human C5 protein that meets the quality standards for commercialisation. A collaborative agreement has been arranged to supply the protein for Hycult Biotech.

3.2.2.1 RO7112689 column preparation

An NHS HiTrap 5ml NHS-Activated HP affinity column was prepared according to the manufacturer's protocol (section 3.2.1.2) and 50mgs of the pH-switch anti-C5 mAb RO7112689 immobilised on the matrix. Before the purification the column was cleaned with 3 CV of wash buffer containing 1M NaCl to remove the storage buffer and any potential contaminants.

3.2.2.2 Glassware/ buffers preparation

All glassware used were washed x 5 with 0.5M NaOH followed by sterile water (Gibco, # PMC0438) in a tissue culture (TC) hood and then autoclaved. All buffers were prepared and sterile filtered in a TC hood; freshly opened bottles of all reagents were used and weighed out in the TC hood.

3.2.2.3 HPLC AKTA purifier sterilisation

The AKTA was cleaned immediately before use by flushing through 50ml of 0.5M NaOH, followed by 1l sterile water and 100ml of sterile run buffer (Table 3.3).

Buffer	Composition
Run Buffer	0.01M HEPES, 0.5M NaCl, 135nM $CaCl_2$, 1mM $MgCl_2$, 0.001% w/v NaN_3, pH 7.4
Column wash buffer	0.01M HEPES, 1M NaCl, 135nM $CaCl_2$, 1mM $MgCl_2$, 0.001% w/v NaN_3, pH 7.4
Elution buffer	0.1M acetate buffer, 0.15M NaCl, pH5.5
Neutralisation buffer;	0.1M HEPES, 0.5M NaCl, pH9
Storage buffer	PBS, 0.001% w/v NaN_3

Table 3.3 *Purification buffers used for human C5 isolation on RO7112689*

3.2.2.4 Purification protocol

Human C5 was purified by passage of 350ml NHS over the 5ml RO7112689 column at 1 – 2 ml/minute on the AKTA purification system, the column washed with 20 CV of run buffer, and the human C5 eluted with 5ml elution buffer pH 5.5, collecting 1ml fractions into 100µl neutralisation buffer. Flow rate was. The column was re-equilibrated immediately by flushing with 5 CV storage buffer and stored at 4°C.

3.2.2.5 Purified endotoxin free human C5 processing

The eluted C5 was immediately pooled (in TC hood) and dialysed (ThermoFisher Scientific, Slide-A-Lyzer™ Dialysis Cassette, #66030) overnight at 4°C against sterile PBS (Gibco, # 10010031). The protein concentration was measured by absorbance at 280nm and confirmed by BCA assay. From ~350ml NHS, 28mgs of pure C5 was obtained (98% yield); this was aliquoted into sterile Falcon tubes (in TC hood) and stored at -80°C.

The protein was tested for endotoxin presence using LAL Chromogenic Endpoint Assay supplied by Hycult Biotech (#HIT302). C5 function was tested in haemolytic assay, specificity in ELISA and purity by SDS-PAGE.

3.2.3 Purification of Cobra Venom Factor (CVF)

CVF was purified using a modification of a published method (Morgan 2000). Freeze-dried whole cobra venom (1g) from the cobra *Naja naja kaouthia (Thailand cobra)* (Sigma, # V-

9125) was dissolved in low salt buffer (5mM PBS containing 10mM EDTA; PBS-EDTA) to prevent CVF degradation by Ca^{2+}-dependent venom proteases. The sample was buffer exchanged using Vivaspin concentrators and applied onto Poros 50 HQ column (Mono Q, IEC) equilibrated in low salt buffer. CVF was eluted with a 600ml linear NaCl gradient elution from 0 to 0.5M NaCl at 1 – 5 ml/ minute. The column was re-equilibrated immediately by flushing with 5 CV ddH_20 and 20% Ethanol and stored at 4°C. Fractions were assessed for protein content by absorbance at 280nm (NanoDrop), tested for function in haemolytic assay and subjected to SDS-PAGE. The identified CVF-containing fractions were pooled, dialysed overnight at 4°C into HBS, 0.5M NaCl pH7.4, concentrated to ~1mg/ml and stored in aliquots at -80°C.

3.2.4 Purification of MAC intermediates

3.2.4.1 C5b6 generation

C5b6 was generated in two ways: 1. using purified terminal and alternative pathway components and CVF (DiScipio *et al* 1983); 2. using C7 depleted serum (protocol adapted from Morgan, 2000).

3.2.4.1.1 C5b6 generation using purified components

In this protocol, C5b6 was generated from purified C5 (using RO11277689, section 3.2.2) and C6 (clone 23D1 used, section 3.2.1) by incubating these proteins with a fluid phase convertase generated from CVF and commercial FB and FD (CompTech). CVF convertase (CVFBb) was generated by incubating CVF (100 µg/ml), FB (10 µg/ml) and FD (1 µg/ml) in a total volume of 1.32 ml in CFD containing 3mM $MgCl_2$ for 45 minutes at 37˚C in a shaking water bath. C5 and C6 (1mg of each) was added to the newly generated CVFBb and incubated overnight at 37˚C in a shaking water bath to allow cleavage of C5 and subsequent C5b-C6 binding. The overnight reaction mixture yielded white precipitate, demonstrated in previous publications to be C5b6 aggregates (DiScipio 1992), that went back into solution after gentle mixing; the protein was dialysed into HBS and subjected to ion exchange chromatography on a POROS™ HQ column (ThermFisher Scientific, # 1255911) equilibrated into HBS. C5b6 was eluted using a salt gradient (HBS 0.1 M – 1 M NaCl pH7.4). Fractions were assessed for protein content, peak pooled, dialysed overnight at 4°C into HBS, 0.5M NaCl pH7.4, concentrated to >1mg/ml with Vivaspin concentrators, and stored in HBS containing 0.5M NaCl and 20% glycerol in aliquots at -20°C.

3.2.4.1.2 C5b6 purification using C789 depleted serum

Serum, prepared as described above, was depleted of C7, C8 and C9 (C789D) using appropriate mAb columns (F10 for C7, E2 for C8, B7 for C9). Depletion was confirmed by CP haemolytic assay. To activate both CP and AP in the depleted serum, Zymosan A (7mg/ml, Cayman Chemical, #CAS 58856-93-2) and in-house heat-aggregated human IgG (1mg/ml) were added and incubated at 37°C in a shaking water bath for 32 hours. Particulates were removed by centrifugation (2500rpm for 15 minutes at 4°C) followed by 0.2 µm filtration. The activated C789D serum was then applied to the RO11277689 anti-human C5 affinity column and C5b6 was purified as described for C5 in section 3.2.2. C5b6 containing fractions were dialysed immediately into HBS containing 0.5M NaCl, assayed for haemolytic activity and checked for purity by SDS-PAGE. Pure, functional C5b6 fractions were pooled and concentrated to >1mg/ml, confirmed by Nanodrop and BCA assay (EA C5b6 = 1.03). The obtained C5b6 was applied to a 24ml SD200 GF column (GE Healthcare, equilibrated in HBS/0.5 M NaCl) to remove aggregates; the functional, pure C5b6 fractions (confirmed by haemolytic assay and SDS-PAGE) were pooled, concentrated and stored in HBS/0.5M NaCl containing 20% glycerol in aliquots at -20°C.

3.2.4.2 Purification of C5b67 and C5b78 intermediates

C5b6 generated using either of the above protocols was used to produce the MAC intermediates; C5b67, C5b678. To do this, C5b6 was incubated sequentially for 2h at RT with in house purified terminal pathway proteins (C7, or C7 and C8 respectively) in molar ratio 1:1. Excess protein was separated from the complex by gel filtration on a Superdex-200 (SD200) gel filtration column (GE Healthcare) pre-equilibrated in HBS/0.5M NaCl at a flow rate of 0.2 ml/minute. Peak fractions were collected, purity confirmed by SDS-PAGE and dot blotting and stored in HBS/0.5M NaCl containing 20% glycerol in aliquots at -20°C.

3.2.5 Generation of sC5b-9

Complement in NHS was activated via both classical and alternative pathways by incubation with Zymosan A (7mg/ml) and aggregated human IgG (1mg/ml) for 32 hours at 37°C in a shaking water bath. The reaction was stopped by centrifugation at 2500rpm for 15 minutes at 4°C, the supernatant (activated serum) collected and 0.2 µm filtered.

3.2.5.1 Purification of sC5b-9 using PEG Precipitation and Immunoaffinity chromatography

The activated NHS was subjected to a precipitation step to enrich the yield of sC5b-9 and reduce the volume to be applied on the affinity column. PEG4000 was added from a 40% w/v stock solution (in run buffer) to a final concentration of 5%, incubated for 20 minutes at

ambient temperature while mixing, then centrifuged at 2500rpm for 20 minutes at 4°C and the supernatant decanted. The pellet containing sC5b-9 was dissolved in a minimum volume of run buffer and applied onto a 1ml HiTrap mAb E2 anti-C8 affinity column. The immunoaffinity purification was carried out as described in section 3.2.5 except that Tris buffered saline (TBS) was used as run buffer.

sC5b-9 containing fractions from immunoaffinity purification were pooled, concentrated and applied to a SD200 gel filtration column equilibrated and run in HBS containing 0.5M NaCl, pH 7.4; fractions containing sC5b-9 were collected, pooled, and purity determined by SDS-PAGE, WB and ELISA. The protein was stored in HBS/0.5M NaCl, containing 20% glycerol in aliquots at -20°C.

3.2.6 Protein polishing

3.2.6.1 Gel Filtration

Affinity purified proteins were subject to GF on a SD200 column (GE Healthcare, Superdex 200, 10/300 GL, # 17-5175-01). Proteins were concentrated to > 5mg/ml using Visaspin concentrators and concentrated protein (200µl or 1ml depending on the superloop used) loaded via the injection loop; 60ml run buffer was passed over the column at 0.3 ml/minute, 1ml fractions collected, assessed for protein content by A280 (NanoDrop) and applied to SDS-PAGE. Peak fractions were pooled and stored at -80°C (for most proteins) or -20°C in run buffer containing 20% glycerol for C8 and complexes.

3.2.6.2 Ion exchange chromatography (IEC)

IEC was used as a polishing step for some of the immunoaffinity purified proteins. A Mono Q column (Poros 50 HQ; ThermoFisher Scientific, # 1-2552-46) was equilibrated with 3 CV of low salt buffer (HBS/10mM NaCl), sample injected via the superloop and eluted with a linear NaCl gradient elution from 0 to 1M NaCl at 1 – 5 ml/ minute. Peak fractions were assessed for protein content as above, tested for functionality in haemolytic assay and subject to SDS-PAGE and/or ELISA. The identified fractions were pooled, concentrated and stored as above.

3.2.7 Purification of monoclonal antibodies

Monoclonal antibodies were purified either using protein G chromatography on the AKTA or by ammonium sulphate precipitation. Prior to purification, cell culture supernatant (cells cultured in Low IgG-F10) was clarified by centrifugation at 2500 rpm for 15 minutes at 4°C and filtered through a 0.2µm filter.

3.2.7.1 Purification of monoclonal antibodies using Protein G columns

IgG isotype mAbs were purified using 5ml HiTrap Protein G sepharose columns (GE Healthcare, #GE17-0405-01). Protein G is an IgG-binding protein from *Staphylococcus aureus* that captures most IgG subclasses from ascites fluid, cell culture supernatants, serum and other sources of IgG protein.

The column was washed, equilibrated with run buffer, then IgG-containing supernatant was applied at 1-2 ml/min, the column washed with 50ml run buffer, and bound antibody eluted with 5ml elution buffer, collecting 1ml fractions into 100µl neutralisation buffer. Peak fractions were identified, pooled and dialysed overnight at 4°C into HBS. Antibody concentration was measured and the purified IgG was stored frozen in aliquots at >1mg/ml.

3.2.7.2 Purification of monoclonal antibodies by ammonium sulphate precipitation

Ammonium sulphate precipitation was used for crude purification of mouse monoclonal antibodies. Stock 100% saturated Ammonium sulphate solution was prepared by dissolving 541.8g of ammonium sulphate into 1l of deionised water at 25°C. Ammonium sulphate stock was added to antibody-containing tissue culture supernatant at 45% final saturation (e.g. 450ml of 100% saturated ammonium sulphate added to 550ml of the tissue culture supernatant), stirred continuously for 30 minutes at 25°C and centrifuged at 2500 rpm for 25 minutes at 25°C. The supernatant was discarded and the pellet (containing antibody) was re-dissolved in HBS and dialysed.

For IgM isotype antibodies the ammonium sulphate precipitation was carried out as above and the re-solubilised pellet subjected to a euglobulin precipitation by dialysing against 10mM Tris pH 8.0 overnight at 4°C. The dialysate was equilibrated to room temperature, removed from the tubing and centrifuged at 2500rpm for 25 minutes at 25°C. Supernatant was discarded and the pellet (mAb) was dissolved in HBS. mAb concentration was determined as described above (EA; IgM = 1.8).

3.5 Results

3.5.1 Characterisation of the purified terminal pathway proteins

Purified human and animal terminal pathway proteins were analysed by SDS-PAGE and/ or WB under non-reducing and reducing conditions. Haemolytic assays were used to assess activity and ELISA for detection. All tested proteins were active in haemolytic assays, and were detected in direct ELISA and by WB (Fig. 3.1 A – D). Example purification chromatograms are in Fig. 3.1 A – D. The affinity purification yields are summarised in Table 3.4.

Protein	Column used	Calculated yield
Human C5	5ml RO7112689	97%
Rat C5	1ml 4G2	73%
Rat C5	5ml OmCI	95%
Human C6	5ml 22D1	87%
Human C6	5ml 8E1	68%
Human C7	5ml F10	91%
Rat C7	1ml H05-40	84%
Mouse C7	1ml 73D1	72%
Human C8	5ml D5	63%
Human C8	5ml E2	73%
Human C9	5ml B7	87%
Human C9	1ml 26	74%

Table 3.4 *Summary of the average purification yields (from at least two purifications) for human and animal proteins. Yields were calculated as described in methods.*

A.

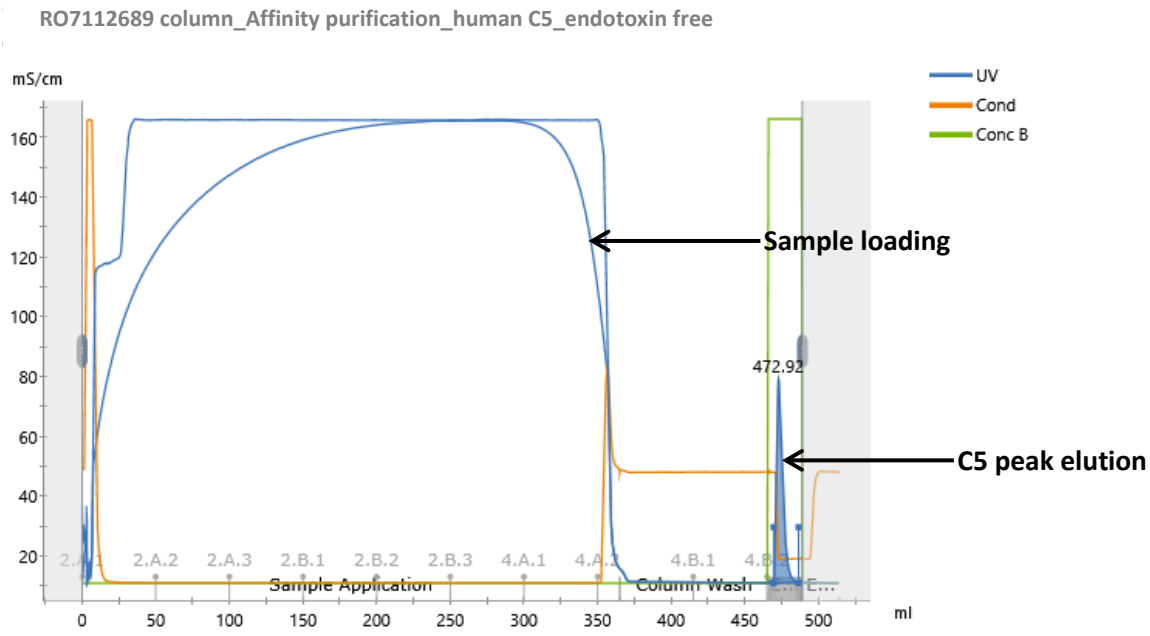
RO7112689 column_Affinity purification_human C5_endotoxin free
mS/cm
UV
Cond
Conc B
Sample loading
472.92
C5 peak elution
Sample Application
Column Wash
ml

B.

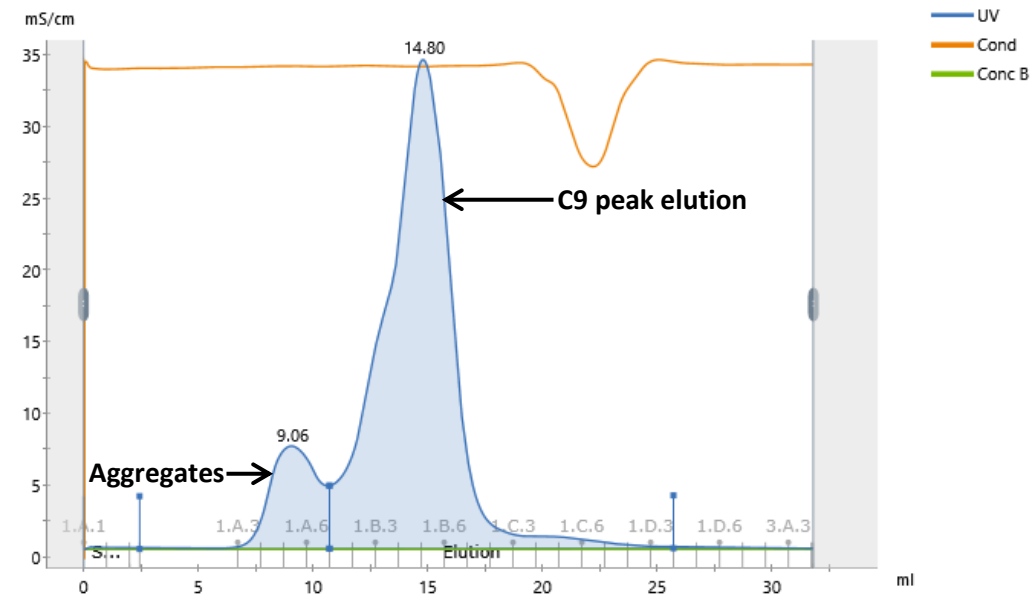
SD20010300GL_human C9
mS/cm
UV
Cond
Conc B
14.80
C9 peak elution
9.06
Aggregates
Elution
ml

C.

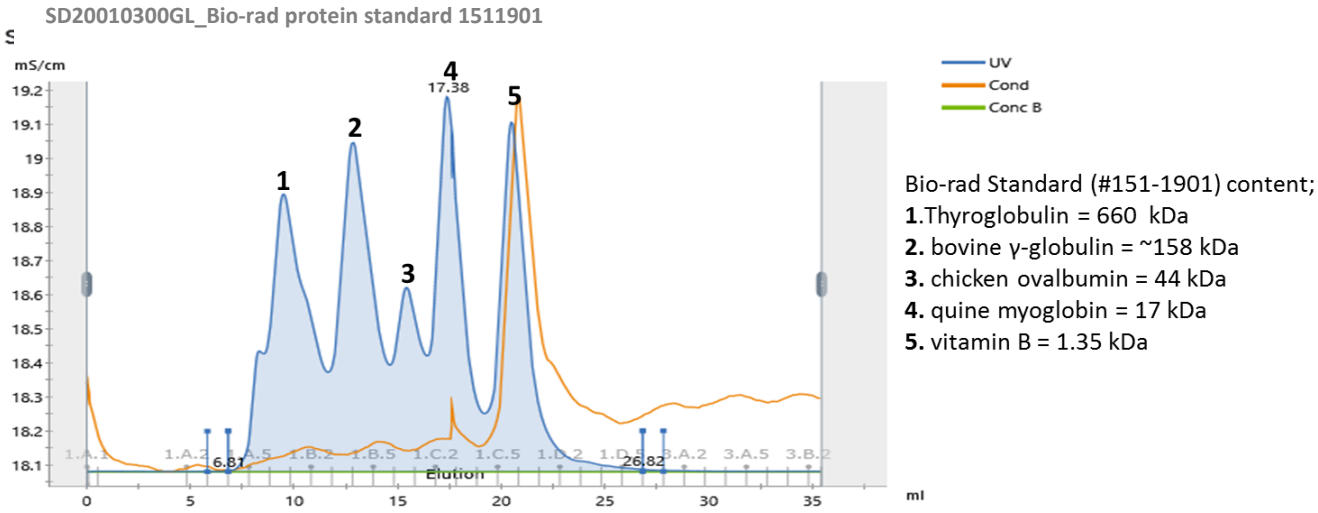

D.

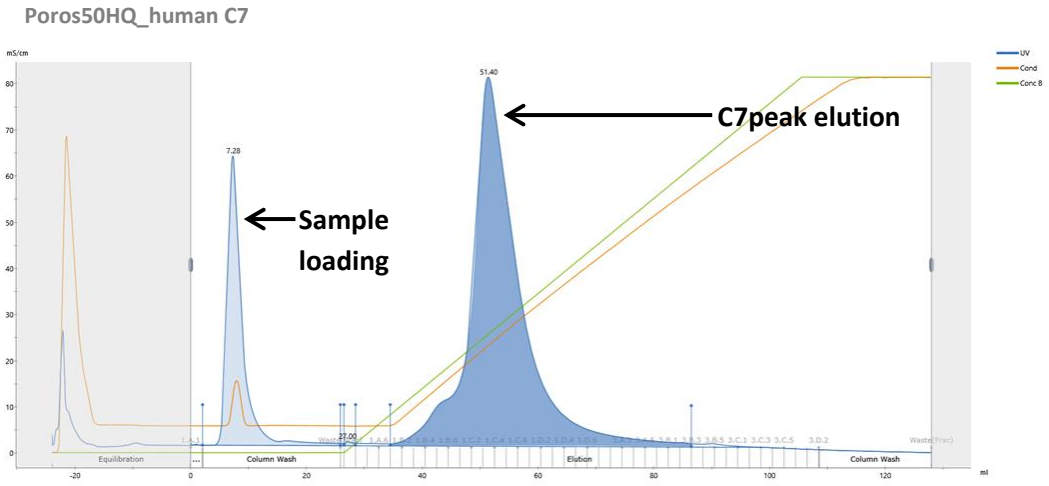

Figure 3.1 Example chromatograms of purification using affinity column, gel filtration and ion exchange chromatography. A*. NHS was passed over RO7112689 column and C5 eluted.* ***B****. Affinity purified human C9 was loaded onto SD200 GF column to remove aggregates.* ***C****. Protein standards (Bio-rad, #151-1901) applied onto SD200 column to calibrate.* ***D****. Affinity purified human C7 was polished using IEC on Poros50 HQ column.*

A.

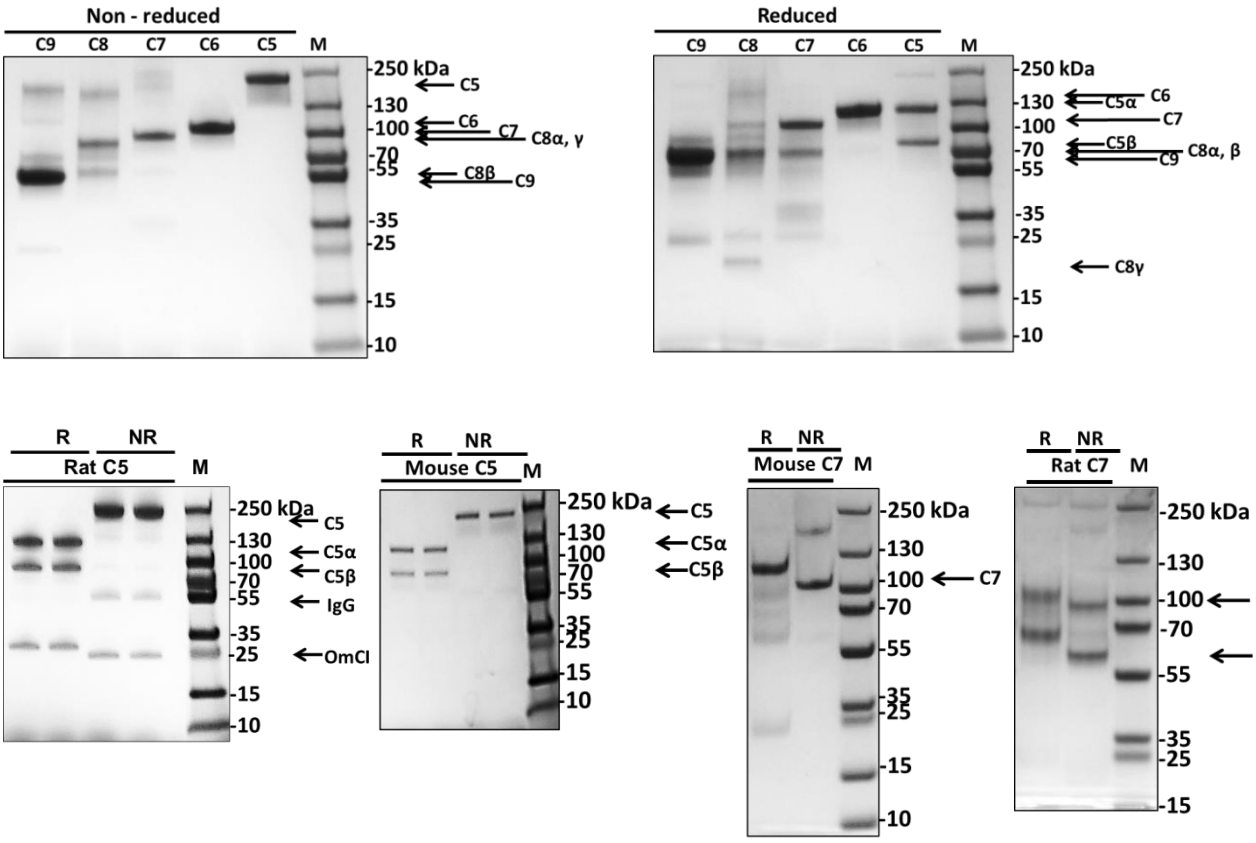
Non - reduced
C9 C8 C7 C6 C5 M
250 kDa
130
100
70
55
35
25
15
10
C5
C6
C7
C8α, γ
C8β
C9
Reduced
C9 C8 C7 C6 C5 M
C5α
C6
C7
C5β
C8α, β
C9
C8γ
R NR
Rat C5 M
C5
C5α
C5β
IgG
OmCl
R NR
Mouse C5 M
C5
C5α
C5β
R NR
Mouse C7 M
C7
R NR
Rat C7 M
C7
Albumin

B.

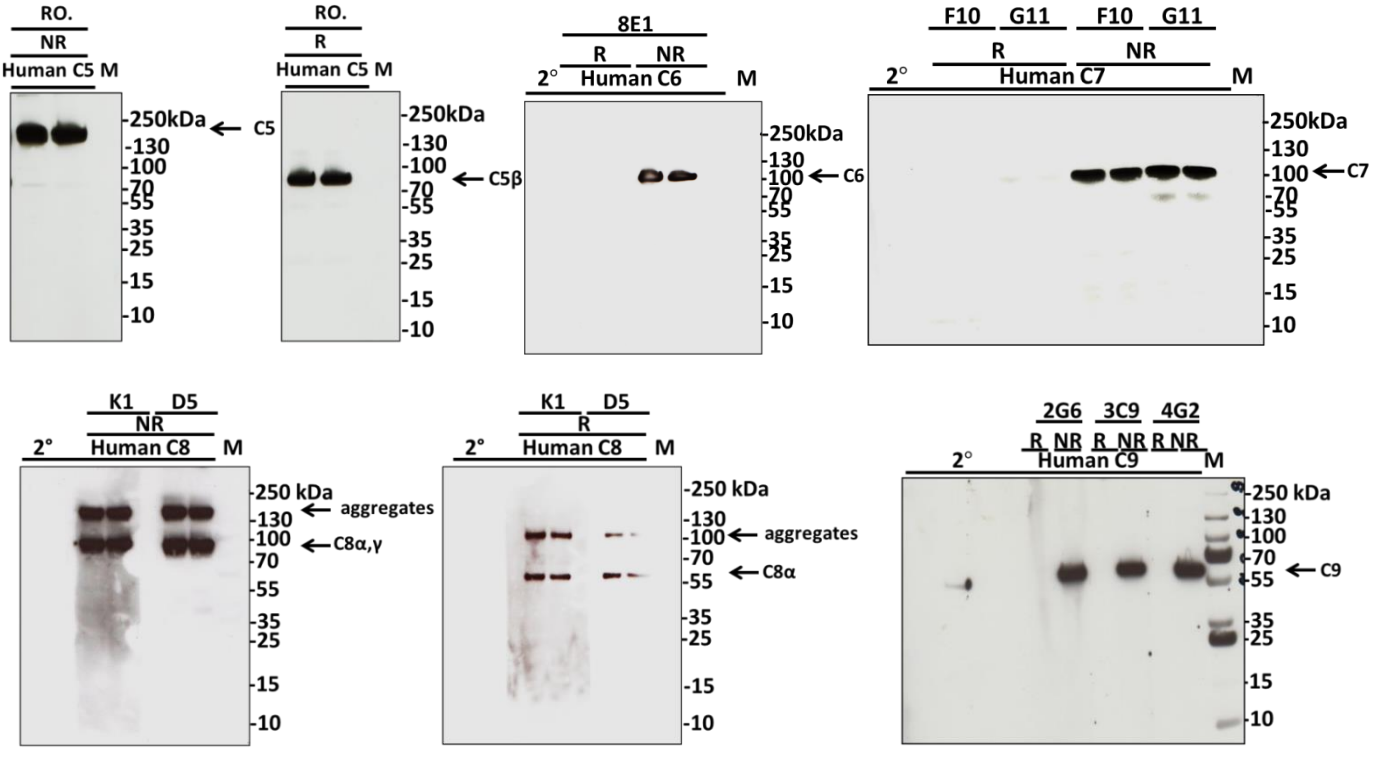
RO.
NR
Human C5 M
250kDa
130
100
70
55
35
25
15
10
C5
RO.
R
Human C5 M
C5β
8E1
R NR
2° Human C6 M
C6
F10 G11 F10 G11
R NR
2° Human C7 M
C7
K1 D5
NR
2° Human C8 M
aggregates
C8α,γ
K1 D5
R
2° Human C8 M
aggregates
C8α
2G6 3C9 4G2
R NR R NR R NR
2° Human C9 M
C9

C.

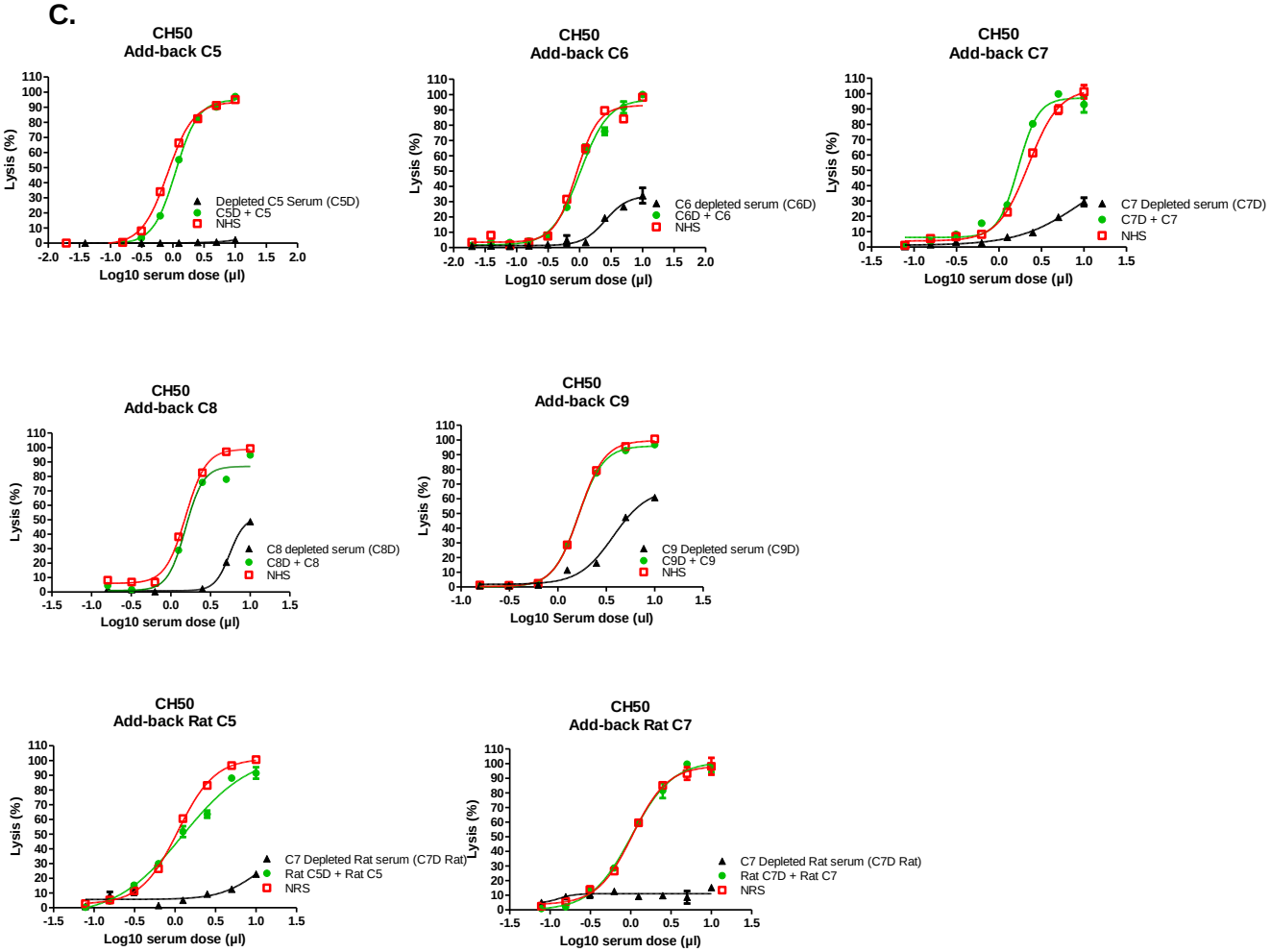
CH50
Add-back C5
Lysis (%)
Log10 serum dose (µl)
Depleted C5 Serum (C5D)
C5D + C5
NHS
CH50
Add-back C6
Log10 serum dose (µl)
C6 depleted serum (C6D)
C6D + C6
NHS
CH50
Add-back C7
Log10 serum dose (µl)
C7 Depleted serum (C7D)
C7D + C7
NHS
CH50
Add-back C8
Log10 serum dose (µl)
C8 depleted serum (C8D)
C8D + C8
NHS
CH50
Add-back C9
Log10 Serum dose (ul)
C9 Depleted serum (C9D)
C9D + C9
NHS
CH50
Add-back Rat C5
Log10 serum dose (µl)
C7 Depleted Rat serum (C7D Rat)
Rat C5D + Rat C5
NRS
CH50
Add-back Rat C7
Log10 serum dose (µl)
C7 Depleted Rat serum (C7D Rat)
Rat C7D + Rat C7
NRS

D.

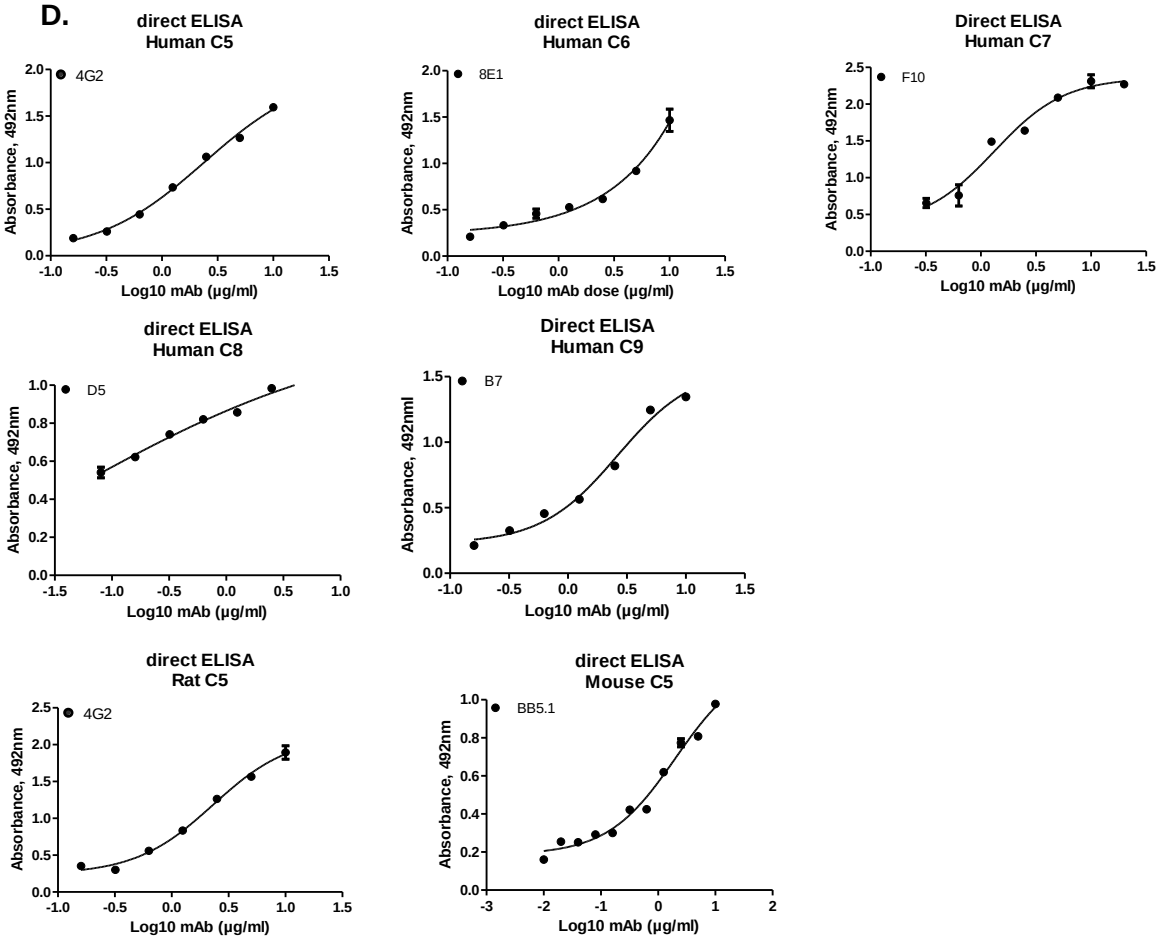
direct ELISA
Human C5
4G2
Absorbance, 492nm
Log10 mAb (µg/ml)
direct ELISA
Human C6
8E1
Log10 mAb dose (µg/ml)
Direct ELISA
Human C7
F10
Log10 mAb (µg/ml)
direct ELISA
Human C8
D5
Log10 mAb (µg/ml)
Direct ELISA
Human C9
B7
Absorbance, 492nml
Log10 mAb (µg/ml)
direct ELISA
Rat C5
4G2
Log10 mAb (µg/ml)
direct ELISA
Mouse C5
BB5.1
Log10 mAb (µg/ml)

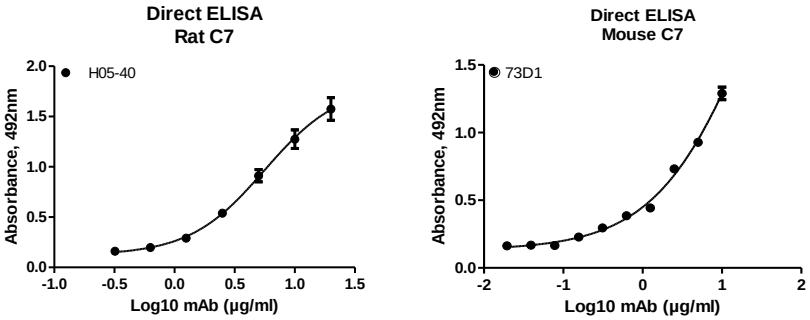

Figure 3.2 Protein characterisation using SDS-PAGE, WB, haemolysis assay and ELISA. A. *SDS-PAGE of affinity purified human, rat and mouse proteins (2µg) resolved on 7.5% or 4 – 20% gels under non-reducing (NR) and reducing (R) conditions, then stained with coomassie blue. Anticipated molecular weights (kDa) of proteins: C5 = 190, C5α = 115, C5β = 75; C6 = 105, C7 = 95; C8; 151, C8α = 64, C8β = 64, C8γ = 22 kDa. M; molecular weight marker (PageRuler, #26620).* ***B.*** *WB analysis of purified proteins (1µg) resolved on 4-20% PAGE gels under NR and R conditions. Blots were probed with mAb RO7112689 for human C5 detection, mAb 4G2 for rat C5, mAb 8E1 for human C6, mAb F10 and G11 for C7, mAb K1 and D5 for C8 and mAb 2G6, 3C9 and 4G2 for C9. Results are representative of multiple analyses. M; protein molecular weight marker, 2°; secondary antibody.* ***C.*** *CP (CH50) haemolytic assays to confirm activity of purified proteins; individual proteins were added-back to respective depleted sera at physiological levels, 10 – 0% serum dilutions prepared. All purified proteins showed efficient restoration of lytic activity after added-back to the depleted sera. NHS, normal human serum, NRS, normal rat serum; C5D, C6D, C7D, C8D, C8D, depleted sera.* ***D.*** *In direct ELISA, plates were coated with protein at 0.5 µg/ml and detected with relevant mAb; 4G2 for human and rat C5 detection, BB5.1 for mouse C5, 8E1 for human C6, 73D1 for mouse C6, F10 for human C7, D5 for human C8 and B7 for human C9. All mAb bound the protein of interest. The error bars are standard errors of triplicates.*

3.3.2 Purification of fully active, endotoxin free human C5 protein using RO7112689

Human and mouse C5 were purified as described in section 3.2 using RO7112689 columns.

3.3.2.1 C5 purified in a single step by immunoaffinity on RO7112689 is homogenous, active and endotoxin-free

In direct comparison with commercial C5 (CompTech), RO7112689-purified human C5 demonstrated similar banding patterns on SDS PAGE under reducing and non-reducing conditions; a single 190 kDa band non-reduced and two bands, 115 kDa (C5α chain) and

75 kDa (C5β chain), under reducing conditions (Fig. 3.3 A, B, C). No other bands were detected in the C5 preparation, confirming the high purity of the protein. Seven separate purifications across 14 months were performed using the same column, producing high quality C5 at high yield each time (Table 3.5). Mouse C5 purified using RO7112689 was also highly homogenous (Fig. 3.3 D). Before the purification, C5 concentration in pooled NHS was measured by ELISA as 81.3 µg/ml, and yield was ~98% (e.g. for purification 6: 350 ml serum, calculated available 28.45mg; purified 27.7mg). The C5 protein was free of endotoxin as confirmed by LAL Chromogenic Endpoint Assay (Fig. 3.3 G). Mouse C5 was also purified to homogeneity on RO7112689 (Fig 3.3 E, F).

Purification No.	**Column**	**Serum applied (ml)**	**Calculated yield**	**Month/year**
Human				
1	5ml	20	-	04/2017
2	5ml	30	96%	05/2017
3	5ml	70	97%	05/2017
4	5ml	180	97%	05/2017
5	5ml	50	98%	09/2017
6	5ml	350	98%	11/2017
7	5ml	332	98%	05/2018
Mouse				
1	1ml	2	92%	02/2018
2	1ml	2	93%	03/2018

Table 3.5 *Purifications performed to date for human and mouse C5 on the RO7112689 columns. The same 5ml column was used for all seven human C5 purifications. Yield was calculated as described in methods for each purification (except for the first purification).*

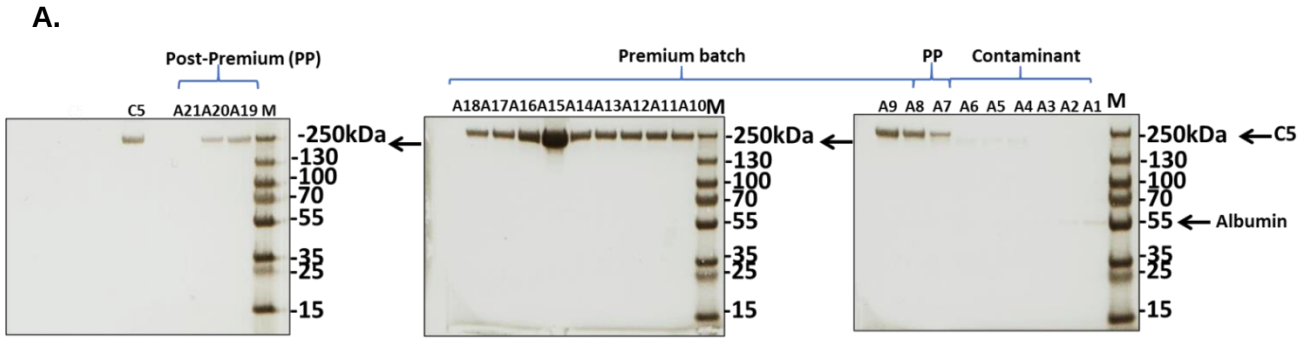
A.
Post-Premium (PP)
Premium batch
PP
Contaminant
C5
A21A20A19 M
A18A17A16A15A14A13A12A11A10M
A9 A8 A7 A6 A5 A4 A3 A2 A1 M
-250kDa
-130
-100
-70
-55
-35
-25
-15
C5
Albumin

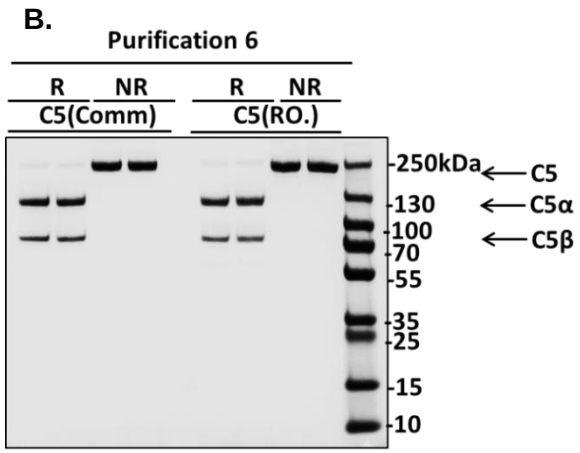
B.
Purification 6
R NR R NR
C5(Comm)
C5(RO.)
250kDa
130
100
70
55
35
25
15
10
C5
C5α
C5β

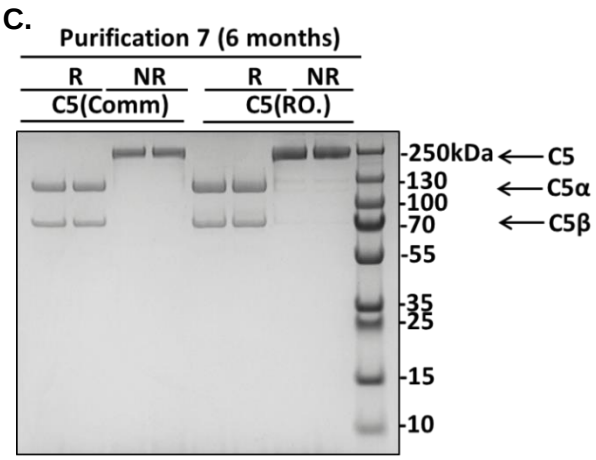
C.
Purification 7 (6 months)
R NR R NR
C5(Comm)
C5(RO.)
250kDa
130
100
70
55
35
25
15
10
C5
C5α
C5β

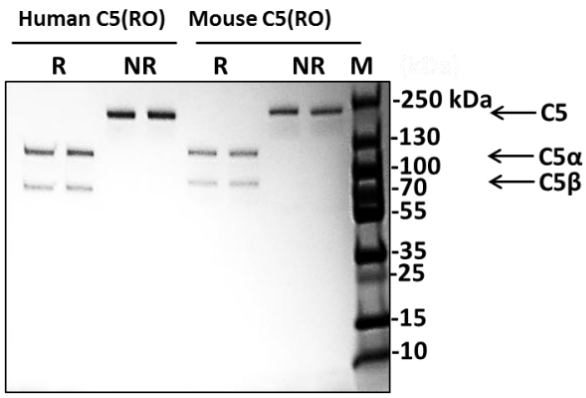
D.
Human C5(RO)
Mouse C5(RO)
R NR R NR M
250 kDa
130
100
70
55
35
25
15
10
C5
C5α
C5β

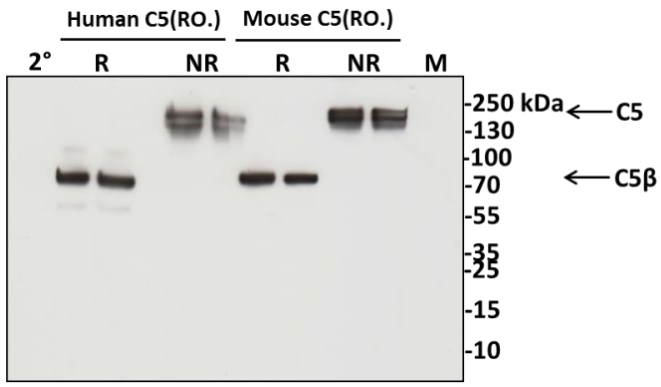
E.
Human C5(RO.)
Mouse C5(RO.)
2° R NR R NR M
250 kDa
130
100
70
55
35
25
15
10
C5
C5β

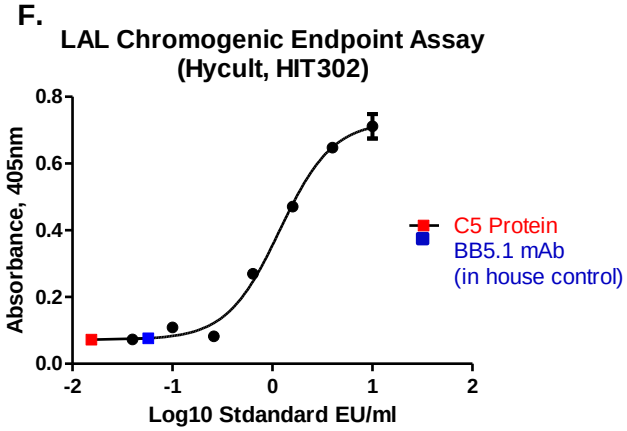
F.
LAL Chromogenic Endpoint Assay
(Hycult, HIT302)
Absorbance, 405nm
0.8
0.6
0.4
0.2
0.0
-2
-1
0
1
2
Log10 Stdandard EU/ml
C5 Protein
BB5.1 mAb
(in house control)

Figure 3.3 Characterisation of purified C5. A. *SDS-PAGE of C5 fractions (purification 6) resolved on 7.5% PAGE gel under non-reduced (NR) conditions, stained with Coomassie Blue. Fractions identified as "Premium" (A8 – A18) contained the most concentrated C5 without contaminant; fractions pre- and post- premium contained lower concentrations of C5 without contaminant (A7, A19 – A21) and were retained separately while fractions A1 – A6 were discarded.* ***B.*** *Premium fractions (prep #6) were pooled and subjected to SDS-PAGE with commercially sourced C5 (CompTech) as a comparator, and stained with Coomassie Blue. NR; 190kDa corresponding to intact C5, R; 115 kDa; C5α chain and 75 kDa; C5β chain. RO; RO7112689.* ***C.*** *As above but with prep #7 performed on the same column 6 months after prep #6 to demonstrate stability of the RO7112689 column and reproducibility of the procedure for purification of human C5.* ***D.*** *SDS-PAGE of human and mouse C5 purified on RO7112689, conditions as described above.* ***E.*** *WB to compare staining of human and mouse C5. Goat anti-human C5 detected the intact C5 in NR conditions and both chains in R conditions in both species, whereas RO7112689 detected intact C5 in NR conditions and only the C5β chain in R conditions for both species. M, molecular marker; Comm., commercial CompTech protein; RO, RO7112689.* ***F.*** *The protein was tested for endotoxin presence using LAL Chromogenic Endpoint Assay (Hycult Biotech, #HIT302); no endotoxin was detected.*

3.3.2.2 Haemolytic assays demonstrate high activity of RO7112689-purified C5

Human C5 was completely removed from 350ml of pooled NHS in a single pass over the RO7112689 column (Fig 3.4 A). Add-back of C5 to C5-depleted serum (C5D) at physiological levels fully restored serum lytic activity, confirming that the C5 depletion was specific and that the purified C5 was fully active (Fig 3.4 B). The C5D reconstituted with RO7112689-purified C5 had a calculated CH50 of 63.4 Units, whereas C5D reconstituted with the same amount of commercial C5 had a CH50 of 40.2 Units. Titration of C5 into a constant dilution of C5D confirmed that commercially sourced C5 was significantly less efficient at restoring haemolytic activity; the dose of C5 restoring to 50% haemolysis in 10% C5D was 221.5 ng/ml for RO7112689 -purified C5 and 714.7 ng/ml for commercial C5 (Fig. 3.4 C). As little as 2ng/ml RO7112689-purified C5 conferred detectable haemolytic activity to 10% C5D (Fig 3.4 D).

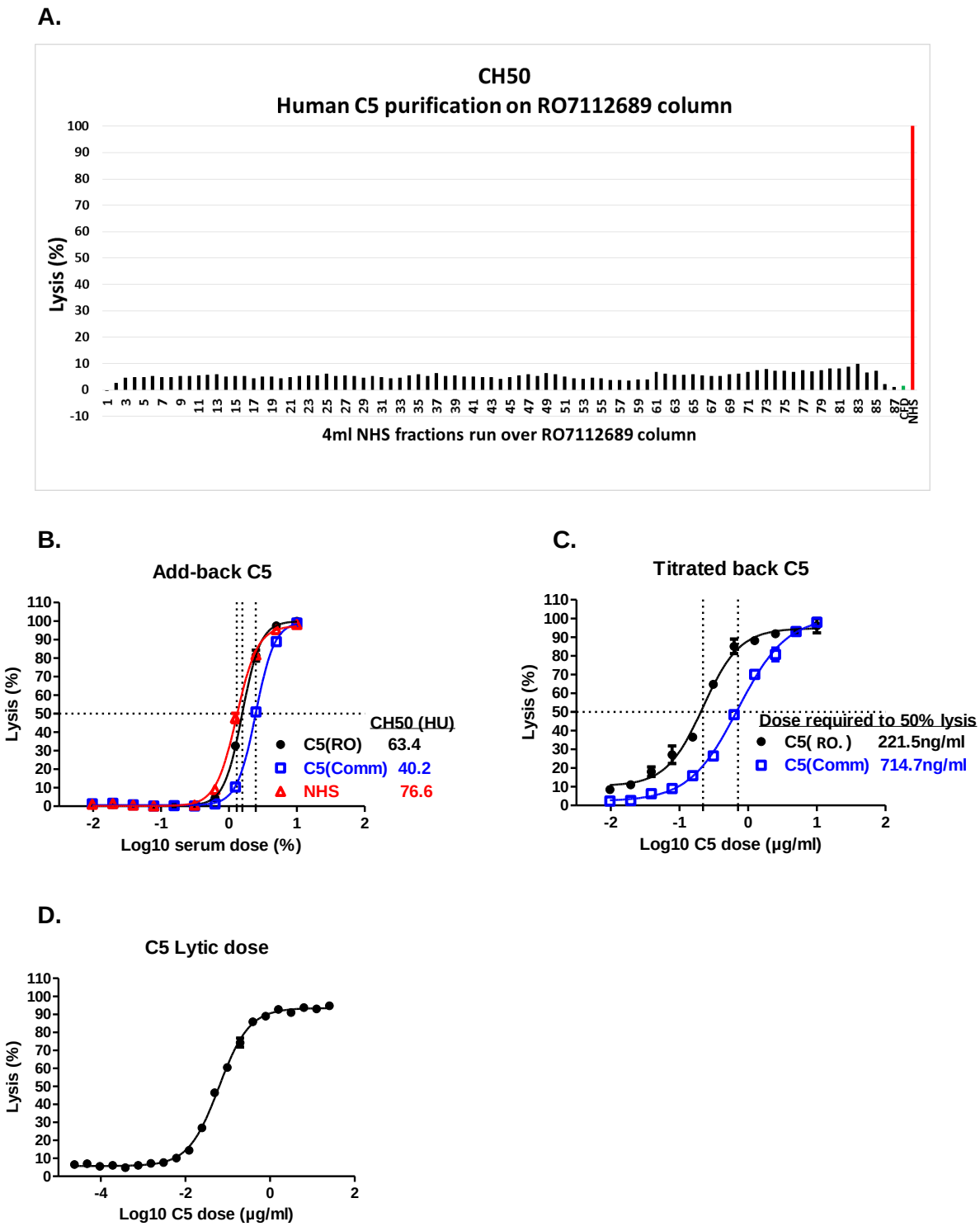

Figure 3.4 Haemolysis assays with human C5 RO7112689-purified

A. *Haemolysis assay on run-through 4ml fractions collected from pooled NHS passed over the RO7112689 column; less than 10% lysis seen in each fraction demonstrating complete depletion of human C5. NHS diluted 1:10 was used as the positive control and showed 100% lysis.* ***B.*** *Repletion with C5; -RO7112689-purified C5 or commercial (CompTech) C5 was added back to neat C5-depleted serum (C5D) at 75 µg/ml; both C5 proteins fully*

restored haemolytic activity but commercial C5 restored serum was less lytic; calculated CH50 values were: RO7112689 C5, 63.4 Units; commercial C5, 40.2 Units. ***C.*** *RO712689-purified C5 or CompTech C5 were titrated back into 10% C5D to measure the dose that restored haemolysis to 50%. The 50% lytic dose of RO7112689-purified C5 was 221.5 ng/ml, whereas that for commercial C5 was 714.7 ng/ml.* ***D.*** *Titration to identify the lowest lytic dose of C5 purified on RO7112689 when added back to C5D; C5 at 2 ng/ml conferred measurable lytic capacity in 10% C5D. RO; RO7112689. The error bars are standard errors of triplicates.*

3.3.3 Purification of CVF

CVF was purified as described in section 3.2.3 using GF followed by Mono Q chromatography. The purified CVF (Figure 3.7) was used for generation of CVFBb convertase, essential for C5b6 production.

3.3.4 Purification of MAC intermediates

C5b6 was purified as described in section 3.2.4.1 according to the two different protocols using serum previously depleted of C7, C8 and C9 (C789D) resulted in a better yield (Table 3.6).

Protein	Method used	Calculated yield
C5b6	Generated from purified components (DiScipio protocol)	25%
C5b6	Generated from activated C789D serum (Morgan protocol)	33%
C5b67	Incubation of C5b6 + C7 (1:1 molar ratio)	74%
sC5b-9	Generated from activated NHS	35%

Table 3.6 *Summary of the average purification yields of TP complexes (from at least two purifications). Yields were calculated as described in methods.*

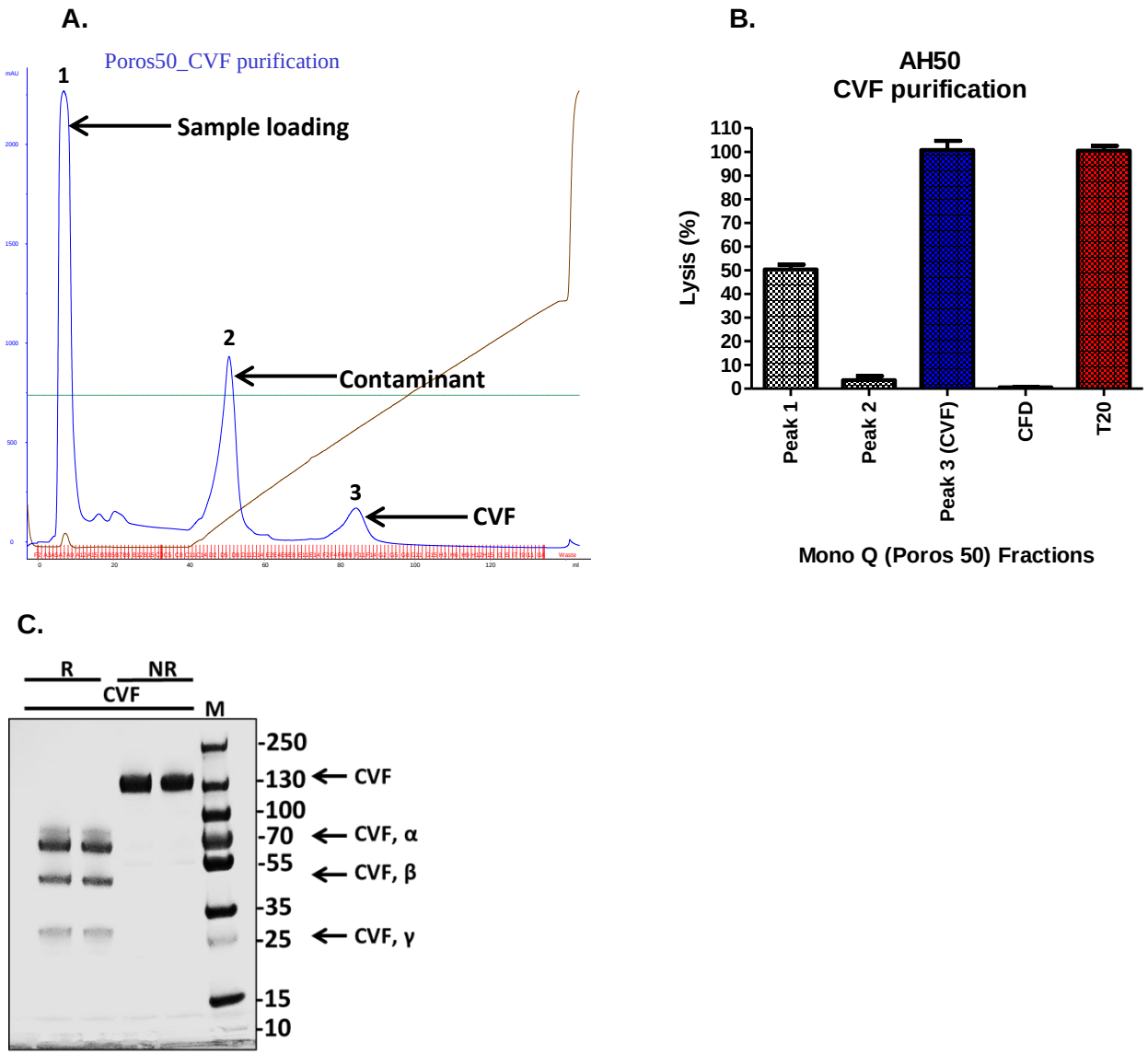

Figure 3.5 Purification and Characterisation of CVF. A. *HPLC AKTA chromatogram from CVF purification using mono Q Poros 50 column; CVF, identified in haemolytic assay (AH50), eluted in peak 3 (**B**). GPE (2% in APB) were incubated with 10% NHS and aliquots of column fractions. C5 cleavage by CVFBb convertase resulted in lysis of GPE. Red bar (T20; 0.1% Tween 20), Blue bar, peak 3 containing CVF. The error bars are standard errors of triplicates.* ***C.*** *SDS-PAGE of purified CVF resolved in 7.5% PAGE gel nNR and R, stained with Coomassie Blue, NR; 146kDa band corresponding to intact CVF, R; bands at 68kDa (CVFα chain), 48kDa (CVFβ chain) and 30kDa (CVFγ chain). M, molecular weight markers.*

3.3.4.1 Generation of C5b6 from purified components

C5b6 was purified as described in section 3.2.4.1.1 The GF fractions were analysed by SDS-PAGE and haemolytic assay (Fig. 3.6 C). GF separated C5b6 from aggregates (Fig. 3.6 A); C5b6-containing fractions showed high efficiency in reactive lysis of GPE (Fig. 3.6 B).

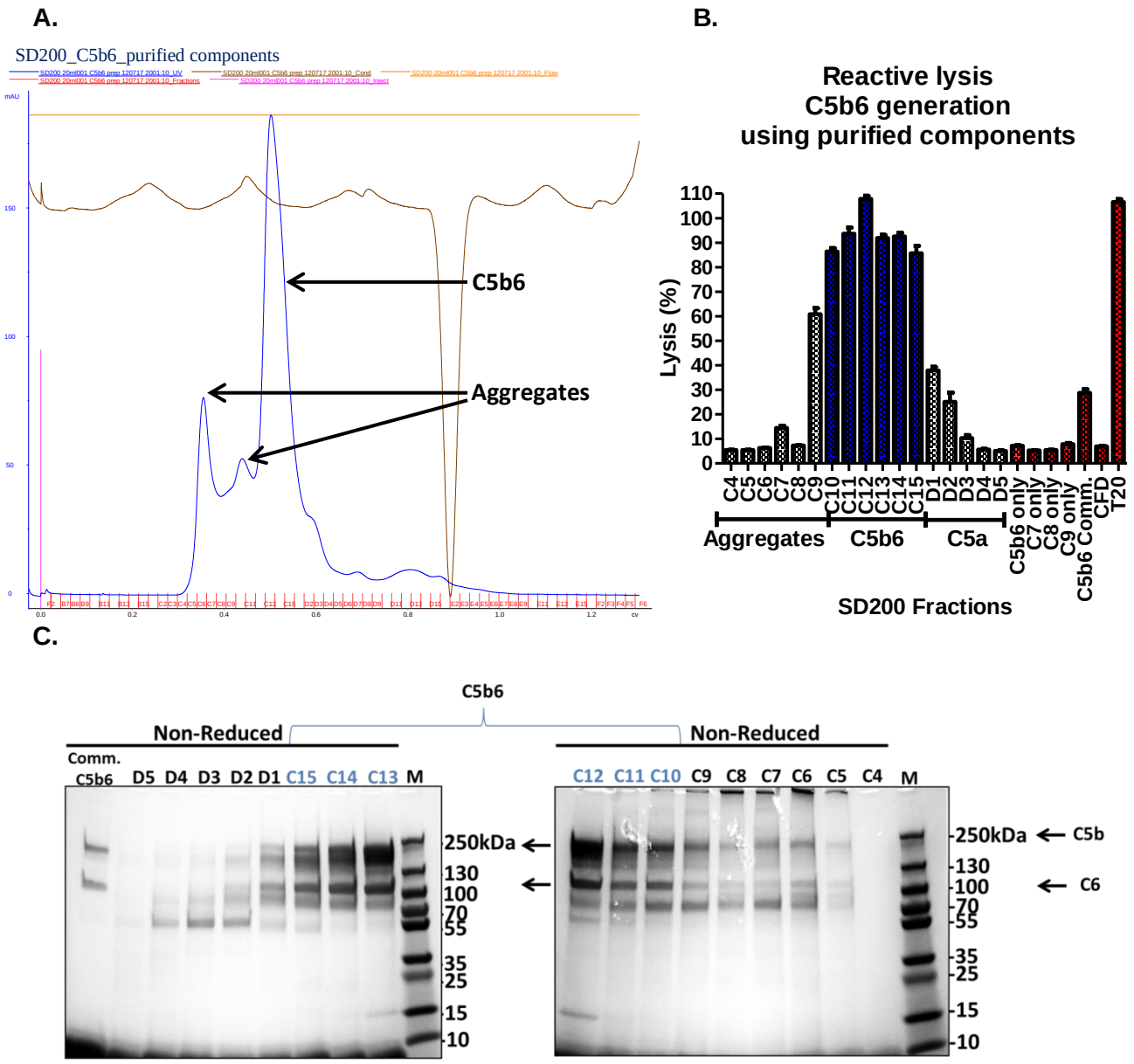

Figure 3.6 Characterisation of C5b6 generated using purified components A. *SD200 chromatogram of C5b6 purification; peak 1 contained C5b6 aggregates; peak 2 active C5b6; peak 3 likely contained C5a.* ***B.*** *Reactive lysis assay; fractions were incubated with 2% GPE in CFD, and then C7, C8 and C9 were added. Fractions C10 – C15 showed strong haemolytic activity. Positive control was 0.1% Tween 20 (red bar; T20). The error bars are standard errors of triplicates.* ***C.*** *SDS-PAGE of purified C5b6; 20µl neat fraction resolved in 4 – 20% PAGE gel under NR conditions, stained with Coomassie Blue., NR; the ~205 kDa band corresponds to C5b and the ~105k Da band corresponds to C6. Comm. C5b6; Commercial C5b6 (CompTech) showed two bands at these same molecular weights but had poor haemolytic activity compared to the in-house generated C5b6. This was a result of subsequent protein degradation, being defrosted in a few days delayed transit.*

SDS-PAGE identified gel bands corresponding to C5b and C6 under NR conditions (Fig. 3.8 C). The calculated purification yield based on input proteins was 25%**.**

3.3.4.2 Generation of C5b6 from C789 Depleted serum

C5b6 was purified from activated C7/C8/C9 depleted serum (C789D) by immunoaffinity and GF columns (section 3.2.4.1.2). The first large peak from the GF (SD200) eluted fractions comprised C5b6 (Fig. 3.7 A-C). The pooled, purified C5b6 showed high efficiency of GPE lysis; total lysis was observed with 125ng/ml C5b6 (Fig. 3.7 D). By dot-blot C5b and C6 were detected in the first peak fractions only (Fig. 3.7 E). Bands corresponding to C5b (~205 kDa) and C6 (105kDa) were observed in SDS-PAGE (Fig. 3.7 F). The calculated purification yield was ~33% based on the estimated amounts of C5 and C6 in the C789D.

3.3.4.3 Generation of C5b67

C5b67 was generated by incubating C5b6 with C7 in 1:1 molar ratio for 2 hours at ambient temperature. The complex was purified by gel filtration showing some aggregates (Fig. 3.8 A). C5 and C7 were detected in the same GF fractions dot-blotted onto nitrocellulose membrane (Fig. 3.8 B). In NR conditions, bands at 95 kDa (C7), 105 kDa (C6) and 205 kDa (C5b) were present (Fig. 3.8 C). The calculated purification yield based on protein input was 74%. To test whether this complex was haemolytically active, reactive lysis with human purified components was performed, when GPE were incubated with C5b67 and C8 and C9 were added lysis was observed, albeit not to the same level as obtained with standard reactive lysis using C5b6 and other components. (Fig. 3.8 D).

3.3.5 Generation of sC5b-9

Human sC5b-9 was generated by serum activation with zymosan and aggregated IgG as described in section 3.4.3. The complex was affinity purified using E2 anti-C8 mAb (Fig. 3.9 A) followed by gel filtration (Fig 3.9 B). sC5b-9 is composed of ~13 polypeptides chains with a combined size of ~1,030 kDa. Variability in molecular weight is a result of different numbers of C9 or S protein/clusterin molecules per complex (usually between 1 – 3 for each). SDS-PAGE of the purified complex showed that it contained each terminal pathway component (Fig. 3.9 C), confirmed by WB and ELISA (Fig. 3.9 D, E). The calculated purification yield was 35% based on C5 turnover.

A.

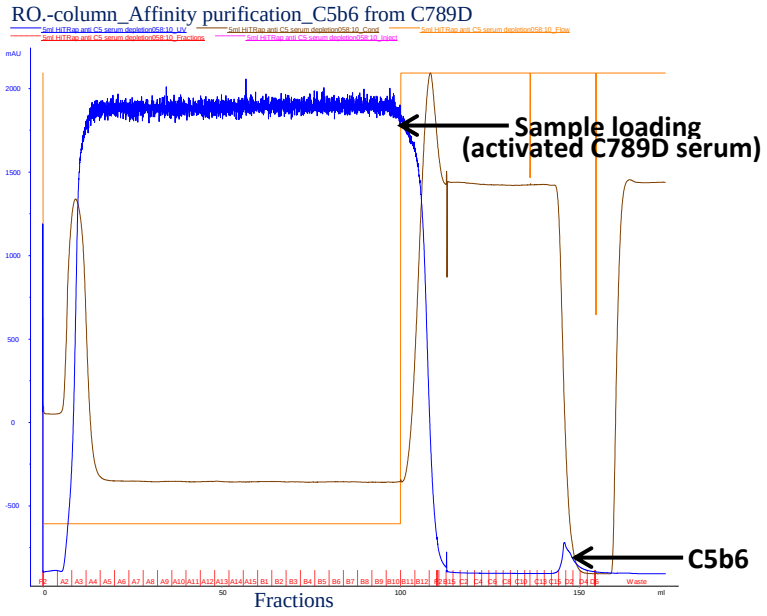
RO.-column_Affinity purification_C5b6 from C789D
Sample loading
(activated C789D serum)
C5b6
Fractions

B.

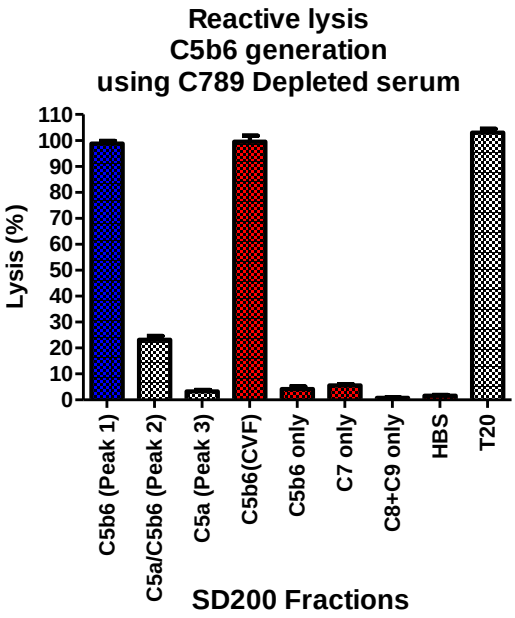
Reactive lysis
C5b6 generation
using C789 Depleted serum
Lysis (%)
C5b6 (Peak 1)
C5a/C5b6 (Peak 2)
C5a (Peak 3)
C5b6(CVF)
C5b6 only
C7 only
C8+C9 only
HBS
T20
SD200 Fractions

C.

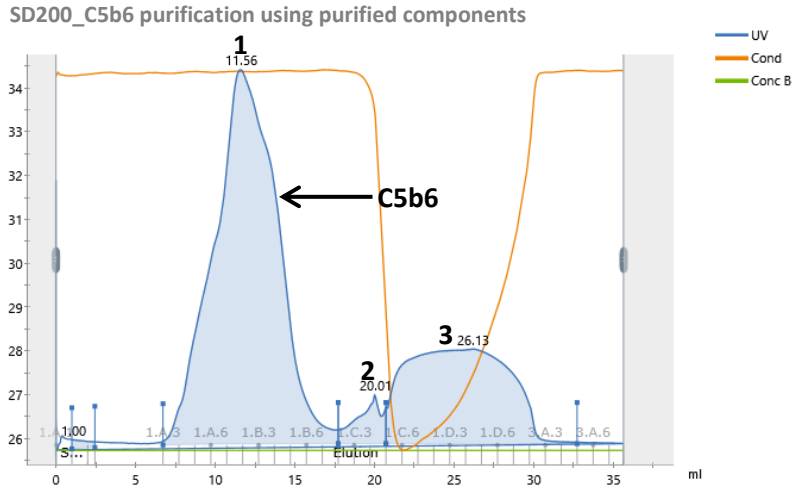
SD200_C5b6 purification using purified components
UV
Cond
Conc B
C5b6
Elution
ml

D.

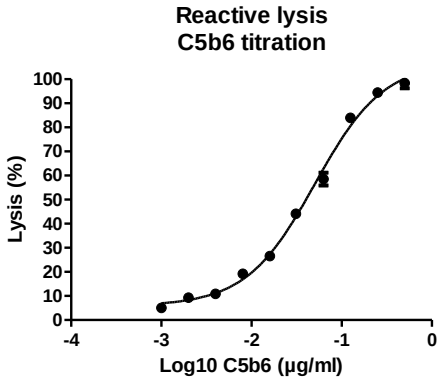
Reactive lysis
C5b6 titration
Lysis (%)
Log10 C5b6 (µg/ml)

E.

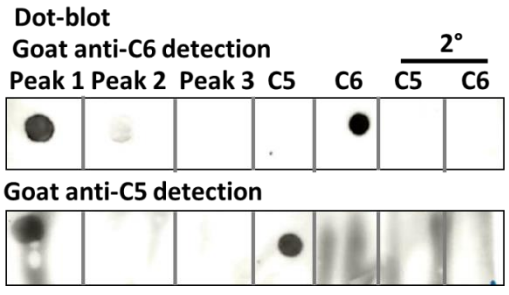
Dot-blot
Goat anti-C6 detection
Peak 1 Peak 2 Peak 3 C5 C6 C5 C6
2°
Goat anti-C5 detection

F.

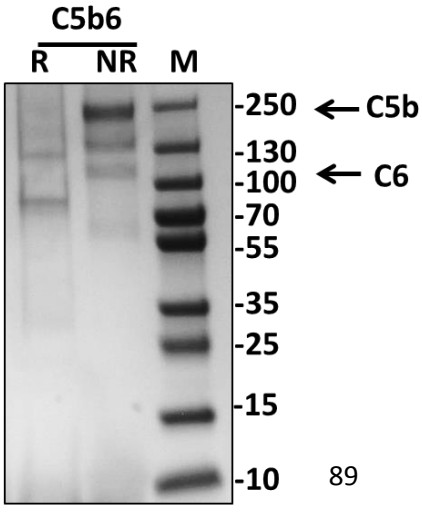
C5b6
R NR M
C5b
C6

Figure 3.7 Characterisation of C5b6 generated from C789D serum. A. *Chromatogram of C5b6 affinity purification using anti-C5 mAb (1ml RO7112689 column). After dialysis to HBS, the eluted peak fractions were concentrated and further purified using SD200 column* ***C****; peak 1 contained C5b6 as demonstrated by haemolytic assay as above (****B****). Activity was confirmed by titration of C5b6; complete lysis was obtained with 125ng/ml C5b6. (****D****). The error bars are standard errors of triplicates.* ***E****. The protein was dot-blotted onto nitrocellulose (5µl) and detected using polyclonal anti-C5 and anti-C6 mAb; both C5 and C6 were detected in the peak.* ***F.*** *SDS-PAGE of C5b6 resolved in 4 – 20% PAGE gel under NR and R conditions, stained with Coomassie Blue. In NR conditions bands at 205 kDa (C5b) and 105 kDa (C6) were present.*

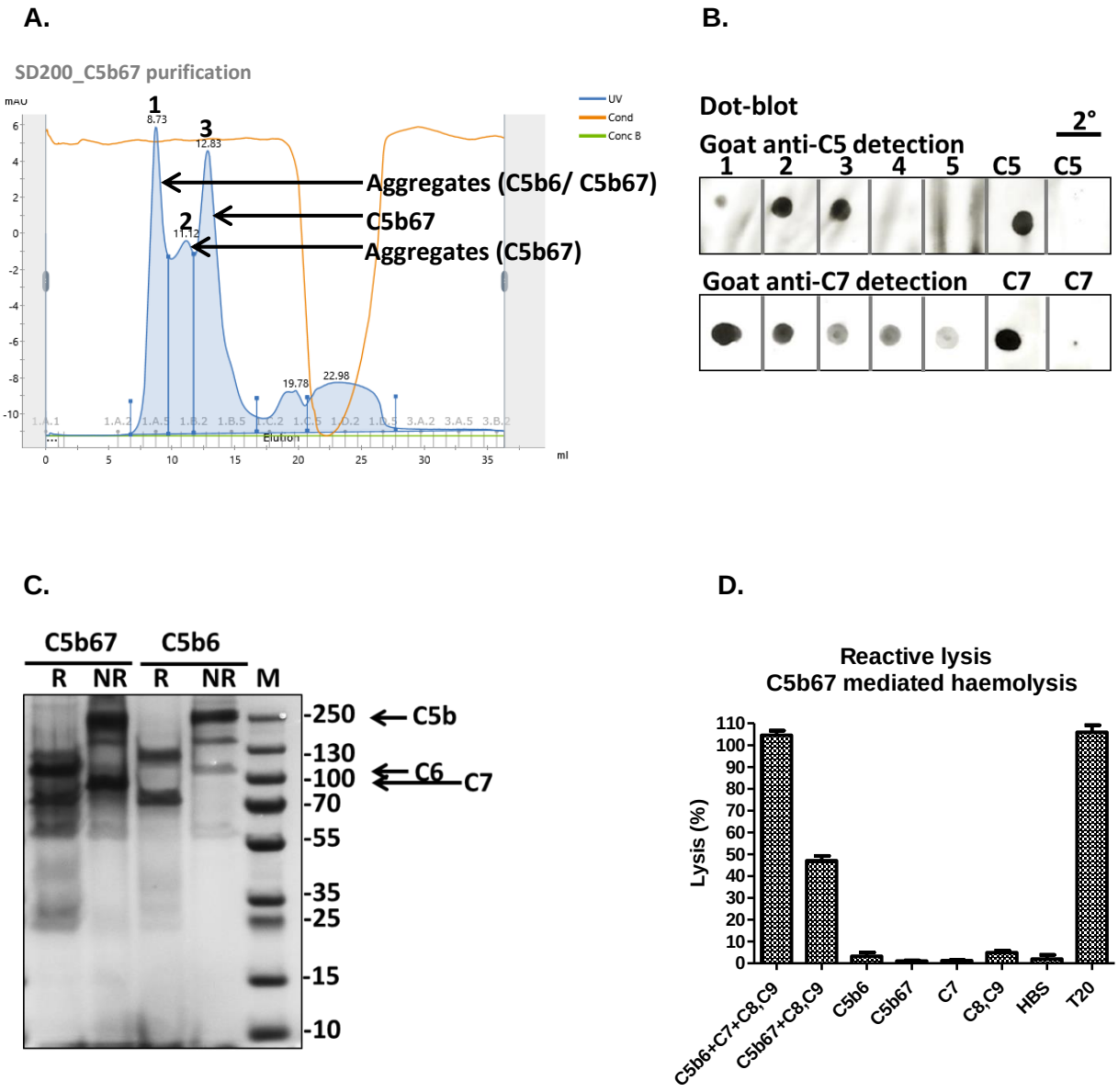

Figure 3.8 Characterisation of C5b67 using purified components; A. *GF chromatogram of C5b67; the first set of peaks all contained C5b67 haemolytic activity, likely representing aggregates and non-aggregated C5b67; unbound C7 eluted in the final peak.* ***B.*** *Peak fractions were pooled, dot blotted onto nitrocellulose and detected using polyclonal anti-C5 and anti-C7; C5 and C7 were detected in the same fractions.* ***C.*** *SDS-PAGE (7.5%) of C5b6 and C5b67 under NR and R conditions, stained with Coomassie Blue. NR; bands were present at 95 kDa (C7), 105 kDa (C6) and 205 kDa (C5b).* ***D.*** *Reactive lysis utilising human; GpE were incubated with C5b67, washed and developed with C8/C9. Controls included individual proteins (no lysis), C5b6 at the same dose plus C7, C8 and C9 (full lysis). T20; 0.1% Tween 20. All experiments were repeated three times with comparable results. The error bars are standard errors of triplicates.*

A.

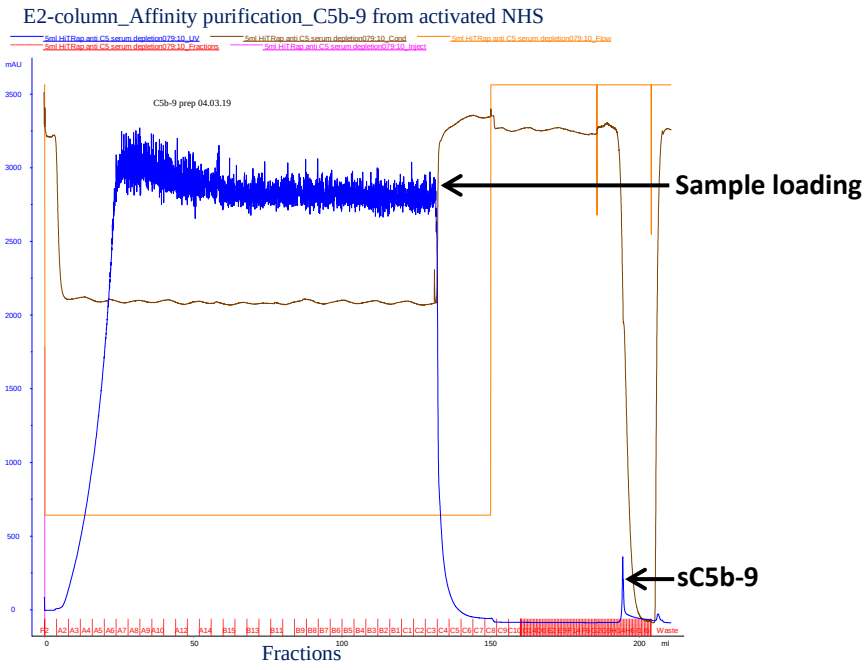

B.

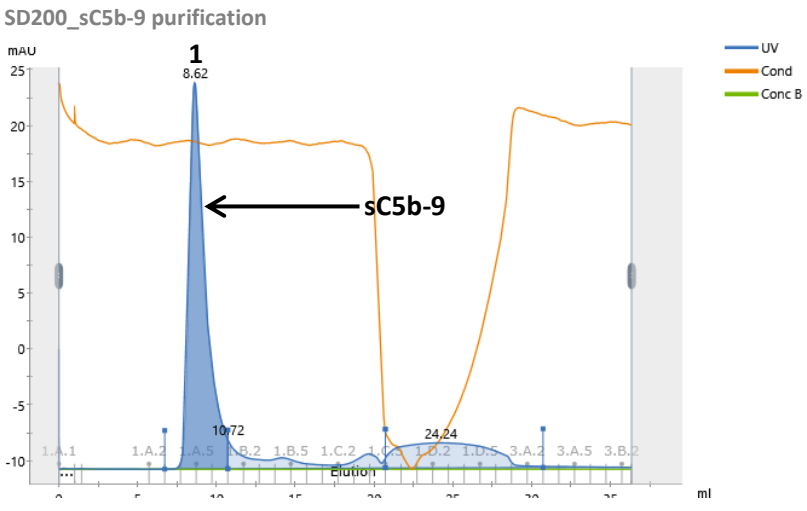

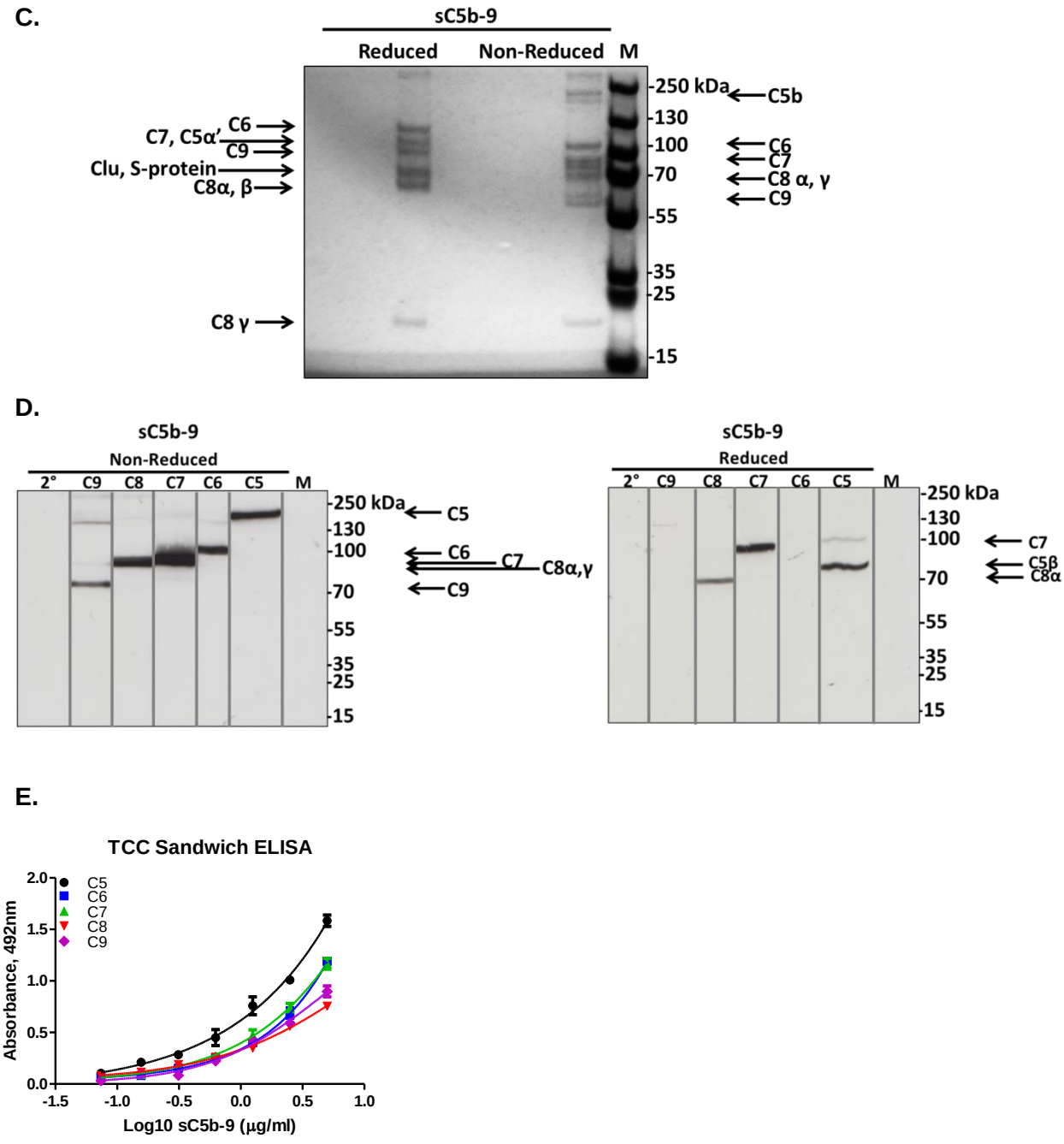

Figure 3.9 Characterisation of sC5b-9 using purified components. *Chromatograms of sC5b-9 affinity purification (**A**) and GF (**B**); the sharp peak 1 from GF contained SC5b-9. Pooled peak 1 fractions were resolved (2µg) in 7.5% SDS-PAGE gel under NR and R conditions, stained with Coomassie Blue (**C**) or subject to WB (**D**). sC5b-9 was probed with the antibodies; Goat anti-C5, 22D1 anti-C6, Goat anti-C7, E2 anti-C8 and B7 anti-C9. NR: C5b, 205 kDa; C6, 105 kDa; C7, 95 kDa, C8αγ; 70 kDa; C9, 65 kDa. R: C6, 110 kDa, C7/ C5α', 100 kDa; C9, 70kDa; C8α/β, 65 kDa; C8γ, 22 kDa; Clusterin (Clu.) and S-protein, 75 kDa. In WB, C6 (22D1) and C9 (B7) were not detectable in R conditions. The blots were*

cut into strips to detect the individual protein and re-aligned. ***E.*** *Sandwich ELISA; the sC5b-9 complex was captured using Goat anti-C9 antibody and detected with in house monoclonal antibodies; 10B6 anti-C5, 22D1 anti-C6, F10 anti-C7, E2 anti-C8 and B7 anti-C9. All experiments were repeated three times with comparable results. The error bars are standard errors of triplicates.*

3.3.6 Purification of mAb

IgG1 and IgG2a/2b isotype mAb (determined with Isostrip, Roche, # 11493027001) were purified using protein G chromatography on an AKTA HPLC purifier. Integra supernatant was filtered prior to purification. An example chromatogram of the purification is shown below (Fig. 3.10 A). For most of the IgG mAb, single-step purification yielded pure IgG with no contaminants (Fig. 3.10 B). IgM mAb was purified using ammonium sulphate precipitation as described in section 3.2.6.2. The concentration of the purified antibodies was measured using NanoDrop and confirmed by BCA assay (yield was ~1mg mAb per ml of Integra supernatant). Protein was concentrated prior to storage frozen in aliquots at >1mg/ml.

A.

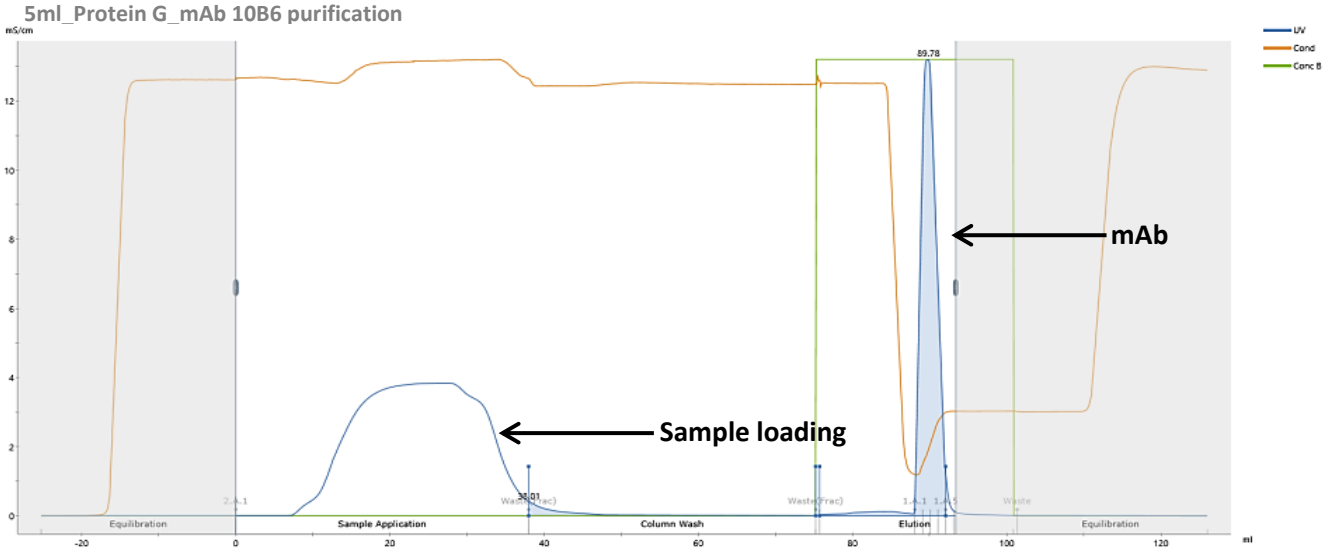

B.

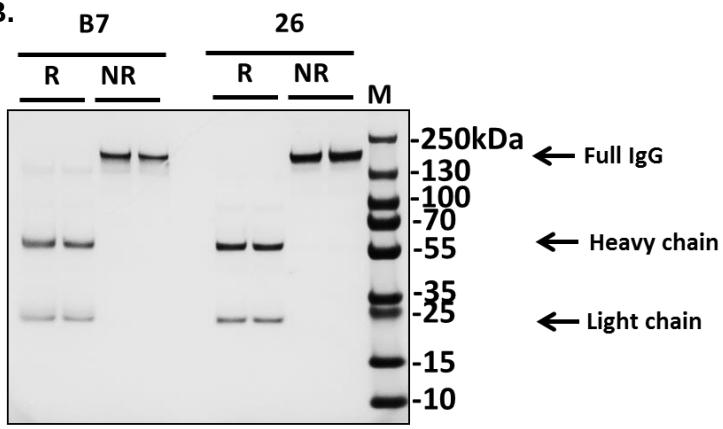

Figure 3.10 A*. *Example chromatogram and SDS-PAGE of mAb purification on Protein G *(10B6 anti-C5). Supernatant was passed over the column and bound IgG eluted as a single peak.* ***B.*** *SDS-PAGE gel of purified IgG; mAb anti-C9 (clone B7 and 26) were resolved on 7.5% gels under NR and R conditions, then stained with coomassie blue. The 150 kDa band corresponds to intact IgG; in R lanes the 55 kDa band corresponds to mAb heavy chain and 25 kDa to mAb light chain. M; molecular weight marker (PageRuler, #26620).*

3.4 Discussion

In this chapter I have described production of human and rodent complement proteins, complexes and other reagents essential for the aims of this project. In the current anti-complement landscape C5 is the favourite target for therapeutic intervention; nearly half of drugs in development target C5 (Harris 2018; Zelek *et al* 2019). The novel C5 purification method I developed using RO7112689 antibody offers many advantages over conventional techniques. C5 purified using this method is highly pure and functionally intact. The great advantage of this method is that is efficient, fast and produces a high yield of fully active C5. C5 was depleted completely from 350ml serum with a single pass over the RO7112689 column (Fig. 3.3, 3.4). By taking advantage of the pH dependence of mAb RO7112689 I eliminated the need for exposure to extremes of pH (shifting form neutral pH to pH 2.5 was damaging for the protein). RO7112689, in Phase 2 clinical trials, has been developed to recycle in vivo by shedding its cargo in acidic pH (~5.5) in endosome (Fukuzawa *et al* 2017). This recycling mechanism enhances the mAb therapeutic potential by reducing dose (Igawa *et al* 2010; 2014). The successful purification of C5 using this mAb is a proof of concept solution for isolation of pH sensitive proteins. A pH dependent antibody can be developed relatively simply through engineering of CDRs or, as in the case of RO7112689, selected by screening for pH sensitivity during the cloning steps.

The functional assays and intermediates developed during this project are powerful tools for exploring interactions in MAC formation; having high-quality, reliable and reproducible protein complexes was fundamental for this work. C5b6 was purified either using purified components or from activated C789 depleted serum; the latter gave higher yield of functional C5b6. C5b6 produced using both methods showed high lytic activity, contained both C5 and C6 as demonstrated by dot-blot and ELISA (Fig. 3.7). Purified C5b6 was used to generate the C5b67 complex by addition of C7 (Fig. 3.8), for functional testing of the mAb (chapter 5); C5b67 made in this way retained the capacity to trigger reactive lysis making it also useful for functional assays of mAb activities. The sC5b-9 complex was also generated, purified and characterised for investigation of mechanisms in terminal pathway fluid phase

interactions. All the terminal pathway proteins were detected in the complex by WB and ELISA and SDS-PAGE (Fig. 3.9).

All mAb were purified with a high yield using standard methods. The hybridoma cell growth was optimised for maximum mAb production by growing in Integra bioreactors (section 2.17.3), producing between 1 – 2mg of mAb per ml of the hybridoma tissue culture supernatant. Addition of the reducing agent β-ME increased cell growth by ~50%, thereby increasing significantly production of the mAb.

The next two chapters will discuss the generation of the function-blocking mAb against terminal pathway proteins and complexes that are the principle outcomes of the project.

CHAPTER 4; DEVELOPMENT AND CHARACTERISATION OF NOVEL ANTI-C5 MONOCLONAL ANTIBODIES CAPABLE OF INHIBITING COMPLEMENT IN MULTIPLE SPECIES

4.1 Introduction

Over the last decade there has been an explosion in complement drug development. Eculizumab, an anti-C5 monoclonal antibody, was a landmark in this work, approved by the US Food and Drug Administration (FDA) in 2007 for use in PNH (Rother *et al* 2007; Hilmen *et al* 2006; Brodsky *et al* 2008), four years later for aHUS (Wong *et al* 2013) and recently for generalised myasthenia gravis (gMG) (news.alexionpharma.com/press-release/product-news/fda-approves-soliris-eculizumab-treatment-patients-generalized-myasthenia) and NMO (https://news.alexion.com/press-release/product-news/alexion-receives-fda-approval-soliris-eculizumab-treatment-adults-neuromy). Eculizumab rapidly became the standard treatment for the two ultra-rare complement driven diseases PNH, aHUS. A host of new agents are in development, targeting the cascade at different stages; however, nearly half of them target C5 (Harris 2018; Morgan and Harris 2015; Zelek *et al* 2019). C5 occupies a central position in the complement cascade; the C5 convertase cleaves C5 into C5a and C5b, the former a powerful driver of inflammation, the latter essential for MAC assembly. Inhibition of C5 is thus an attractive therapeutic target and the focus of several drugs in development (Morgan 1999; Morgan and Harris 2015; Ricklin *et al* 2018, Ricklin and Lambris 2019). Eculizumab prevents cleavage of C5 by the C5 convertase, blocking generation of the two most inflammatory products of the complement cascade; C5a anaphylatoxin and MAC. The risk of blocking C5 is relatively low; the sole iatrogenic impact of treatment with Eculizumab is an increased risk of Neisserial infections, resolved by vaccination prior to treatment and prophylactic use of antibiotics.

Despite abundant interest in complement drugs, only three are currently FDA approved; Eculizumab and a recently approved variant engineered for extended half-life, Ravalizumab (ALXN1210; https://ascopost.com/News/59600), and serum-derived and recombinant C1-Inhibitor marketed as Cinryze or Berinert and used in a single, rare indication, hereditary angioedema (Harris 2018; Zelek *et al* 2019). As noted above, Eculizumab has changed outlook in patients with PNH and aHUS, is now in the clinic for gMG, NMO and in clinical trials for many other diseases. Although effective in these rare diseases, the cost of treatment and high dosage are huge disadvantages for extending use to more common diseases; annual cost of Eculizumab treatment of a PNH patient is £340,000 in the UK, and the antibody must be administered bi-weekly by intravenous infusion (900mg/dose) (Morgan and Harris 2015). There are several agents in development that target C5, for

example, SKY59 (RO7112689; RG6107; Crovalimab) an anti-C5 mAb, now in phase 2 clinical trials for PNH, that incorporates a pH dependent recycling technology to increase half-life and decrease dose required for efficient C5 inhibition (Fukuzawa *et al* 2017). The modified form of Eculizumab, Ravulizumab, uses a similar pH switch technology to increase recycling efficiency and drug half-life (Lee *et al* 2018; Sheridan *et al* 2018). (Zelek *et al* 2018). Commercial RO7112689 and Eculizumab were used in this study for comparison with the novel in-house mAb.

In this chapter I describe the development and characterisation of novel mAb that inhibit human C5 activity. The mAb were further tested to determine whether any of these mAb recognised and functionally inhibited C5 from other species as this would make them powerful tools for proof-of-concept animal studies. One of these mAb was shown to efficiently inhibit complement *in vivo* in rats and to prevent disease in a rat EAMG model. The binding affinities of mAb for C5, measured using Surface Plasmon Resonance (SPR) analysis of selected mAb, demonstrated strong and stable binding to both human and rat C5, making these antibodies strong candidates for tool therapeutics.

4.2 Specific methods

All chemicals, except where otherwise stated, were obtained from either Fisher Scientific UK (Loughborough, UK) or Sigma Aldrich (Gillingham, UK), and were of analytical grade. All tissue culture reagents and plastics were from Invitrogen Life Technologies (Paisley, UK). Sheep and guinea pig erythrocytes in Alsever's solution were from TCS Biosciences (Claydon, UK). Eculizumab was kindly donated by Prof David Kavanagh (Newcastle University, UK), and RO7112689 by Roche Diagnostics (Basel, Switzerland).
Human and animal sera were prepared as described in chapter 2.

4.2.1 Generation of anti-C5 mAb

Mouse mAbs to C5 were generated by immunization of C6-deficient mice (bred in-house) with C5b6 using standard schedules (Kohler and Milstein 1975). C5b6 was used as immunogen to increase the likelihood of obtaining function-blocking mAbs. The C6 deficient mice were derived from a spontaneously arising C6 deficient mouse (Orren *et al* 1986), back-crossed 8 generations onto C57Bl/6. C5b6 was prepared in house as described in chapter 3. Immunised mice were screened for antibody responses by ELISA, mice with the highest titre response selected and re-boosted prior to sacrifice and harvesting of spleens. Plasma cells were harvested, fused with SP2 myeloma and aliquoted to 96-well plates. Positive hybridomas were selected by direct ELISA on immobilised C5b6 and by haemolysis

assay for blocking activity as described below. C5b6-positive complement inhibitory mAb-secreting clones were sub-cloned by limiting dilution to monoclonality.

4.2.2 Haemolytic Assays

The inhibitory activity of mAbs in human and animal sera was investigated by CP haemolysis assay using ShEA or AP assays utilising rabbit erythrocytes (RabE) as described in 2.17.5. Hybridoma supernatants were screened for blocking mAbs using the same assay but with neat tissue culture supernatant in place of the purified mAb. C5a generation in CP haemolysis assay supernatants was measured using an ELISA kit (Hycult Biotech, # HK349-02).

4.2.3 Characterisation of mAb by ELISA

Direct and sandwich ELISA were used to test whether the new mAbs bound C5, C6 or C5b6. Sandwich ELISA were used to confirm C5 binders in order to eliminate issues around denaturation and demonstrate whether the test mAbs bound the same or separate epitopes to control mAbs RO7112689 or Eculizumab used as capture. Standard curves were generated using in-house C5, C5b6 and C6 purified as previously described (Zelek *et al* 2018; 2018).

In the direct ELISA, Maxisorp (Nunc, Loughborough, UK) 96-well plates were coated with C5, C5b6 or C6 (0.5µg/ml in bicarbonate buffer pH 9.6) prior to incubation with purified mAb or tissue culture supernatant. In the sandwich ELISA, Maxisorp plates were coated with RO7112689 or Eculizumab then incubated sequentially with purified proteins C5, C5b6 or C6, in-house mAb anti-C5, HRP-labelled anti-mouse IgG and OPD developer as described in chapter 2 (2.2.1). Assays detection limits, working ranges and assay performance were determined as described (Ingram *et al* 2012).

4.2.4 Characterisation of mAb by WB

C5, C5b6 and C6 (in house; 1µg in 25µl PBS in SDS PAGE running buffer) were placed in separate wells in 4-20% SDS-PAGE gels (Biorad, #4561093), resolved under R and NR conditions, electrophoretically transferred to nitrocellulose, then probed with individual test or control mAbs or polyclonal (goat) anti-human C5 (CompTech; A220; 2µg/ml) followed by respective HRP labelled secondary antibodies as described in chapter 2. After washing, the blots were developed with ECL and visualised by autoradiography.

4.2.5 Testing impact of mAb on atypical cleavage of C5 by neutrophil elastase

C5 was incubated with test mAb at 5x molar excess (C5: mAb; 736.84: 3684.2 nM) in HBS for 15 minutes at RT. Neutrophil elastase (NE, Athens Research, Athens, Georgia; # 16-14-051200) was added at 420nM final concentration, incubated 30 minutes at 37°C in a shaking water bath, and the reaction stopped by addition of 61nM protease cocktail inhibitors (CI, Sigma Aldrich, #P8340). C5 cleavage was determined by measuring generation of C5a, detected by WB and by ELISA (Hycult Biotech, # HK349-02). For WB, samples were diluted 1 in 2 in HBS, separated and transferred as above. Blots were probed with anti-C5a mAb (Hycult Biotech, #HM2079), detected using donkey anti-mouse IgG-HRP (Jackson ImmunoResearch, 715-035-150). Positive controls included intact C5 (in house), C5a (CompTech, Texas, USA), NE and CI diluted in HBS.

4.2.6 SPR analysis to determine mAb binding affinity to human rat or mouse C5

The mAb to C5 protein interactions were measured in real time using Surface Plasmon Resonance (SPR) (Douzi, 2017). The SPR assays were run on a Biacore™ T200 or S200 System at a flow rate of 30µl/minute with 0.01M HEPES pH 7.4, 0.15M NaCl, 3mM EDTA, 0.005% w/v Surfactant P20 (EP-HBS) as the running buffer. The anti-human C5 mAb binding analyses were carried out on a Biacore S200, while anti-rat/ mouse C5 mAb binding was tested using a Biacore T200 instrument (GE Healthcare, Amersham, UK). Mouse Antibody Capture kit (GE Healthcare, # BR-1008-38) was used to immobilise the mAb on a CM5 sensor chip (GE Healthcare, #29-1496-03) as recommended by the manufacturer. Briefly; the chip surface was activated with a 400 second injection of 11.5mg/ml N-Hydroxysuccinimide (NHS) and 75mg/ml 1-Ethyl-3-(3-dimethylaminopropyl) carbodiimide hydrochloride (EDC) mixed 1:1 at a flow rate of 30µl/minute. Polyclonal anti-Mouse Fc antibody was diluted to 7µg/ml in 10mM sodium acetate pH4.5 and injected for 180 seconds over each flow cell at a flow rate of 30µl/ minute (target RU for human C5 = 500 and for rat C5 = 400). Residual active groups on flow cells (1-2) were deactivated with a 400 second injection of 1M ethanolamine hydrochloride-NaOH pH8.5 at a flow rate of 30µl/ minute. The flow cell surface was then washed with a 60 second injection of 50mM NaOH. Flow cell 2 was used to capture the test mAb (with target RU between 40 – 60) and flow cell 1 was used as the reference surface. The SPR assay protocol was as follow; test mAb were flowed to saturate the surface, then C5 protein diluted in EP-HBS buffer (usually 0 – 68nM) flowed over the immobilised mAb. For kinetic analysis the flow rate was maintained at 30 µl/minute, and data were collected at 25°C. Data from a reference cell were subtracted to control for bulk refractive index changes. The Rmax was kept low and the flow rate high to eliminate mass transfer. All reagents used were of high purity, polished by size exclusion

chromatography immediately before use to ensure removal of any aggregates. Data were evaluated using the software appropriate to the instrument (Biacore Evaluation Software). BB5.1 anti-Mouse C5 mAb was tested using Biacore T200 instrument and data analysed as described above, except that the mAb was directly immobilised onto the CM5 sensor-chip at RU approximately 200.

4.2.7 Passive Transfer Experimental Autoimmune Myasthenia Gravis (EAMG) in rats

To test in vivo effects and therapeutic efficacy of test mAb, Wistar Han IGS rats (100 – 150g) were obtained from Charles River Laboratories (Edinburgh, UK) and allowed to acclimatize for one week prior to disease induction by intraperitoneal administration of anti-Acetylcholine receptor (AChR) mAb35 at 1 mg/kg in PBS as described previously (Chamberlain–Banoub *et al* 2006). MAb35 binds the main immunogenic region of AChR, activating complement and damaging the neuromuscular junction endplates, causing severe muscle weakness. Animals were assessed hourly post-disease initiation as described previously (Chamberlain–Banoub *et al* 2006; Morgan *et al* 2006). mAb35-injected rats were split into two groups: Group one (n = 4) was treated with test mAb at 40 mg/kg dose (selected dose determined in a pilot study), subcutaneously (SC) at time zero, with a second SC dosage of 13 mg/ kg at 24 hours. The second group (n = 3) received an irrelevant isotype control antibody at the same times, routes and doses. All animals were euthanised at 40 hours post-induction, blood taken for serum assays, and soleus muscles harvested and frozen in OCT mounting medium for sectioning as 10µm as described previously (Chamberlain–Banoub *et al* 2006; Morgan *et al* 2006).

4.2.8 Immunostaining of rat soleus muscles for end-plate damage and complement deposition

Soleus sections were fixed in ice cold acetone for 15 min at -80°C and then blocked for 30 minutes in 10% horse serum 2% BSA. After washing in PBS, sections were stained overnight at 4°C with primary antibodies, C3/30 anti-C3b/iC3b mAb (in house) at 10µg/ml, and rabbit anti-rat C9/MAC polyclonal IgG (in house) at 50µg/ml, both in the block buffer. Anti-C3b/iC3b sections were washed and incubated for 15 min at RT with amplifier antibody goat anti-mouse (Vector Labs, Peterborough, UK, VectaFluor DyLight 488, # DK-2488). After washing, secondary antibody, horse anti-goat IgG–Alexa Fluor 488 (DyLight 488, # DK-2488) for C3b/ iC3b or goat anti-rabbit-FITC (Oxford Biomedical Research, #45002) for anti-C9/MAC were added as appropriate, together with alpha-bungarotoxin-TRITC (BtX) (labels AChR; Boitum, # 00012) at 0.5% and Hoechst stain 1:10 000 (ThermoFisher, # 62249), then incubated 40 minutes at RT in dark. Sections were washed in PBS and mounted in VectorShield Vibrance (Vector labs, #H-1700-2) before analysis using an

Apotome fluorescent microscope (Zeiss Apotome Axio Observer microscope). Slides were prepared from each test and control group animal to obtain at least ten fields captured from comparable regions of muscle in each sample at the same exposure and magnification (x 40). The number of BuTx-reactive endplates in each section was measured using density slicing in an image analysis system (ImageJ). Appropriate controls; secondary antibody only, primary only and no staining visualised. For co-localisation of complement activation products, sections were additionally imaged on a Zeiss confocal microscope (Zeiss LSM800 confocal laser scanning microscope).

4.2.9 Generation of Fab antibody fragments

Fab fragments were generated from intact mAb to determine binding sites on C5 using cryoelectron microscopy (Cryo-EM) and to investigate tissue penetrance. The mAbs, stored in HBS buffer, were buffer exchanged using zebra spin desalting columns (7KMWCO, Pierce, # 89889) to freshly prepared digestion buffer (1mM EDTA, 50mM sodium phosphate, 0.2mM Cysteine-HCl-H_20, pH7). Immobilised papain (Pierce, #20341) was used for IgG2b isotype mAb digestion and ficin (Pierce, #44881) to digest IgG1 isotype antibody. Immobilised papain or ficin (1ml of the suspension) was washed by centrifugation three times in the digestion buffer and resuspended in 2ml of the buffer exchanged antibody (10mg of each), incubated for 2 hours at 37°C followed by 24 hours incubation at RT, gently mixing during the incubation. The resin was washed three times by centrifugation with 5ml PBS, the wash fractions containing the digested antibody combined and applied to a Protein A column (GE Healthcare, #17-0402-01). The run through containing Fab fragments was collected, and the bound Fc and residual intact mAb was eluted using 0.1M glycine pH2.5. The Fab fragments were analysed on SDS-PAGE, dialysed against HBS buffer and stored at -20°C.

4.3 Results

4.3.1 Generation of anti-C5 mAb

C6 deficient mice were immunised with C5b6 protein, those with the highest titre of anti-C5b6 antibodies in ELISA selected (Fig. 4.1 A, B), sacrificed, spleens harvested and used in the fusion. Clone supernatants were screened using direct ELISA for specificity as described in 2.11.1 (Figure 4.1 C) and high throughput classical pathway haemolysis assay for function blocking as stated in section 2.19.3 (Fig. 4.1 D) to assess the clones for complement inhibition. The selected clones were expanded and re-screened to confirm the C5 specificity and inhibition (Fig. 4.1 E, F). In total, 9 fusions were performed, ~9.000 hybridoma clones were generated and screened, 139 antibodies were selected from ELISA,

12 of these confirmed to be inhibitory and three of these, 4G2, 7D4 and 10B6, chosen for full characterisation based on the mAb IgG isotype, species cross – reactivity and specificity to either C5α or C5β chain. 4G2 and 10B6 clones were obtained from different original clones from fusion 4, 7D4 was from fusion 7 (Fig 4.1 C, D). The inhibitory clones were also positive in ELISA and were expanded in Integra flasks as described in chapter 2.

A.

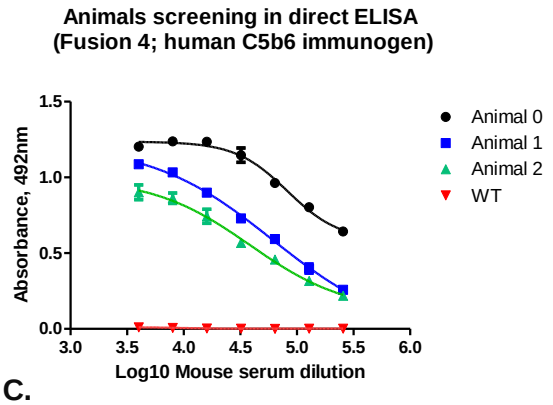

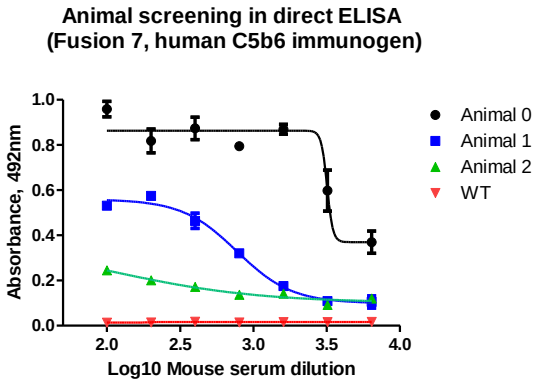

C.

Plate 7	direct ELISA; Fusion 7 clones screening											
A	0.193	0.109	0.1416	0.1313	0.11	0.0974	0.1294	0.1226	0.6115	0.837	0.1361	0.1294
B	0.1637	0.1394	0.1322	0.0753	0.1475	0.0707	0.095	0.1205	0.1818	0.298	0.0967	0.0846
C	0.2071	0.0902	0.1103	0.0714	0.1316	0.2055	0.0969	0.0844	0.1251	0.24	0.1214	0.0845
D	0.2481	0.1575	0.0931	**0.7274**	0.1648	0.0824	0.09	0.0883	0.1022	0.135	0.1277	0.1043
E	0.0943	0.087	0.0884	0.0882	0.0891	0.124	0.0868	0.1079	0.1037	0.157	0.1007	0.0941
F	0.172	0.0968	0.0845	0.0834	0.0856	0.0721	0.0821	0.0897	0.0859	0.328	0.1146	0.1096
G	0.1009	0.1519	0.2312	0.1011	0.1337	0.0784	0.0848	0.1459	0.1094	0.232	0.099	0.1165
H	0.0783	0.1497	0.1219	0.1348	0.1084	0.4397	0.103	0.083	0.0896	0.286	0.0966	0.1348

D.

Plate 7	Haemolysis assay (CH50); Fusion 7 clones screening											
A	0.6976	0.6558	0.6527	0.6797	0.7045	0.7069	0.674	0.6638	0.6436	0.6112	0.547	0.577
B	0.6646	0.6578	0.6336	0.6402	0.6638	0.6441	0.6656	0.6332	0.6563	0.5926	0.613	0.6469
C	0.6836	0.4919	0.5108	0.5232	0.6967	0.4611	0.6428	0.5152	0.609	0.5953	0.592	0.6622
D	0.6788	0.675	0.6505	**0.1692**	0.6921	0.3634	0.666	0.7345	0.6906	0.6763	0.66	0.6486
E	0.7222	0.7003	0.6263	0.703	0.5281	0.7002	0.624	0.7123	0.7035	0.6993	0.449	0.6212
F	0.704	0.699	0.6363	0.6699	0.6756	0.739	0.6813	0.7036	0.6609	0.6693	0.468	0.6758
G	0.6815	0.4439	0.4237	0.6902	0.5298	0.6533	0.6517	0.7023	0.7056	0.7065	0.644	0.6473
H	0.7332	0.7028	0.6059	0.6975	0.715	0.7346	0.7442	0.7223	0.7296	0.7239	0.71	0.7051
							Negative	0.1205	0.1437	Positive	1.003	0.9875
								Average	0.1321		Average	0.9953

Plate 7	Calculated %Lysis											
A	50.16	46.452	46.177	48.572	50.772	50.985	48.066	47.162	45.37	42.496	36.81	39.462
B	47.233	46.629	44.483	45.068	47.162	45.414	47.321	44.447	46.496	40.846	42.63	45.663
C	48.918	31.914	33.591	34.69	50.08	29.182	45.299	33.981	42.301	41.086	40.77	47.02
D	48.492	48.155	45.982	**3.2908**	49.672	20.516	47.357	53.433	49.539	48.27	46.86	45.813
E	52.342	50.399	43.835	50.639	35.125	50.39	43.631	51.464	50.683	50.31	28.12	43.383
F	50.727	50.284	44.722	47.703	48.208	53.832	48.714	50.692	46.904	47.649	29.77	48.226
G	48.732	27.657	25.865	49.503	35.276	46.23	46.088	50.577	50.869	50.949	45.4	45.698
H	53.317	50.621	42.026	50.151	51.703	53.442	54.293	52.351	52.998	52.492	51.28	50.825

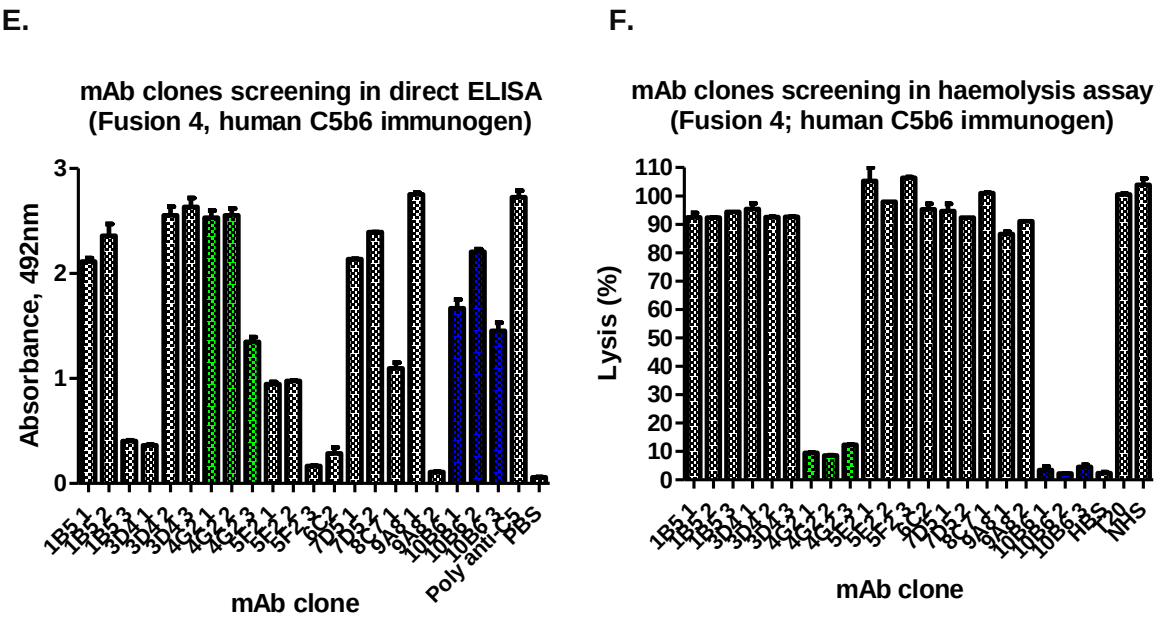

Figure 4.1 Screening Assays for mAb detection. A, B. *Screening in direct ELISA to determine the mouse with the highest anti-human C5b6 antibody titre; mice used in fusions 4 and 7 shown as examples. All animals showed good anti-C5b6 antibody titres; spleens were collected and used in fusion. mAb 4G2 and 10B6 clones were obtained from Animal 0 Fusion 4, 7D4 from Animal 0 fusion 7. The fused hybridoma clones were screened at every stage from the original fusion plates (**C, D**) throughout the re-cloning for specificity in direct ELISA and for complement inhibition using high-throughput classical pathway haemolysis assay; the example, clone 7D4 showed positive signals in ELISA and inhibition of complement in the haemolysis assay**. E, F.** Representative data from Fusion 4 clone screens after expansion to 24 well plate, 4G2 and 10B6 showed strong signals to C5b6 in ELISA and efficient complement inhibition in haemolysis assay. Samples were not corrected for IgG levels therefore some show moderate or low binding in ELISA but strong inhibition in haemolytic assay (e.g. clone 4G2 3). Also, some low binding clones showed high haemolysis more likely due to the poor expression of mAb. The error bars are standard errors of triplicates. WT, wild type non-immune mouse serum; T20, 0.1% Tween 20.*

4.3.2 Isotyping and purification of the anti-C5 mAb

Antibody clones; 4G2 and 7D4 were identified as isotype IgG2b*κ*, 10B6 as IgG1*κ* (Isostrip, Roche, # 11493027001) and were purified using protein G chromatography on an AKTA HPLC purifier. Integra supernatant was filtered prior to purification. Purity of the antibodies was determined using SDS-PAGE (Fig. 4.2); concentration of the purified antibodies was

measured using BCA assay (yield was ~1mg mAb per ml of Integra supernatant). Protein was concentrated if necessary prior to storage frozen in aliquots at >1mg/ml.

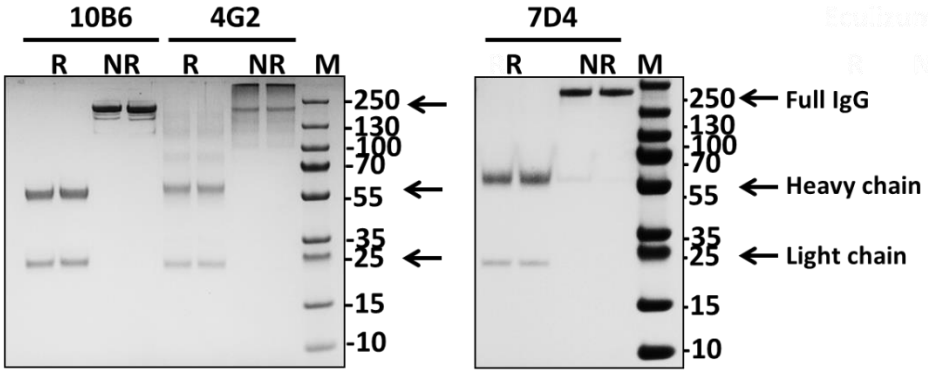

Figure 4.2 SDS-PAGE of the purified mAb 4G2, 7D4, 10B6. *mAb were resolved on 7.5% gels under NR and R conditions, then stained with coomassie blue. The ~150 kDa band corresponds to intact IgG, in R lanes the 55 kDa band corresponds to mAb heavy chain and 25 kDa to mAb light chain. M; molecular weight marker (PageRuler, #26620).*

4.3.3 Cross-species complement inhibition by mAb in haemolysis assays

Hybridoma clones were initially selected for further characterisation based upon the capacity of clone supernatants to cause inhibition of CP haemolysis in NHS; three of the selected monoclonal clones; 4G2, 7D4, 10B6, were expanded for further characterisation, secreted mAbs purified and tested in haemolysis assays with different species sera. As expected, each of the selected mAbs efficiently inhibited NHS-induced CP haemolysis, with clone 10B6 showing equivalent dose-response performance to the benchmark mAbs RO7112689 and Eculizumab (Fig. 4.3 A). When the impact of the mAbs on CP haemolysis induced by other species sera was tested, mAb 4G2 and 7D4 efficiently inhibited haemolysis mediated by either rat or rabbit serum (Fig. 4.3 B, C) and weakly inhibited haemolysis by guinea pig and mouse serum (Fig. 4.3 D, E). In contrast, neither the new mAb 10B6 nor Eculizumab inhibited any of these non-human sera, while RO7112689 inhibited mouse, guinea pig and rabbit but not rat serum induced haemolysis. The calculated 50% complement inhibitory doses of all mAbs are shown (Fig. 4.3 F); Guinea pig serum is not included in this summary as levels of inhibition did not reach 50% for any of the mAbs. The novel mAbs 10B6, 4G2 and 7D4 also showed efficient inhibition of AP lysis in human serum (Fig. 4.3 G), while 4G2 and 7D4 efficiently inhibited rat AP (Fig. 4.3 H). C5a release was inhibited by the novel mAbs at the same levels as haemolysis inhibition (66nM) in the human CP assay (Fig. 4.3 I).

A.

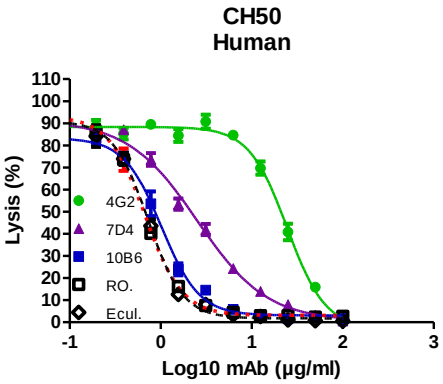

B.

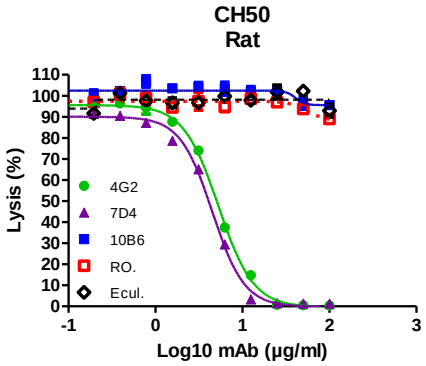

C.

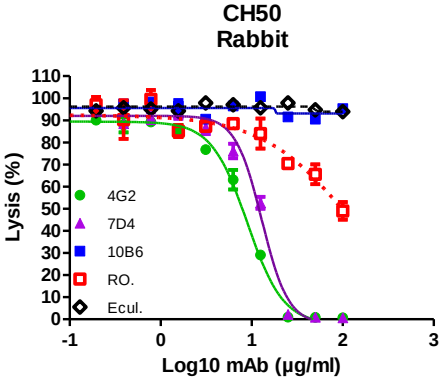

D.

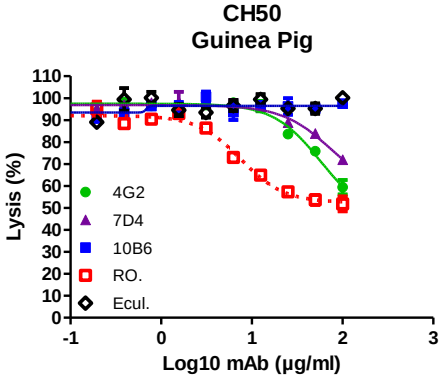

E.

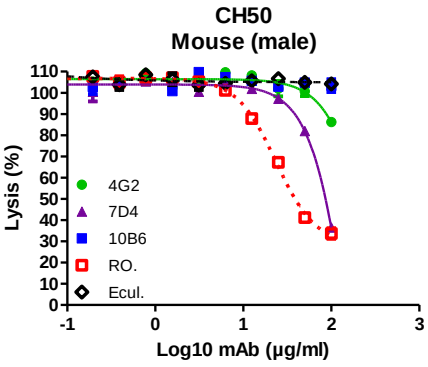

F.

Antibody	50% Complement inhibitory dosage (ng/ml)			
	Human	Rat	Rabbit	Mouse
4G2	20417.4	5105.0	8091.0	-
7D4	2187.8	4385.3	10964.8	87096.4
10B6	841.4	-	-	-
RO7112689	668.3	-	95499.3	40738.0
Eculizumab	695.0	-	-	-

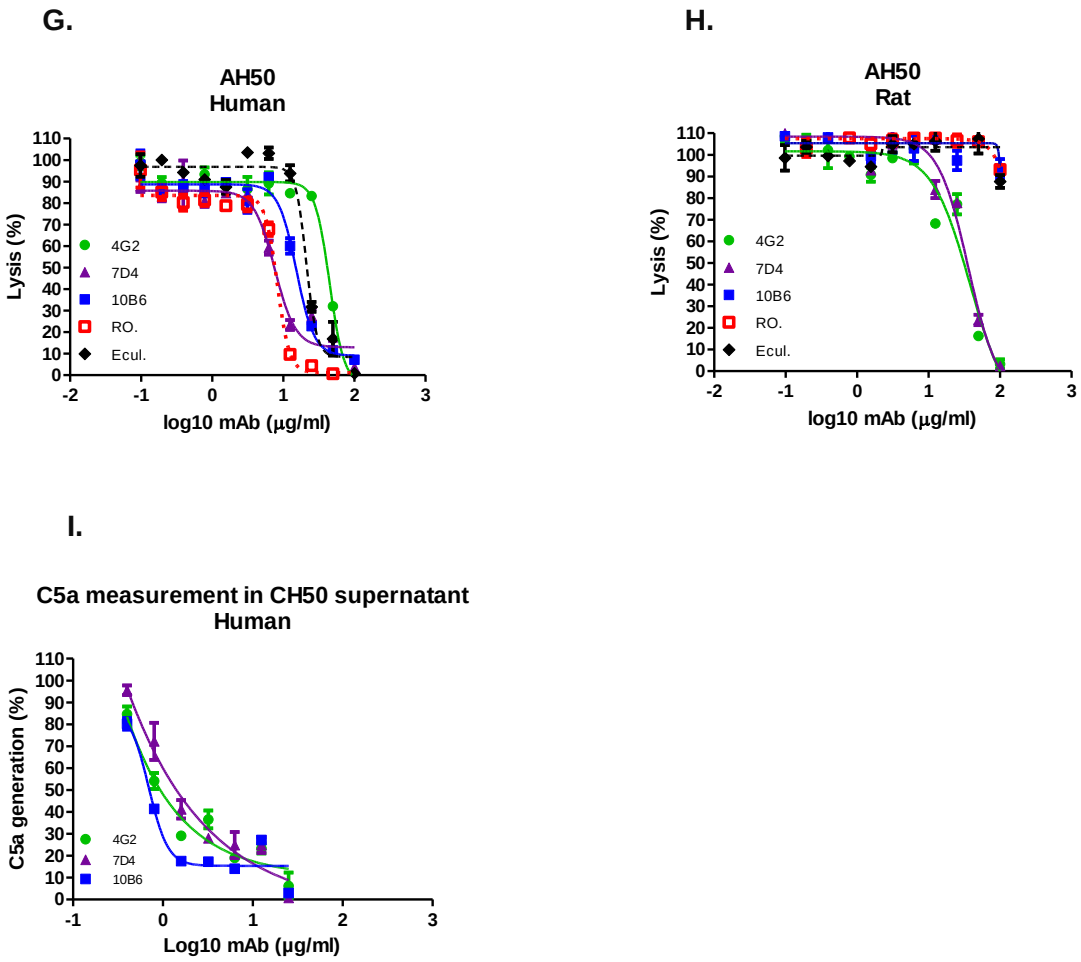

Figure 4.3 Haemolytic assays to investigate whether the anti-C5 mAb 4G2, 7D4, 10B6 inhibit complement mediated lysis across species. A – E*. Functional assays to determine whether mAb 4G2, 7D4 and 10B6 inhibit complement classical pathway haemolysis (CH50) in different species. Sera tested were human (**A**), rat (**B**), rabbit (**C**), guinea pig (**D**) and mouse (**E**). Commercial mAb RO7112689 and Eculizumab were used as comparators. **F.** Calculation of 50% inhibitory dose showed that human C5 inhibition by mAb 10B6 was equivalent to the two commercial mAb; RO7112689 and Eculizumab, and that 4G2 most strongly inhibited rat C5. G, H. Impact of mAb on alternative pathway haemolysis (AH50) assay utilising human (**G**) and rat (**H**) serum. **I.** Inhibition of C5a generation by the novel mAbs in a classical pathway assay with human serum. All experiments were repeated three times with comparable results. The error bars are standard errors of triplicates. The dashed lines correspond to the commercial mAb.*

4.3.4 Determination of 4G2, 7D4 and 10B6 binding to human C5 and C5b6 by ELISA

The direct ELISA showed that all the selected new mAbs recognised C5 and C5b6 and none recognised C6 (Fig. 4.4 A – C). In a sandwich ELISA with RO7112689 (anti-C5β) as capture and 4G2 mAb as detection, C5 and C5b6, but not C6, were detected demonstrating that mAb 4G2 and RO7112689 antibodies recognised different epitopes on C5 and C5b in the C5b6 complex (Fig. 4.4 D).

To test whether the novel anti-C5 mAb recognised epitopes distinct from the commercial mAb, sandwich ELISA were developed utilising RO7112689 or Eculizumab as the capture mAb. With RO7112689 (anti-C5β) as capture, the mAb (7D4 and 4G2) bound strongly but 10B6 did not bind (Fig. 4.4 E). With Eculizumab (anti-C5α) capture, the mAb 10B6 bound most strongly while the other mAb bound weakly (4G2) or not at all (7D4), suggesting that they competed for similar epitopes (Fig 4.4 F).

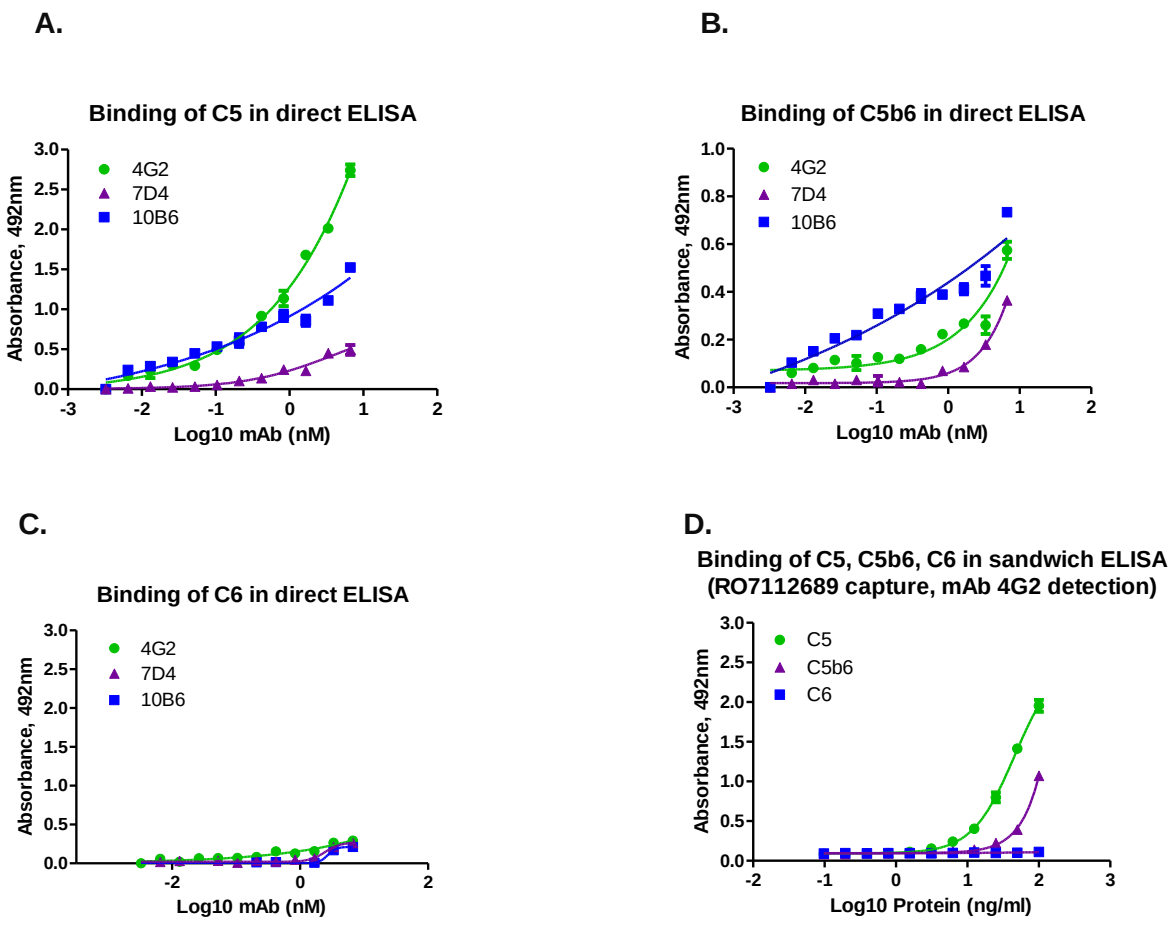

E.

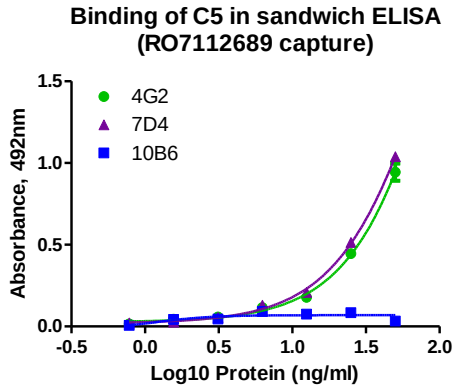

F.

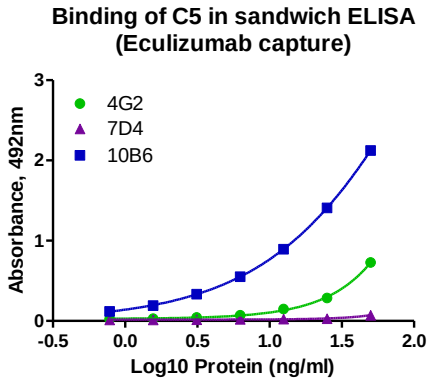

Figure 4.4 Direct and sandwich ELISA to determine 4G2, 7D4 and 10B6 binding to human and rat C5 and competition with commercial mAb A – C*. In direct ELISA, plates were coated with human C5 (**A**), C5b6 (**B**) or C6 (**C**). All new mAbs detected C5 and C5b6 complex, but not C6.* ***D.*** *In sandwich ELISA with RO7112689 as capture and 4G2 mAb as detection, both C5 and C5b6, but not C6 were detected showing that mAb 4G2 and RO7112689 antibodies recognised different epitopes of C5.* ***E, F.*** *Sandwich ELISA comparing RO7112689 (anti-C5β) and Eculizumab (anti-C5α) as the capture mAb showed that both the C5α-specific mAb (7D4 and 4G2) bound strongly to RO7112689 captured C5 but the C5β-specific 10B6 did not bind; the β-chain specific mAb 10B6 bound most strongly to Eculizumab captured C5 while the anti-C5α mAb bound weakly (4G2 or not at 7D4), suggesting that they competed for similar epitopes. All experiments were repeated three times with comparable results. The error bars are standard errors of triplicates.*

4.3.5 Testing 4G2, 7D4 and 10B6 binding to human and rat C5 and C5b6 by WB

To confirm which chains of C5 the new mAb bound, western blotting was performed on purified C5. The blots demonstrated that mAb 4G2 and 7D4 bound the α-chain in C5; of note, while 7D4 recognised both residual α-chain and the α'-chain in C5b6, 4G2 only bound residual intact α-chain (Fig. 4.5 A, B). 10B6 recognised the β-chain of C5 (Fig. 4.5 C); RO712689 also recognised the β-chain (Fig. 4.5 D), while Eculizumab is known to bind the macroglobulin 7 domain in the α-chain (Dhilion *et al* 2018). Polyclonal anti-C5 recognised both C5 α- and β-chains (Fig. 4.5 E). Cross-reactivity of mAb 4G2 to rat C5 was confirmed by western blotting on purified rat C5. As expected from the human data, the blot demonstrated that mAb 4G2 strongly bound the α-chain in rat C5 (Fig. 4.5 F).

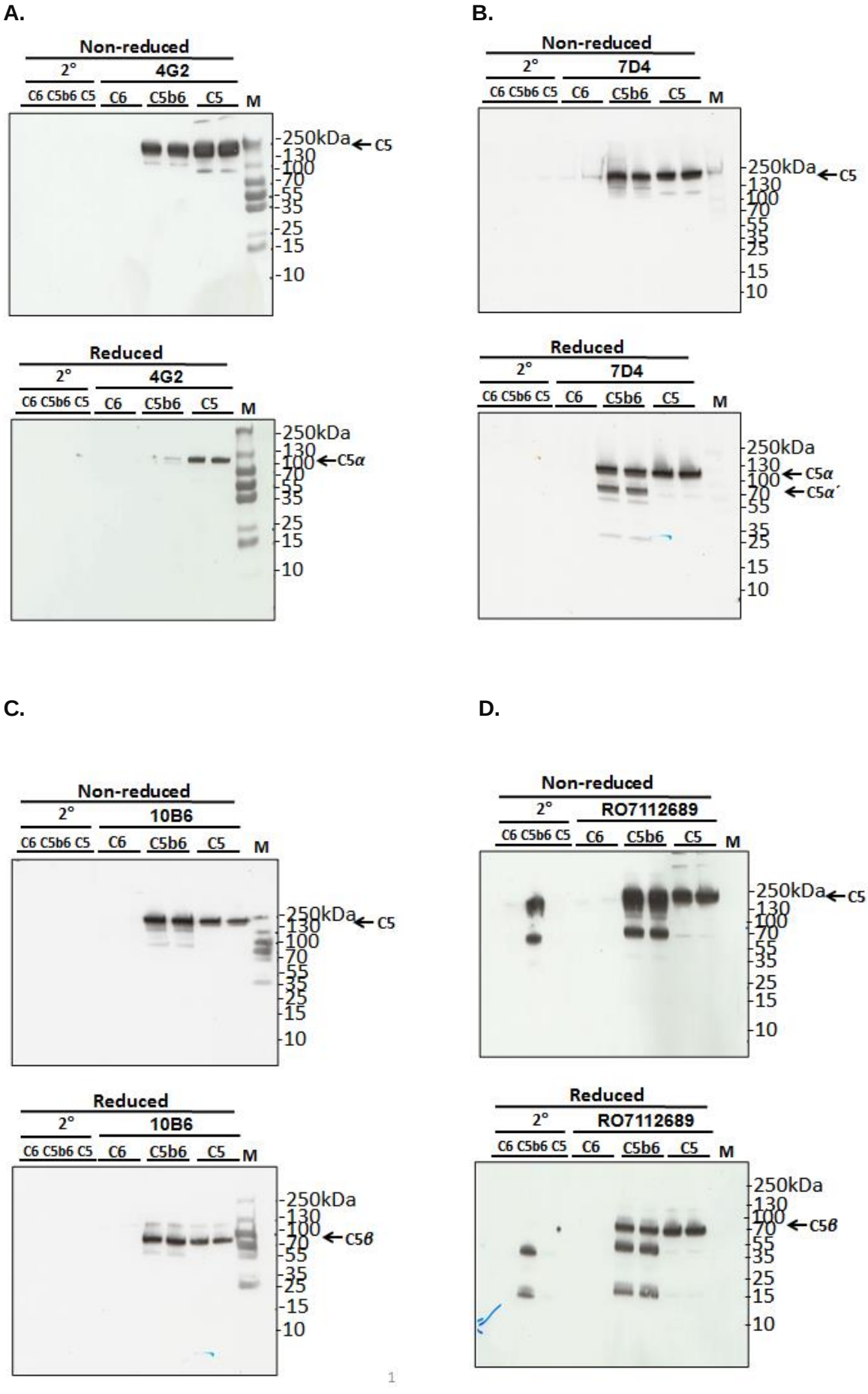
A.
Non-reduced
2°
4G2
C6 C5b6 C5
C6
C5b6
C5
M
250kDa
130
100
70
55
35
25
15
10
C5
Reduced
2°
4G2
C6 C5b6 C5
C6
C5b6
C5
M
250kDa
130
100
70
55
35
25
15
10
C5α
B.
Non-reduced
2°
7D4
C6 C5b6 C5
C6
C5b6
C5
M
250kDa
130
100
70
55
35
25
15
10
C5
Reduced
2°
7D4
C6 C5b6 C5
C6
C5b6
C5
M
250kDa
130
100
70
55
35
25
15
10
C5α
C5α´
C.
Non-reduced
2°
10B6
C6 C5b6 C5
C6
C5b6
C5
M
250kDa
130
100
70
55
35
25
15
10
C5
Reduced
2°
10B6
C6 C5b6 C5
C6
C5b6
C5
M
250kDa
130
100
70
55
35
25
15
10
C5β
D.
Non-reduced
2°
RO7112689
C6 C5b6 C5
C6
C5b6
C5
M
250kDa
130
100
70
55
35
25
15
10
C5
Reduced
2°
RO7112689
C6 C5b6 C5
C6
C5b6
C5
M
250kDa
130
100
70
55
35
25
15
10
C5β

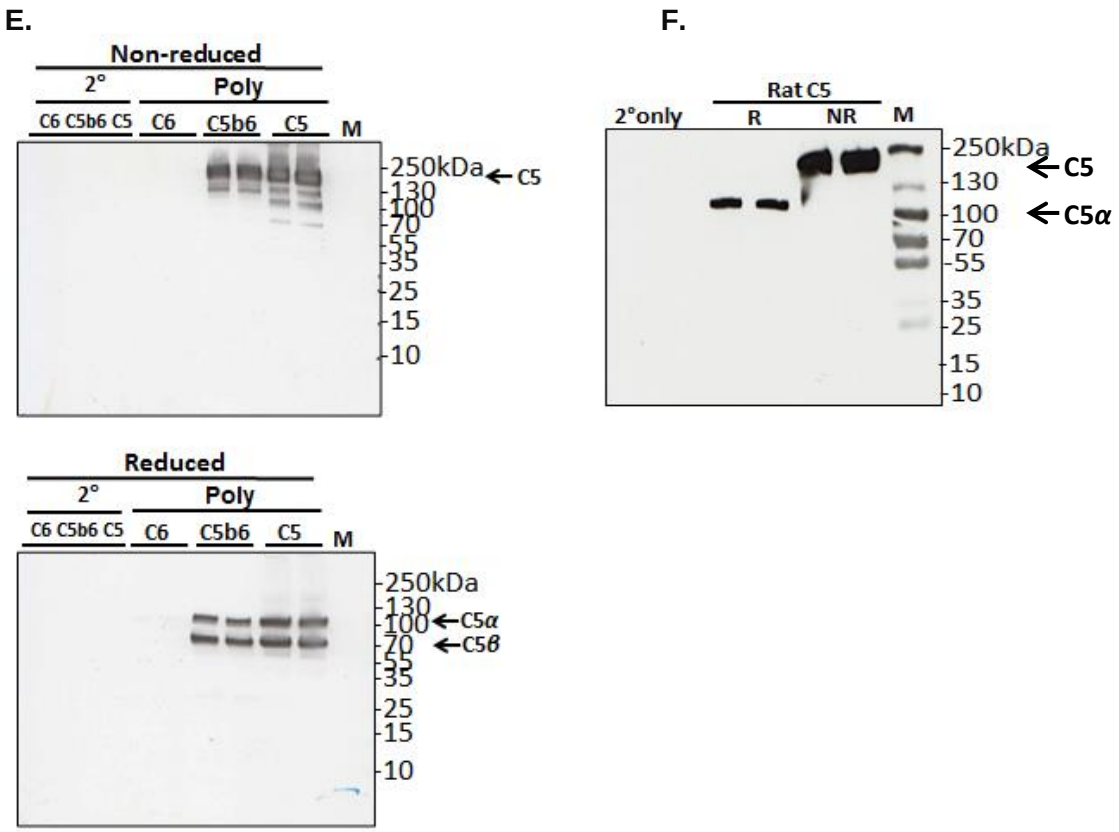

Figure 4.5 Detection of human C5 and C5b6 by 4G2, 7D4 and 10B6 mAb. A – F. *WB using novel mAbs (4G2, 7D4, 10B6) in comparison to anti-C5 mAb RO7112689 and polyclonal (in house) anti-human C5. Proteins; human C5, C5b6 and C6 or rat C5 (1µg) were resolved on 4-20% PAGE gels under NR and R (5% β-mercaptoethanol) conditions. Blots were probed with mAb 4G2 (**A**), 7D4 (**B**), 10B6 (**C**), RO7112689 (**D**). All mAbs detected intact C5 and C5b in the C5b6 complex, but not C6. mAb 4G2 and 7D4 bound the C5α chain, while mAb 10B6 and RO7112689 bound the C5β chain. All mAb except 4G2 detected C5b6 in R conditions. mAb 4G2 detected rat C5 α - chain (**F**). Polyclonal anti-C5 recognised both C5 α- and β-chains (**E**). C5b6 probed with RO7112689 showed trace contaminating human antibody bands from the immunoaffinity purification process detected by the anti-human IgG secondary. Results are representative of multiple analyses. M; protein molecular weight marker, 2°; secondary antibody.*

4.3.6 SPR analysis to determine test mAbs binding affinity to human and rat C5

SPR analysis on immobilised antibody with human C5 flowed over (Fig. 4.6 A – C) showed binding between human C5 and each of the novel mAb. The mAb 10B6 and 7D4, showed very strong binding to human C5 in SPR analyses (KD = 4.105 x 10^{-10}, 1.264 x 10^{-9} respectively) with negligible off rates, suggesting that 10B6 and 7D4, respectively targeting the β and α chains of C5, might be promising candidates for therapeutics.

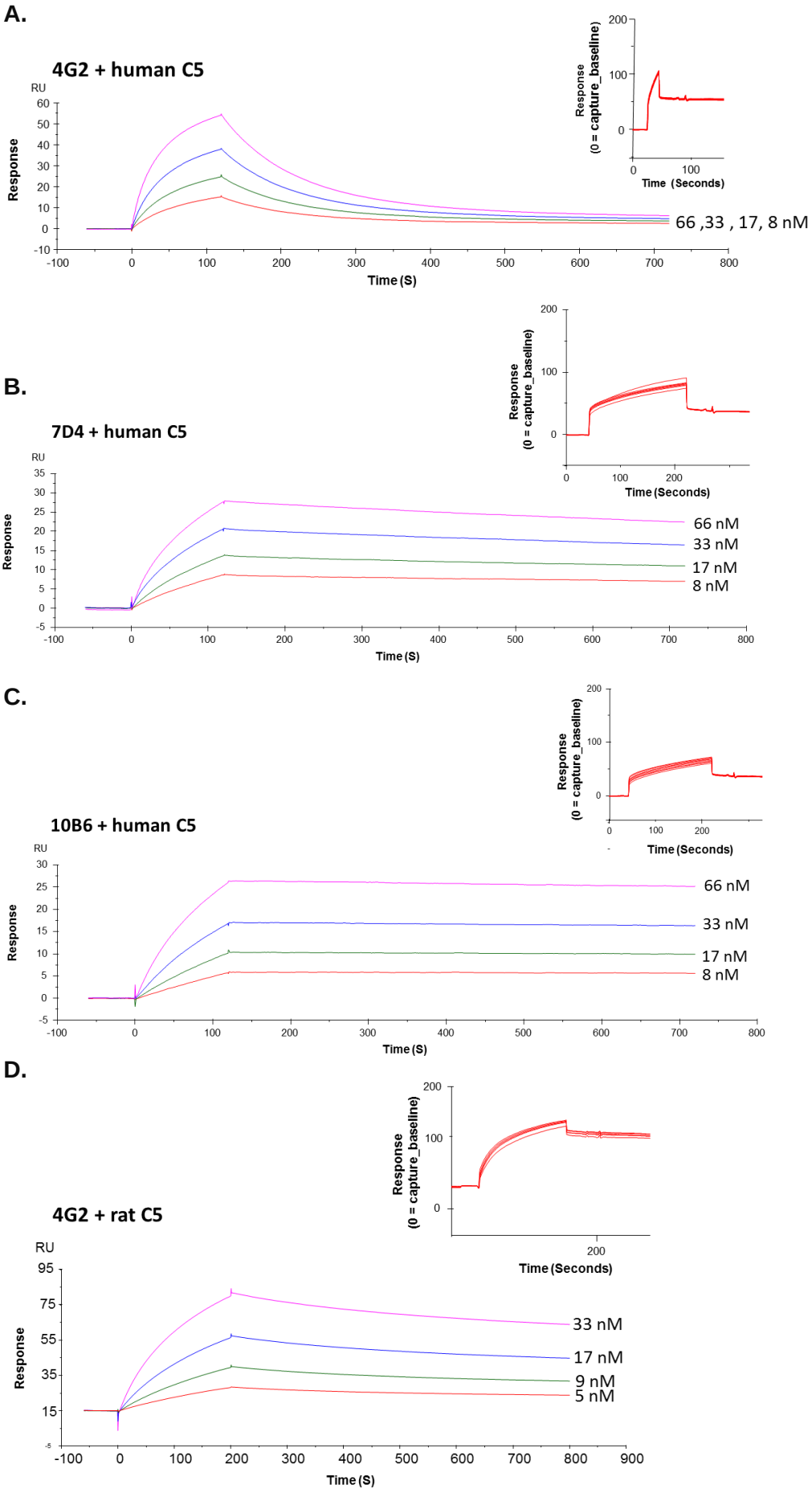
A.
4G2 + human C5
RU
Response
Time (S)
66 ,33 , 17, 8 nM
Response (0 = capture_baseline)
Time (Seconds)
B.
7D4 + human C5
RU
Response
Time (S)
66 nM
33 nM
17 nM
8 nM
Response (0 = capture_baseline)
Time (Seconds)
C.
10B6 + human C5
RU
Response
Time (S)
66 nM
33 nM
17 nM
8 nM
Response (0 = capture_baseline)
Time (Seconds)
D.
4G2 + rat C5
RU
Response
Time (S)
33 nM
17 nM
9 nM
5 nM
Response (0 = capture_baseline)
Time (Seconds)

E.

Antibody	ka (1/Ms)	kd (1/s)	KD (M)
Rat C5			
4G2	1.66E5	6.05E-4	3.68E-9
Human C5			
4G2	8.998E+5	0.01250	1.389E-8
7D4	2.801E+5	3.539E-4	1.264E-9
10B6	1.652E+5	6.783E-5	4.105E-10

Figure 4.6 Analysis of the binding affinity of mAb 4G2 to human and rat C5 and 7D4, 10B6 to human C5. A – E. *Each mAb (4G2, 7D4, 10B6) was immobilised on the mouse IgG capture sensor chip (GE Healthcare) at approximately 60 RU (insets in each). C5 was flowed in HBS at 66 to-8nM for human and 33 to 5nM for rat C5 and interactions with the immobilised mAbs analysed. Sensorgrams were collected and KDs calculated using the Langmuir 1:1 binding model with RI value set to zero. Representative sensorgrams are shown with fitted data in colour (n = 3).* ***A****. mAb 4G2 binding human C5****; B.*** *mAb 7D4 binding human C5;* ***C.*** *mAb 10B6 binding human C5;* ***D.*** *mAb 4G2 binding rat C5;* ***E.*** *Summary table of KDs from the aggregate studies.*

Binding of human C5 to 4G2 was relatively weak (KD = 1.389 x 10^{-8}; Fig. 4.6 A); in contrast, binding of rat C5 to 4G2 was strong and stable (KD = 3.68 x 10^{-9}, Fig. 4.6 D, summary table; E). The relatively slow off rate of rat C5 from mAb 4G2 suggested that this mAb offered promise for use *in vivo* in rats because 4G2 and C5 will form a stable complex, delivering prolonged inhibition. Technical issues precluded the analysis by SPR of 7D4 binding to rat C5.

4.3.7 Induction of EAMG in rats and effect of mAb 4G2 on clinical disease and pathology

Rats given mAb35 at 1mg/kg intraperitoneally began to lose weight and show signs of hind limb weakness within 12 hours (Fig. 4.7 A) (Chamberlain – Banoub *et al* 2006). Clinical symptoms, comprising limp tails, piloerection, hind limb weakness and reduced grip strength, were detectable in isotype control treated animals by 18 hours post-induction, and all exhibited severe disease with hind limb weakness and/or partial paralysis, reaching clinical score 4 on a standardised scale (0, no disease; 1, reduced grip strength in front legs

(can grip cage lid but cannot lift) and floppy tail ; 2, loss of grip in front legs; 3, loss of grip and hind limb weakness and wasting; 4, loss of grip and hind limb paralysis; 5, moribund) by endpoint. In contrast, animals given mAb 4G2 subcutaneously at the time of disease induction continued to gain weight over the time course of the experiment and did not develop detectable weakness or other clinical manifestations for the duration of the experiment (Fig. 4.7 B). Animals were sacrificed by a Schedule 1 method when weight loss was equal to or exceeded 20% of original bodyweight, or when clinical score reached 4. CP haemolytic activity in serum was essentially absent at 2 hours post-induction in 4G2-treated animals but at later time points, residual haemolytic activity of approximately 35% of controls was detected (Fig. 4.7 C), likely due to the high sensitivity of the haemolytic assay for residual C5 (Zelek *et al* 2018). As expected, serum from the untreated control animals retained full haemolytic activity across the time course.

Soleus muscles were harvested from each animal at sacrifice (40 hours), sections (10µm) were prepared, fixed in acetone and endplates identified by staining AChR with α-Bungarotoxin-TRITC (4.2.8). Receptor numbers were quantified across 10 different representative fields in an automated imaging system and analysed using ImageJ software. The number of endplates in isotype control animals was significantly decreased compared to mAb 4G2 treated animals (~2-fold less; Fig. 4.7 D); endplate numbers in the 4G2 group were not significantly different to numbers in naïve animals (data not shown). Residual endplates were frequently fragmented in isotype control animals, while most endplates in 4G2-treated animals displayed the typical continuous, linear character. The α-Bungarotoxin fluorescence intensity was significantly higher in the 4G2-treated animals ($P = 0.002$, Fig. 4.7 E). Whereas C3 fragment staining intensity was similar between the groups, C9/MAC staining was reduced more that 3-fold in the 4G2-treated group ($P<0.0001$; Fig. 4.7 F, G). Representative confocal images and co-localisation of C3b/iC3b and C9/MAC deposition at the endplate are shown (Fig. 4.7 H).

A.

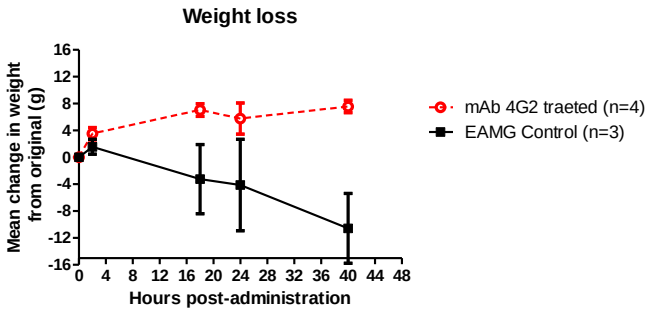

B.

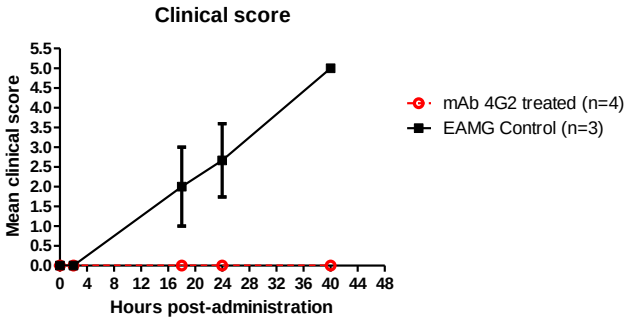

Clinical Score;
1). Reduced grip strength in front legs and floppy tail
2). loss of grip in front legs
3). loss of grip and hind limb weakness and wasting
4). loss of grip and hind limb paralysis
5). Moribund

C.

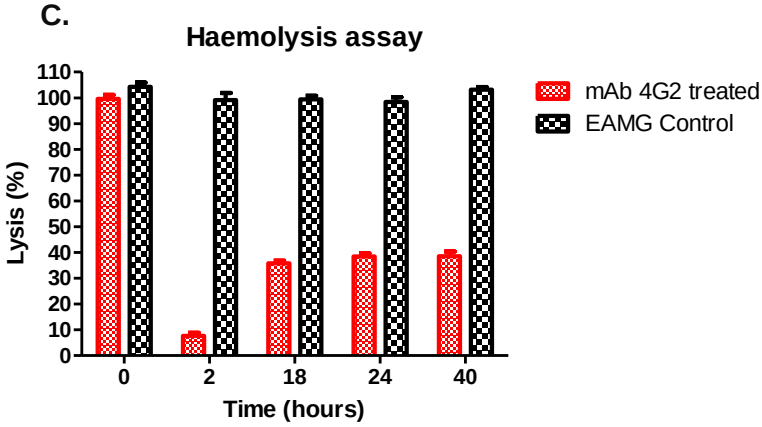

D.

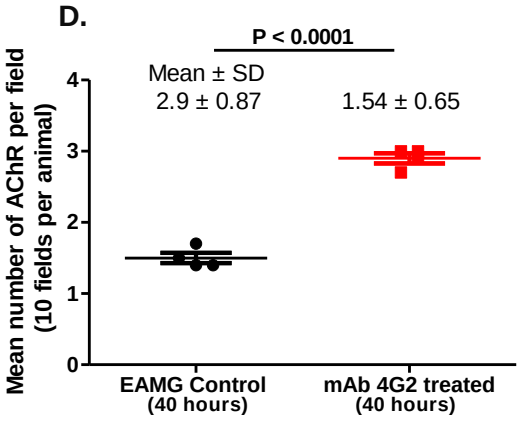

E.

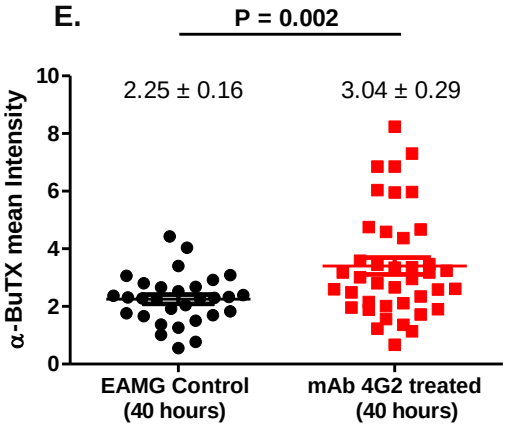

F.

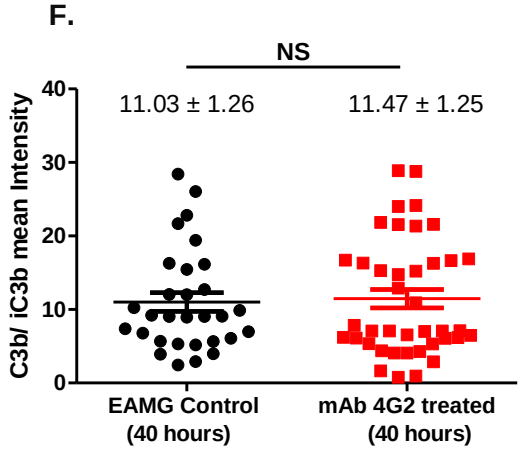

G.

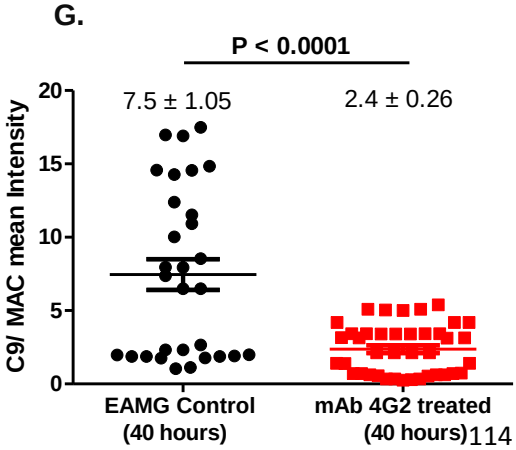

H.

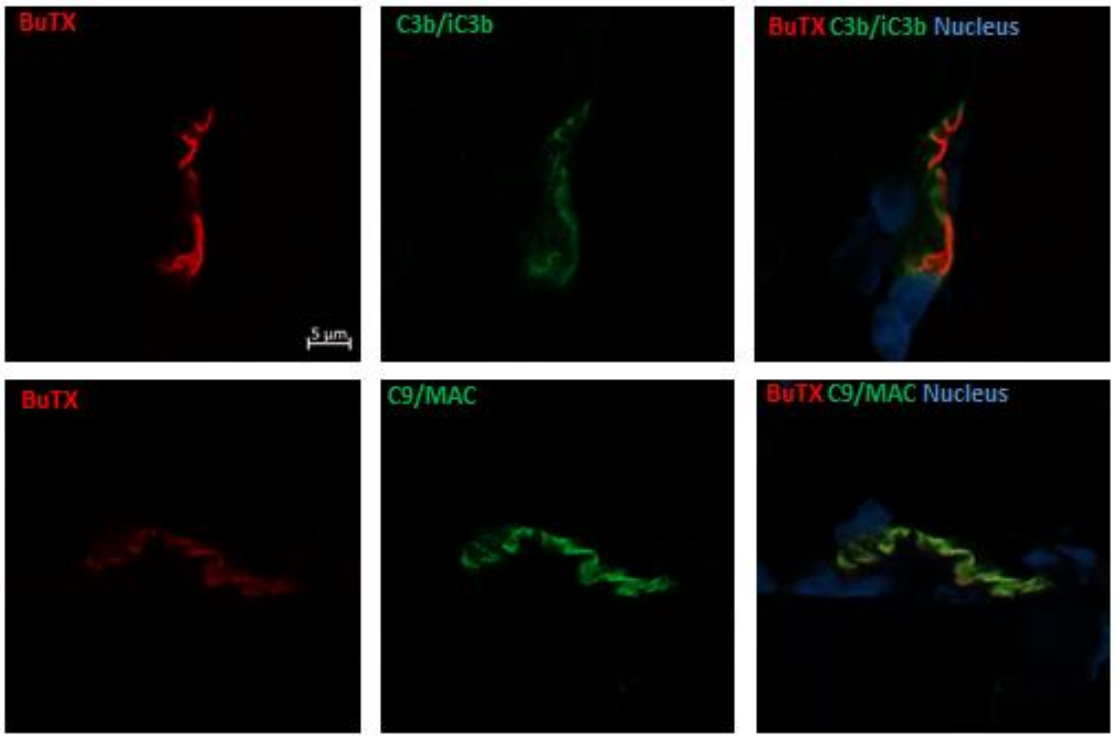

EAMG controls (40 hours)

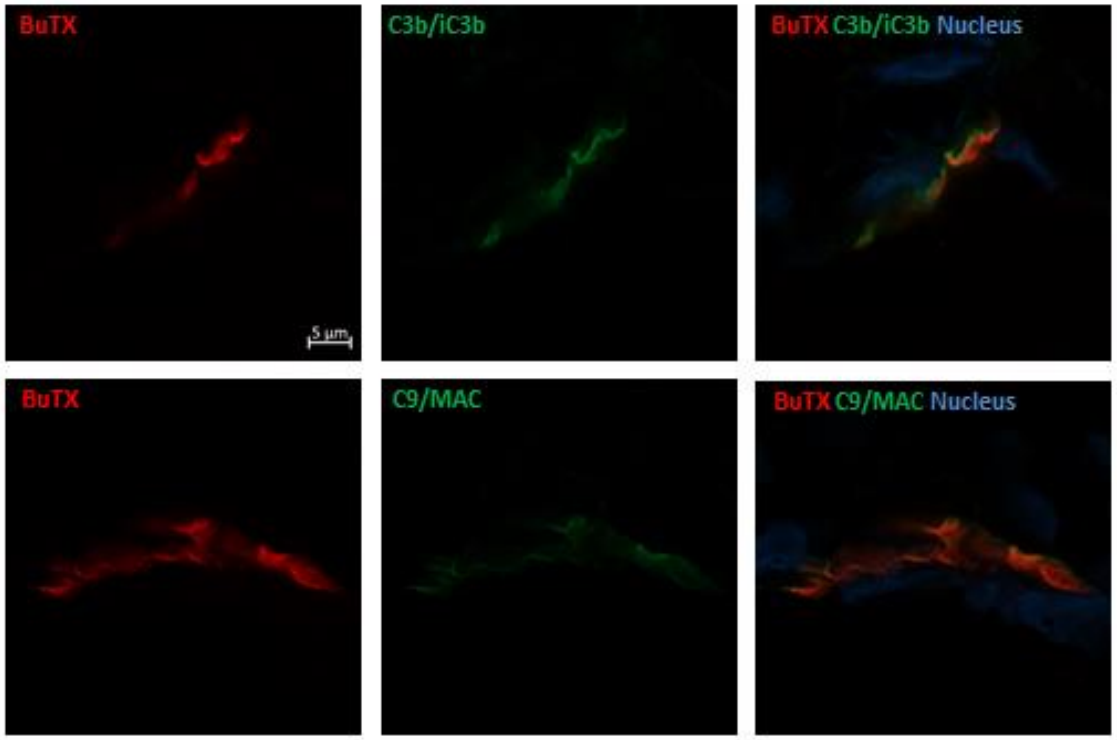

4G2 treated (40 hours)

Figure 4.7 In vivo testing of mAb 4G2 in EAMG model. A, B. *EAMG was induced in rats; weight loss and clinical score were monitored. Isotype control treated animals (EAMG)*

rapidly developed weight loss and muscle weakness, reaching clinical scores of four or five and all were sacrificed at 40 hours. The mAb 4G2 treated animals were protected from disease and weight loss; all were sacrificed at 40 hours. ***C.*** *Serum lytic activity was measured at multiple time points (0, 2, 18, 24 and 40 hours) in each animal. Results are means of determinations from four 4G2-treated and three isotype control treated EAMG animals and vertical bars represent SD.* ***D.*** *Soleus muscles were harvested at sacrifice and snap frozen in OCT. Sections (10μm) were stained for AChR with TRITC-conjugated α-BuTX and visualised on a Zeiss Apotome microscope; AChR-positive endplates were counted in ten fields from each animal using ImageJ software.* ***E.*** *Mean fluorescence intensity of BuTx staining in the sections (mean pixel intensity values from ten fields per animal from ImageJ analysis as above) was significantly higher in 4G2 treated animals compared to controls (P = 0.002).* ***F.*** *Mean fluorescence intensity of C3b/iC3b (mean pixel intensity values from ten fields per animal from ImageJ analysis as above) was not significantly (NS) different between the two groups.* ***G.*** *C9/MAC (mean pixel intensity values from ten fields per animal from ImageJ analysis as above) staining was markedly reduced in 4G2 treated animals (P<0.0001). Statistical significance was obtained by t-test and p<0.05 was considered as significant.* ***H.*** *Tissue sections from isotype control or 4G2-treated animals were double stained for AChR together with anti-C3b/iC3b (top panel) or C9/MAC (bottom panel). Pictures imaged on a Zeiss confocal microscope. For each analysis, statistical significance was obtained by t-test and p<0.05 was considered as significant. The scale bar is shown in the first plate; all images were captured at identical magnification.*

4.3.8 mAb 4G2 but not mAb 7D4 and 10B6 block atypical cleavage of C5 by neutrophil elastase

To test whether any of the new mAb inhibited atypical cleavage of C5, C5 was incubated with NE with or without an excess of each of the mAb; C5a generation, detected by WB, was used as an index of C5 cleavage. Although C5 cleavage products were present in all cases, complete inhibition of NE-mediated C5a generation was observed when mAb 4G2 was used, while 10B6 and 7D4 caused a partial inhibition of C5a generation compared to the no-mAb control (Fig. 4.8 A). When tested in this assay, RO7112689 completely inhibited C5a generation while Eculizumab had no effect on C5a production; an irrelevant non-blocking anti-C5 (3D3) also did not inhibit C5a generation (Fig. 4.8 A). Densitometric analysis of the C5a band showed a ~95% inhibition of C5a generation by 4G2 and RO7112689, 40% by 10B6 and 20% by 7D4 compared to cleavage in absence of antibody (Fig. 4.8 B). These data were confirmed by ELISA; when compared to the amount of C5a generated by NE in the absence of antibody (670ng/ml in the assay; 100%), the amount of

C5a generated was reduced to ~4% by inclusion of 4G2 or RO7112689; 73% by 7D4; 59% by 10B6; Eculizumab did not inhibit C5 cleavage in this assay (Fig. 4.8 C).

A.

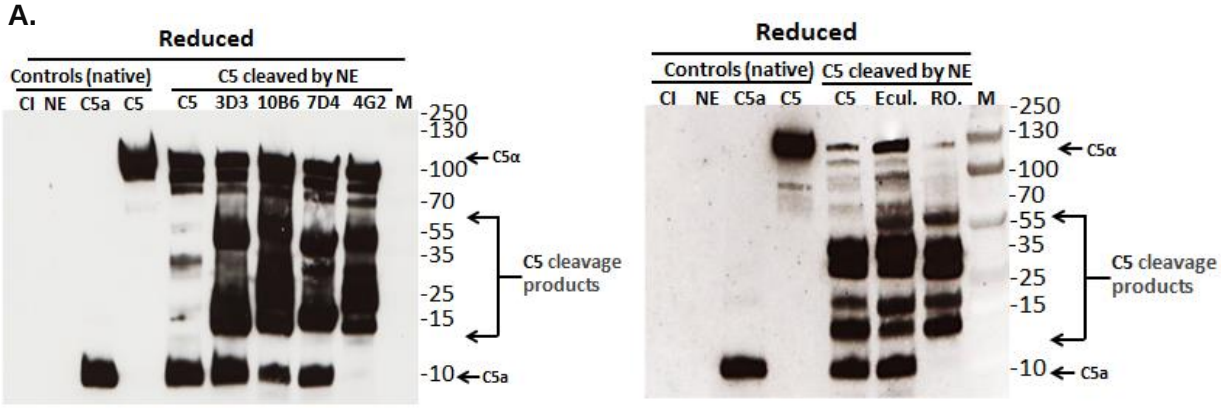

B.

Sample	Densitometry (%)
C5 cleaved by NE + mAb 4G2	5.6
C5 cleaved by NE + mAb 7D4	79.9
C5 cleaved by NE + mAb 10B6	60.2
C5 cleaved by NE + RO7112689	4.8
C5 cleaved by NE + Eculizumab	98.3
C5 cleaved by NE	100.0

C.

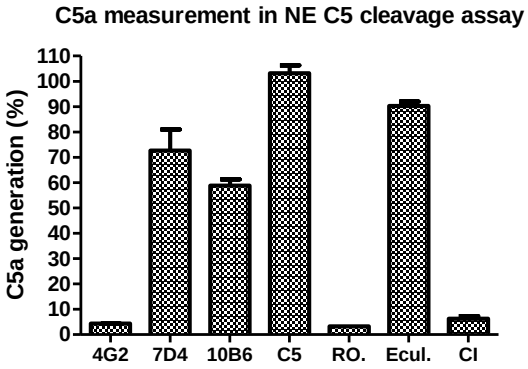

Figure 4.8 Detection of C5a generated by atypical cleavage of C5 by neutrophil elastase A. *Western blot of C5 subjected to atypical cleavage by neutrophil elastase (NE) with and without anti-C5 mAb. Intact or cleaved C5 and C5a were detected using anti-C5a mAb (Hycult). C5; NR; 190 kDa (intact C5), R; 75 kDa (C5β chain), C5α (115 kDa), C5a (10.4 kDa), CI; proteases cocktail inhibitors, Ecul.; Eculizumab, RO; RO7112689, 3D3; irrelevant mAb.* ***B.*** *Densitometry analysis using ImageJ.* ***C.*** *C5a ELISA confirmed that mAb 4G2 and commercial mAb RO7112689 efficiently inhibited generation of the C5a cleavage product. Densitometry and ELISA percentage calculated relative to C5a in C5 + NE lane = 100% (measured as 669.7 ng/ml in C5a ELISA). Results are representative of three independent experiments. The error bars are standard errors of triplicates.*

4.3.9 Fab fragments of the mAb retain their functional activity

Fab fragments were generated by digestion with papain for 4G2 and 7D4 mAbs and ficin for 10B6 mAb. The Fab(s) functionality was tested in CP haemolysis assay. Each of the

Fab(s) inhibited lysis of ShEA by NHS, with 7D4 Fab showing the same activity as intact antibody, whereas 4G2 and 10B6 Fab were less effective (Fig 4.9 A). All Fab(s) showed strong signals in direct ELISA confirming that their binding ability was not affected by the enzymatic digestion (Fig. 4.9 B). The Fab(s) purity was confirmed by SDS-PAGE (Fig. 4.9 C) with single bands visible at 50 kDa (NR) and 25 kDa (R), corresponding to Fab fragments.

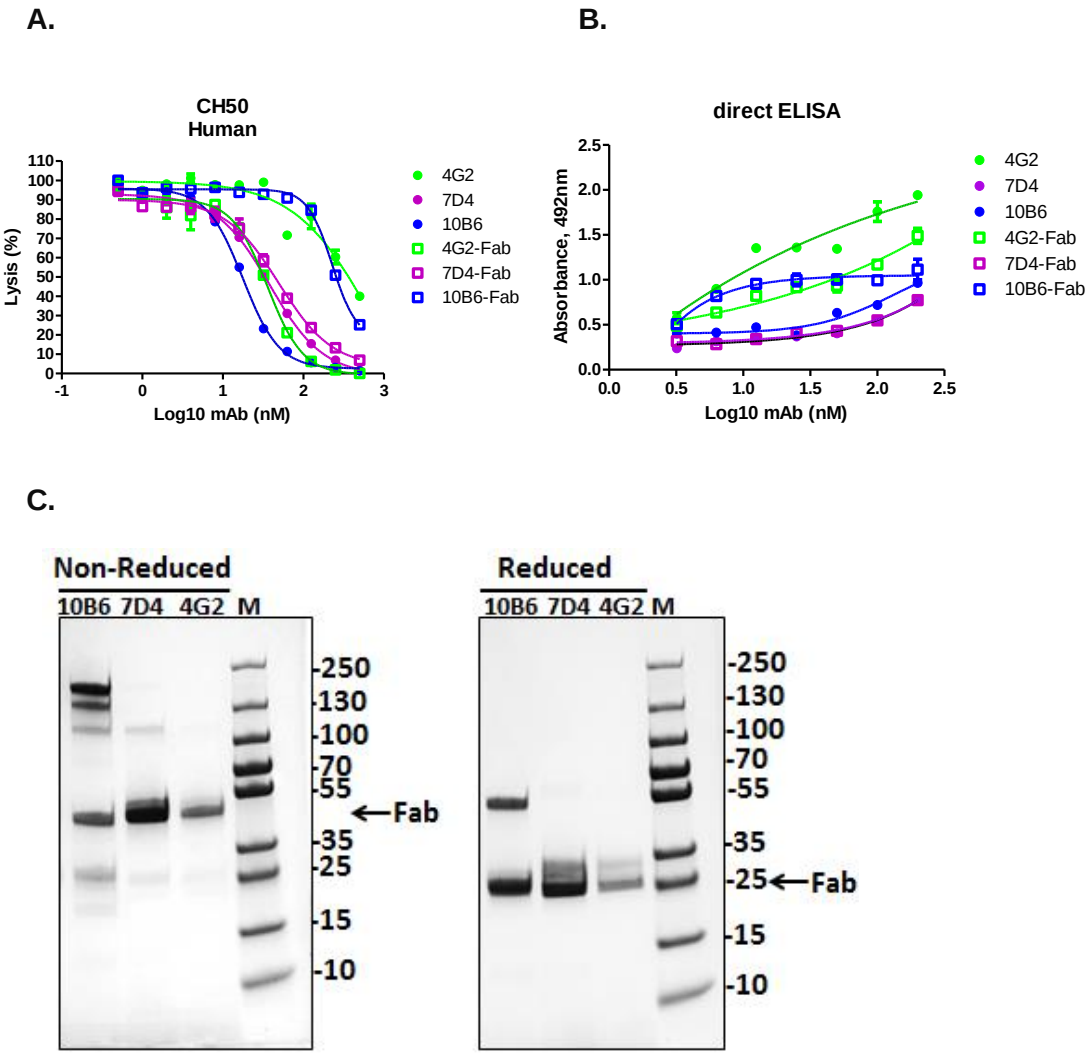

Figure 4.9 Testing of generated Fab(s) A. *CP haemolytic assay utilising NHS; all Fab(s) inhibited lysis.* ***B.*** *Direct ELISA; plates were coated with human C5; all Fab(s) detected C5. The error bars are standard errors of triplicates.* ***C.*** *Purity of the Fab(s) was assessed by SDS-PAGE on 7.5% gel under non-reducing (NR) and reducing (R) conditions, stained with coomassie blue. NR; the 150 kDa band corresponds to full IgG, 50 kDa to Fab fragment, R; 25 kDa to Fc. 7D4 and 4G2 Fab(s) showed no contamination, 10B6 was contaminated with undigested IgG. M; molecular weight marker (PageRuler, #26620).*

4.3.10 Summary of the characterisation of the novel anti-C5 mAb. Table 4.1 summarises the properties of the novel anti-C5 mAb generated in this project.

Antibody	Isotype	Target	Cross-species reactivity/ inhibition *in vitro*	Cross-species reactivity/ inhibition *in vivo*	Inhibition of atypical cleavage by NE	C5 chain specificity	IP
4G2	IgG2b, K	C5 / C5b6	Strong; Hu, Rt, Rb. Weak; Gp, Ra	Rat	Yes	α-chain	Licence agreement in progress
7D4	IgG2b, K	C5 / C5b6	Strong; Hu, Rt, Rb. Weak; Gp, Rb, Mo	Not tested	No	α-chain	
10B6	IgG1, K	C5 / C5b6	Strong; Hu	N/A	No	β-chain	N/A

Table 4.1 *Summary of the new anti-C5 mAbs and the plans for further development.*

4.4 Characterisation of mAb BB5.1 anti-mouse C5

The first report on a functional inhibitor mAb targeting C5 was published nearly 35 years ago. The monoclonal anti-C5 antibody BB5.1 was generated in C5 deficient mice and inhibited haemolysis in mouse serum (Frei *et al* 1987). BB5.1 was used as proof of concept for safe and effective inhibition of MAC in many mouse models (Wang *et al* 1995; Huugen *et al* 2007; Copland *et al* 2010; Raedler *et al* 2011). The success of BB5.1 in mice initiated research for anti-human complement blocking agents, notably the development of Eculizumab (Thomas *et al* 1996; Adis *et al* 2007). Although BB5.1 was developed many years before Eculizumab, its mechanism of inhibition is still unknown. Here I further characterised the BB5.1 antibody for cross-species inhibition, binding affinity and chain specificity.

4.4.1 Cross-species complement inhibition in haemolytic assays

The hybridoma cell line producing BB5.1 (a gift of Prof. Brigitta Stockinger) was re-cloned (section 2.15.6), expanded, the mAb produced in large quantities using Integra flask (section 2.15.3) and purified on protein G column (section 3.2.7.1). The purified mAb was tested in CP haemolysis assays using various species sera. BB5.1 efficiently inhibited haemolysis mediated by mouse serum only (Fig. 4.10 A - D) As noted above, Eculizumab inhibited only human complement, while RO7112689 additionally inhibited mouse, guinea pig and rabbit but not rat serum induced haemolysis. The calculated 50% complement inhibitory doses of all mAbs are shown (Fig. 4.10 F).

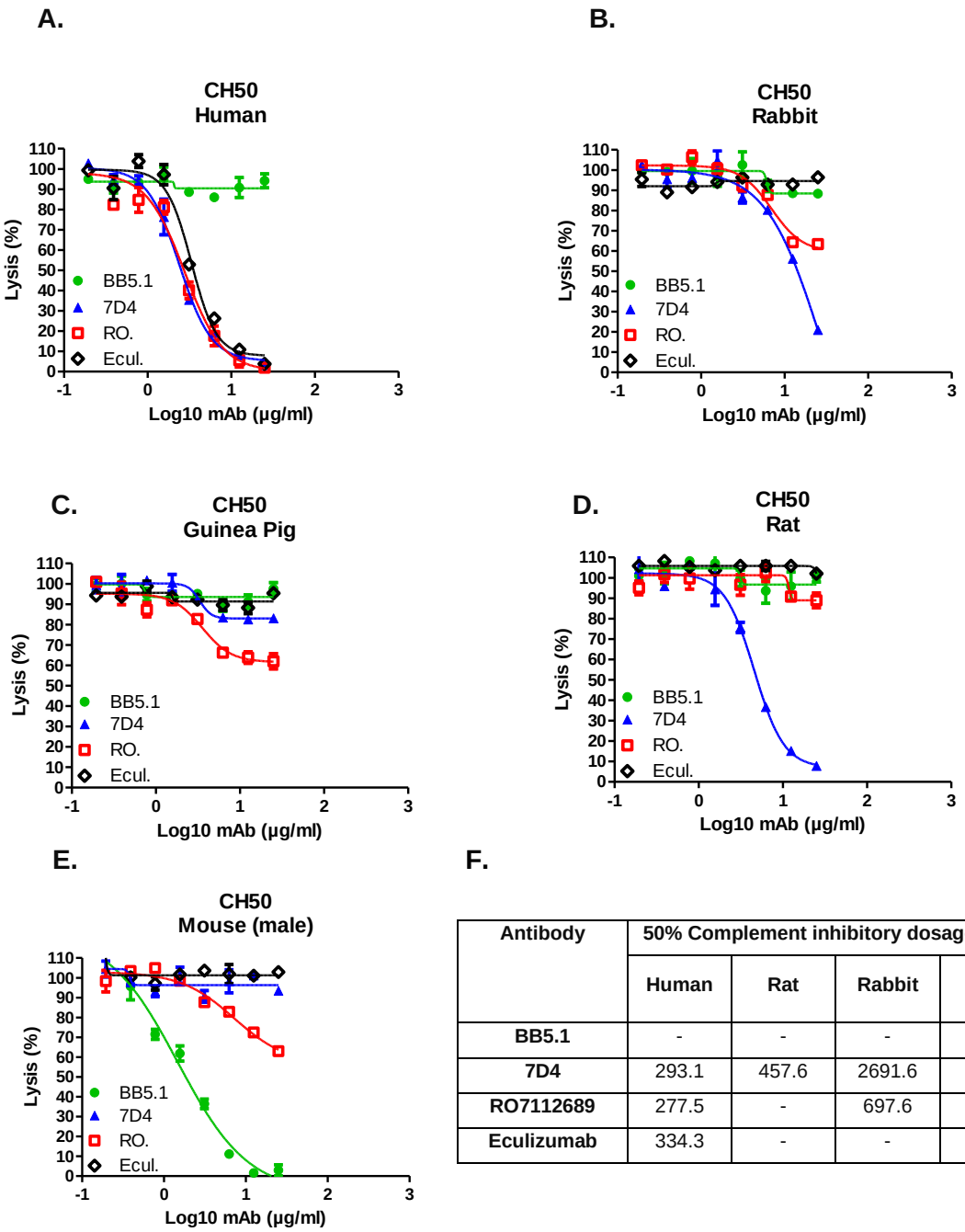

F.

Antibody	50% Complement inhibitory dosage (ng/ml)			
	Human	Rat	Rabbit	Mouse
BB5.1	-	-	-	147.5
7D4	293.1	457.6	2691.6	-
RO7112689	277.5	-	697.6	564.3
Eculizumab	334.3	-	-	-

Figure 4.10 Haemolytic assays to investigate whether the anti-C5 mAb BB5.1 inhibits complement mediated lysis across species. A – E. *Functional assays to determine whether mAb BB5.1 inhibits complement classical pathway haemolysis (CH50) in different species. Sera tested were human (**A**), rabbit (**B**), guinea pig (**C**), rat (**D**) and mouse (**E**). Commercial mAb RO7112689 and Eculizumab were used as comparators. All experiments were repeated three times with comparable results. The error bars are standard errors of triplicates.* ***F.*** *Calculation of 50% inhibitory dose showed that mAb BB5.1 inhibited C5 only in mouse.*

4.4.2 Determination of BB5.1 binding to mouse C5 by ELISA and WB

The direct ELISA (section 2.11.1) showed that BB5.1 recognized mouse C5 (Fig. 4.11 A). Western blotting (section 2.9) was used to confirm BB5.1 antibody binding to mouse C5. The blots demonstrated that BB5.1 bound the β-chain in C5 (Fig 4.11 B).

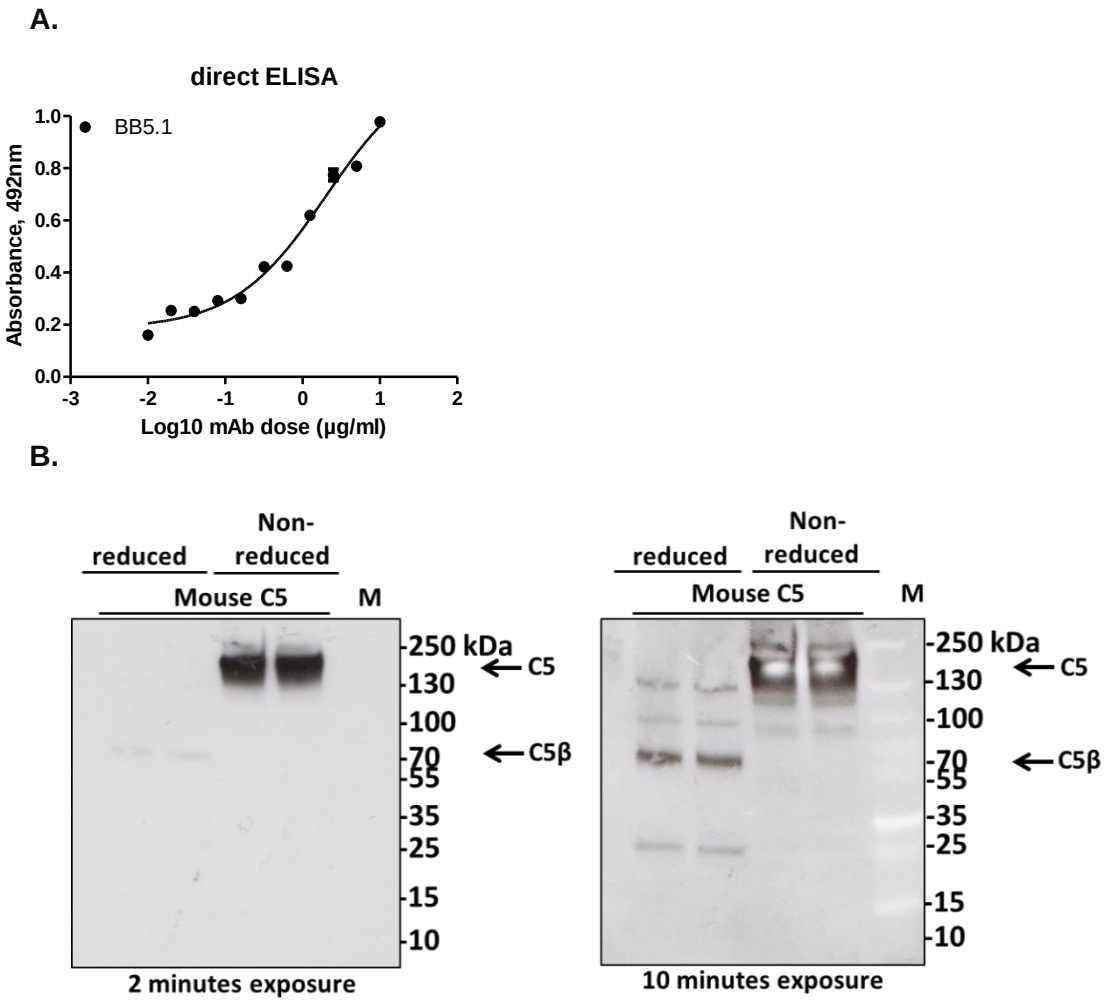

Figure 4.11 Detection of mouse C5 by BB5.1 mAb A. *Direct ELISA; plates were coated with mouse C5 (purified using OmCI column) at 0.5µg/ml, than incubated with BB5.1 mAb diluted from 10 – 0µg/ml, detected with secondary donkey anti-mouse IgG diluted 1 in 1000. The assay was repeated three times with comparable results. The error bars are standard errors of triplicates.* ***B.*** *Mouse C5 was diluted in PBS, separated on 4-20% SDS-PAGE under R and NR conditions, transferred to nitrocellulose then probed with mAb BB5.1 (1µg/ml) and HRP labelled donkey anti-mouse IgG (diluted 1:10000). Bands were detected with ECL and visualised by autoradiography. M; protein molecular weight marker. BB5.1 detected intact mouse C5 in NR and, weakly, C5 β-chain in R conditions.*

4.4.3 Testing of binding of BB5.1 Fab fragments to mouse C5 by ELISA and purity verification by SDS-PAGE

BB5.1 fragments were generated as described in section 4.2.9, tested in direct ELISA (section 2.11.1) to confirm binding to mouse C5 after the enzymatic digestion (Fig. 4.12 A) and resolved in SDS-PAGE gel to verify their purity. The latter showed that Protein A purification was much more efficient compared to Protein G at removing contaminating Fc and intact IgG (Fig. 4.12 B).

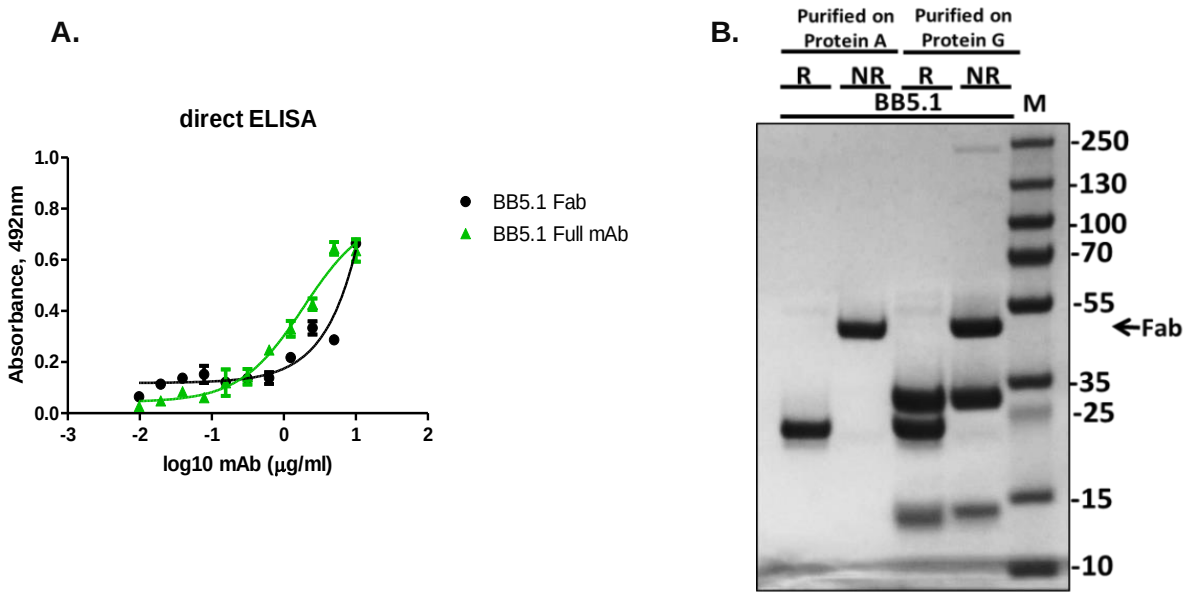

Figure 4.12 Testing of Fab(s) generated from BB5.1. A. *Direct ELISA; plates were coated with mouse C5; BB5.1 Fab detected mouse C5 to a similar degree compared to intact mAb.The assay was repeated three times with comparable results. The error bars are standard errors of triplicates.* ***B.*** *Purity of the Fab(s) was assessed by SDS-PAGE on 4 – 20% gel under non-reducing (NR) and reducing (R) conditions, stained with coomassie blue. NR; the 50 kDa corresponds to Fab fragment, R; 25 kDa to Fab. M; molecular weight marker.*

4.4.4 SPR analysis to determine BB5.1 mAb binding affinity to mouse C5

SPR analysis (section 4.2.6) on immobilised BB5.1 mAb (~200RU) with mouse C5 flowed over confirmed strong binding between mouse C5 and BB5.1 (KD = 8.1 x 10^{-9}) (Fig. 4.13). The very slow off rate of mouse C5 from mAb BB5.1 explains why this mAb is an efficient inhibitor of complement *in vivo*.

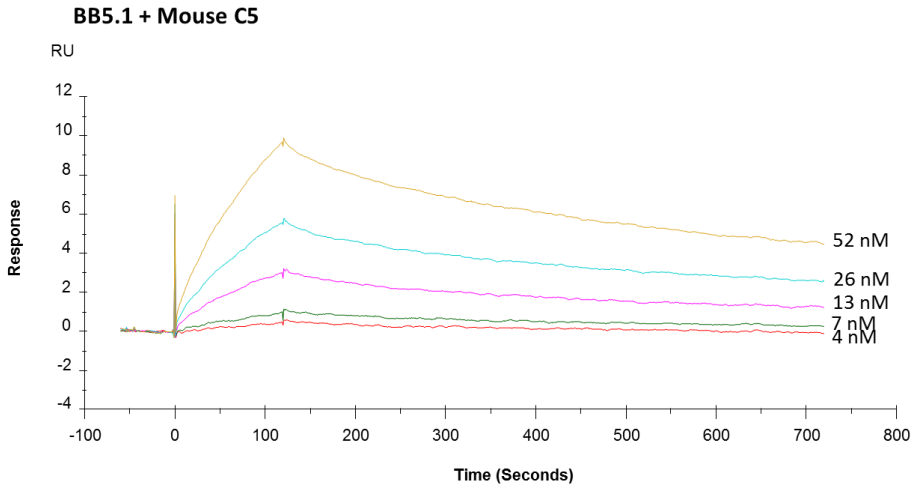

Antibody	ka (1/Ms)	kd (1/s)	KD (M)
Mouse C5			
BB5.1	1.56E5	0.0013	8.10E-9

Figure 4.13 Analysis of the binding affinity of BB5.1 to mouse C5. *BB5.1 was immobilised directly onto the CM5 sensor chip by amine coupling (GE Healthcare) at approximately 200 RU. Mouse C5 was flowed in HBS-EP at 52 to 4 nM and interactions with the immobilised mAbs analysed. Sensorgrams were collected and KDs calculated using the Langmuir 1:1 binding model. Representative sensorgrams are shown with fitted data in colour (n = 3).*

4.4.5 BB5.1 CDR sequences determination

The sequences were determined by Absolute Antibody as stated below;

Full VH Sequence

QVQLQQPGAELVRPGTSVKLSCKASGYTFTSSWMHWVKQRPGQGLEWIGVIDPSDSYT NYNQKFKGKATLTVDTSSSTAYMQLSSLTSEDSAVYYCARGGGSSYNRYFDVWGTGTT VTVSS

CDR-H1	CDR-H2	CDR-H3
SSWMH	VIDPSDSYTNYNQKFKG	GGGSSYNRYFDV

Full VL Sequence

NIMMTQSPSSLAVSAGEKVTMSCKSSQSVLYSSNQKNYLAWYQQKPGQSPKLLIYWAS TRESGVPDRFTGSGSGTDFTLTISSVQAEDLAVYYCHQYLSSRTFGGGTKLEIK

CDR-L1	CDR-L2	CDR-L3
KSSQSVLYSSNQKNYLA	WASTRES	HQYLSSRT

4.5 Further characterisation of RO7112689 anti-human C5

4.5.1 mAb RO7112689 inhibits CP haemolysis and RL in other species

The mAb was tested using ShEA and NHS or other species sera at a dose selected to cause ~80 - 100% target lysis. The antibody efficiently inhibited lysis by NHS and normal male mouse serum (NMS), inhibited rabbit serum (NRbS) weakly and did not inhibit rat serum (NRS)-mediated haemolysis (Fig. 4.14 A – D). In the reactive lysis system using human proteins, pre-incubation of C5b6 with RO7112689 efficiently blocked lysis on subsequent addition of C7-C9 (complete inhibition at a molar ratio C5b6: RO7112689 of 1:2; Fig.4.14 E). In contrast, incubation of GPE pre-coated with C5b6 with RO7112689 caused no inhibition of lysis on addition of C7-C9, even at the highest mAb doses (Fig. 4.14 F). These data demonstrate that, in addition to its impact on C5 cleavage, RO7112689 may inhibit the terminal pathway by binding and blocking the C5b6 complex before that complex binds the membrane. Of note, Eculizumab did not inhibit in the reactive lysis system at all, suggesting its sole action is to block C5 cleavage.

4.5.2 Quantification of human and mouse C5 by ELISA

RO7112689 was used a as capture antibody and Goat anti-human C5 (CompTech) was used as detection antibody. The sandwich ELISA showed very high sensitivity for measuring human and mouse C5 (Fig. 4.15 A, B) with working range of 0.2 – 250ng/ml for human and 50 – 500ng/ml for mouse C5. The assay did not detect C3, C3a or C5a, tested using purified proteins (Fig. 4.15 C). NHS samples from 25 healthy donors and NMS samples from 11 male C57/Bl mice were measured; mean C5 concentration in NHS was 79.6µg/ml (range; 56.0 – 130.7), and in NMS was 102.7 µg/ml (range; 92.7 – 130.6) (Fig. 4.15 D). The assay detected C5b6 but not C6 (Fig 4.15 E); the signal for C5b6 was lower by ~50% compared to the same molar dose of C5, suggesting some hindrance of binding of the antibodies to C5b in the C5b6 complex. Binding of C5b6 in the ELISA supports the above data demonstrating capacity of RO7112689 to inhibit reactive lysis when pre-incubated with C5b6.

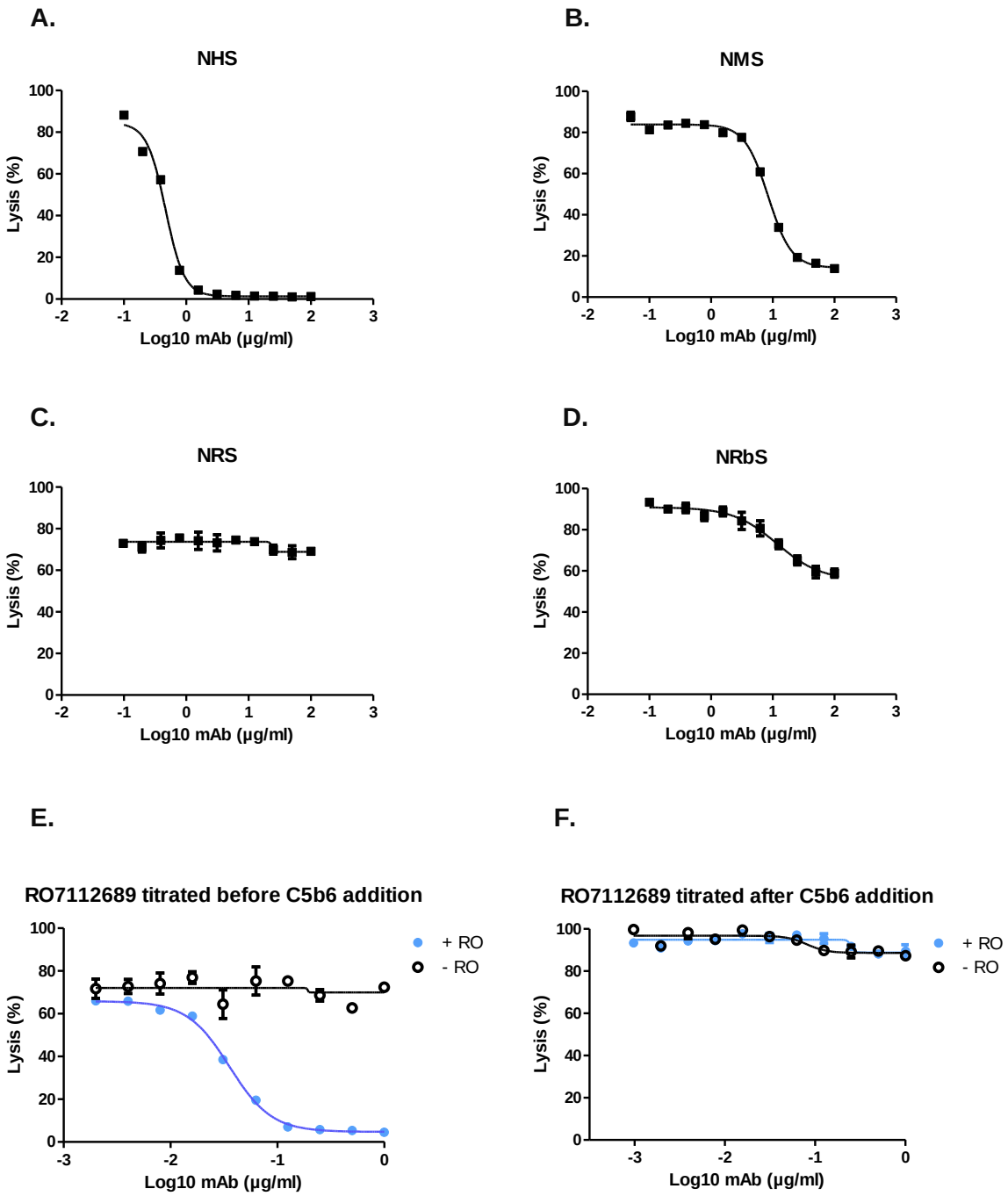

Figure 4.14 Haemolytic assays to investigate whether RO7112689 inhibits complement mediated lysis across species. A – D*. Functional assays to determine whether mAb RO7112689 inhibits complement classical pathway haemolysis (CH50) in different species. Sera tested were human (**A**), mouse (**B**), rat (**C**) and rabbit (**D**). **E, F**. Reactive lysis assays using human proteins. GPE were incubated with RO7112689 before and after C5b6 addition followed by sequential addition of C7, C8 and C9. RO7112689 efficiently blocked lysis when added before C5b6 addition but not after. All experiments were repeated three times with comparable results. The error bars are standard errors of triplicates.*

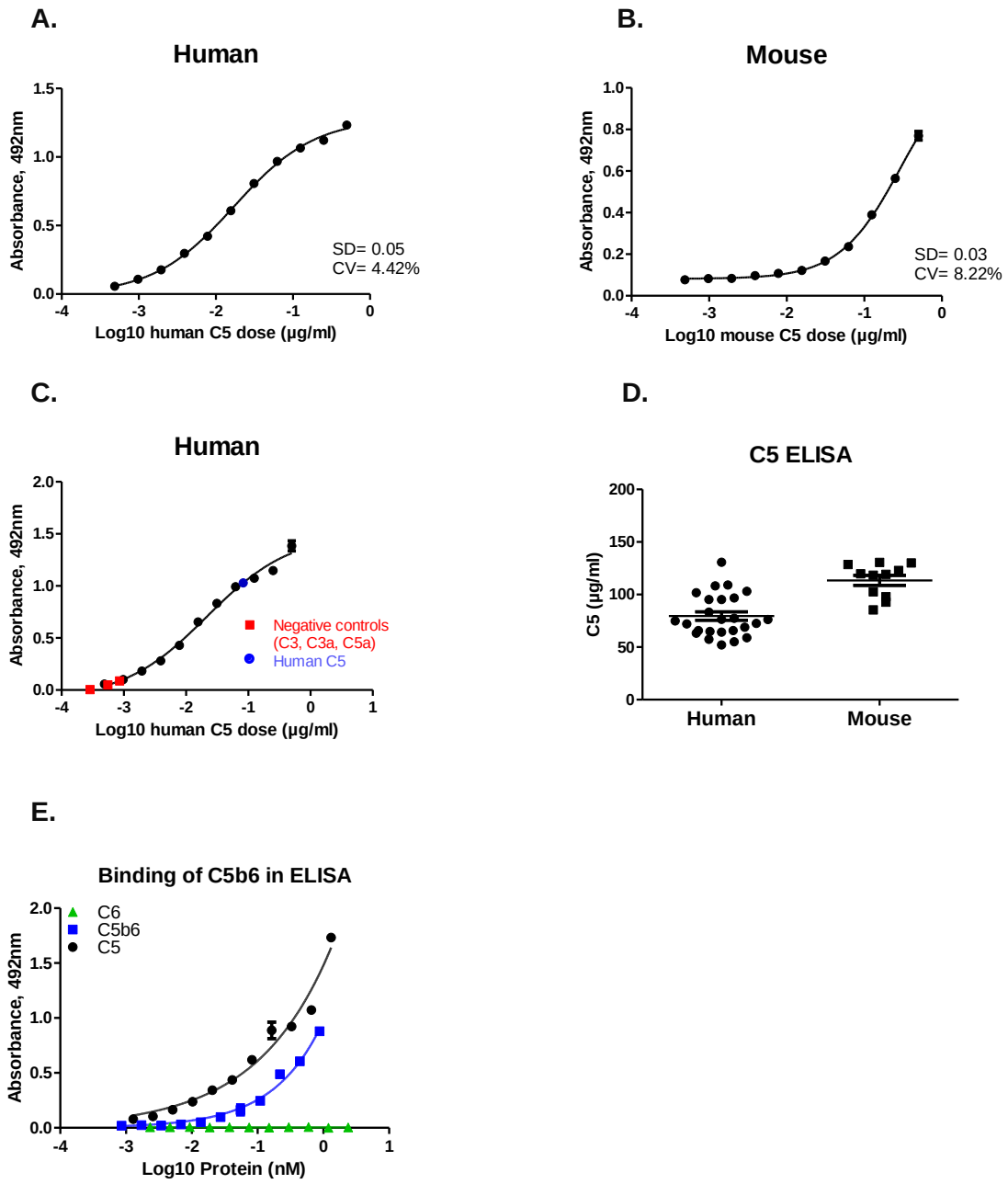

Figure 4.15 ELISA for human and mouse C5 detection A. B. *C5 sandwich ELISA was generated using RO7112689 as capture antibody and polyclonal anti-human C5 as detection. Standard curves were generated using either human C5 or mouse C5.* ***C.*** *Measurement of C3, C3a, C5a showed no cross-reactivity in the human C5 assay.* ***D.*** *Measurement of human and mouse C5 in the sandwich ELISA; serum from 25 healthy donors and 11 male C57/Bl mice (NMS) were measured. The average level of C5 in NHS was 79.6µg/ml (range; 56.0 – 130.7), and in NMS was 102.7 µg/ml (range; 92.7 – 130.6).* ***E.*** *Detection of human C5 and C5b6, but not C6; signal intensities of C5b6 were ~50% less intense compared to the same amount of C5.*

4.6 Discussion

The discovery of Eculizumab (anti-C5 mAb) and its dramatic success catalysed Pharma interest in anti-complement drugs (Morgan and Harris 2015; Harris 2018). Cost and convenience are limiting factors in broadening anti-complement drug use; current cost and dosing schedules for Eculizumab are incompatible with use in treatment of common, chronic diseases. Other limiting factor is that the currently available agents are human-specific, restricting proof-of-concept of efficacy of C5 inhibition in rodent disease models. The mAb BB5.1 has been widely used in mouse models (Copland *et al* 2010; Raedler *et al* 2011), and a single report described a blocking anti-rat C5 mAb that was not further utilised (Zhou *et al* 2007), apart from these, no anti-C5 mAb inhibiting in other animal species have been described.

Here I immunised C6-deficient mice with C5b6 in order to develop functionally optimal mAb, selecting from the outset for function-blocking activity. From nine fusions approximately 88,000 hybridoma clones were obtained and screened, 139 antibodies were selected in ELISA, 12 of these inhibited human complement. All of the mAb selected based on blocking activity bound native C5 and C5b6 (the immunogen), but not C6, in ELISA. Three of these were selected for further characterisation; testing for inhibition in other species showed that two of the mAb, 7D4 and 4G2 (both against C5α chain), inhibited C5 in rat, rabbit, guinea pig and mouse sera, whereas 10B6 (against C5β chain) was human-specific. RO7112689 bound the C5β chain, and was a weak inhibitor of guinea pig and mouse C5 (Fig. 4.3), while Eculizumab bound C5α and was human-specific (Schatz-Jakobsen *et al* 2016). The critical residue in the Eculizumab binding site that dictates human specificity is Trp917, replaced by Ser in other species, including non-human primates, rat, mouse, rabbit, guinea pig, sheep, pig and horse as reported (Schatz-Jakobsen *et al* 2016; Brachet *et al* 2016), and from my data base search (www.ncbi.nlm.nih.gov/protein). The fact that the two blocking anti-C5α mAb 7D4 and 4G2 work across species suggests that they bind an epitope distinct from that in C5α bound by Eculizumab; this is supported by the demonstration that these mAb bind C5b6 (the immunogen) in the direct ELISA while Eculizumab does not. The mAb 4G2 detected C5 captured on Eculizumab in a sandwich assay, confirming that the epitopes are distinct; however, 7D4 did not bind in this assay, indicating that its epitope overlaps that of Eculizumab. When RO7112689 (C5β-specific) was used as capture in the assay, both the C5α-binding mAb detected the bound C5 as anticipated; in contrast, the C5β-specific mAb 10B6 gave no signal, demonstrating that its epitope was masked by the capture mAb. Of note, RO7112689, like 10B6, also binds C5b6 (Fig. 4.4). These data indicate that the epitopes for these two mAb are overlapping; the fact that RO7112689 inhibits across species while 10B6 is human-specific suggests that the epitopes are non-identical. It is clear

from the above findings, and from published work comparing tick-derived C5 inhibitors with Eculizumab, that there are numerous sites on C5 where binding of an inhibitor can effectively block function (Jore *et al* 2016). This supports the suggestion that these diverse inhibitors act as conformation locks, preventing a structural "priming" event that is necessary for cleavage of C5 by the convertase.

The mAb were also tested for their capacity to block the atypical cleavage of C5 by neutrophil elastase (NE), a process that has been implicated in the generation of C5a and MAC at inflammatory sites such as in the rheumatoid joint and cystic fibrosis lung (Giles *et al* 2015; Vogt *et al* 2000; Fick *et al* 1986); mAb that inhibited this cleavage might therefore have additional value as therapeutics. The mAb 4G2 strongly inhibited NE-mediated C5 cleavage and C5a generation *in vitro*, whereas the other two novel mAbs weakly inhibited atypical C5 cleavage. Eculizumab did not inhibit C5 cleavage by NE but RO7112689 effectively blocked generation of C5a by NE (Fig. 4.8).

SPR analysis (Biacore) showed very strong and stable binding of 7D4 and 10B6 to human C5 with dissociation rates and calculated affinities comparable to RO7112689 (Fukuzawa *et al* 2017) (Fig. 4.7). In contrast, 4G2 binding to human C5 was much weaker – but this mAb bound rat C5 much more strongly than human (KD 4.872×10^{-9} for rat and 3.68×10^{-9} for human) and with a slow off-rate; these binding data support the functional assays where 4G2 was a more potent inhibitor of rat C5 than human (Fig. 4.3 A). The 4G2 mAb was tested *in vivo* as a prophylactic therapy in a model of MG, previously demonstrated to be dependent on MAC assembly in man and rodents and suppressed by TP deficiencies or inhibition (Ingram *et al* 2012; Morgan *et al* 2006). While control animals developed severe muscle weakness and weight loss, mAb 4G2 treated rats were protected from disease and weight loss (Fig. 4.7 A, B). Endplates in controls were reduced in number, fragmented and richly decorated with C3b/iC3b and C9/MAC, whereas in 4G2 treated animals endplates were preserved in number and integrity; although endplates were strongly C3b/iC3b-positive in these animals, C9/MAC deposition was markedly reduced or absent (Fig. 4.8 D - I). Although mAb 4G2 proved to be an efficient blocker of EAMG, assays of serum haemolytic activity showed ~35% residual lysis after the 2-hour time-point in 4G2 treated animals (Fig. 4.7 C). I have previously demonstrated that as little as 2 ng/ml C5 added back to undiluted C5-depleted serum is sufficient to cause measurable lysis, and 50% lysis in the assay was attained at 2µg/ml C5 added back to undiluted C5-depleted serum (Zelek *et al* 2018). These findings illustrate the exquisite sensitivity of the haemolytic assay and show that it is not a good predictor of efficacy of C5 inhibition in disease. We have not yet tested this mAb for amelioration of established disease in the EAMG model, difficult given the

acute nature of the model, or in more chronic disease models; such studies are planned in the future.

The novel mAbs CDR sequences have been defined as an external service. This, in combination with cryo-EM analysis, will enable me to define precisely their binding sites on C5. Fab generated here will be used for this work.

The novel mAbs described here are efficient blockers of human C5, with binding sites and other properties distinct from existing anti-C5 mAb. All three mAb bind C5b6, used as the immunogen, and block reactive lysis, a property absent from Eculizumab, that may provide a therapeutic advantage. Notably, two of the mAb inhibit C5 in common laboratory animal species, raising the prospect of their use as tools in proof-of-concept studies, illustrated here using EAMG as an example. One of the new mAb (4G2) was a strong inhibitor of elastase-mediated C5 cleavage, raising the possibility of testing the impact of blocking atypical C5 cleavage in inflammatory diseases where neutrophil activation predominates in rodents or man.

BB5.1 is an efficient inhibitor of mouse complement widely used in animal models (Wang *et al* 1995; Huugen *et al* 2007; Copland *et al* 2010; Raedler *et al* 2011). Although BB5.1 was the first functional blocker of complement and it has been around for many years (Frei *et al* 1987), little was known about its mechanism of C5 inhibition. My data show that BB5.1 is mouse C5-specific and binds the C5β chain (Fig. 4.10 and 4.11 B). The Biacore testing showed very strong and stable binding of BB5.1 to mouse C5 with slow dissociation rate and affinities comparable to Eculizumab (Fig. 4.13). The fact that BB5.1 recognises the C5β-chain suggests that BB5.1 and Eculizumab (C5α-chain specific) are quite different antibodies, further supporting the concept of C5 having multiple surface sites that can be targeted by mAb or other agents to cause inhibition of C5 cleavage and function, likely through conformational locking (Jore *et al* 2016).

A further characterisation of mAb RO7112689 showed that the mAb binds and inhibits not only human C5 as stated in the previous report (Fukuzawa *et al* 2017) but also mouse C5; this was confirmed by ELISA and WB detecting C5β chain of mouse and human C5 (Fig. 4.5 D, 4.15 B, 4.15 B). The cross-reactive sandwich ELISA allows quantification of C5 in mouse serum (mean of 102.7µg/ml from 11 male mice), a useful tool for future studies (Fig. 4.16). The original report on RO7112689 (Fukuzawa *et al* 2017) stated that the antibody inhibits C5 cleavage by the C5 convertase, the same mechanism as Eculizumab, despite the fact that these mAb bind different chains of C5 (Fukuzawa *et al* 2017; Schatz-Jakobsen *et al* 2016; Rother *et al* 2007). I confirmed that RO7112689 inhibited C5 cleavage, but also showed that it binds C5b6 which suggests that it inhibits its association with the membrane.

In a reactive lysis system (2.17.6) using purified C5b6, when added to C5b6 prior to (but not after) incubation with the target GpE, RO7112689 efficiently inhibited reactive lysis (Fig. 4.15 E, F). This finding was supported by the demonstration that RO7112689 binds C5b6 in ELISA (Fig. 4.15 E). The ability to inhibit C5b6-mediated lysis is an important second mode of action for this mAb, particularly given the growing list of situations where C5 is atypically activated by proteases to generate a C5b-like fragment capable of triggering MAC assembly (Foley *et al* 2016; Huber-Long *et al* 2006; Amara *et al* 2010). The capacity of RO7112689 (and my novel mAbs) to block atypical cleavage of C5 by neutrophil elastase (Fig. 4.8) and to inhibit after C5 cleavage may contribute substantially to its mechanism of action for complement inhibition *in vivo*.

In summary, I have generated several anti-C5 blocking mAb with diverse binding sites, properties and cross-species activities and have further characterised commercial (RO7116829) and donated (BB5.1) anti-C5 mAbs. These findings add to understanding of C5 targeting by mAbs and provide new tools for human and animal studies; further analyses in progress will provide fundamental information for future structure-based drug design. The primary purpose of the current project was to find antibodies that inhibited MAC formation beyond C5; however, the fact that all the blocking mAb generated using C5b6 as immunogen in C6D mice were anti-C5 necessitated their characterisation. The next chapter takes the work back on mission and beyond C5.

CHAPTER 5; DEVELOPMENT AND CHARACTERISATION OF NOVEL ANTIBODIES CAPABLE OF INHIBITING COMPLEMENT DOWNSTREAM OF C5

5.1 Introduction

A step change is now needed to enable the use of anti-complement drugs in less rare (and common) diseases such as MS, AMD and AD. In these common diseases proportion of patients do not respond to currently available agents. Taking anti-complement approaches into these diseases requires a new generation of drugs that are safer, cheaper and easier to administer. The field of anti-complement drugs is pretty crowded with numerous agents being developed, some of which have already reached the clinic and become blockbusters (Morgan and Harris 2015; Ricklin *et al* 2018). The complement cascade can be targeted at many stages; however, the current anti-complement drugs are focussed on very few targets, with agents targeting the complement protein C5 or its breakdown products predominating. The focus on C5 and relative neglect of other targets has been opportunistic and not based on evidence of best target. The lesson taken from my development of novel C5 blocking mAbs (chapter 4) is that generation of C5 inhibitory mAb is relatively easy and expedient - one in twelve of the anti-C5 clones obtained was a functional C5 blocker! In this chapter I have explored other terminal pathway targets downstream of C5 and assessed their therapeutic potential in animals.

To date there are only few reports targeting MAC beyond C5. An anti--C8 mAb was tested in hyperacute rejection (HAR) and cardiopulmonary bypass (CPB) rodent models (Rollins *et al* 1995; Rinder *et al* 1999); in HAR, mAb treatment protected hearts perfused with human serum while in CPB the mAb reduced platelet activation. A polyclonal antibody against C6 inhibited clinical symptoms of EAMG in rats (Biesecker *et al* 1989). These experiments not only demonstrate the crucial role of MAC as a pathology driver, but also highlight the therapeutic potential of developing anti-terminal pathway drugs beyond C5. Currently, an anti-C6 mAb (CP010) developed by Complement Pharma is in pre-clinical development for neurological disorders (Ricklin *et al* 2018). Currently there is only one drug targeting MAC downstream of C5 in clinical trials, a gene therapy agent (AAVCAGsCD59) in development for AMD (Cashman *et al* 2011).

I selected C7 as the optimal target; however, as the project developed, C6 and MAC intermediate inhibitors were also generated. I focused on C7 as a target for a number of reasons:

- Unique among the terminal pathway components, C7 is not an acute phase reactant (Würzner *et al* 1994; Barnum and Schein 2018); therefore, the plasma levels remain stable in disease making it an easier target;
- as a consequence of this, the dose needed to inhibit complement will likely be less

compared to the current treatment with Eculizumab and the duration of inhibition is likely to be longer;

- inhibiting C7 is likely to be less of an infection hazard compared to current therapies because C5a-mediated neutrophil recruitment is unimpaired -indeed, the majority of patients with C7 deficiency are healthy (Würzner *et al* 1992);
- C7 has been neglected as a target, unlike C5 where numerous Pharma companies are developing mAb or other drugs to target C5 (Harris 2018; Ricklin *et al* 2018; Zelek *et al* 2019).

C7 and C5b67 complex are essential building blocks of MAC assembly (Hadders *et al* 2012). In the fluid phase C7 can also assemble into soluble (s) complexes such as C5b-7, C5b-8, C5b-9. Naturally occurring terminal pathway inhibitors such as S – protein (vitronectin) and clusterin associate with the soluble complexes mediating their clearance (Murphy *et al* 1989; Fernie-King *et al* 2001).

In this chapter I will describe the generation and characterisation of a panel of anti-C7 mAbs, all of which are efficient inhibitors of human and rodent complement. The mAb inhibited complement *in vivo*. One of the mAb, 2H2, showed long lasting (up to one week) inhibition with a single dose in rats; this and other data suggest that this mAb inhibits complement by binding C5b-7 complex resulting in lower dose and long-lasting neutralisation of complement.

5.2 Specific methods

5.2.1 Breeding of C7 deficient mice

Two pairs of mice heterozygous for a CRISPR-generated knock-out mutant of the C7 gene were purchased from Jackson Laboratory (C57BL/6NJ-C7em1(IMPC)J/Mmjax, MMRRC Stock No: 42133-JAX). These mice were generated by the Knockout Mouse Phenotyping Program (KOMP2). The deletion removed 247 bp of the C7 coding sequence, resulting in the deletion of exon 2, and a frame shift causing early termination. The mice were back-crossed to obtain homozygous C7 deficient mice and establish a colony. WB and haemolysis assays were used to confirm heterozygous and homozygous C7 deficiency in the back-crosses.

5.2.2 High-throughput classical pathway (CP) haemolysis assay for screening of mouse serum complement lytic activity

The assay obviates the need for large amounts of animal (in this case mouse) serum to determine complement mediated lysis and the impact of blocking mAb. NHS depleted of the specific protein (in this case C7) is the source of the rest of the complement proteins; the missing protein is reconstituted from the animal serum. Mouse blood was collected and processed as described in section 2.12. The assay was performed as described in section 2.17.8.

5.2.3 *In vivo* testing of mAb for the capacity to inhibit complement

Clones 17E7 and 73D1 were tested in mouse to determine their capacity to inhibit complement *in vivo*. To test clone 17E7, C7 deficient mice (10) were injected intraperitoneally with human C7 (500µg), then split into test and control groups (5 in each). The test group animals were injected subcutaneously with 17E7 mAb (1mg), while control group mice were injected with an irrelevant mAb (1mg, JC-3); blood was collected from all the animals just before the experiment, one hour after C7 administration (immediately before giving the mAb) and at intervals after mAb injection. Serum was prepared (section 2.12) and tested for lytic activity as above.

5.2.4 *In vivo* testing of mAb for the capacity to inhibit disease in experimental autoimmune myasthenia gravis (EAMG) model in rats

The therapeutic effect of mAb 2H2 was tested in the EAMG model as described in section 4.2.7 with following amendments; Lewis rats used (100 – 150g, Charles River Laboratories, Edinburgh, UK), lower dose of mAb (10mg/kg) and different isotype control (mAb; D1.3).

5.2.5 Measuring kinetics and affinity of mAb using Biacore

The SPR assays were run on a Biacore™ T200 System as described in section 4.2.6 at a flow rate of 30 µl/minute with EP-HBS running buffer. For mAb of isotype IgG, a Mouse Antibody Capture kit (GE Healthcare, # BR-1008-38) was used to immobilise the mAb on a CM5 sensor chip (GE Healthcare, #29-1496-03) as recommended by the manufacturer. mAb isotype IgM was immobilised on a Protein L Series S sensor chip (GE Healthcare #29-2051-38). mAb were flowed to saturate the surface, then C7, human, rat or mouse, diluted in EP-HBS (usually 0 – 68nM) flowed over the immobilised mAb. For kinetic analysis the flow rate was maintained at 30µl/minute, and data were collected at 25°C. All reagents used

were of high purity, polished by GF immediately before use to ensure removal of any aggregates. Data were evaluated using Biacore Evaluation Software.

5.2.6 Pull-down assay to identify whether mAb 2H2 inhibits one of the TP complexes

Complement in serum (rat or human ~3ml) was activated via both classical and alternative pathways by incubation with Zymosan A (7mg/ml) and aggregated human IgG (1mg/ml) in the presence of biotinylated mAb 2H2 (section 2.2.2). The mixture was incubated for 32 hours at 37°C in a shaking water bath to ensure that all the C5 was converted into the complex. The reaction was stopped by centrifugation at 2500rpm for 15 minutes at 4°C, the supernatant (activated serum) collected and mixed with 1ml Avidin beads (taken from a 1ml HiTrap NHS activated column with 1mg of Avidin immobilised as described in section 2.15 and re-suspended to 7ml total volume). The mixture was incubated for one hour at ambient while mixing gently, then beads washed five times by centrifugation and the bound mAb 2H2-complex eluted by incubation (10 minutes at 100°C) in reduced or non-reduced SDS-PAGE running buffer. Supernatants were subjected to SDS-PAGE and WB (section 2.9). The activated serum containing the complex with mAb 2H2 was also tested in ELISA (section 2.11.2). Briefly, plates were coated with Avidin (10µg/ml); after BSA blocking the sample was added and detected with Goat anti-C5, C6, C7, C8 or C9 antibodies, then developed with rabbit anti-Goat-HRP. Appropriate controls included; C7 pre-incubated with biotinylated mAb 2H2, mAb 2H2-Biotin only.

5.2.7 Testing whether mAb bind fluid phase or membrane bound MAC precursors by flow cytometry

To investigate whether inhibition of MAC formation occurred through mAb binding intermediates in the fluid phase or on the cell surface, CP haemolysis assay utilising ShEA and human or rat serum, was performed as described in section 2.17.4. The mAb was added at total concentration of 100µg/ml to ensure complete MAC inhibition. After incubation, cells were pelleted, supernatants were removed and the ShEA, washed into HBS containing 5% w/v FBS, 1% w/v BSA (FACS buffer); anti-mouse IgG-FITC diluted 1 in 50 in FACS buffer was added to detect bound mAb, incubated for 30 minutes on ice, cells were washed twice in FACS buffer and analysed by flow cytometry using a Becton Dickinson FACSCalibur. ShEA yielded a single population when analysed for forward and side scatter; the entire population was gated for analysis of fluorescent staining. Relevant negative controls of unstained, secondary mAb only and a positive control for MAC formation of aE11 anti-C9 neo-specific monoclonal antibody (Hycult Biotech, #HM2167) were prepared. The data was analysed using FlowJo software version 10.

5.3 Results

5.3.1. Breeding of C7 deficient mouse

CRISP-generated heterozygous C7 knock-out mice (C57BL/6NJ-C7em1(IMPC)J/Mmjax) were back-crossed to obtain homogenous C7 deficient mice as described in section 5.2.1. Litters were screened for C7 deficiency using the modified haemolytic assay (section 5.2.2) and WB (section 2.9) and homozygotes were selected for further breeding (Fig. 5.1). The data also show that mouse serum alone (NMS controls; Fig 5.1 A) at the dose used caused no lysis in this system, demonstrating the value of the modified assay. The obtained C7 deficient mice colony showed no lytic activity and absence of C7 by WB (Fig. 5.1 B). No health issues were observed with these mice.

5.3.2. Generation of anti-human, rat, mouse C7 mAb

C7 deficient (C7D) mice were immunized with human C7 and/or rat C7 (both purified in-house). The C7D mice were also used as a source of macrophages during the cloning process as a feeding support for hybridoma cell lines. Clone 17E7 was generated in wild type mice as no C7D mouse was available at that time. The immunised animals were tail bled, the collected blood allowed to clot and serum prepared; direct ELISA was used to determine which mouse had the highest antibody titre as described in Methods. Animals with the highest titre were sacrificed, spleens harvested and used in the fusion. Supernatants of the fused clones were screened the same way as for C5 blockers in direct ELISA for C7 specificity (section 2.11.1) and high throughput classical pathway haemolysis assay for complement inhibition (section 2.17.3). In total, 15 fusions were performed; ~15,000 hybridoma clones were generated and screened, 7 confirmed to be inhibitory, and five of these, 2H2, 3B11, 17E7, 59E7 and 73D1, chosen for full characterisation. Clone 17E7 was obtained from fusion 1 (WT animals immunised with human C7), 2H2 from fusion 7 (C7D animals immunised with rat C7), 3B11 and 59E7 from fusions 14 and 15 respectively (C7D animals immunised with both human and rat C7). The inhibitory clones that were also positive in ELISA were expanded in an Integra flask as described in Methods.

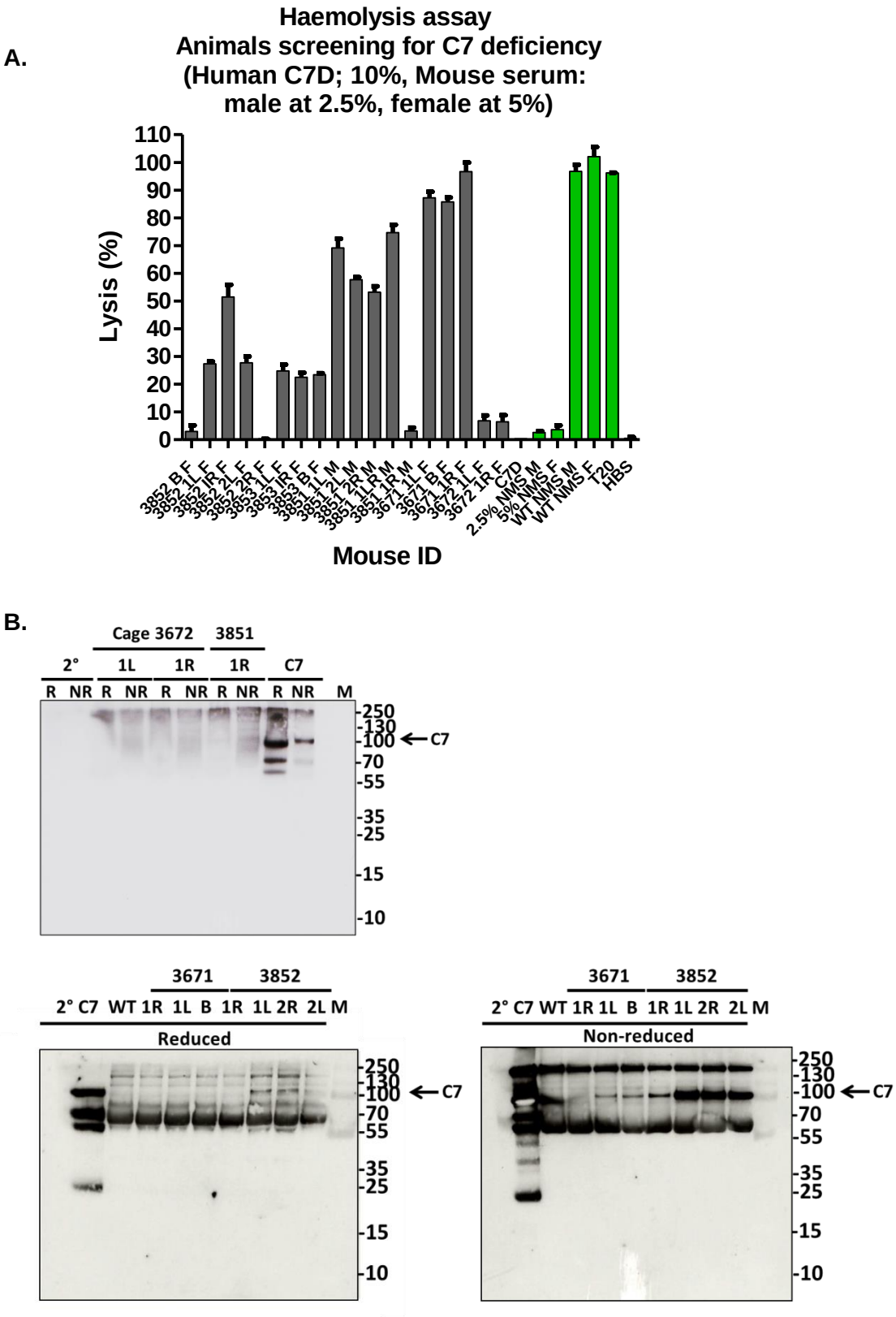

Figure 5.1 Screening mice for C7 deficiency. *Litters from the heterozygote back-crosses were screened; example data are shown.* ***A.*** *Haemolytic assay to identify mice with no complement lytic activity; here, mice 3852-B, 3852-2R, 3851-1R, 3672-1L and 3672-1R showed no haemolysis of ShEA. Controls in green, NMS, normal mouse serum without human C7D; M, male; F, female; T20, 0.1% tween 20.* ***B.*** *The error bars are standard errors*

of triplicates. The absence of C7 in animals 3851-1R, 3671-1R, 3672-1L and 3672-1R was confirmed by WB; Mouse sera (1 in 100 dilution in PBS) and human C7 (1µg) were resolved on 7.5% gels under NR and R conditions and transferred to nitrocellulose membrane. Blots were probed with in house rabbit anti-C7 (5 µg/ml) and detected with Donkey anti-rabbit-HRP. The 95 kDa band corresponds to intact C7. M; molecular weight marker (PageRuler, #26620), WT; wild type.

5.3.3 Isotyping and purification of the anti-C7 mAb

Antibody clones; 17E7 and 73D1 were identified as isotype IgG2aκ, 2H2 and 59E7as IgG2bκ and 3B11 as IgMκ (Isostrip, Roche, # 11493027001). All clones except 3B11 were purified using protein G chromatography (section 3.2.7.1); clone 3B11 was purified with ammonium sulphate precipitation as described in section 3.2.7.2. Purity of the antibodies was determined using SDS-PAGE (Fig. 5.2).

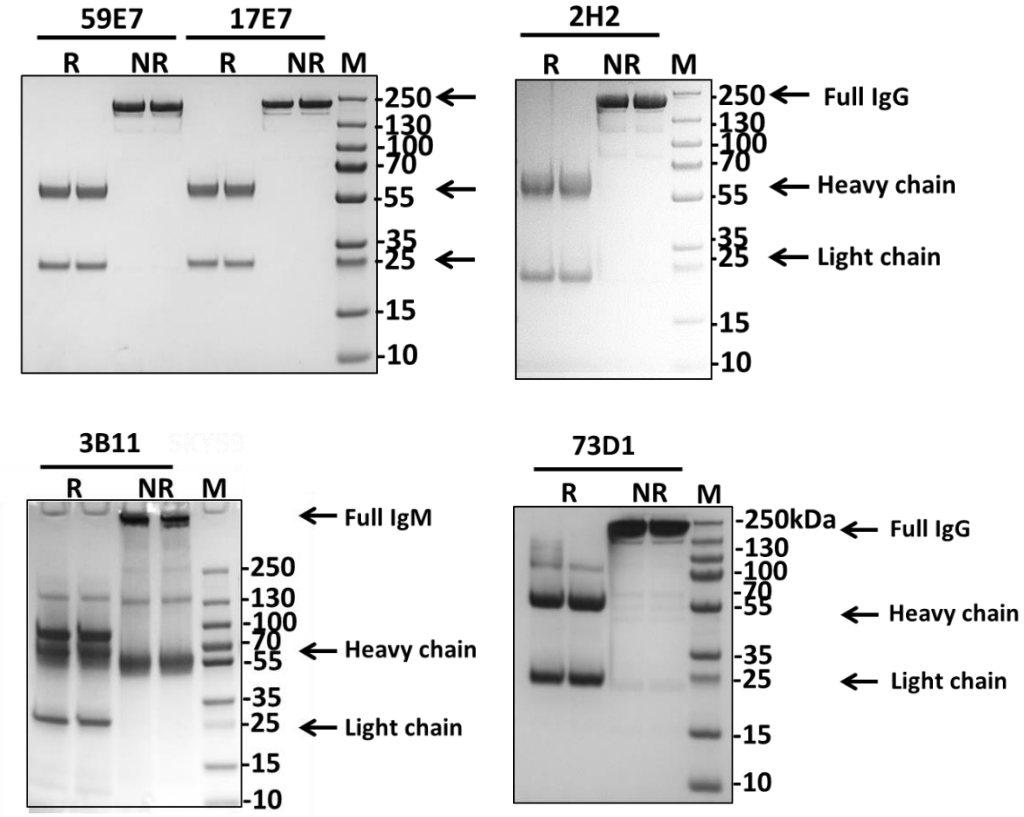

Figure 5.2 *SDS-PAGE of the purified mAb. mAb (2µg) were resolved on 7.5% gels under non-reducing (NR) and reducing (R) conditions, then stained with coomassie blue. The 150 kDa band (NR) corresponds to intact IgG, in R lanes the 55 kDa band corresponds to mAb heavy chain and 25 kDa to mAb light chain. M; molecular weight marker (PageRuler, #26620). Albumin contaminant was observed at ~55 kDa in IgM mAb 3B11.*

5.3.4 Cross-species complement inhibition by mAb anti-C7 in haemolysis assays

Hybridoma clones were initially selected for further characterisation based upon the capacity of clone supernatants to cause inhibition of CP haemolysis in NHS and/or NRS; five of the selected monoclonal clones, 2H2, 3B11, 17E7, 59E7, 73D1, were expanded for further characterisation, secreted mAbs purified and tested in haemolysis assays with different species sera (Fig. 5.3 A – D). As expected, each of the selected mAbs efficiently inhibited CP haemolysis in some species sera; clones 3B11, 17E7 and 59E7 predominantly in NHS, clone 2H2 predominantly in NRS and clone 73D1 in NMS (Fig. 5.3 A – C); 7D4 alone efficiently inhibited lysis of ShEA in NRbS (Fig. 4.3 D). All tested mAbs showed some cross-species inhibition. Anti-C5 mAb were used as positive controls; Eculizumab and RO7112689 for NHS, BB5.1 for NMS and 7D4 for NRS complement. The calculated 50% complement inhibitory doses and haemolytic units (HU) of all mAbs are shown (Table 5.1). A serum excess assay was used to test mAb 17E7 and 2H2 in conditions that better reflect those prevailing in whole blood (Fig. 5.3 E, F).

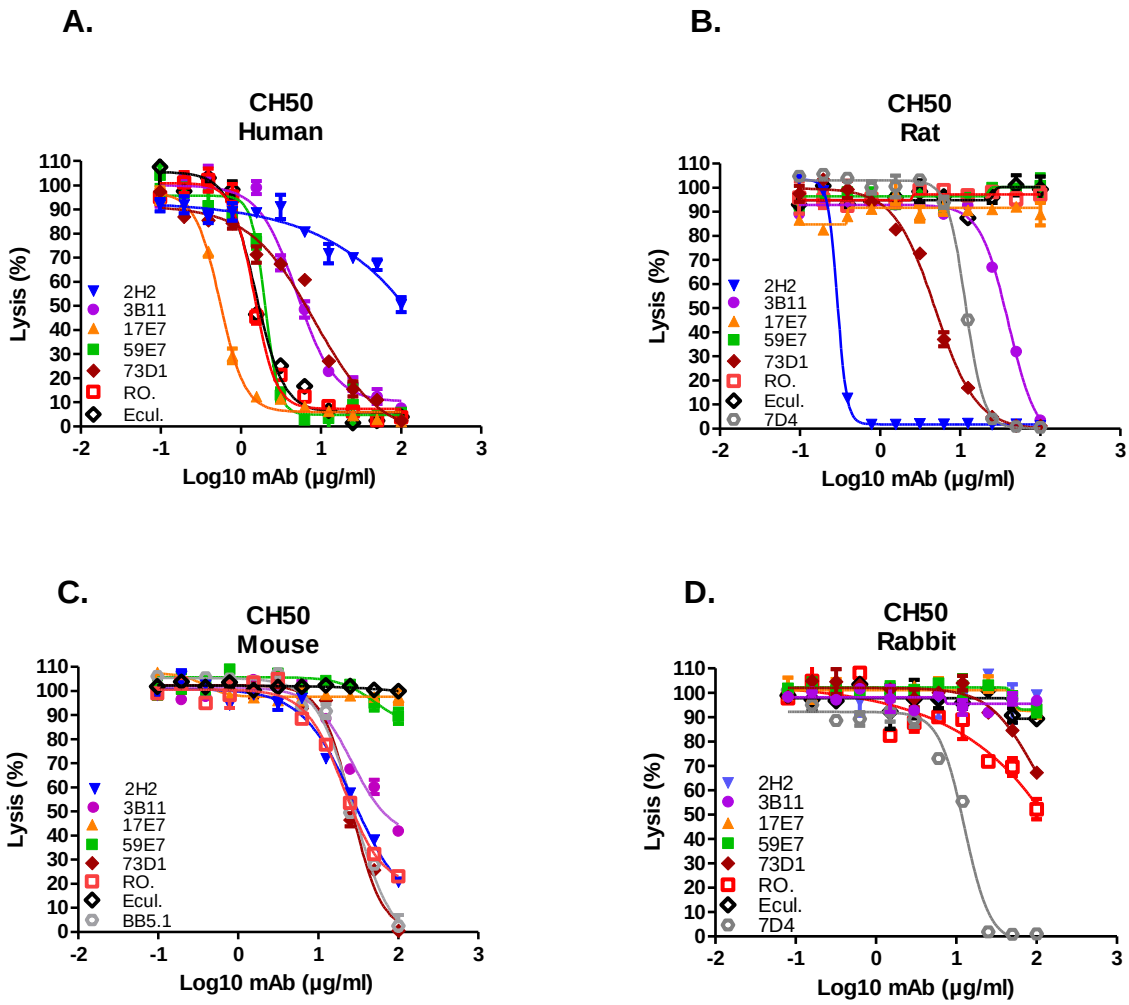

E.

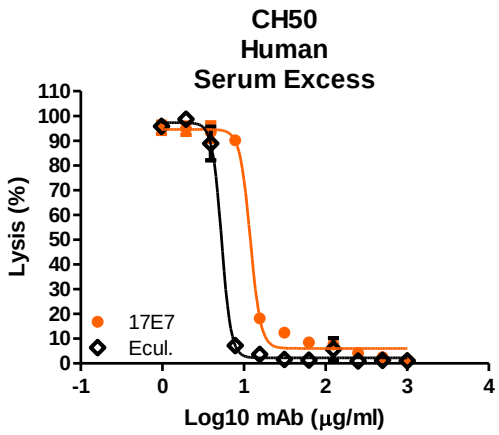

F.

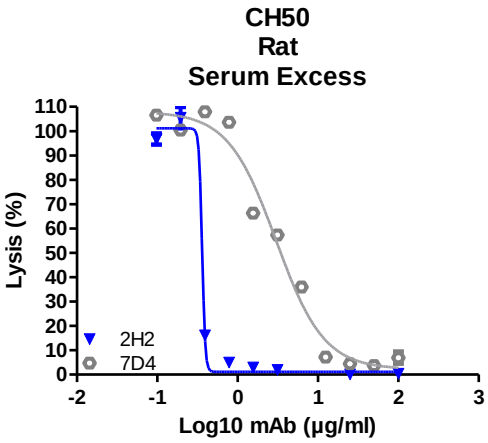

Figure 5.3 Haemolytic assays to investigate whether the anti-C7 mAbs inhibit complement mediated lysis across species. *Sera tested were human (**A**), rat (**B**), mouse (**C**) and rabbit (**D**). Anti-C5 mAb RO7112689, Eculizumab, BB5.1 and 7D4 were used as comparators. **E. F.** Serum excess assay performed utilising NHS or NRS concentration 10-fold that used in the standard CP assay. Test and control mAb were titrated in range 0 – 100µg/ml. All experiments were repeated at least three times with comparable results. The error bars are standard errors of triplicates.*

Antibody	Isotype	Haemolytic Units (HU)	50% Inhibitory Dose (ng/ml)	Cross-species reactivity
17E7	IgG2a, K	Human = 55.1	Human = 181.6	Strong; Human
59E7	IgG2b, K	Human = 47.7	Human = 209.7	Strong; Human
3B11	IgM, K	Human = 19.9 Rat = 11.9	Human = 501.9 Rat = 839.5	Strong; Human, Rat
2H2	IgG2b, K	Human = 1.0 Rat = 264.8 Mouse =2.7	Human = 9977.0 Rat = 33.9 Mouse = 3715.4	Strong; Rat Weak; Mouse, Human
73D1	IgG2a, K	Human = 17.2 Rat = 19.8 Mouse =13.9	Human = 581.8 Rat = 505.5 Mouse = 720.3	Strong; Mouse, Weak; Human, Rat
7D4	IgG2b, K	Human = 69.3 Rat = 9.5	Human = 144.2 Rat = 1054.4	Strong; Human, Rat
BB5.1	IgG1, K	Mouse =16.3	Mouse = 613.6	Strong; Mouse
RO7112689	IgG1, K	Human = 49.9 Mouse = 1.4	Human = 212.3 Mouse = 1862.1	Strong; Human Weak; mouse
Eculizumab	IgG2/4, K	Human = 47.1	Human = 181.6	Strong; Human

Table 5.1 *Calculated HU and 50% dose (ng/ml) required to inhibit lysis for each antibody tested.*

5.3.5 Reactive lysis to identify mechanism of mAb anti-C7 inhibition

GPE were first incubated with C5b6 (section 2.17.6) then mAb (17E7, 59E7, 73D1, 2H2) at various doses (0 – 1µg/ml) added either before or after C7 addition, followed by C8, C9 (Fig. 5.4 A – D). All mAb except 2H2 were tested with human purified proteins, mAb 2H2 using purified rat C7 or EDTA-NRS as a source of rat C8 and C9. The tested mAbs showed strong inhibition when added to GPE-C5b6 before C7 was added, but only mAb 2H2 inhibited when added after C7, implying that this mAb, and only this mAb, worked in part by blocking C8 binding to C5b67 on the target surface and suggesting that this mAb had a distinct mechanism of inhibition. To further test mode of inhibition, mAb 17E7 was either incubated with GPE-C5b6 before C7 addition or pre-incubated with C7 before exposure to GPE-C5b6 (Fig. 5.4 E); inhibition of lysis was essentially the same in both conditions confirming that the mAb captures fluid-phase C7 and prevents formation of an active C5b67 complex, either by preventing C7 binding to C5b6 or by permitting C7 binding but preventing its unfolding and/or capacity to bind C8. In a reactive lysis system using human C5b6, rat C7 and either human C8/C9 or NRS as a source of C8/C9, ~60% lysis was obtained (Fig. 5.4 G). In the latter system, mAb 2H2 effectively blocked lysis when pre-incubated with GPE-$C5b67_{(rat)}$ (Fig. 5.4 F).

5.3.6 Add-back haemolytic assays to investigate the species selectivity of mAb 2H2

To investigate further the selectivity of mAb 2H2 for rat; human or rat C6 and C7 were used in add back assays (section 2.17.9). Both depleted and deficient sera are labelled D. The proteins were added at physiological levels to human or rat C7D or C6D sera and the restored sera titrated to give ~80% lysis of ShEA in a CP assay. mAb 2H2 was diluted at concentrations 0 – 25µg/ml. As anticipated, mAb 2H2 inhibited lysis of rat C7D restored with rat C7 (Fig. 5.5 A); surprisingly, mAb 2H2 also inhibited lysis by rat C7D restored with human C7 (Fig. 5.5 B). The mAb also inhibited lysis by rat C6D restored with human C6 (Fig. 5.5 C) and rat C6D/C7D restored with human C6 and human C7 (Fig. 5.5 D; these data imply that the species specificity of this mAb extends beyond the native proteins. In support of this, mAb 2H2 did not significantly inhibit lysis by human C7D restored with rat C7 demonstrating that rat C7 alone was not sufficient for effect of the mAb (Fig 5.5 E).

5.3.7 ELISA to confirm mAb binding to human, monkey, rat and mouse C7

The direct ELISA (2.11.1) showed that all novel mAb bind human C7; mAb 2H2, 3B11 and 73D1 also bound rat C7, while mAb 73D1 bound mouse C7 (Fig. 5.6 A – C). mAb 17E7 was strongly cross-reactive with non-human primate (cynomolgus) C7 (Fig. 5.6 D). In a sandwich ELISA (2.11.2) using mAb 2H2 as capture and goat anti-C7 as detection, human

and rat C7 were detected demonstrating that mAb 2H2 can bind C7 from both species (Fig. 5.6 E). To investigate whether the mAb recognised the same or closely apposed epitopes on C7, the antibodies were paired in sandwich ELISA; C7 was not detected with any mAb pair suggesting that they competed for similar epitopes; all mAb worked in sandwich ELISA with goat anti-C7 as either capture or detect (Fig. 5.6 F – K). In sandwich ELISA with mAb 2H2 and goat anti-C5 detection all MAC (with rat C7) intermediates except C5b-9 were detected suggesting a steric hindrance upon the C5 binding (Fig. 5.6 L).

5.3.8 SPR analysis to determine test mAb binding affinity to human and rat C7

SPR analysis on immobilised antibody with human or rat C7 flowed over (Fig. 5.7) showed binding of each of the novel mAb to human and/or rat C7. The mAb 17E7 and 59E7, showed very strong binding to human C7 in SPR analyses (KD = 1.02 x 10^{-9}, 9.31 x 10^{-10} respectively) (Fig. 5.7 A, B) with negligible off rates, suggesting that 17E7 and 59E7 might be promising candidates for human therapeutics. Binding of mAb 3B11 and 73D1 to human or rat C7 was relatively weak (human KD = 2.30 x 10^{-7} and 5.55 x 10-8; rat KD =1.93 x 10^{-7} and 8.17 x 10-8) (Fig. 5.7 C – F); however, these both mAb showed a relatively slow off rate for rat C7 offering promise for use *in vivo*. Technical issues precluded the analysis by SPR of 2H2 binding to human, rat or mouse C7 and 73D1 binding to mouse C7. The measured kinetics/affinity are summarised in Table 5.2.

Antibody	Ka (1/Ms)	Kd (1/s)	KD (M)
17E7	Human; 6.83 x 104	6.94 x 10-5	1.02 x 10-9
59E7	Human; 1.45 x 106	1.4 x 10-3	9.31 x 10-10
3B11*	Human; 5.05 x 103 Rat; 2.91 x 103	1.20 x 10-3 5.61 x 10-4	2.30 x 10-7 1.93 x 10-7
73D1	Human; 2.63 x 104 Rat; 6.98 x 103 Mouse; to be determined	1.5 x 10-3 5.70 x 10-4 to be determined	5.55 x 10-8 8.17 x 10-8 to be determined
2H2	Human; to be determined Rat; to be determined	to be determined	to be determined

***** *Protein L capture*

Table 5.2 *Kinetics and Affinity of the mAb anti--C7 produced.*

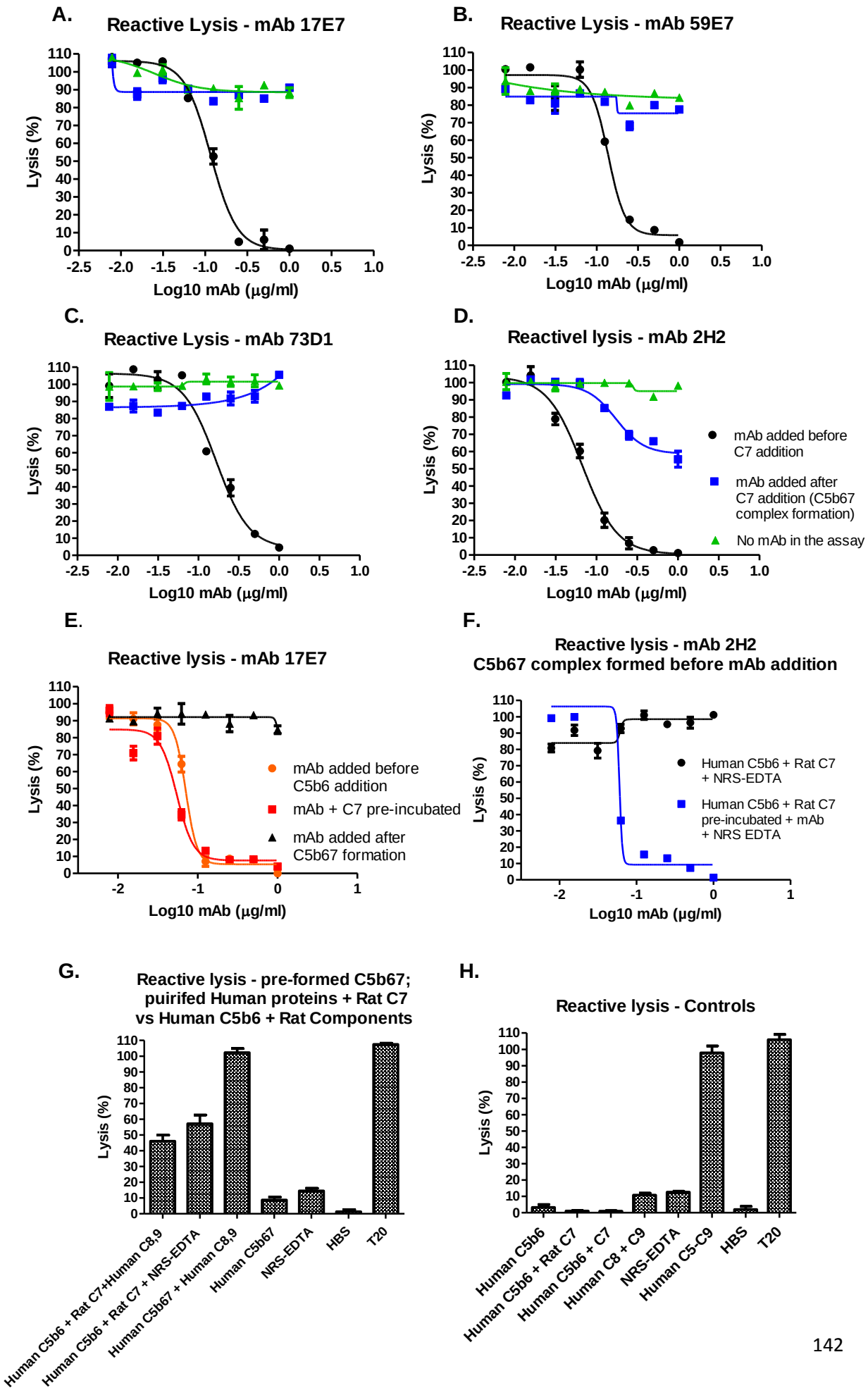
A.
Reactive Lysis - mAb 17E7
Lysis (%)
Log10 mAb (µg/ml)
B.
Reactive Lysis - mAb 59E7
Lysis (%)
Log10 mAb (µg/ml)
C.
Reactive Lysis - mAb 73D1
Lysis (%)
Log10 mAb (µg/ml)
D.
Reactivel lysis - mAb 2H2
Lysis (%)
Log10 mAb (µg/ml)
mAb added before C7 addition
mAb added after C7 addition (C5b67 complex formation)
No mAb in the assay
E.
Reactive lysis - mAb 17E7
Lysis (%)
Log10 mAb (µg/ml)
mAb added before C5b6 addition
mAb + C7 pre-incubated
mAb added after C5b67 formation
F.
Reactive lysis - mAb 2H2
C5b67 complex formed before mAb addition
Lysis (%)
Log10 mAb (µg/ml)
Human C5b6 + Rat C7 + NRS-EDTA
Human C5b6 + Rat C7 pre-incubated + mAb + NRS EDTA
G.
Reactive lysis - pre-formed C5b67; puirifed Human proteins + Rat C7 vs Human C5b6 + Rat Components
Lysis (%)
Human C5b6 + Rat C7+Human C8,9
Human C5b6 + Rat C7 + NRS-EDTA
Human C5b67 + Human C8,9
Human C5b67
NRS-EDTA
HBS
T20
H.
Reactive lysis - Controls
Lysis (%)
Human C5b6
Human C5b6 + Rat C7
Human C5b6 + C7
Human C8 + C9
NRS-EDTA
Human C5-C9
HBS
T20

Figure 5.4 Reactive lysis assays. Guinea-pig erythrocytes (GpE) and purified human complement proteins *(C5b6, C7, C8 and C9) were used for testing mAb 17E7 and 59E7 (**A, B**); for mAb 2H2 and 73D1 human C5b6, and either human or rat C7 were used with NRS or NMS with 5mM EDTA as the source of rodent C8 and C9 (**C, D, F**). All mAb when added to GpE before C5b67 formation efficiently inhibited reactive lysis (**A – E**). mAb 2H2 also inhibited lysis after C7 addition (**D**) and efficiently inhibited reactive lysis when added to pre-formed C5b-7$_{(rat)}$ complexes (**F**). **G.** Reactive lysis using human proteins or combination of human and animal proteins. **H.** Controls for reactive lysis include the individual proteins (no lysis), C5b-9 (full lysis). T20; 0.1% Tween 20. All experiments were repeated three times with comparable results. The error bars are standard errors of triplicates.*

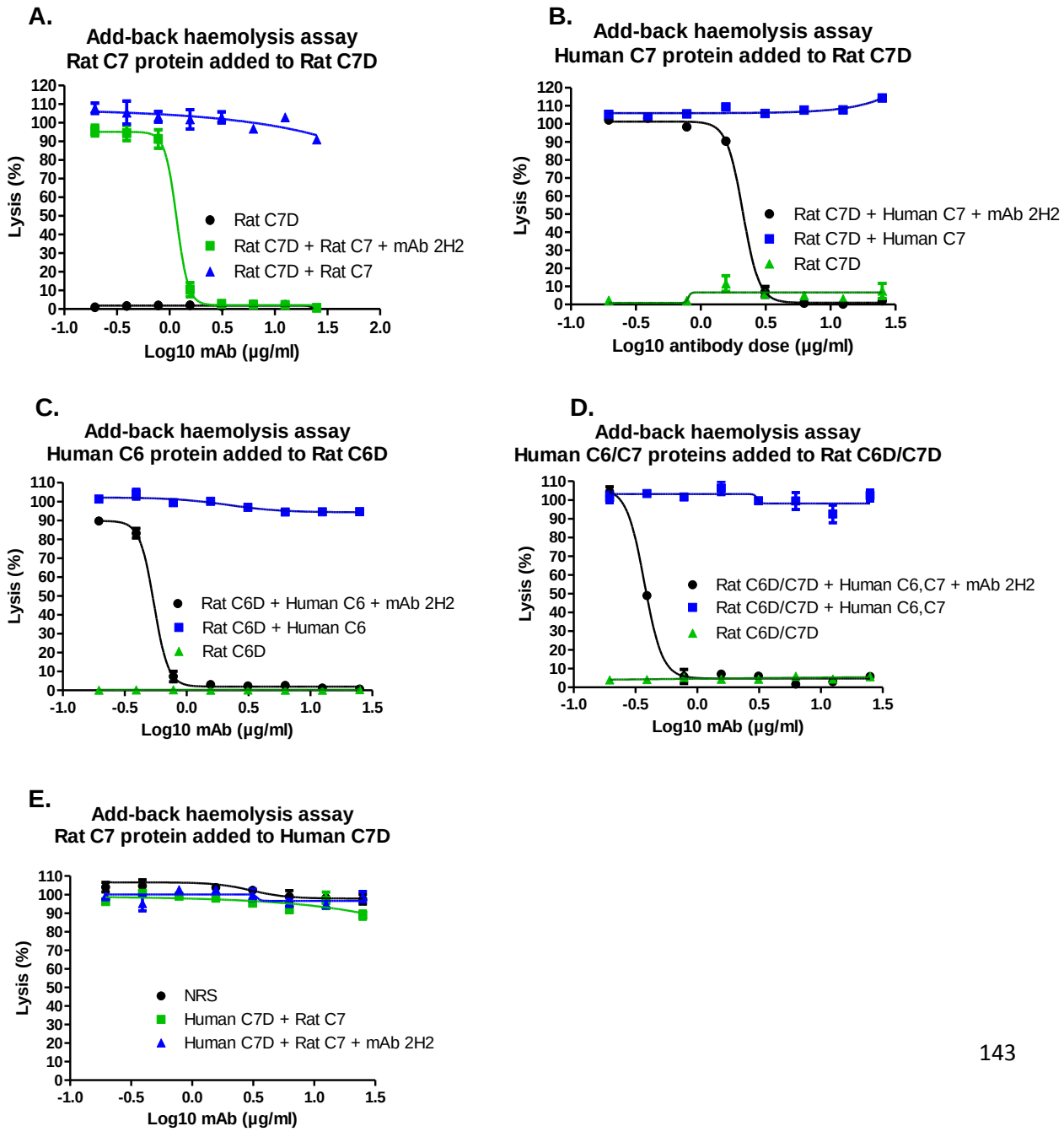

Figure 5.5 Add-back haemolysis assays to test species selectivity of mAb 2H2. A, B. *Adding back either human or rat C7 at physiological levels to C7D serum restored serum lytic activity; addition of mAb 2H2 inhibited lysis in each case.* ***C, D.*** *Adding back human C6 to rat C6D or human C6/C7 to rat C6D/C7D restored lysis and in each case the mAb inhibited lysis.* ***E.*** *Adding back rat C7 to human C7D restored lysis but mAb 2H2 did not inhibit at any dose. All experiments were repeated three times with comparable results. The error bars are standard errors of triplicates.*

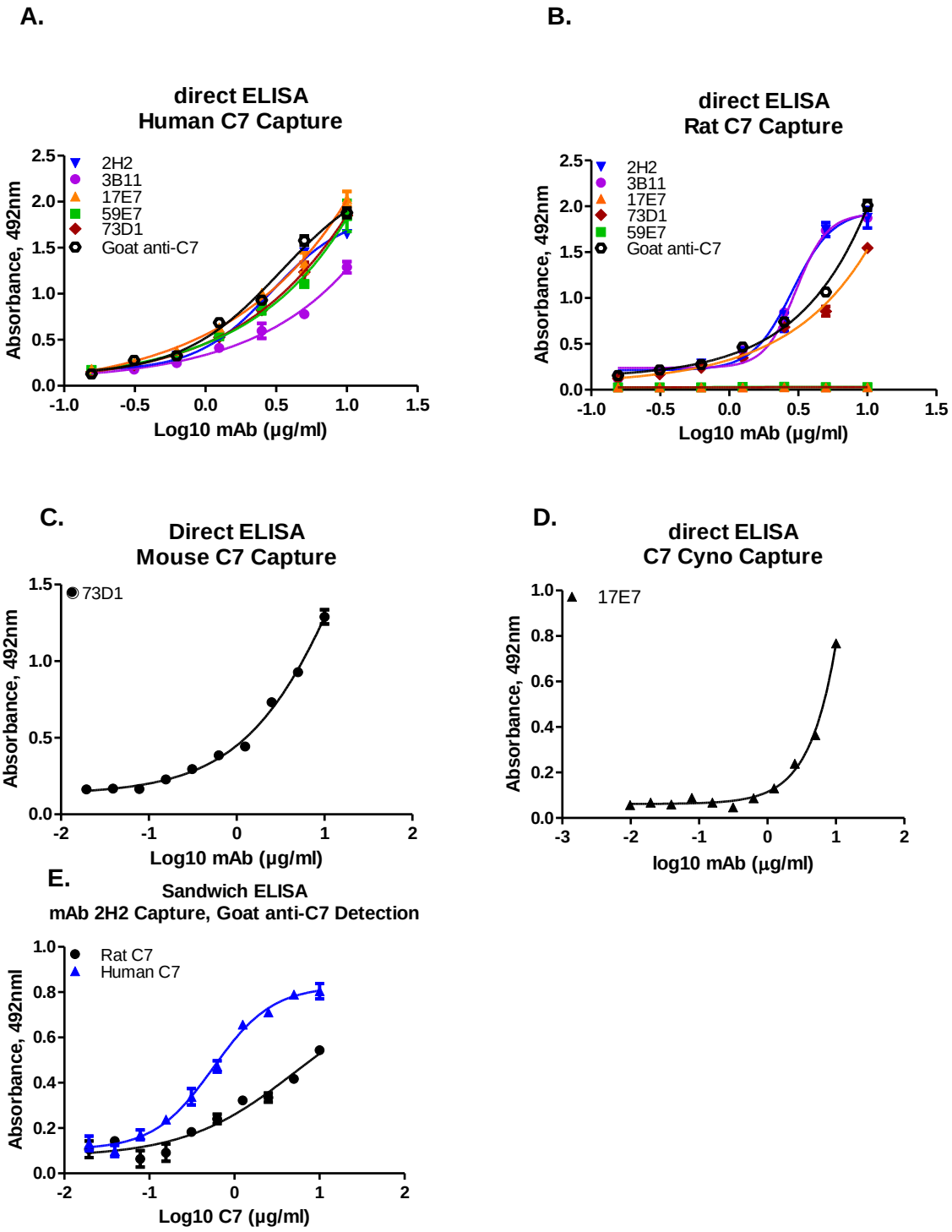

F.

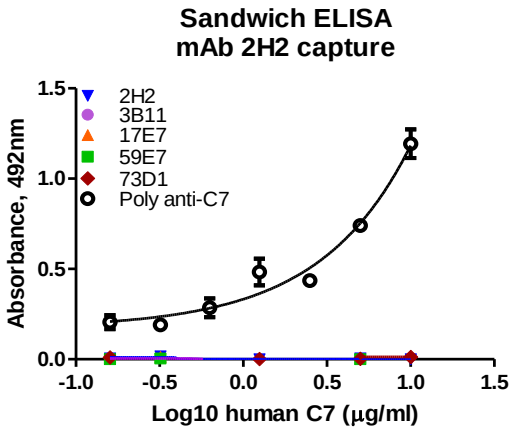
Sandwich ELISA
mAb 2H2 capture
2H2
3B11
17E7
59E7
73D1
Poly anti-C7
Absorbance, 492nm
Log10 human C7 (µg/ml)

G.

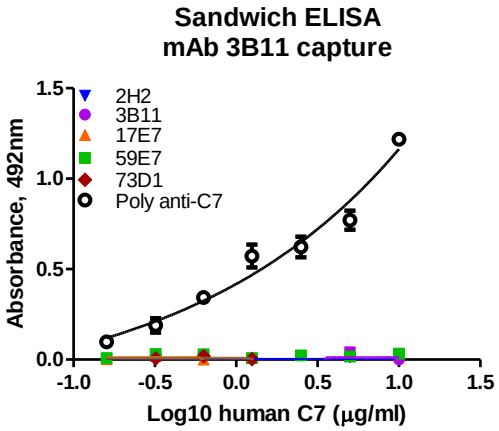
Sandwich ELISA
mAb 3B11 capture
2H2
3B11
17E7
59E7
73D1
Poly anti-C7
Absorbance, 492nm
Log10 human C7 (µg/ml)

H.

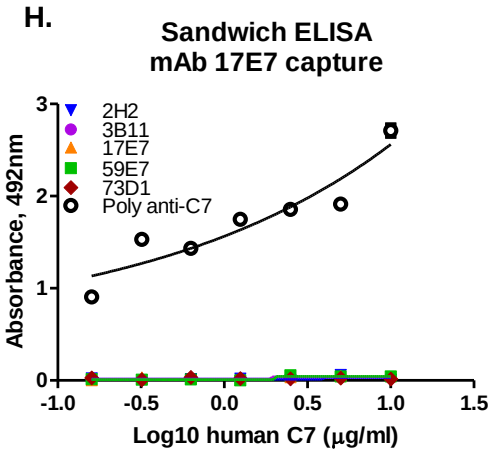
Sandwich ELISA
mAb 17E7 capture
2H2
3B11
17E7
59E7
73D1
Poly anti-C7
Absorbance, 492nm
Log10 human C7 (µg/ml)

I.

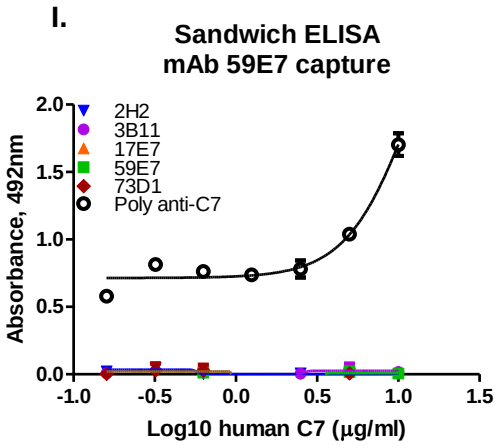
Sandwich ELISA
mAb 59E7 capture
2H2
3B11
17E7
59E7
73D1
Poly anti-C7
Absorbance, 492nm
Log10 human C7 (µg/ml)

J.

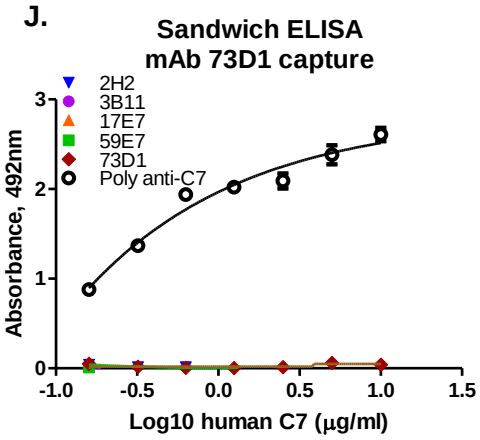
Sandwich ELISA
mAb 73D1 capture
2H2
3B11
17E7
59E7
73D1
Poly anti-C7
Absorbance, 492nm
Log10 human C7 (µg/ml)

K.

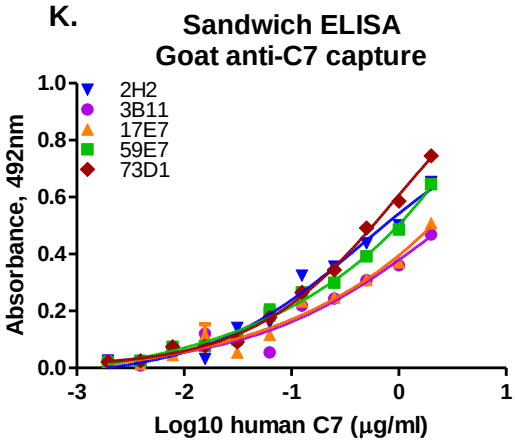
Sandwich ELISA
Goat anti-C7 capture
2H2
3B11
17E7
59E7
73D1
Absorbance, 492nm
Log10 human C7 (µg/ml)

L.

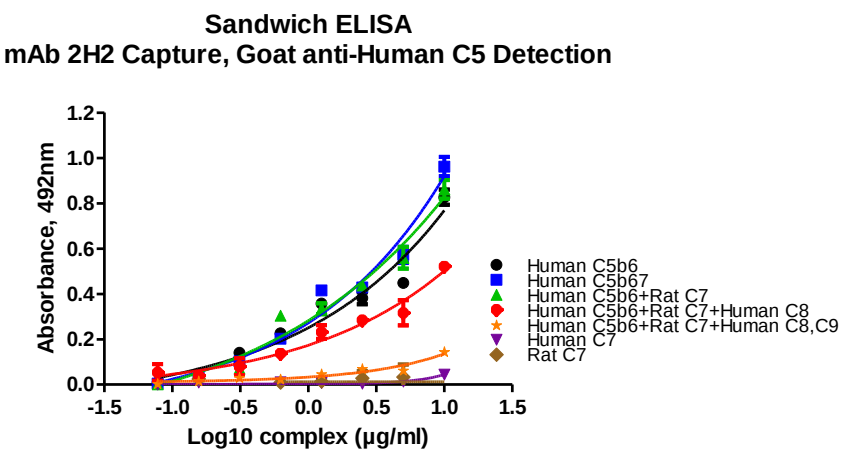
Sandwich ELISA
mAb 2H2 Capture, Goat anti-Human C5 Detection
Human C5b6
Human C5b67
Human C5b6+Rat C7
Human C5b6+Rat C7+Human C8
Human C5b6+Rat C7+Human C8,C9
Human C7
Rat C7
Absorbance, 492nm
Log10 complex (µg/ml)

Figure 5.6 Direct and sandwich ELISA to determine mAb binding to human, rat and mouse C7 and epitope binding *In direct ELISA, plates were coated with human (**A**), rat (**B**) or mouse C7 (**C**). All new mAbs detected human C7 and mAb 2H2, 3B11, 73D1 bound rat C7; mAb 73D1 also detected mouse C7.* ***D.*** *mAb 17E7 detected non-human primate C7. In sandwich ELISA using mAb 2H2 as capture and Goat anti-C7 as detection, both human and rat C7 were detected (**E**). When the mAb were paired in sandwich ELISA no signal was observed suggesting that all the antibodies recognised the same or closely related epitopes on C7 (**F – J**). Polyclonal anti-C7 as detect gave a signal with each of the mAb as capture (F-J) and when used as capture, all mAb worked as detect for C7 (**K**). All MAC intermediates generated with human proteins and rat C7 were detected except for C5b-9 complex possibly due to the conformational change (**L**). All experiments were repeated three times with comparable results. The error bars are standard errors of triplicates.*

A.

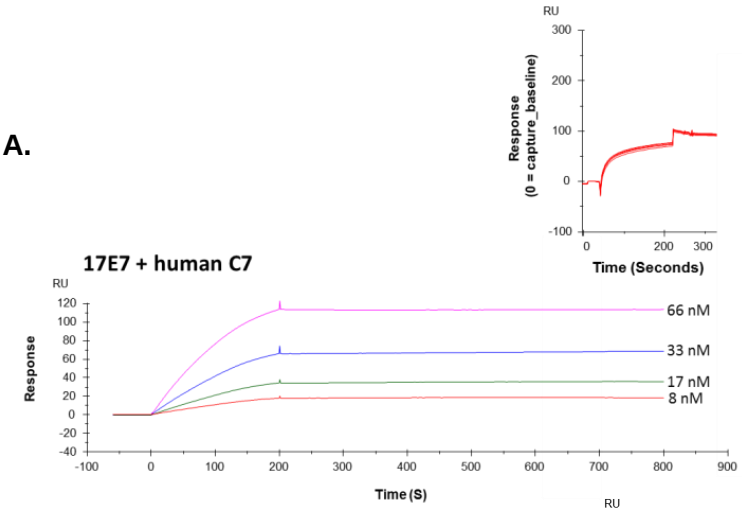
17E7 + human C7
RU
Response
Time (S)
66 nM
33 nM
17 nM
8 nM
Response (0 = capture_baseline)
Time (Seconds)

B.

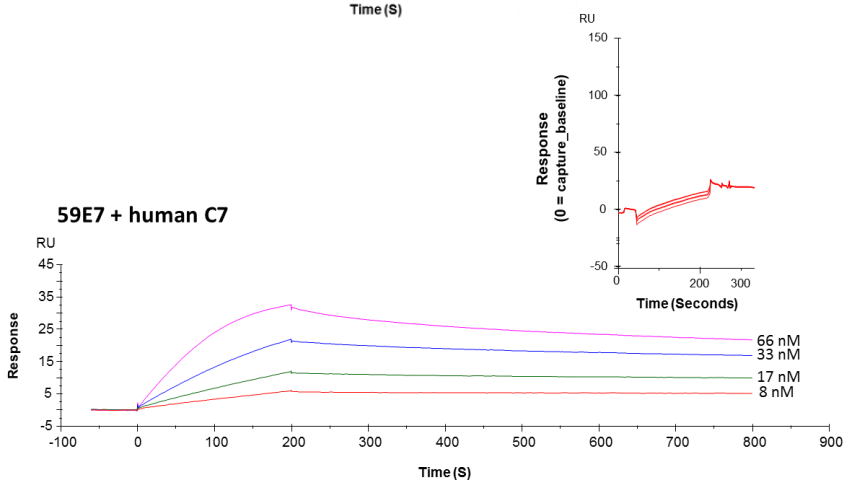
59E7 + human C7
RU
Response
Time (S)
66 nM
33 nM
17 nM
8 nM
Response (0 = capture_baseline)
Time (Seconds)

C.

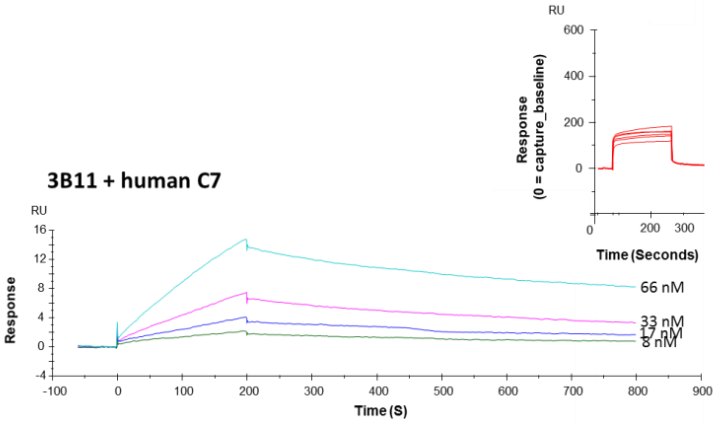
3B11 + human C7
RU
Response
Time (S)
66 nM
33 nM
17 nM
8 nM
Response (0 = capture_baseline)
Time (Seconds)

D.

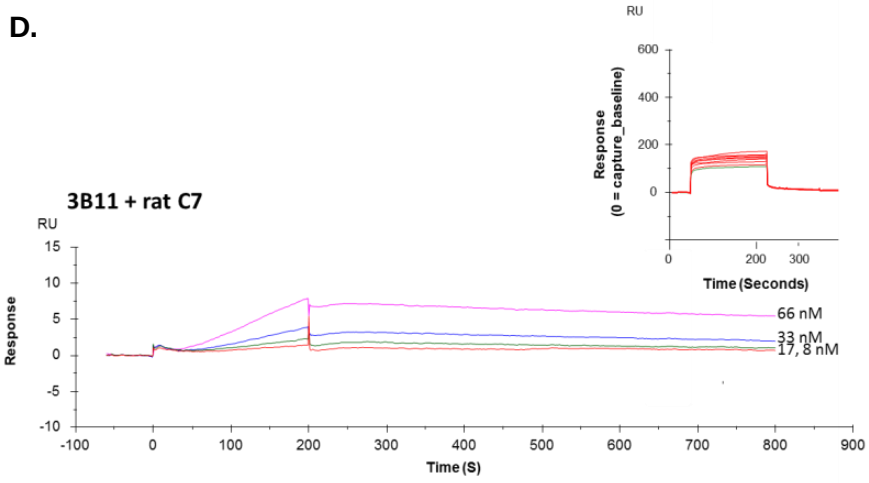
3B11 + rat C7
RU
Response
Time (S)
66 nM
33 nM
17, 8 nM
Response (0 = capture_baseline)
Time (Seconds)

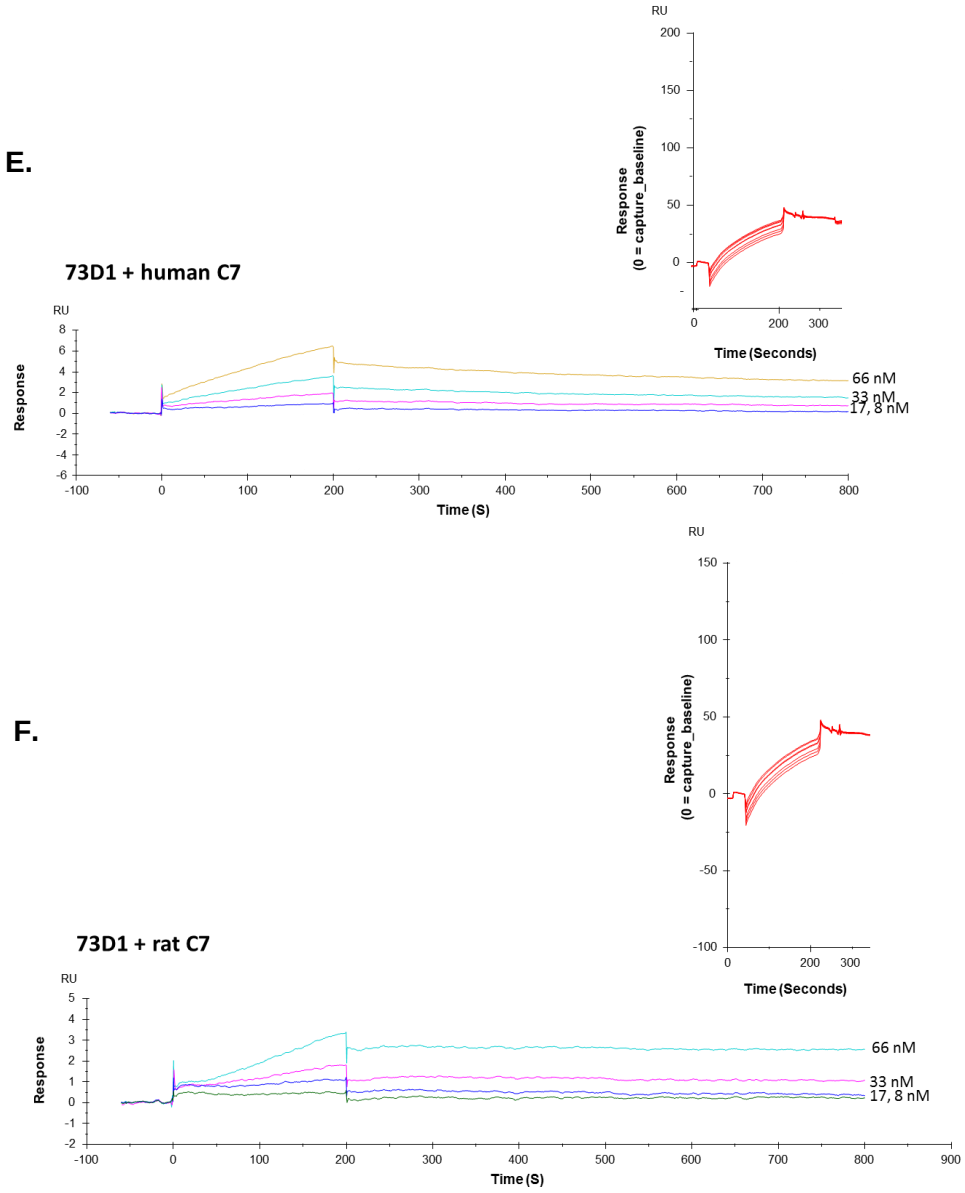

Figure 5.7 Analysis of the binding affinities of anti-C7 mAb to human or rat C7 *mAb 17E7, 59E7, 73D1 were immobilised on the mouse IgG capture sensor chip (GE Healthcare) at approximately 60 RU (insets in each). Protein L series S sensor chip (#29205138, GE Healthcare) was used for testing mAb 3B11 (IgM) at approximately 60 RU. C7 was flowed in HBS-EP at 66 to 8nM for human or rat protein and interactions with the immobilised mAbs analysed. Sensorgrams were collected and KDs calculated using the Langmuir 1:1 binding model with RI value set to zero. Representative sensorgrams are shown with fitted data in colour (n = 3).* ***A.*** *mAb 17E7 binding human C7;* ***B.*** *mAb 59E7 binding human C7;* ***C.*** *mAb 3B11 binding human C7;* ***D.*** *mAb 3B11 binding rat C7;* ***E.*** *mAb 73D1 binding human C7;* ***F.*** *mAb 73D1 binding rat C7. Summary of KDs from the aggregate studies in Table 5.2.*

5.3.9 Testing anti-C7 mAb binding to human, rat, mouse and monkey C7 by WB and ELISA

To confirm binding of mAb to C7 WB was performed on human and animal sera. The human-specific mAb 59E7 and 17E7 specifically detected C7 in NR but not R serum (Fig. 5.8 A); the species cross-reactive mAb 2H2, 73D1 and 3B11 specifically detected C7 in human, rat, mouse and monkey sera under NR conditions (Fig. 5.8 B – D). Most of the mAb have not detected C7 under reducing conditions (data not shown).

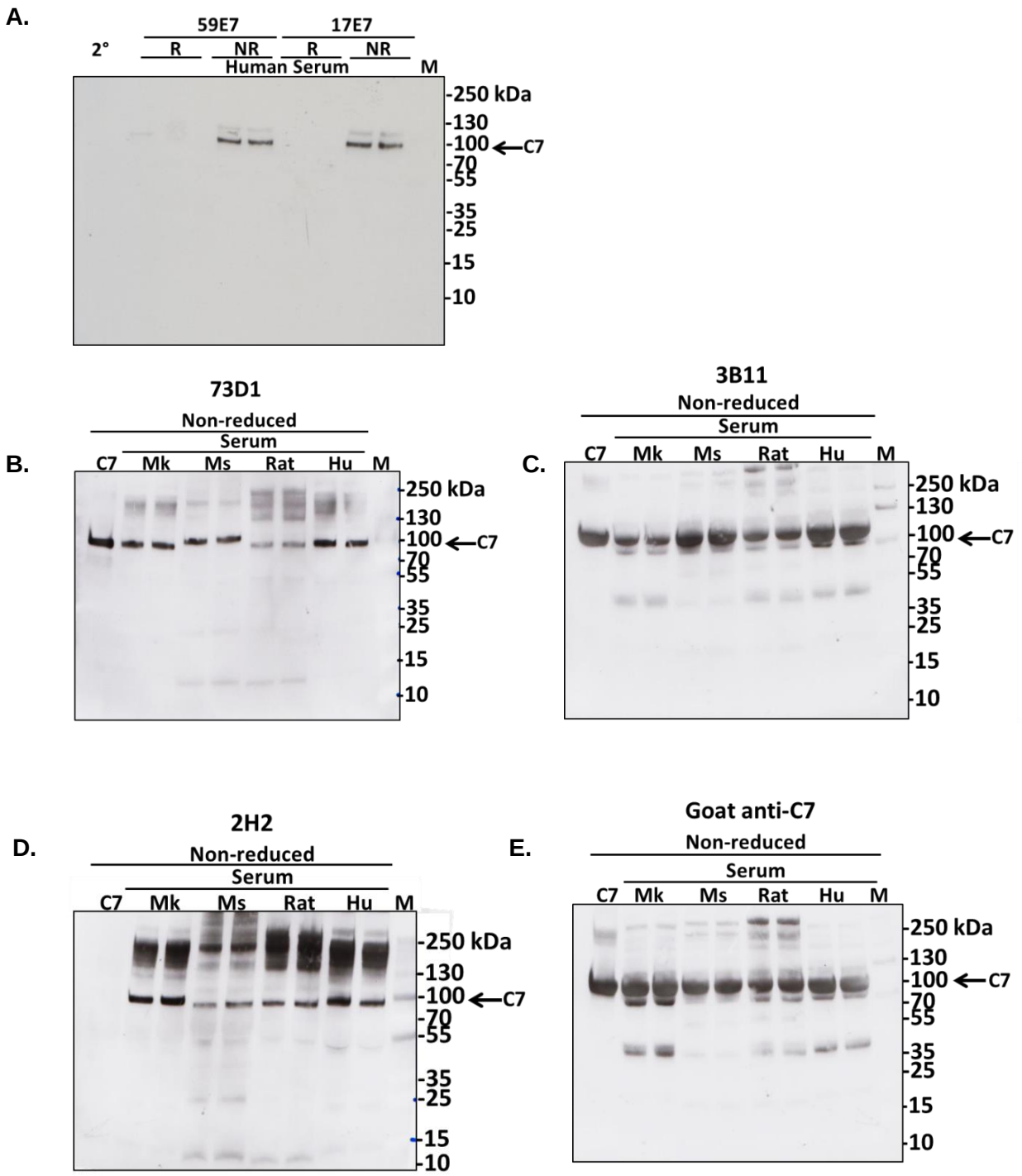

Figure 5.8 Detection of C7 by anti-C7 mAb in WB *Sera; human, rat, mouse and monkey were diluted 1 in 100 in PBS and resolved on 4-20% PAGE gels under NR conditions. Blots were probed with mAb 17E7, 59E7 (**A**), 73D1 (**B**), 3B11 (**C**), 2H2 (**D**), and goat anti-C7 (**E**) Results are representative of multiple analyses. M; protein molecular weight marker, 2°; secondary antibody; Hu, human; Ms, mouse; Mk, monkey.*

5.3.10 WB and ELISA on mAb 2H2-complex to identify the composition of the 2H2 pull-down complex.

mAb 2H2 have not detected NR human C7 protein by WB (Fig. 5.9 D). To further explore this surprising result pull-down assay from activated with zymosan and aggregated human or rat serum was performed as described in section 5.2.6. mAb 2H2 pulled down all the terminal pathway proteins (Fig. 5.9 A, B). In Sandwich ELISA on pulled down rat or human protein with mAb 2H2 all terminal pathway proteins: C5, C6, C7, C8 and C9 were detected; the strongest signals were observed with C5, C6 and C7 proteins (Fig. 5.9 C, D). Taken together, the above WB data and this assay suggest that mAb 2H2, when present in the fluid phase during serum activation, captures fluid phase complexes that contain all terminal pathway proteins. Presence of S-protein or Clusterin in the pulled-down complex has not been checked. This suggests that one possibility for the mechanism of inhibition of haemolysis by 2H2 is that this occurs in the fluid phase, capturing intermediates, thereby abolishing attachment to the membrane and MAC formation, but allowing fluid-phase TCC formation.

5.3.11 Purification of C7 using novel anti-C7 mAb

HiTrap NHS-activated columns were prepared with mAb 17E7. 59E7, 2H2 or 73D1, and control antibodies F10 (in house non-blocker anti-human C7) and HO5-40 (non-blocker anti-rat C7 from GSK) (2mgs each) and protein was purified from human, rat or mouse serum as described in section 3.2.1. The purified protein was subject to SDS-PAGE and stained with coomassie blue. For the human-specific mAb, protein eluted from the F10 column gave a single major band of 105 kDa NR, 115 kDa R corresponding to human C7; eluted protein from both 17E7 and 59E7 gave no band corresponding to C7, instead both had major bands at ~200 and 60 kDa NR and 100, 65, 40 and 20 kDa R (Fig. 5.10 A). For the rat-selective mAb, protein eluted from the H05-40 column contained bands corresponding to rat C7 (95 kDa NR, 110 kDa R) but also contained a major contaminant; (60 kDa NR, 65 kDa R); 2H2 eluate contained these same bands although the C7 bands were faint in comparison to the

contaminant (Fig. 5.10 B). Eluate from the mouse C7-specific non-blocker mAb 73D1 gave clean C7-specific bands (Fig 5.10 C). It is surprising that the best C7 blocking mAbs failed to effectively purify C7 from the relevant sera and failed to deplete C7 from the serum (Fig 5.10 D). The observed contaminants for the human-specific mAb likely represent IgG (human or murine) and albumin; the contaminant for the rat-specific mAb may also be albumin. To eliminate the possibility that the ~65kDa contaminant was (~65 kDa on SDS-PAGE), the eluates were subjected to WB and goat anti-C9 was used to detect, no C9 reactivity was present in any of the eluates (Fig. 5.10 E).

A.

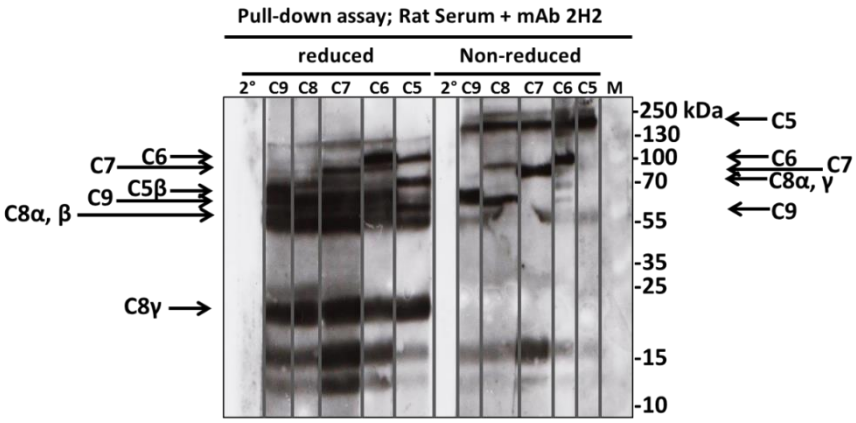

B.

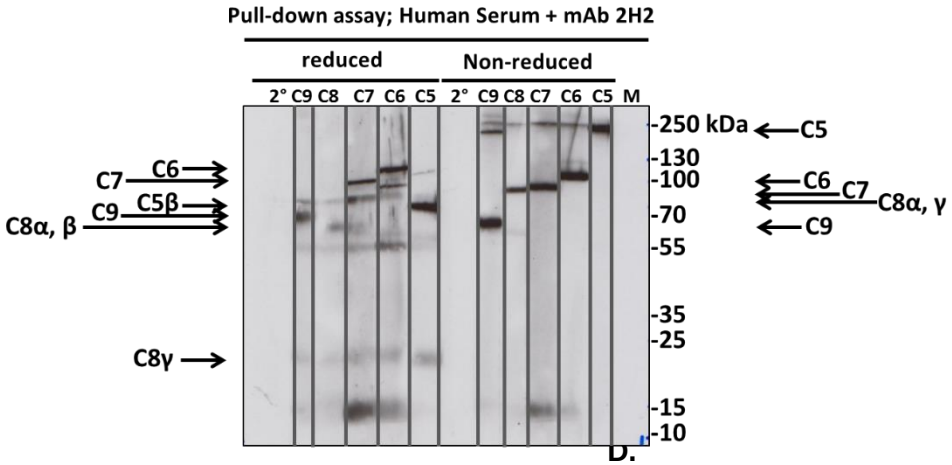

C. **D.**

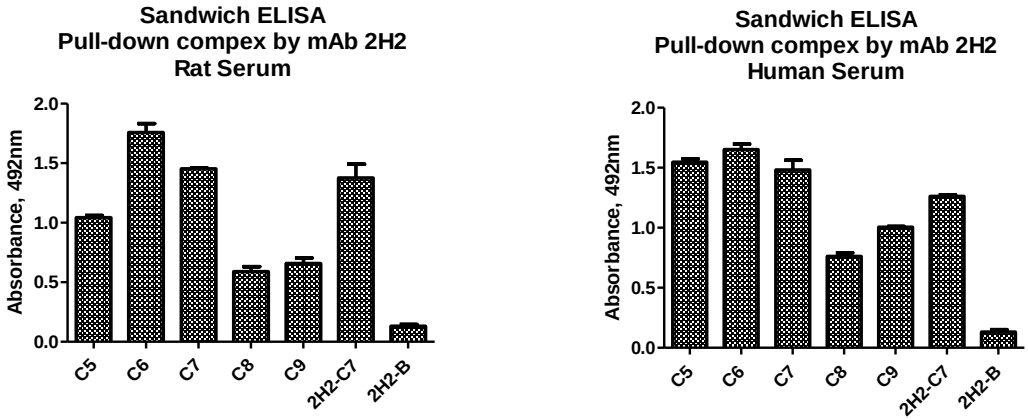

Figure 5.9 WB and ELISA to identify the composition of the 2H2 pull-down complex. *The 2H2 pull-downs from rat (**A**) and human (**B**) serum were subject to WB; protein (1µg) was resolved in 7.5% SDS-PAGE gel and transferred onto nitrocellulose membrane. The protein was probed with goat anti-C5, C6, C7, C8, C9 mAb. The blots were cut into strips to detect the individual protein and re-aligned. NR: C5, 190 kDa; C6, 105 kDa; C7, 95 kDa, C8αγ; 70 kDa; C9, 65 kDa. R: C6, 110 kDa; C7, 95 kDa; C5β, 75 kDa; C9, 70 kDa; C8α/β, 65 kDa; C8γ, 22 kDa. Results are representative of multiple analyses. M; protein molecular weight marker, 2°; secondary antibody; Hu, human; Ms, mouse; Mk, monkey.* ***C, D.*** *In sandwich ELISA with avidin as capture, Biotin-2H2-complex from rat or human activated serum was bound; composition of the complex was interrogated by adding goat anti-C5, -C6, -C7, -C8 or -C9. In both rat and human, the strongest signals were observed with anti-C5, -C6 and -C7 antisera. Controls were biotinylated mAb 2H2 alone (2H2-B) and 2H2-B pre-incubated with C7 (2H2-C7), each detected with anti-C7. All experiments were repeated three times with comparable results. The error bars are standard errors of triplicates.*

5.3.12 Testing whether mAb bind membrane bound MAC precursors by flow cytometry

ShEA were incubated with NHS or NRS in the presence of each of the blocking mAb, 17E7, 59E7 and 2H2; the cells were then pelleted, washed and stained for mAb binding. Binding of the mAb to MAC intermediates on erythrocytes was not detected for any of the blocking mAb using flow cytometry (section 5.2.7) confirming that all of the mAb are fluid phase inhibitors and none bind into the forming MAC on the cell surface. As a control for MAC formation in the absence of blocking mAbs, ShEA exposed to human serum were strongly stained with the anti-human C9 neo-specific mAb aE11, demonstrating that MAC formed on the cells under the conditions used (Fig. 5.11).

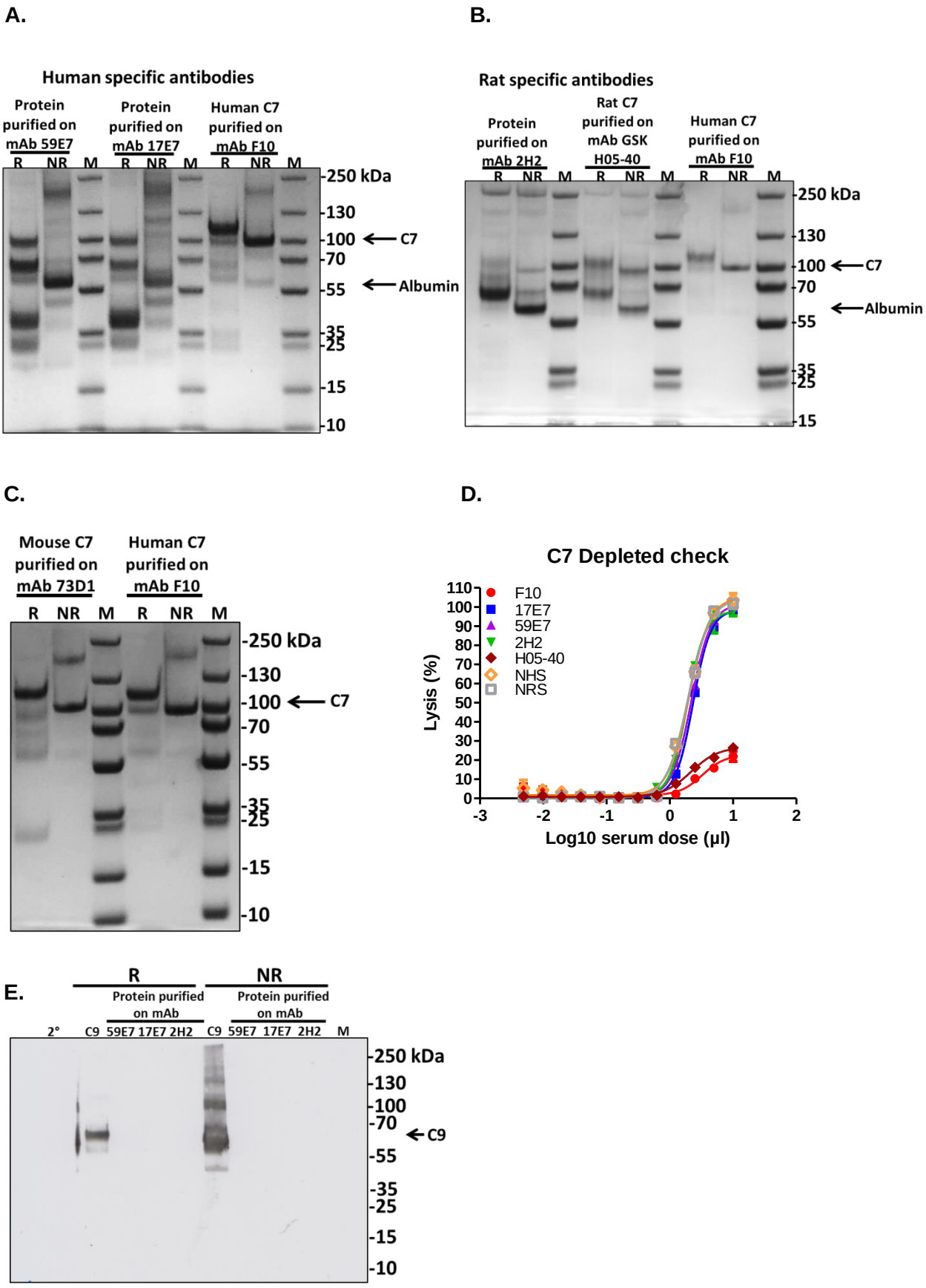

Figure 5.10 Characterization of purified proteins using mAb 2H2, 17E7, 59E7 and 73D1 A – C. *SDS–PAGE of eluates (3µg) from human (17E7, 59E7 or F10), rat (2H2, H05-*

*40) or mouse (73D1) serum (using 73D1) resolved on 7.5% gels either NR or R conditions then stained with Coomasie Blue. NR. For the anti-human C7 mAbs only the non-blocker F10 isolated proteins of the anticipated Mr for human C7 (105 kDa NR, 115 KDa R). For anti-rat C7 mAbs H05-40 isolated protein of the expected Mr for rat C7 along with a major contaminant, while 2H2 isolated small amounts of rat C7 together with a major contaminant identical to that from H05-40. The anti-mouse C7 mAb 73D1 isolated clean C7 from mouse serum. To identify the contaminant, WB of eluates were probed with goat anti-C9; no bands apart for C9 protein were observed (**E**). M; protein molecular weight marker, 2°; secondary antibody. The sera post-purification were tested in haemolytic assay showing that most mAb failed to deplete C7 from the serum (**D**). The error bars are standard errors of triplicates.*

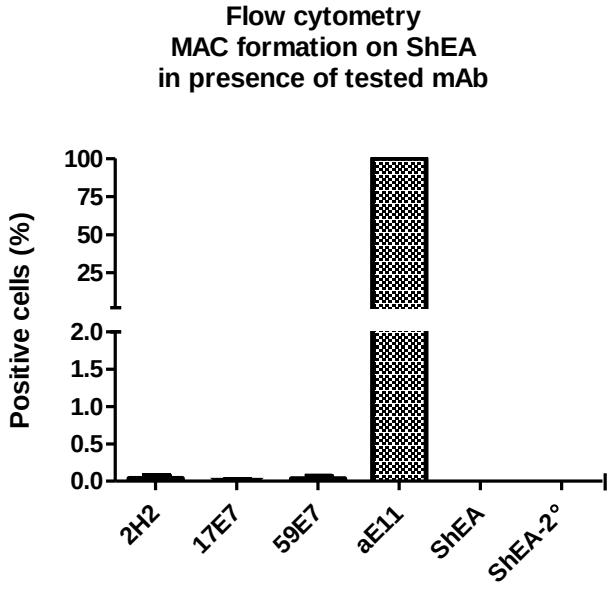

Figure 5.11 Flow cytometry to determine binding of the mAb to erythrocytes. *CP activation (section 2.19.4) using 5% rat (for 2H2) or human (for 17E7, 59E7, aE11) serum; and a blocking dose (100µg/ml) mAb. Post-incubation, ShEA were washed with FACS buffer, stained on ice with donkey anti-mouse FITC antibody. Cells were subsequently washed into FACS buffer and analysed on the FACS Calibur flow cytometer. None of the mAb tested showed binding to the ShEA post-attack. As positive control aE11 C9 neo-specific antibody was used. Negative controls included ShEA cells and secondary antibody only (ShEA-2°), duplicates used. ShEA positive gate used for quantification displayed.*

5.3.13 mAb 17E7 was an efficient complement inhibitor *in vivo*

An animal study was conducted to demonstrate the capacity of mAb 17E7 to inhibit the complement system in vivo (5.2.3). To test the capacity of mAb 17E7 to inhibit C7 in vivo,

mAb was administered to C7-deficient mice reconstituted with human C7. Human C7 effectively restored haemolytic activity in the mice, tested one hour after administration; levels were indistinguishable from wild-type mouse serum. Administration of mAb 17E7 efficiently inhibited haemolytic activity in the mice (>70% inhibited at 3 hours post-administration) compared to irrelevant antibody, demonstrating that the mAb efficiently blocked human C7 in vivo (Fig. 5.12).

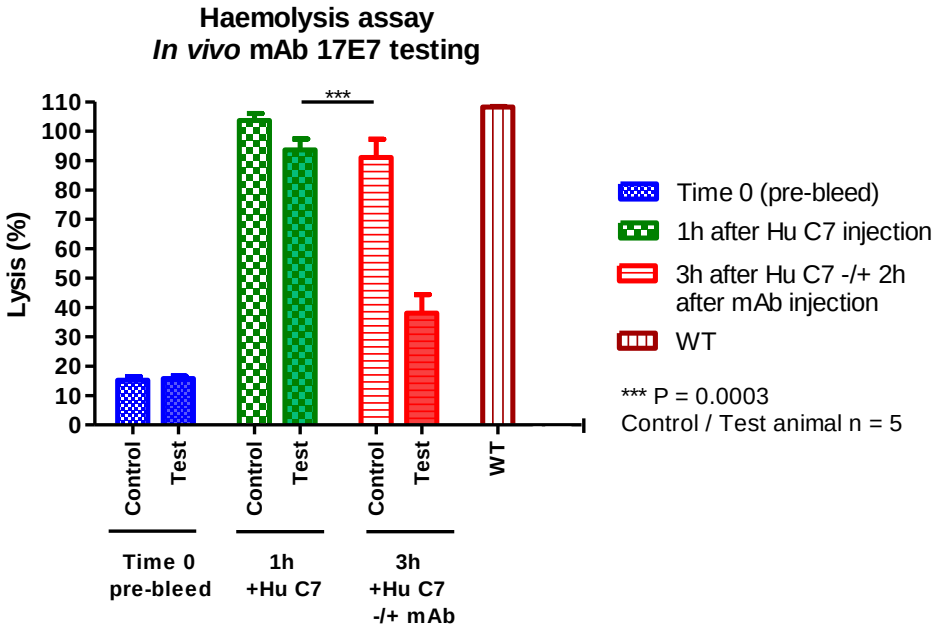

Figure 5.12 Haemolysis in sera of human C7 reconstituted mice treated with mAb 17E7 *C7 deficient mice (10 females) were injected intraperitoneally with human C7 (500µg), then split into test and control groups (5 in each). The test group animals were injected subcutaneously with 17E7 mAb (1mg), while control group mice were injected with an irrelevant isotype control mAb (JC-3 anti-human FB, 1mg); blood was collected from all the animals just before the experiment, one hour after human C7 administration, and at intervals after mAb injection. C7D, C7 deficient mouse serum; WT, wild type. The error bars are standard errors of triplicates.*

5.3.14 mAb 73D1 efficiently inhibited complement in mice

To test the capacity of the anti-mouse C7 mAb 73D1 to inhibit complement in vivo (5.2.3), mice were administered 73D1 or as a positive control the blocking anti-mouse C5 mAb BB5.1. Wild type mice (C57BL/6J) were pre-bled and IP injected with mAb 73D1 or BB5.1 (5 mice each). Complement activity was monitored by testing animal sera in the haemolytic assay over a time course of 48 hours using the add-back (to human depleted sera) assay

described in section 2.17.8. Complement was inhibited by both mAb over the full course of the experiment from 2 – 48 hours (Fig. 5.13). BB5.1 has been widely used in animal models and set the scene for current anti-C5 therapeutics; 73D1 was administered at the same dose as BB5.1 and the efficient inhibition of mouse complement by this mAb make it a valuable candidate for animal studies targeting MAC specifically without interfering with C5a generation.

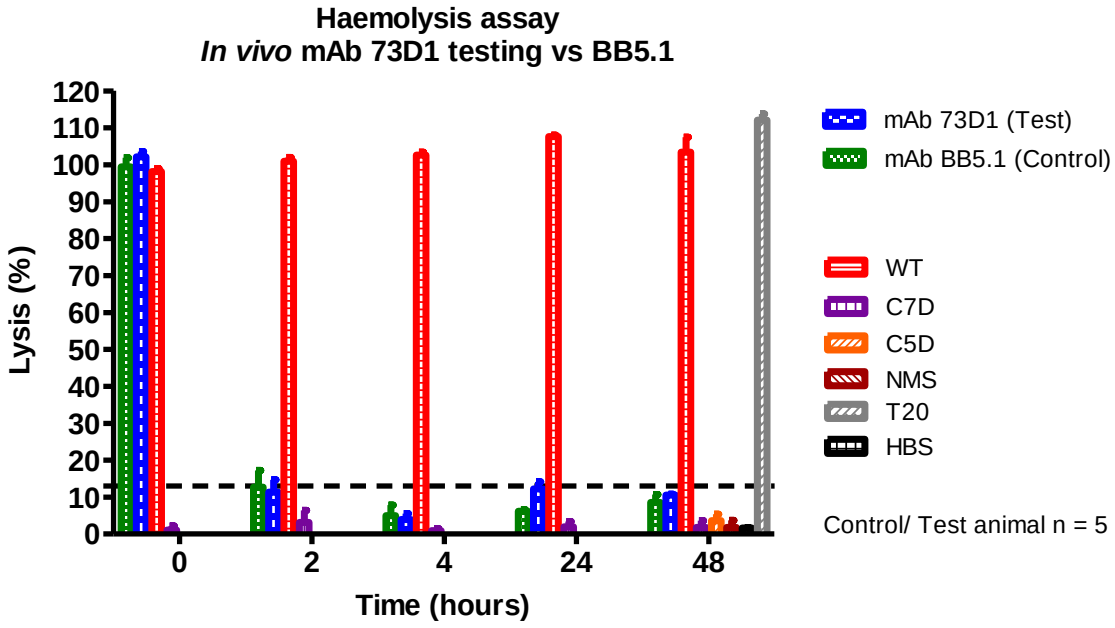

Figure 5.13 Haemolytic assay in sera of mice treated with mAb 73D1 and BB5.1 *Haemolytic assays were used to monitor complement activity in mice (groups of 5 each, females) treated with mAb. 73D1 and BB5.1 were IP administered at a dose of 1 mg/kg, blood samples were collected at time points; 0, 2, 4, 24 and 48 hours, serum prepared (section 2.14) and tested in haemolytic assays utilising human C5D or C7D serum in combination with the mouse serum. Controls included C7D and C5D human sera at the same dose, NMS to demonstrate the requirement for human depleted sera and Tween and HBS to set 100% and 0% lysis in the assay. C7D, C7 human depleted serum; NMS, normal mouse serum; T20, 0.1% Tween 20 complete lysis as positive control; HBS, buffer only as no lysis negative control; NMS, normal mouse serum; WT, wild type. The error bars are standard errors of triplicates.*

5.3.15 *In vivo* complement inhibition dose experiment for mAb 2H2 administration

mAb 2H2 was tested for complement inhibition in rats to determine dose requirement and antibody half-life. Rats were injected with mAb 2H2 at 10, 20 and 40 mg/kg and blood collected at intervals for testing haemolytic activity. Even at the lowest dose, the mAb was

an effective inhibitor for >48 hours, and at the highest was effective for one week (Fig. 5.14 A – C). The 10mg/kg dose was used for the induced EAMG experiment described below. Of note, the standard dose for C5 inhibiting mAb use in rodents is 40 mg/kg to obtain inhibition for >48 hours. mAb 2H2 inhibits lytic activity at much lower dose and for much longer, supporting the hypothesis that mAb 2H2 inhibits by binding C5b67 or other intermediate complexes.

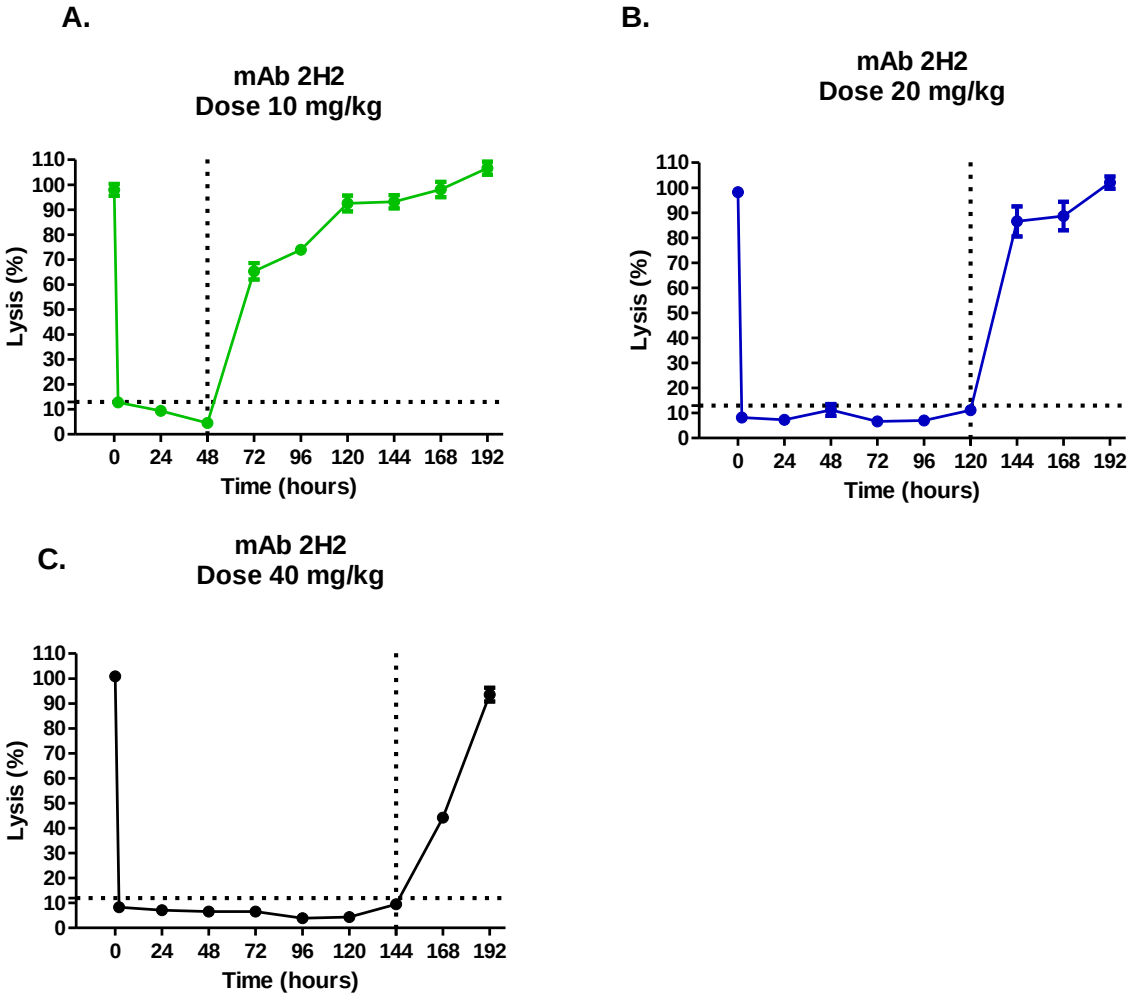

Figure 5.14 In vivo dosing experiment for mAb 2H2 *Six Lewis rats were divided into three groups (2 females in each) and injected intraperitoneally with mAb 2H2 at doses of 10, 20 and 40 mg/kg; blood was collected from all the animals just before the experiment, two hours after mAb 2H2 administration, and then every 12 hours, sera prepared and haemolytc activity tested in standard CP assays. The lowest dose of 10 mg/kg efficiently blocked complement activity up to 48 hours (**A**), 20 mg/kg for up to 5 days (**B**), and for 7 days in animals injected with the highest dose of 40 mg/kg (**C**). The error bars are standard errors of triplicates.*

5.3.16 Induction of EAMG in rats and effect of mAb 2H2 on clinical disease and pathology

The rat EAMG model is described in detail in section 5.2.4 and is described here in brief and with modifications where appropriate. Rats were given mAb35 at 1mg/kg intraperitoneally and at the same time a subcutaneous injection of 2H2 mAb or isotype control (10mg/kg; 5 per group). As expected, isotype control treated rats began to lose weight and show signs of hind limb weakness within 20 hours (Fig. 5.15 A). Clinical symptoms, comprising limp tails, piloerection, hind limb weakness and reduced grip, were present in all isotype control treated animals by 24 hours post-induction, and all exhibited severe disease with hind limb weakness and/or paralysis, reaching clinical score 4 on a standardised scale (0, no disease; 1, reduced grip strength in front legs and floppy tail ; 2, loss of grip in front legs; 3, loss of grip and hind limb weakness and wasting; 4, loss of grip and hind limb paralysis; 5, moribund) by endpoint. (Fig. 5.15 B, D). In contrast, animals given mAb 2H2 sc at disease induction continued to gain weight over the course of the experiment and did not develop detectable weakness or other manifestations for the duration of the experiment (Fig. 5.15 B, D). Animals were sacrificed by a Schedule 1 method when weight loss exceeded 20% of original, or when clinical score reached 4. CP serum haemolytic activity was absent in 2H2-treated group throughout the experiment while serum from untreated controls retained haemolytic activity (Fig. 5.15 C). Soleus muscles were harvested at sacrifice (48 hours) for future staining for endplate damage (AChR detection) and complement deposition (C3b/iC3b and C9/MAC) as described in chapter 4.

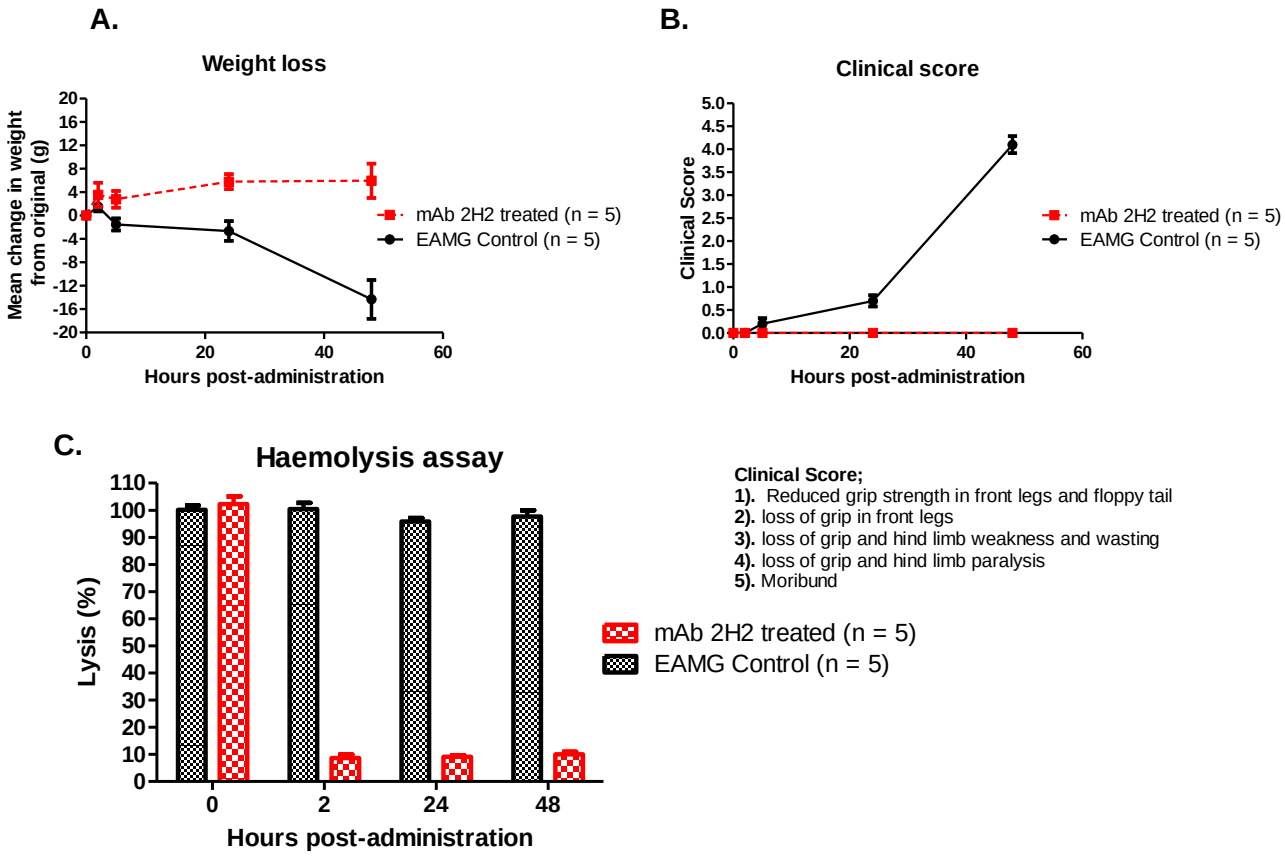

Figure 5.15 In vivo testing of mAb 2H2 in EAMG model *EAMG was induced with mAb35 (1 mg/kg) administered IP; at the same time mAb 2H2 or isotype control mAb (D1.3) at 10 mg/kg was administered SC.* ***A, B.*** *Assessment of the weight loss and clinical score. Isotype control treated animals (EAMG) rapidly developed weight loss and muscle weakness, reaching clinical scores of four or five and all were sacrificed at 48 hours. The mAb 2H2 treated animals were protected from disease and weight loss; all were sacrificed at 48 hours.* ***C.*** *Serum haemolytic activity was measured at time points: 0, 2, 24 and 48 hours. Results are means of determinations from 2H2-treated and isotype control treated EAMG animals (five per group), all samples run in triplicate and vertical bars represent SD.*

5.3.17 Generation of anti-C6 monoclonal antibodies

Although the development of anti-C6/C5b6 antibodies was not an aim of this thesis, these were generated as by-products of C7 blocking mAb development. Presumably, targeting C6 would have the same effect as C7; inhibition on formation of the pro-inflammatory MAC that drives pathology. The difference would be the dose of drug needed to neutralise. In brief, C7 is not an acute phase reactant hence it is likely that less mAb will be required in comparison to C6 synthesis of which is increased in an acute phase manner. An anti-C6 mAb has been developed by Complement Pharma (CP010) and it is in pre-clinical trials for CNS diseases treatment (Harris 2018, Zelek *et al* 2019). CP010 is a human-specific antibody, therefore here I will investigate whether the in house developed mAb are cross-species inhibitors which would make them useful tools for animal models. The mAb will not be pursued as drugs because they lack novelty with CP010 already in development.

5.3.17.1 Isotyping and purification of the anti-C6 mAb

Antibody clones; 1G8 and 9E8 were identified as isotype IgG2bκ (Isostrip, Roche, # 11493027001) and were purified using protein G chromatography as described in section 3.2.7.1. Purity of the antibodies was determined using SDS-PAGE (Fig. 5.16).

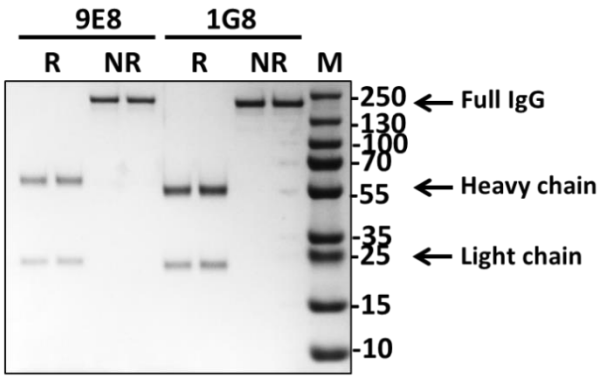

Figure 5.16 SDS-PAGE of the purified anti-C6 mAb*. mAb (2µg) were resolved on 7.5% gels under non-reducing (NR) and reducing (R) conditions, then stained with coomassie blue. The 150 kDa band (NR) corresponds to intact IgG, in R lanes the 55 kDa band corresponds to mAb heavy chain and 25 kDa to mAb light chain. M; molecular weight marker. (PageRuler, #26620).*

5.3.17.2 Cross-species C6 inhibition by novel mAb in haemolysis assays

Haemolysis-blocking anti-C6 clones were also generated in C7 deficient mice immunised with human and rat C7 in fusions: 13 – 15 (section 2.16). This was a surprising finding given that the mice had not been immunised with C6; the mAb were only identified because the initial screens were for blocking function. Initially, seven C6-reactive hybridoma clones were selected for further characterisation based upon the capacity of clone supernatants to cause inhibition in CP haemolysis assays using NHS, and detection of human C6 in ELISA; two of the selected monoclonal clones; 1G8 and 9E8 were expanded for further characterisation, secreted mAbs purified and tested in haemolysis assays with different species sera. As expected, the selected mAb efficiently inhibited lysis of ShEA mediated by human complement with equivalent dose-response performance to the benchmark Eculizumab (Fig. 5.17 A). mAb 1G8 also inhibited rat serum induced haemolysis at the same level as in house anti-C7 mAb 7D4 , but less efficient than mAb 2H2 (Fig. 5.17 B). Neither of the novel mAb inhibited mouse or rabbit complement *in vitro* (Fig. 5.17 C, D).

5.3.17.3 Determination of 1G8 and 9E8 binding to human C6 and C5b6 by ELISA/ WB

In direct ELISA mAb 1G8 and 9E8 detected C6 and C5b6 complex (Fig. 5.18 A, B). In sandwich ELISA with mAb 1G8 or 9E8 used as a capture and polyclonal anti-C6 used as detection, both C6 and C5b6 were detected (Fig. 5.18 C, D), when goat anti-C5 antibody used as detection, only C5b6 was detected (Fig. 5.18 E, F). In assays using the novel anti-C6 mAb 1G8 as capture and anti-C5 mAb (4G2, 7D4, 10B6) or polyclonal anti-C5 as detect, C5b6 was strongly detected by mAb 4G2 (and polyclonal anti-C5) and weakly by 10B6, demonstrating that the epitopes for these mAb are simultaneously accessible on C5b6 (Fig. 5.18 G, H). The binding of the novel mAb to human C6 was confirmed with WB; both mAb detected a major band at 105kDa together with high molecular weight contaminants under NR conditions, as did several other uncharacterised anti-C6 clones; Banding patterns under R conditions were complex and suggested contamination with human IgG (Fig. 5.18 I).

5.3.18 Summary of the characterisation of the novel anti-C7/ C6 mAb. The properties of the newly generated anti-C6 and anti-C7 mAbs are shown in Table 5.3.

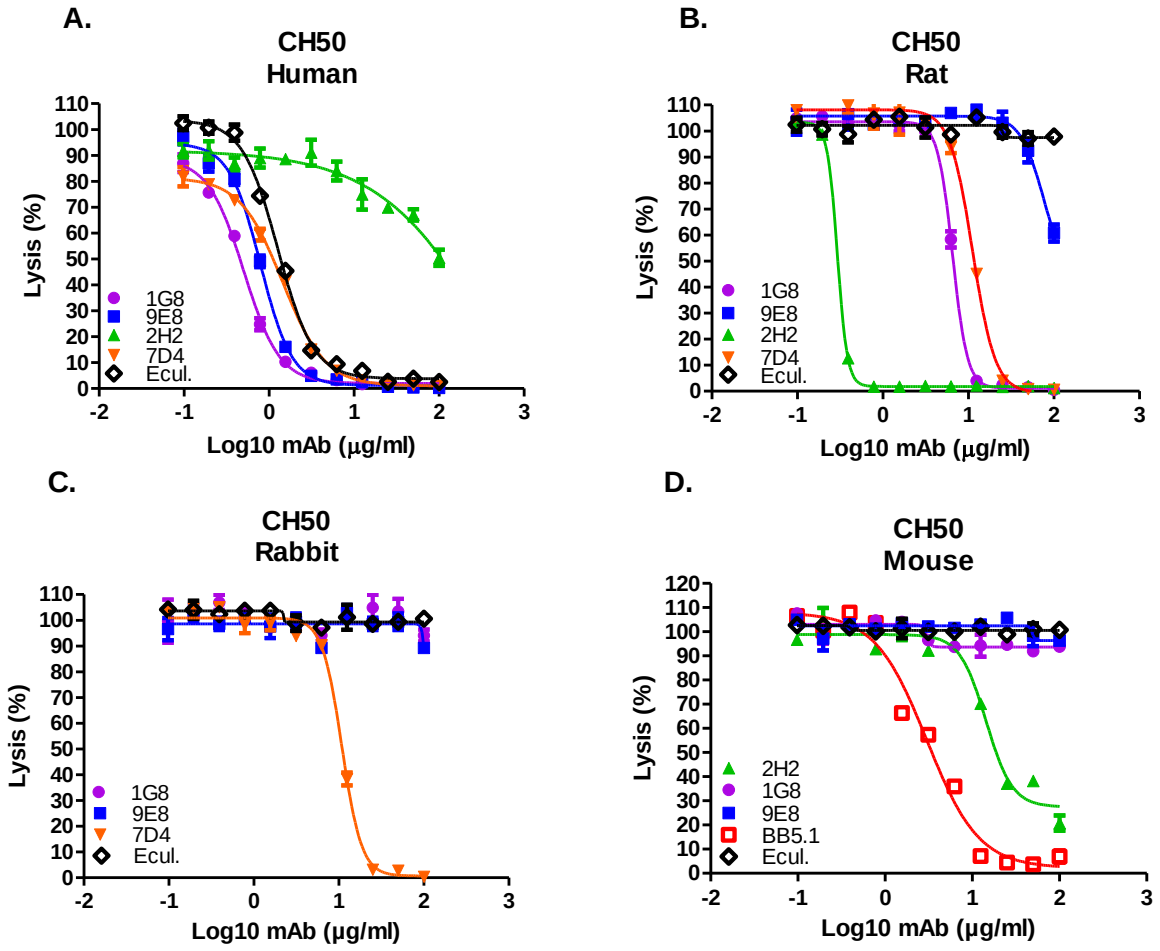

E.

Antibody	50% Complement inhibitory dosage (ng/ml)			
	Human	Rat	Rabbit	Mouse
1G8	194.9	653.6	-	-
9E8	130.9	-	-	-
7D4	144.2	1174.9	1088.9	-
2H2	-	29.4	-	1438.8
BB5.1	-	-	-	301.6
Eculizumab	127.3	-	-	-

Figure 5.17 Haemolytic assays to investigate whether the anti-C6 mAbs 1G8 and 9E8 inhibit C6 across species. A – E. *Functional assays to determine whether mAb 1G8 and 9E8 inhibit CP haemolysis (CH50) in different species. Sera tested were human (**A**), rat (**B**), rabbit (**C**) and mouse (**D**). Anti-C5 mAb Eculizumab and in house anti-C7 mAbs 7D4 and 2H2 were used as comparators. All experiments were repeated three times with comparable results. The error bars are standard errors of triplicates.* ***E.*** *Calculation of 50% inhibitory dose showed that the efficiency of human C6 inhibition by mAb 1G8 and 9E8 were equivalent to Eculizumab, and in house mAb 7D4 (anti-C5). mAb 1G8 also strongly inhibited rat C7.*

Antibody	Isotype	Target	Cross-species reactivity/ inhibition *in vitro*	Cross-species reactivity/ inhibition *in vivo*	IP
2H2	IgG2b, K	C7/ C5b-7	Strong; Rt; Weak; Mo, Hu	Rat	Patent application in progress
3B11	IgM, K	C7	Strong; Hu, Rt	Not tested	
17E7	IgG2a, K	C7	Strong; Human	Human	
59E7	IgG2b, K	C7	Strong; Human	Not tested	
73D1	IgG2a, K	C7	Strong; Mo; Weak; Hu, Rt	Mouse	
1G8	IgG2b, K	C6/ C5b6	Strong; Hu, Rt	Not tested	Licence agreement in progress
9E8	IgG2b, K	C6/ C5b6	Strong; Hu	Not tested	

Table 5.3. *Summary data of the new anti-C7 and anti-C6 mAb and the plans for further development.*

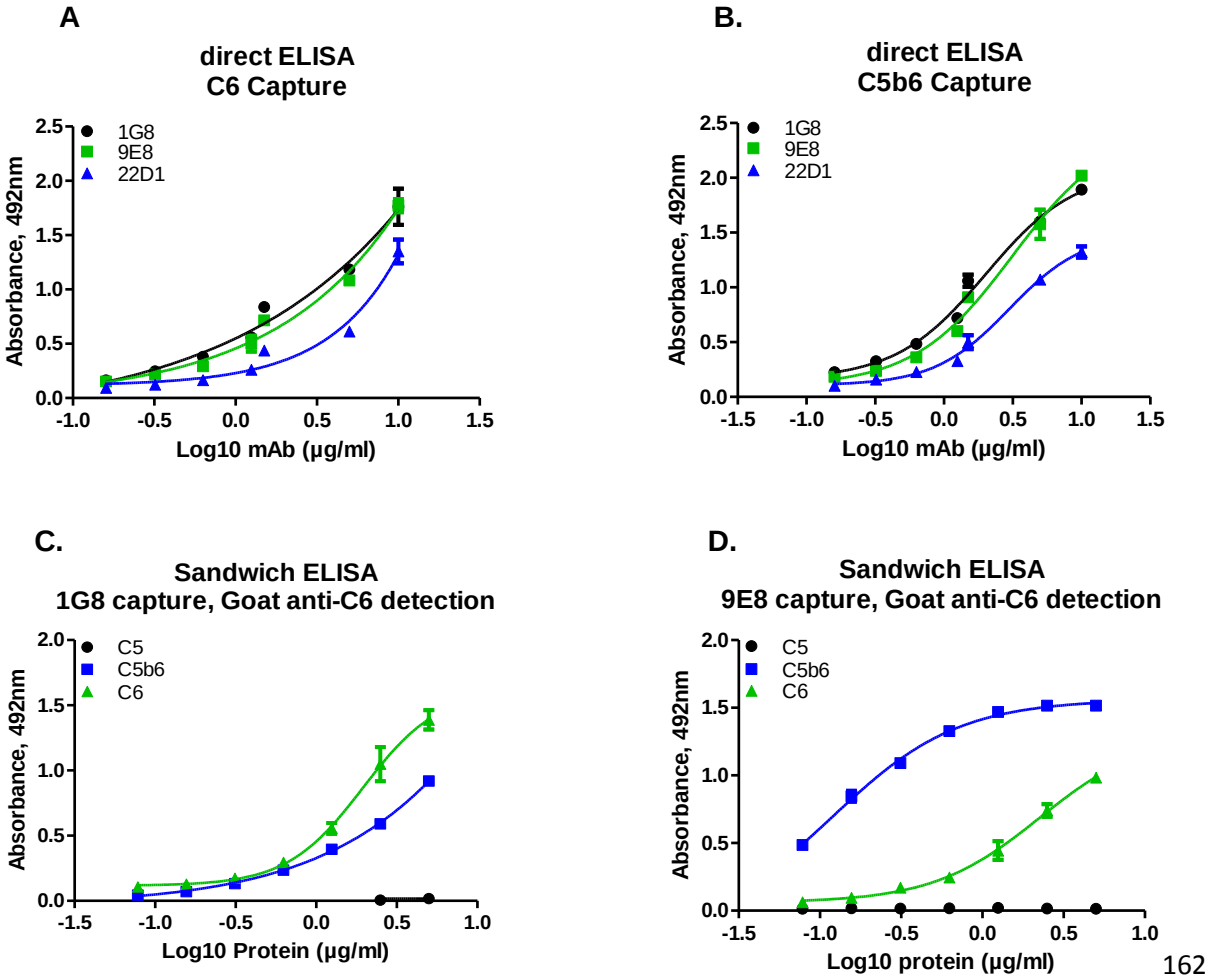

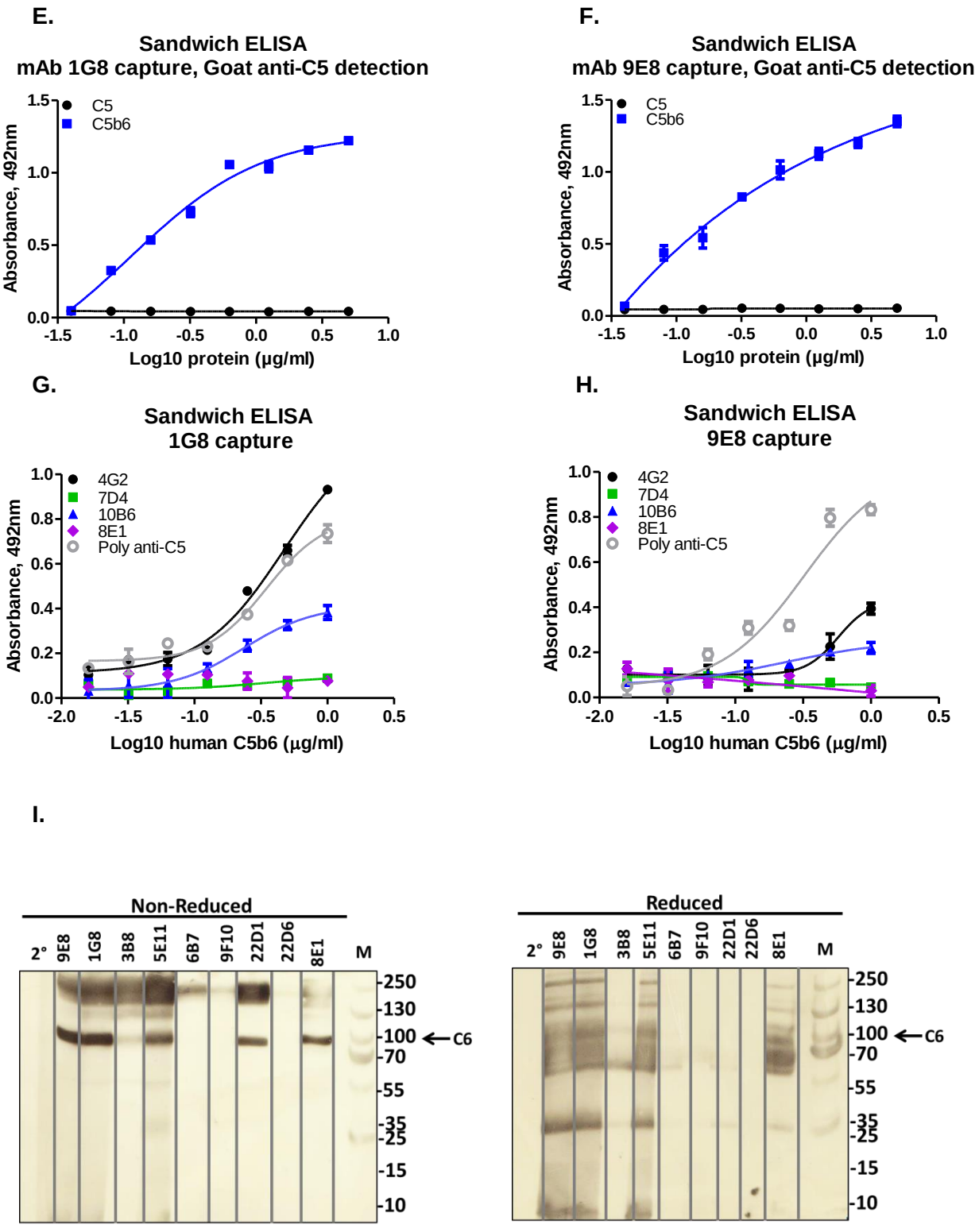

Figure 5.18 ELISA and WB to determine 1G8 and 9E8 binding to human C6 and C5b6 ***A, B.*** *In direct ELISA mAb 1G8 and 9E8 detected human C6 and C5b6 proteins.* ***C – F.*** *In sandwich ELISA with 1G8 and 9E8 as capture and polyclonal anti-C5 or C6 as detection, both C6 and C5b6, but not C5 were detected.* ***G, H.*** *In sandwich ELISA with the novel anti-C6 mAb as capture and 4G2 anti-C5 mAb as detection, C5b6 was detected showing that*

epitopes for both these mAbs are available on C5b6. Weak or no signals with the other mAb used as detection (7D4, 10B6 anti-C5, 8E1 anti-C6) suggests that binding of these mAb is restricted by steric hindrance. All experiments were repeated three times with comparable results. The error bars are standard errors of triplicates. ***I.*** *WB of novel mAb (1G8, 9E8) and supernatants from several uncharacterised clones (3B8, 5E11, 6B7, 9F10) and in house anti-C6 non-blockers (22D1, 22D6, 8E1) detecting C6 in human serum diluted 1 in 100 in PBS. Samples were resolved on 7.5% SDS PAGE under NR and R conditions. Blots were probed with the anti-C6 mAb and donkey anti-mouse IgG secondary antibody. The blots were cut into strips to detect the individual protein and re-aligned. M; protein molecular weight marker, 2°; secondary antibody.*

5.4 Discussion

In this chapter I have described the generation of a panel of mAb raised against human C7 and C6 proteins cross-reacting with rat and/or mouse. All mAb except clone 17E7 were generated in C7 deficient mice immunised with human or/and rat C7 purified in house. Prior to this work, no C7 blocking mAb had been described. Generation anti-C7 blocking mAb was more challenging compared to C5 mAb described in chapter 4 with ratios for C7: 1 in 2143, C5: 1 in 750 clones. All of the selected anti-C7 mAb bound C7 in ELISA and inhibited lysis of ShEA in CP assays with mAb 17E7 and 59E7 being the most efficient for human serum, mAb 2H2 most effective for rat and 73D1 for mouse complement. mAb 3B11 efficiently inhibited both human and rat serum. In a modified CP assay using a ten-fold higher serum dilution than standard to more closely mimic the in vivo situation, inhibition by 17E7 and 2H2 was also effective (Fig. 5.3). The efficiency of complement inhibition in CP assays by the human specific mAb 17E7 and 59E7 was similar to the currently available therapeutic anti-C5 mAb Eculizumab and RO7112689, used here as positive controls. The promising *in vitro* species–cross reactivity data led to testing of the mAb in animals. Clone 17E7 showed efficient inhibition of complement *in vivo* (tested in C7-deficient mice administered human C7) (Fig. 5.12), while mAb 73D1 efficiently inhibited mouse complement tested in parallel with the well-characterised anti-mouse C5 mAb BB5.1 (Fig. 5.13). mAb 17E7 and 59E7 showed strong and stable binding to C7 in SPR (KD = 1.02 x 10^{-9}, 9.31 x 10^{-10} respectively; Fig. 5.7) suggesting that they bind tightly to C7 in plasma to effect complement inhibition. The demonstration that both of these mAb were ineffective in purifications of C7 from serum may suggest that they bind conformational epitopes of C7 as has been suggested in other contexts (Aleshin *et al* 2012; Wurzner *et al* 1995). Further

studies are required to better characterise the mode of action and pharmacokinetics of these mAb *in vivo*.

Blocking anti-C6 mAb were also generated in C7 deficient mice using human or rat C7 immunogen. This is somewhat surprising given that the mice had not been immunised with C6 and these mAb were only identified because the first screening assay was for functional blocking activity. It is possible that these are a result of trace contamination of C7 preparations with the highly homologous C6 protein, although I found no evidence for this. A speculative explanation might be that immunisation with C7 in the C7D mice leads to the production of C5b67 complexes that expose new, immunogenic epitopes on C6; such mAb might be expected preferentially bind C5b6 and be blocking. Indeed, the two mAb selected showed efficient inhibition of human (clone 1G8 and 9E8) or rat (1G8) complement (Fig. 5.17) and both mAb showed strong binding to human C6 and C5b6 (Fig. 5.18). These interesting mAb were not further characterised because they were not the focus of this work and lacked novelty. CP010 (Complement Pharma) anti-C6 mAb is in clinical trials phase I (http://www.complementpharma.com/product-development/small-molecule-program; Harris 2018; Zelek *et al* 2019).

Unique among the mAb generated, the rat-selective mAb 2H2 was a highly efficient complement inhibitor *in vitro* and *in vivo*, requiring much lower doses than other in house or external control mAbs, Rats treated with mAb 2H2 showed complete loss of haemolytic activity and were protected from EAMG compared to controls (Fig. 5.14). The dose used for the animal experiment was 10 mg/kg, a quarter of the dose used for terminal pathway inhibitory mAb (such as BB5.1 or the in-house 4G2 anti-C5, or 73D1 anti-C7 mAb) described in this thesis (Wang *et al* 1995; Huugen *et al* 2007; Copland *et al* 2010; Raedler *et al* 2011; Zelek *et al* 2019); for these other mAb this dose is insufficient to fully inhibit complement in vivo, likely because it does not sufficiently exceed plasma levels of C7. The estimated amount of plasma in 200g rat is 8.4ml (Bijsterbosch *et al* 1981). C7 concentration in plasma is ~100µg/ml so this gives ~840µg of C7 per rat. The calculated C7: mAb 2H2 molar ratio (1: 1.5) is much lower compared to the standard dose (C5; 4G2 of 1: 12); but, the dose effectively blocked complement for seven days in rats (Fig.5.14).

Reactive lysis assays demonstrated that the 2H2 mAb inhibited efficiently binding of C5b6 to C7, and weakly C5b67 binding to C8 (Fig. 5.4 D). Interestingly, the mAb showed strong inhibition of C5b67 binding to C8 when the complex was pre-formed on GpE (C5b67-erythrocytes were washed after the complex formation) showing that 2H2 is capable of binding to C5b67 even when attached to erythrocytes suggesting that the mAb binds neo-specific epitope on C5b67 complex responsible for association to C8 to form MAC (Fig. 5.4 F). The capacity of mAb 2H2 to inhibit fluid-phase C5b67 complex was confirmed by flow

cytometry where no binding to cells was observed (Fig. 5.11). The inhibitory mechanism preventing the C5b67 association with the membrane is similar to how clusterin inhibits MAC. Clusterin binds to C5b67 preventing membrane insertion of the complex thus formation of C5b-9 (TCC) (Choi *et al* 1989; Jenne and Tschopp 1989). In reactive lysis in presence of clusterin haemolysis was inhibited ~50% and no inhibition was observed when C5b67 was pre-formed (clusterin added after the complex formation) suggesting that clusterin interferes with membrane binding of nascent C5b67 (Hallström *et al* 2015; Jenne and Tschopp 1989).

S-protein (vitronectin) is another TP regulator that binds C5b67 complex and blocks its insertion into the cell membrane. It was also showed that S-protein added to pre-formed C5b67 or C5b678 complex inhibited polymerisation of C9 (Podack *et al* 1984; Singh and Riesbeck 2010; Preissner and Jenne 1991; Preisner 1985). This dual function on C5b-9 assembly is very similar to mAb 2H2 action. Both S-protein and clusterin are weak inhibitors of haemolysis (~50%) and their role is more to downregulate complement rather than completely switching it off. In this respect mAb 2H2 mimics this mechanism but with much greater efficiency inhibiting lysis completely. The strength of S-protein or clusterin binding to C5b67 is unknown. A precise binding/ kinetics analysis would help to understand interactions between the MAC regulators or mAb 2H2 and the complexes; this can be investigated further by structural studies to determine the binding epitopes.

Of note, all the other novel mAb blocked reactive lysis *before* C7 addition, but not after the cells were decorated with C5b67 complex (Fig. 5.4) supporting the hypothesis that they associate with unfolded C7 epitope exposed only on C7 binding to C5b6 complex, yet structural studies are in progress to confirm this.

Despite the apparent rat specificity of 2H2, when rat serum depleted of C6 and C7 and restored with the human proteins was tested, 2H2 caused inhibition of lysis; when rat C6/C7 was added back to double-depleted human serum, 2H2 did not inhibit (Fig. 5.5). These confusing data imply a specificity for rat MAC intermediates rather than individual components that requires further exploration. The ELISA demonstrated that all mAb bind similar epitope of C7 or there is a steric hindrance preventing the pair mAb binding; no signals were observed when the mAb were used as capture or detection antibody (Fig. 5.6 A – K). A competition assays in ELISA or using SPR need to be performed to investigate this further. In WB, mAb 2H2 detected C7 in serum, but did not detect purified non-reduced rat C7 protein, again suggesting a complex binding action (Fig. 5.8). Pull-downs from serum activated in the presence of 2H2 mAb included all terminal pathway proteins C5 – C9 (Figs. 5.8, 5.9) suggesting that the mAb captures intermediates in the fluid phase, preventing their

association with membrane to seed MAC but permitting binding of later components to generate a TCC-like complex. The concept of 2H2 as a fluid-phase inhibitor was supported by activating serum on ShEA in the presence of the mAb; lysis was blocked but no mAb was detected on the target surface by flow cytometry (Fig. 5.11). Moreover, mAb 2H2 binds pre-formed C5b67, but usually prevents the complex even forming (Fig. 5.4 F). Attempts to deplete serum of C7 and purify C7 on mAb 2H2 were unsuccessful, yielding only small amounts of C7 and abundant non-specific proteins, predominantly albumin (Fig. 5.10); these data further support the complex-specific binding of 2H2.

Taken together, all of these data lead me to speculate that mAb 2H2 inhibitory mechanism resembles that of the mammalian fluid-phase inhibitors clusterin and S-protein, and the bacterial product, Streptococcal inhibitor of complement (SIC) protein (Hadders *et al* 2012; Fernie-King, *et al* 2001). These proteins bind fluid-phase intermediates (predominantly C5b67) and block the capacity of the complex to associate with membranes. A comprehensive study to compare mAb 2H2 with SIC and clusterin or S-protein and to test the presence of these latter proteins in the 2H2-complex would help to elucidate the precise mechanism of action of the mAb. My current hypothesis is that 2H2 acts as a "super-clusterin" to capture with high affinity the nascent fluid-phase C5b67 complex to prevent its association with membrane. Structural studies are in progress to determine the binding site of the mAb to C7 and C5b67 complex. Regardless of the precise mechanism of action, mAb 2H2 is a game-changing antibody with a novel mechanism that points the way to better, longer-acting, lower dose and less toxic anti-complement drugs; unfortunately, 2H2 is predominantly a rat-specific inhibitor, hence current efforts are focussed on finding human-specific mAb with similar properties and exploring ways of modifying 2H2 to increase its activity as a human inhibitor.

Overall in this chapter I explored a different approach to inhibiting complement beyond C5 inhibition by developing antibodies that specifically target only the terminal pathway downstream of C5. These MAC-targeting drugs are anticipated to replicate the therapeutic impact of current treatment (blocking C5 by Eculizumab) but with a reduced infection risk and lower dose requirement. My data shows that targeting C6 or C7 is just as effective as targeting C5 at inhibiting MAC formation; as a consequence, they are good drug candidates for diseases purely driven by MAC, for example, PNH and MG, as demonstrated here in the animal model, but likely not for diseases in which C5a/ C5aR pathway is implicated (e.g. ANCA-vasculitis). The 2H2 complex specific antibody with significantly reduced dose has potentially great advantages and will open-up new therapeutic fields for anti-complement drugs with significantly lower cost of treatment, with less risk of iatrogenic infection, and more suited to therapy of common, chronic diseases.

CHAPTER 6; DISCUSSION

6.1 Resume

The pathological role of complement has been known for more than fifty years (Pickering *et al* 1968; Schur *et al* 1968; Nesargikar *et al* 2012; Sim *et al* 2016;). Despite this long history, to date, the use of anti-complement drugs has been restricted to a handful of rare diseases, including haemolytic disorders and renal diseases, where they have had a transformational impact (Harris and Morgan 2015; Ricklin *et al* 2018; Zelek *et al* 2019). A step change is now needed to enable the use of anti-complement drugs in less rare (and common) diseases such as MS, AMD and AD. There is considerable unmet need in many of these diseases where a significant proportion of patients do not respond to currently available agents. Taking anti-complement approaches into these diseases requires a new generation of drugs that are safer, cheaper and easier to administer.

6.1.1 Success of inhibition of MAC by targeting C5

Over 30 years ago, the first functional C5 blocker was developed. The mAb BB5.1 provided proof of concept that inhibition of complement in animal models is safe and effective (Frei *et al* 1987, Wang et al. 1995; Huugen et al. 2007; Copland *et al* 2010; Raedler *et al* 2011). A few years later, guided by the success of BB5.1, an anti-human C5 blocking mAb was developed (Adis 2007). Treatment with this mAb, later named Eculizumab, proved successful with life-transforming outcomes, first for PNH and later for aHUS patients, rapidly becoming a blockbuster drug. Ravulizumab (the modified version of Eculizumab with prolonged half-life) was approved by FDA in December 2018 for PNH treatment and recently for gMG. Inhibition of MAC by blocking C5 with Eculizumab proved to be successful in these and other diseases, although numerous issues were raised; these included ineffective treatment for patients with the C5 variant p.Arg885His because Eculizumab didn't bind (Fukuzawa *et al* 2017), highly variable residual haemolysis in *ex vivo* assays using PNH patient sera treated with Eculizumab (Harder *et al* 2019), continuing transfusion need in PNH despite the treatment (Hillmen *et al* 2013), and breakthrough haemolysis in up to 37% of PNH patients on Eculizumab due to high turnover of C5 (Harder *et al* 2019). Even with Ravulizumab, some PNH patients experienced breakthrough haemolysis (5 of 125 patients stated in the recent report) (Lee *et al* 2019).

Other huge disadvantages are cost of the treatment and dosage. For example, yearly treatment cost for a PNH patient is £340 000, and the mAb is administered biweekly by intravenous infusion, 900 milligrams per dose. The cost of Ravulizumab is not yet known, although it is unlikely to be significantly cheaper despite the fact that the dose is reduced by ~50% (Sheridan *et al* 2018).

In chapter 4 I described generation of in-house C5 blocking mAb. From the numerous blocking anti-C5 mAb generated, three clones, 4G2, 7D4 and 10B5, were selected for full characterisation. mAb 4G2 and 7D4 showed efficient inhibition of human and rat complement *in vitro*, clone 4G2 also inhibited complement *in vivo* proving its usefulness for animal models. Clone 10B6 was equivalent to Eculizumab and the Roche mAb RO7112689 (now termed Crovalimab) in inhibition of ShEA lysis mediated by NHS. The rat cross-reactive mAb are under licence agreement with Cedarlane Ltd for research use only to detect rat C5.

The anti-C5 mAb were generated in C6 deficient mice immunised with C5b6 protein in an attempt to generate C5b6 neo-specific mAb; unfortunately, these were not found. All mAb generated bound C5 and C5b6; none bound C5b6 only. Perhaps using the C5b6 immunogen in C5 deficient (or C5/C6 double-deficient) mice would have been more successful.

C5 is a protein with multiple potential function-blocking binding sites on its surface as demonstrated by structural studies on tick-derived inhibitors (OmCI, RaCI) and Eculizumab, each of which inhibit but bind to distinct sites on C5 (Jore *et al*. 2016). My data support the hypothesis that C5 interactions with these different inhibitors causes a conformational lock, preventing the conformational changes in C5 necessary for its cleavage and thus inhibiting MAC formation; locking rather than binding to a specific epitope on C5 is therefore responsible for the inhibition. The high yield of functional C5 blockers (1 in 12 anti-C5 clones) from my work supports this hypothesis. Structural studies using non-inhibitory anti-C5 mAb (Table 6.2) are planned to confirm the conformational C5 locking mechanism. In contrast, generation of blocking anti-C7 mAb has been much more challenging (1 in 206 anti-C7 clones).

.

6.1.2 Inhibition of MAC beyond C5

By definition, any drug blocking complement activation would be anti-inflammatory due to the pro-inflammatory nature of complement. The TP is the source of two of the most potent complement pro-inflammatory products; MAC and C5a. The successful treatment of PNH and aHUS patients with Eculizumab showed that inhibition of C5 is relatively safe with manageable side effects, including increased risk of Neisseria infections. Eculizumab inhibits cleavage of C5 and thus blocks not only MAC formation but also generation of C5a, an important chemoattractant. The benefit of complement inhibition in the TP downstream of C5 is that there is no interference with neutrophil recruitment to areas of inflammation, reducing the risk of infections. Lessons from complement deficiencies suggest that

depletion any of the terminal pathway component is relatively low risk and easy to overcome with prophylactic antibiotic treatment or vaccination against Neisserial infections (Skattum *et al* 2011; Grumach and Kirschfink 2014).

Although the field of development of complement therapeutics is very competitive, it has become highly focused on just a few targets, C5 in TP specifically. Some other TP targeting anti-complement approaches have been suggested but none have progressed beyond models to clinical trials (Harris and Morgan 2015; Harris 2018; Ricklin *et al* 2018, Zelek *et al* 2019). Currently there is only one drug targeting MAC specifically in phase 1 clinical trials, AAVCAGsCD59, a viral construct that has been developed to increase CD59 expression in the retina in AMD (Cashman *et al* 2011). One other agent is in pre-clinical trials, CP10 a blocking mAb against C6. In contrast twelve agents are currently under development targeting native C5 (Zelek *et al* 2019).

In this project I have explored different ways of inhibiting MAC, breaking away from the dogma of C5 being the best therapeutic target. In the course of the work I have developed panels of mAb inhibiting individual MAC proteins; C6 (clones 1G8, 9E8) and C7 (clones 17E7, 59E7, 3B11 and 73D1), and also mAb that likely target the C5b67 complex, an essential intermediate in formation of the MAC (2H2).

The anti-C6 mAb were not completely characterised because of lack of novelty; however, preliminary data showed that they inhibited complement to a similar degree to commercial anti-C5 mAb Eculizumab and RO7112689. Further testing is needed to investigate binding affinities of these novel mAb to C6 and C5b6 complex. These mAb are the subject of a licence agreement with Complement Pharma.

All of the anti-C7 mAb described in chapter 5 were produced in the C7 deficient mouse; all inhibited human complement with mAb 17E7 and 59E7 being the most efficient blockers. The mAb 17E7 effectively inhibited human C7 when tested *in vivo* using human C7 in the C7 deficient mouse. mAb 73D1 is predominantly an anti-mouse C7 mAb, inhibiting mouse complement *in vivo* at the same levels as the broadly used anti-C5 mAb BB5.1. mAbs 3B11 and 2H2 showed good inhibition of rat serum-mediated haemolysis. Overall, mAb 2H2 was the most effective complement inhibitor out of all of the mAb tested, inhibiting at much lower doses compared to the other mAb. Clone 2H2 also showed prolonged half-life

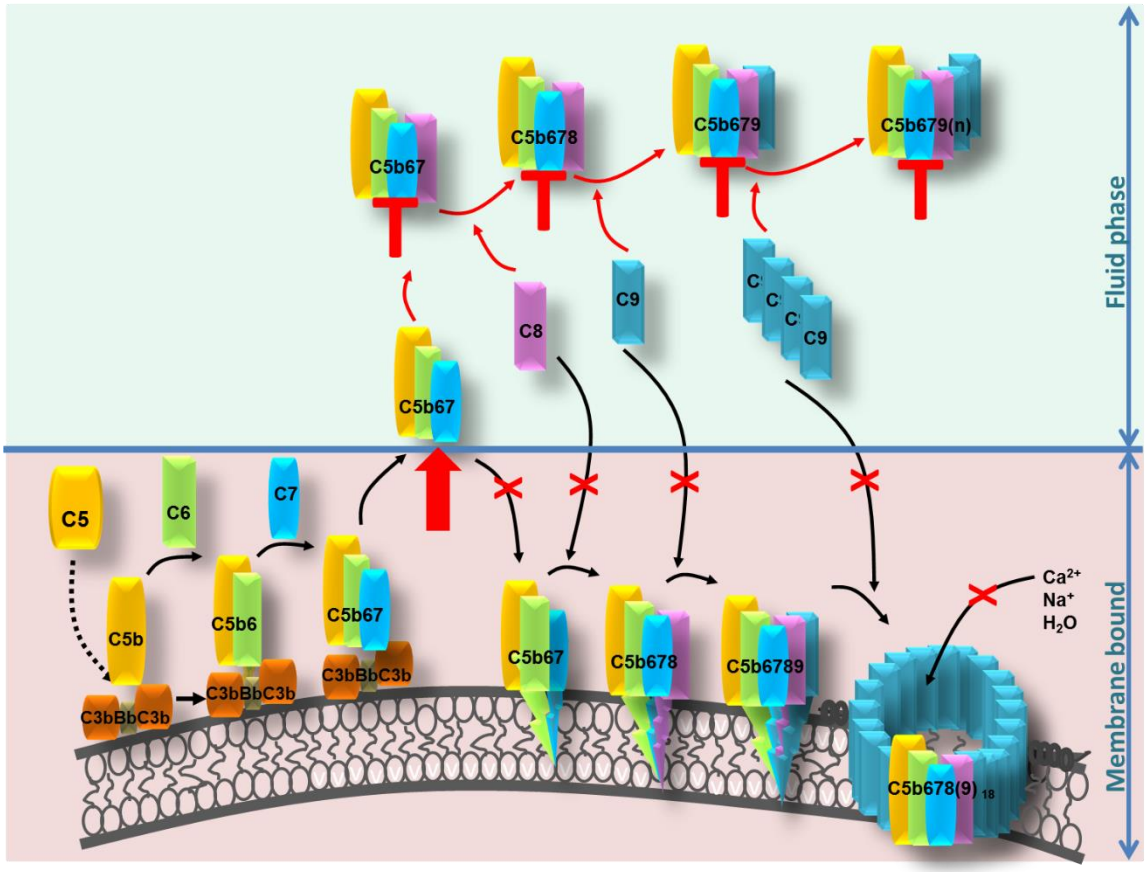

Figure 6.1 Schematic of mechanism of MAC inhibition by mAb 2H2 in fluid phase; *preventing C5b-7 complex assembly on the cell membrane and thus MAC formation by sequential recruitment of the terminal pathway components.*

when tested in rat; the standard dose used (40 mg/kg) inhibited complement for a week whereas the same dose of the anti-C5 mAb (4G2 in rat or BB5.1 in mouse) inhibited for 24 hours. The data suggest that mAb 2H2 illustrates a novel mechanism of MAC inhibition, acting in the fluid phase to prevent the C5b67 complex association with the membrane (Fig. 6.1). The proposed mechanism of preventing MAC assembly on a cell surface by blocking the membrane binding site of the nascent C5b67 complex is not without precedent - the natural fluid-phase regulators clusterin and S-protein (and indeed C8) work in this way to inhibit complement mediated cytolysis (Preissner *et al* 1989; Podack *et al* 1978; Podack and Muller–Eberhard 1978; Jenne and Tschopp 1989; Kriszbaum *et al* 1989; Murphy *et al* 1988; 1989; O'Bryen *et al* 1990; Falk *et al* 1987; Nemerow *et al* 1979). Both S-protein and clusterin bind to the C5b67 complex, blocking membrane association but allowing binding of C8 and C9 to yield the inactive fluid-phase sC5b-9 complex (terminal complement complex; TCC) (Preissner *et al* 1989; Podack *et al* 1978; Podack and Muller – Eberhard 1978; Jenne and Tschopp 1989; Kriszbaum *et al* 1989; Murphy *et al* 1988; 1989). The C5b67 complex is also targeted by bacteria as one of an array of mechanisms to evade

host defence; the Streptococcal inhibitor of complement (SIC) blocks lysis by MAC in haemolytic assays (Åkessont *et al* 1996; Fernie-King *et al* 2001). Like clusterin, SIC binds the C5b67 complex; direct comparison of SIC and clusterin showed that they are equally efficient at inhibiting MAC (Åkessont *et al* 1996; Fernie-King *et al* 2001). In this respect, mAb 2H2 is likely mimicking this mechanism, albeit with considerably greater efficiency as demonstrated by the functional and *in vivo* analyses described in chapter 5.

6.1.3 Summary of the novel anti-terminal pathway mAb developed in the project

Table 6.1 summarises the function-blocking mAb developed and characterised in the course of the work while Table 6.2 notes the non-blockers taken forward as tool antibodies for detection and/or purification of the relevant proteins.

Antibody	**Isotype**	**Target**	**Cross-species reactivity/ inhibition *in vitro***	**Cross-species reactivity/ inhibition *in vivo***	**IP**
4G2	IgG2b, K	C5 / C5b6	Strong; Hu, Rt, Rb. Weak; Gp, Rb	Rt	Licence agreement in progress
7D4	IgG2b, K	C5 / C5b6	Strong; Hu, Rt, Rb. Weak; Gp, Rb, Mo	Not tested	N/A
10B6	IgG1, K	C5 / C5b6	Strong; Hu	N/A	N/A
1G8	IgG2b, K	C6/ C5b6	Strong; Hu, Rt	Not tested	Licence agreement in progress
9E8	IgG2b, K	C6/ C5b6	Strong; Hu	Not tested	
2H2	IgG2b, K	C7/ C5b-7	Strong; Rt. Weak; Mo, Hu	Rt	Patent application in progress
3B11	IgM, K	C7	Strong; Hu, Rt	Not tested	
17E7	IgG2a, K	C7	Strong; Hu	Hu	
59E7	IgG2b, K	C7	Strong; Hu	Not tested	
73D1	IgG2a, K	C7	Strong; Mo. Weak; Hu, Rt	Mo	
1G8	IgG2b, K	C6/ C5b6	Strong; Hu, Rt	Not tested	Licence agreement in progress
9E8	IgG2b, K	C6/ C5b6	Strong; Human	Not tested	

Table 6.1 *Summary of the new anti-C5, C6 and C7 mAb and the plans for further development. Hu, human; Rt, rat; Mo, mouse; Gp, guinea pig; Rb, rabbit.*

Antibody	Isotype	Target
2B1	IgG	C5
2C3	IgG	C5
6G1	IgG	C5
6D9	IgG	C5
8C11	IgG	C5
8E1	IgG1, K	C6
C26*	IgG1, K	C6
F10*	IgG2a, K	C7
D5*	IgG	C8
J1*	IgG	C8
K1*	IgG	C8
26*	IgG1	C9
B7*	IgG	C9

Table 6.2 *Summary of the in-house anti-human terminal pathway non-inhibitory mAb; mAb were used for protein purification, WB, ELISA or other applications. * In-house developed hybridoma cell lines that were re-cloned (section 2.17.6), screened in direct ELISA (section 2.13.1), scaled up in Integra flasks (2.17.3) and purified (section 3.2.7). All mAb were negative in screening for complement inhibition (data not shown).*

6.2 Future prospects

6.2.1 Targeting complement in more common diseases

Rare complement driven-diseases such as PNH and aHUS are caused by inherited or acquired genetic defects, but in many more common diseases complement dysregulation exacerbates/perpetuates pathology. In aHUS and PNH the MAC causes cell damage and drives inflammation. Blocking MAC assembly with the anti-C5 mAb Eculizumab, one of the most expensive drugs in the world, prevents these effects and transforms patient outcomes. To extend therapy to common complement dysregulation diseases, we need simpler, cheaper, easily administered and safe anti-complement drugs. Therapeutic MAC blockade is attractive because, while reducing inflammation and direct damage, it leaves intact critical bactericidal opsonic activities which, if lost, severely compromise defence against infection (Socie *et al* 2019). In recent years, complement has been implicated in various conditions, including more common diseases such as AMD, RA, MS and HS. GWAS studies and biomarkers measurement in plasma and CSF provide solid evidence of complement pathological roles in these diseases (Harris 2018, Ricklin *et al* 2018; Zelek *et al* 2019). It is likely that anti-complement therapy in these conditions would involve downregulation of

complement rather than a complete inhibition, and targeted inhibition to treat tissue damage resulting from local activation of complement where systemic treatment might not be appropriate. There is therefore an urgent need for new ways of regulating complement.

6.2.2 Alternative approaches to targeting MAC

Among the TP proteins, targeting C7 to inhibit MAC is the most logical approach. C7 is the central TP protein, essential for MAC generation. Unique among the TP proteins, the liver is not the principle source of C7 and as a consequence C7 is not an acute phase reactant (Würzner *et al* 1994). Local synthesis of C7 may provide an efficient source of the protein for initiating MAC formation for lysis of intruders and activating neutrophils and endothelial cells at the site of inflammation (Würzner 2000). The fact that C7 is the only TP protein that is not an acute phase reactant means that synthesis and hence plasma levels will not increase during inflammation, eliminating the risk of breakthrough haemolysis, a major issue with C5 inhibitors as described above and enabling the use of much lower doses of drug compared to the other TP proteins. Targeting C7 is a novel way to inhibit MAC and, as I demonstrated here, very effective *in vitro* and *in vivo*. Both mAb 17E7 and 73D1 completely blocked C7 in animals; no residual lysis was detected even 48 hours post-injection, this contrasts to mAb 4G2 anti-C5 where ~40% lysis was seen two hours post administration and throughout the rest of the study.

It has been suggested that C7 and C6 bind reversibly to non-activated C5 (Kolb *et al* 1973; Arroyave and Müller-Eberhard 1973). These interactions are mediated by C345C domain of C5 and are distinct from the irreversible interactions that take place within the MAC. C5-C345C binds directly to the tandem pair of approximately 75-residue factor I modules from C7 (C7-FIMs), an essential step in MAC assembly. SPR analysis showed that C7 binds to C5b6 with a KD ~3pM, and that micromolar concentrations of either rC5-C345C or rC7-FIMs inhibit this early step in MAC formation. It is an attractive idea to target C7-FIMs to inhibit the conformational changes that expose a membrane-binding site in C7 when it binds to C5b6 complex to assemble MAC. The hypothesis could be tested by raising mAbs against C7-FIMs and exploring inhibition of MAC formation. Indeed, my preliminary data suggest that mAb 17E7 binds rC7-FIMs (data not shown; requires replication) which indeed suggests additional mechanism of inhibiting MAC, yet this needs to be explored.

6.2.3 Other potential ways of inhibiting MAC

Recently, an interesting study on C9 binding to C5b-8 complex was published (Spicer *et al* 2018). The data show that polymerisation of C9 is dependent on its TMH1 domain which, in the presence of C5b-8, changes conformation and enters the membrane exposing the

elongation face of newly bound C9 for next C9 monomer to bind to form the pore. Recombinant C9 variant in which TMH1 is disulphide locked is able to bind C5b-8, but unable to bind next C9 molecule as the TMH1 domain of C9 cannot be released (Spicer *et al* 2018). mAb or other agents that mimic this "locked" form of C9 may have potential for inhibiting MAC at this very late stage of formation. *In vivo* experiments are needed to investigate this and establish the impact of the C5b-9_1 pre-pore on cells and in disease pathology.

Studies using rapid atomic force microscopy (AFM) underpinned molecular mechanism and kinetics of MAC assembly (Parsons *et al* 2019). The stepwise kinetics at the single molecule level showed that binding of C9 to C5b-8 after C9 addition is slow (much slower than C5b-8 formation), and the next step, polymerisation of C9, occurs rapidly, as a consequence, binding of the first C9 molecule to C5b-8 is the slowest step in MAC assembly (Parsons *et al* 2019). This creates a great opportunity to interfere with this association and/or C9 polymerisation. Indeed, the time window might explain the efficiency of MAC inhibition mediated by CD59 (Farkas *et al* 2002; Huang *et al* 2006). CD59 plays a double act in MAC assembly; it binds C8α-chain in C5b-8 complex preventing membrane perforation, and/or it binds C9 carboxy-terminal b domain in C5b-9_1 complex inhibiting polymerisation of C9. (Ninomiya *et al* 1992). Soluble recombinant CD59 efficiently inhibits MAC in a purified protein system *in vitro*, but weakly when plasma used, limiting *in vivo* application. Its activity is significantly higher when positioned in close proximity to the target membrane at the site of MAC assembly (Zhang *et al* 1999; Song *et al* 2003). A better understanding of CD59 mode of action in the fluid phase or in association with the membrane in combination with the reported kinetics/reaction times would assist design of therapeutics for modulation of MAC activity based on the first C9 interactions with C5b-8.

6.2.4 Next generation complement drugs

The field of anti-complement agents under development is changing rapidly. However, the only two currently approved anti-complement drugs are Eculizumab (its successor Ravulizumab) and C1INH. In more than twelve years no other new agents have been approved. Ravulizumab is a pH switch (recycling) mAb variant of Eculizumab with extended half-life. Recycling mAb characteristics are improved pharmacokinetics and less frequent dosing. The pH-switch mAb can also be selected at screening stage for pH dependence as was applied for Crovalimab (RO7112689) (Fukuzawa et al. 2017; Sampei *et al* 2018). Another advantage of the pH dependent mAb binding demonstrated in this thesis is the use of these mAb for affinity purification of proteins that are sensitive to pH shifts; here I demonstrated the benefit of C5 purification without exposure to pH extremes using

Crovalimab (chapter 3), but this trick would also be applicable to other difficult to purify proteins.

Of note, the mechanism of complement inhibition by Crovalimab is distinct from Eculizumab, as it inhibits not only C5 cleavage but also binding of C5b6 to C7 as demonstrated by reactive lysis assays and atypical cleavage of C5 with neutrophil elastase (Zelek *et al* 2018; chapter 4). Crovalimab was effective in patients carrying the p.Arg885His C5 variant mutation. The reported trials suggest significant reduction of dose compared to Eculizumab (340 mg every two weeks) (Risitano *et al* 2019). Crovalimab is progressing fast through the clinical trials (currently phase 2) and will certainly challenge Eculizumab and/or Ravulizumab in the near future.

Several of the mAb developed in this project are, without any modifications, just as good as the commercial Eculizumab and RO7112689 at least in *in vitro* assays. To be used in the clinics they will need to be humanised and can also be further improved using various techniques to enhance their therapeutic potential such as affinity maturation, class switching, and pH switching. This would result in more effective treatment with presumably lower dose of mAb. The C5b67 complex specific mAb (2H2) already shows competitive dosing in rats with ~four times less mAb used compared to anti-C5 mAb (4G2). However, this mAb is predominantly a rat specific blocker and is thus not directly suitable for further development. Attempts to develop human specific mAb acting the same way as clone 2H2 are ongoing. The CDR sequences of mAb 2H2 have been determined and it may be possible to introduce changes in the CDRs that make this mAb more human-specific. It is also possible that small molecule drug(s) can be developed based on the CDRs; however, obtaining the structure of the mAb 2H2 in complex with C5b67 is crucial for drug design. The human specific anti-C7 mAb show interesting characteristics that suggest that they bind C7 conformational epitopes (Aleshin et al 2012; Wurzner et al 1995); however, this needs to be confirmed by structural studies. The availability of tool anti-C7 mAb that inhibit rodent C7 enables proof-of concept studies in rodent models, as shown here using rat EAMG; nevertheless, the true therapeutic potential of anti-C7 mAb will only be proven when they enter clinical trials.

6.2.5 Drug delivery

In recent years a lot of effort has been expended to expand the routes available for anti-complement drug administration. Until recently, the only approach available was intravenous with all its restrictions but now a range of other systemic approaches and even oral administration are being explored. The routes are very dependent on the type of drug used; for instance, mAbs can only be delivered through injection be it intravenous,

subcutaneous, intraocular etc. Several promising orally administered small molecules are under development; for example, by RaPharma (targeting amplification loop and C5), Novartis (LNP023 FB inhibitor given twice daily) (Schubart *et al* 2019; Zelek *et al* 209). These are in development for various diseases but mainly focusing on rare disorders; PNH and renal diseases *(*Schubart *et al* 2019). As orally bioavailable small molecules progress through clinical trials in these rare conditions, and if they show promising results, they will offer greater flexibility in drug administration in comparison to mAb and enable attention to be given to more common diseases as noted above. Although the dosage is more frequent (usually twice a day), ease of administration will be a huge advantage, cost should be much lower and even the short half-life might be an advantage in terms of infection risk.

6.2.6 Drug design and modifications

The great advantage of use of mAb as therapeutics is their high specificity; however, their size (~150 kDa) might be an issue in delivery to the difficult targets for example to cross BBB. Numerous modifications can be applied to overcome this including generation of small, tissue-penetrant fragments or variants (fAb; nanobodies, peptides, etc.) *In silico* modelling and structural characterisation of the blocking mAb would help to design small molecule-based drugs for specific purposes – for example, crossing the BBB. The mAb developed in this project are as good as or better than the commercial mAb (Eculizumab and RO7112689) at inhibiting complement in standard lytic assays. Antibody fragments or small drugs designed based on the mAb CDRs would be better able to reach difficult tissue targets including brain. The mAb itself can be fragmented to generate active fragments (e.g. fAb, Fv); indeed, I show in chapter 4 that Fab fragments (~50 kDa) of the mAb retain inhibitory activity. Even smaller fragments will be needed in order to cross the intact BBB. Phage display can be used to generate a vast diversity of recombinant antibody fragments, usually including the whole VH or the CDRH3 mAb domain, allowing generation of small mAb fragments (scFv; nanobodies etc.) that retain the binding properties of a full length IgG (Reader *et al* 2019); these methods could be applied to the novel mAb.

Other small, tissue penetrant agents can be developed based on the novel mAb sequence by identifying peptides that target the specific mAb binding site on the antigen. Once again, computational modelling and/or structural studies to define the mAb–antigen binding site are required to inform design of a successful drug. Complement-inhibiting peptides targeting at several stages are under development; for example, by RaPharma and Achillion, and are progressing through clinical trials (*Zelek et al* 2019). Avacopan (a C5aR-blocking cyclic peptide) was shown to have similar efficacy to high dose corticosteroids in AVV patients with far fewer side effects (Tesar *et al* 2018)

6.3 Conclusions

In this thesis I have described novel approaches for inhibiting complement by targeting MAC components and intermediates downstream of C5. I have shown that, although challenging, it is possible to develop neoepitope-specific mAb against MAC complexes; mAb 2H2 is an inhibitor of C5b67 and offers a novel mechanism of inhibition of MAC with significantly reduced dosage as demonstrated by *in vitro* and *in vivo* assays. Unfortunately, 2H2, a powerful inhibitor in the rat, is a weak inhibitor of human complement. The screening methods I have developed and the optimised purification protocols of proteins and complexes were fundamental tools for the success of this project and will enable identification in future of 2H2-like mAbs that work better in human plasma. mAb 2H2 and the other anti-C7 blockers (clone 17E7, 59E7, 73D1 and 3B11) are the subject of a patent application (1911931.2). The other inhibitory mAb (anti-C5, anti-C6) I developed are subject to licence agreements. The long-term goal is to translate these novel mAb into the clinic to improve therapy of inflammatory disease.

BIBLIOGRAPHY;

Abdul Razzak, R., Florence, G. J., & Gunn-Moore, F. J. (2019). Approaches to CNS Drug Delivery with a Focus on Transporter-Mediated Transcytosis. *International Journal of Molecular Sciences*, 25; 20(12). https://doi.org/10.3390/ijms20123108

Adis Data Information BV. Eculizumab: 5G1.1, h5G1.1, long-acting anti-C5 monoclonal antibody 5G1-1, long-acting anti-C5 monoclonal antibody 5G1.1. (2007). *Drugs in R and D*, *8*(1), 61–68. https://doi.org/10.2165/00126839-200708010-00006

Aeinehband, S., Lindblom, R. P. F., Al Nimer, F., Vijayaraghavan, S., Sandholm, K., Khademi, M., Piehl, F. (2015). Complement component C3 and butyrylcholinesterase activity are associated with neurodegeneration and clinical disability in multiple sclerosis. *PloS One*, *10*(4), e0122048. https://doi.org/10.1371/journal.pone.0122048

Ahrenstedt, R., Knutson, L., Nilsson, B., Nilsson-Ekdahl, K., Odlind, bo, & Hällgren, R. (1990). Enhanced Local Production of Complement Components in the Small Intestines of Patients with Crohn's Disease. *New England Journal of Medicine*, *322*(19), 1345–1349. https://doi.org/10.1056/NEJM199005103221903

Åkessont, P., Sjöholm, A. G., & Björck, L. (1996). Protein SIC, a novel extracellular protein of Streptococcus pyogenes interfering with complement function. *Journal of Biological Chemistry*, *271*(2), 1081–1088. https://doi.org/10.1074/jbc.271.2.1081

Alcorlo, M., Martínez-Barricarte, R., Fernández, F. J., Rodríguez-Gallego, C., Round, A., Vega, M. C., Llorca, O. (2011). Unique structure of iC3b resolved at a resolution of 24 Å by 3D-electron microscopy. *Proceedings of the National Academy of Sciences of the United States of America*, *108*(32), 13236–13240. https://doi.org/10.1073/pnas.1106746108

Alcorlo, M., Tortajada, A., De Córdoba, S. R., & Llorca, O. (2013). Structural basis for the stabilization of the complement alternative pathway C3 convertase by properdin. *Proceedings of the National Academy of Sciences of the United States of America*, *110*(33), 13504–13509. https://doi.org/10.1073/pnas.1309618110

Aleshin, A. E., DiScipio, R. G., Stec, B., & Liddington, R. C. (2012). Crystal structure of C5b-6 suggests structural basis for priming assembly of the membrane attack complex. *Journal of Biological Chemistry*, *287*(23), 19642–19652. https://doi.org/10.1074/jbc.M112.361121

Al Salihi, A., Ripoche, J., Pruvost, L., & Fontaine, M. (1982). Purification of complement components by hydrophobic affinity chromatography on phenyl-Sepharose. Purification of human C5. *FEBS Letters*, *150*(1), 238–242. https://doi.org/10.1016/0014-5793(82)81342-2

Antony, P. M. A., Diederich, N. J., & Balling, R. (2011). Parkinson's disease mouse models in translational research. *Mammalian Genome: Official Journal of the International Mammalian Genome Society*, *22*(7–8), 401–419. https://doi.org/10.1007/s00335-011-9330-x

Arroyave, C. M., & Müller-Eberhard, H. J. (1973). Complement components C5 and C7: recombinant factor I modules of C7 bind to the C345C domain of C5. *Journal of Immunology*, 536–545. http://www.ncbi.nlm.nih.gov/pubmed/4268733

Asgari, E., Le Friec, G., Yamamoto, H., Perucha, E., Sacks, S. S., Köhl, J., … Kemper, C. (2013). C3a modulates IL-1β secretion in human monocytes by regulating ATP efflux and subsequent NLRP3 inflammasome activation. *Blood*, *122*(20), 3473–3481. https://doi.org/10.1182/blood-2013-05-502229

Aslam, M., & Perkins, S. J. (2001). Folded-back solution structure of monomeric factor H of human complement by synchrotron X-ray and neutron scattering, analytical ultracentrifugation and constrained molecular modelling. *Journal of Molecular Biology*, *309*(5), 1117–1138. https://doi.org/10.1006/jmbi.2001.4720

Barcellini, W. (2015). Current treatment strategies in autoimmune hemolytic disorders. *Expert Review of Hematology*, 2015 Oct;8(5):681-91. https://doi.org/10.1586/17474086.2015.1073105

Barkas, T., & Irvine, W. J. (1977). A mild method for decomplementation of human sera. *Clinical and Experimental Immunology*, *29*(2), 355–359. http://www.ncbi.nlm.nih.gov/pubmed/332423

Barnett, M. H., Parratt, J. D. E., Cho, E. S., & Prineas, J. W. (2009). Immunoglobulins and complement in postmortem multiple sclerosis tissue. *Annals of Neurology*, *65*(1), 32–46. https://doi.org/10.1002/ana.21524

Barnum S., Schein T. The complement factsbook. (2018). *Academic Press.*Elsevier. https://doi.org/10.1016/c2015-0-06595-9

Bauer, J., Podack, E. R., & Valet, G. (1979). Determination of the number of lytic sites in biconcave and spheroid erythrocyte ghosts after complement lysis. *Journal of Immunology*, *122*(5), 2032–2036. http://www.ncbi.nlm.nih.gov/pubmed/448115

Beck, L. H., Bonegio, R. G. B., Lambeau, G., Beck, D. M., Powell, D. W., Cummins, T. D., Salant, D. J. (2009). M-type phospholipase A2 receptor as target antigen in idiopathic membranous nephropathy. *New England Journal of Medicine*, *361*(1), 11–21. https://doi.org/10.1056/NEJMoa0810457

Bergelson, J. M., Chan, M., Solomon, K. R., St. John, N. F., Lin, H., & Finberg, R. W. (1994). Decay-accelerating factor (CD55), a glycosylphosphatidylinositol-anchored complement regulatory protein, is a receptor for several echoviruses. *Proceedings of the National Academy of Sciences of the United States of America*, *91*(13), 6245–6248. https://doi.org/10.1073/pnas.91.13.6245

Bergelson, J. M., Mohanty, J. G., Crowell, R. L., St John, N. F., Lublin, D. M., & Finberg, R. W. (1995). Coxsackievirus B3 adapted to growth in RD cells binds to decay-accelerating factor (CD55). *Journal of Virology*, *69*(3), 1903–1906. http://www.ncbi.nlm.nih.gov/pubmed/7531780

Bhakdi, S., Fassbender, W., Hugo, F., Carreno, M. P., Berstecher, C., Malasit, P., & Kazatchkine, M. D. (1988). Relative inefficiency of terminal complement activation. *Journal of Immunology*, *141*(9), 3117–3122. http://www.ncbi.nlm.nih.gov/pubmed/3262681

Bickel, U. (1995). Antibody delivery through the blood-brain barrier. *Advanced Drug Delivery Reviews*, *15*(1–3), 53–72. https://doi.org/10.1016/0169-409X(95)00005-R

Biesecker, G., & Gomez, C. M. (1989). Inhibition of acute passive transfer experimental autoimmune myasthenia gravis with Fab antibody to complement C6. *Journal of Immunology*, *142*(8), 2654–2659. http://www.ncbi.nlm.nih.gov/pubmed/2703710

Bijsterbosch, M. K., Duursma, A. M., Bouma, J. M. W., & Gruber, M. (1981). The plasma volume of the Wistar rat in relation to the body weight. *Experientia*, *37*(4), 381–382. https://doi.org/10.1007/BF01959874

Blom, A. M., Kask, L., & Dahlbäck, B. (2003). CCP1-4 of the C4b-binding protein α-chain are required for factor I mediated cleavage of complement factor C3b. *Molecular Immunology*, *39*(10), 547–556. https://doi.org/10.1016/S0161-5890(02)00213-4

Bomback, A. S., Markowitz, G. S., & Appel, G. B. (2016). Complement-Mediated Glomerular Diseases: A Tale of 3 Pathways. *Kidney International Reports*, 1(3):148-155. https://doi.org/10.1016/j.ekir.2016.06.005

Bora, N. S., Gobleman, C. L., Atkinson, J. P., Pepose, J. S., & Kaplan, H. J. (1993). Differential expression of the complement regulatory proteins in the human eye. *Investigative Ophthalmology & Visual Science*, *34*(13), 3579–3584. http://www.ncbi.nlm.nih.gov/pubmed/7505007

Boyd, J., Burton, D. R., Perkins, S. J., Villiers, C. L., Dwek, R. A., & Arlaud, G. J. (1983). Neutron scattering studies of the isolated C1r2C1s2 subunit of first component of human complement in solution. *Proceedings of the National Academy of Sciences of the United States of America*, *80*(12 I), 3769–3773. https://doi.org/10.1073/pnas.80.12.3769

Brachet, G., Bourquard, T., Gallay, N., Reiter, E., Gouilleux-Gruart, V., Poupon, A., & Watier, H. (2016). Eculizumab epitope on complement C5: Progress towards a better understanding of the mechanism of action. *Molecular Immunology*, *77*, 126–131. https://doi.org/10.1016/j.molimm.2016.07.016

Bradt, B. M., Kolb, W. P., & Cooper, N. R. (1998). Complement-dependent proinflammatory properties of the Alzheimer's disease β-peptide. *Journal of Experimental Medicine*, *188*(3), 431–438. https://doi.org/10.1084/jem.188.3.431

Brennan, F. H., Gordon, R., Lao, H. W., Biggins, P. J., Taylor, S. M., Franklin, R. J. M., Ruitenberg, M. J. (2015). The complement receptor C5aR controls acute inflammation and astrogliosis following spinal cord injury. *Journal of Neuroscience*, *35*(16), 6517–6531. https://doi.org/10.1523/JNEUROSCI.5218-14.2015

Brenke, R., Hall, D. R., Chuang, G. Y., Comeau, S. R., Bohnuud, T., Beglov, D., Kozakov, D. (2012). Application of asymmetric statistical potentials to antibody-protein docking. *Bioinformatics*, *28*(20), 2608–2614. https://doi.org/10.1093/bioinformatics/bts493

Brodbeck, W. G., Liu, D., Sperry, J., Mold, C., & Medof, M. E. (1996). Localization of classical and alternative pathway regulatory activity within the decay-accelerating factor. *Journal of Immunology*, *156*(7), 2528–2533. http://www.ncbi.nlm.nih.gov/pubmed/8786315

Brodbeck, W. G., Mold, C., Atkinson, J. P., & Medof, M. E. (2000). Cooperation Between Decay-Accelerating Factor and Membrane Cofactor Protein in Protecting Cells from

Autologous Complement Attack. *The Journal of Immunology*, *165*(7), 3999–4006. https://doi.org/10.4049/jimmunol.165.7.3999

Brodeur, S. R., Angelini, F., Bacharier, L. B., Blom, A. M., Mizoguchi, E., Fujiwara, H., Geha, R. S. (2003). C4b-binding protein (C4BP) activates B cells through the CD40 receptor. *Immunity*, *18*(6), 837–848. http://www.ncbi.nlm.nih.gov/pubmed/12818164

Brodsky, R. A., Young, N. S., Antonioli, E., Risitano, A. M., Schrezenmeier, H., Schubert, J., Hillmen, P. (2008). Multicenter phase 3 study of the complement inhibitor eculizumab for the treatment of patients with paroxysmal nocturnal hemoglobinuria. *Blood*, *111*(4), 1840–1847. https://doi.org/10.1182/blood-2007-06-094136

Bruce, M. A., Hall, S. D., Haehner-Daniels, B. D., & Gorski, J. C. (2001). In vivo effect of clarithromycin on multiple cytochrome P450s. Drug Metabolism and Disposition: The Biological Fate of Chemicals, 29(7), 1023–1028. http://www.ncbi.nlm.nih.gov/pubmed/11408369

Budding, K., Van De Graaf, E. A., Kardol-Hoefnagel, T., Kwakkel-Van Erp, J. M., Luijk, B. D., Oudijk, E. J. D., Otten, H. G. (2016). Soluble CD59 is a Novel Biomarker for the Prediction of Obstructive Chronic Lung Allograft Dysfunction after Lung Transplantation. *Scientific Reports*, *6*. https://doi.org/10.1038/srep26274

Buddles, M. R. H., Donne, R. L., Richards, A., Goodship, J., & Goodship, T. H. J. (2000). Complement Factor H Gene Mutation Associated with Autosomal Recessive Atypical Hemolytic Uremic Syndrome. *The American Journal of Human Genetics*, *66*(5), 1721–1722. https://doi.org/10.1086/302877

Bunggulawa, E. J., Wang, W., Yin, T., Wang, N., Durkan, C., Wang, Y., & Wang, G. (2018, October 16). Recent advancements in the use of exosomes as drug delivery systems 06 Biological Sciences 0601 Biochemistry and Cell Biology. *Journal of Nanobiotechnology*. BioMed Central Ltd. https://doi.org/10.1186/s12951-018-0403-9

Burgess, R. R. (2009). Protein precipitation techniques. *Methods in Enzymology*, *463*, 331–342. https://doi.org/10.1016/S0076-6879(09)63020-2

Cain, S. A., & Monk, P. N. (2002). The orphan receptor C5L2 has high affinity binding sites for complement fragments C5a and C5a des-Arg74. *Journal of Biological Chemistry*, *277*(9), 7165–7169. https://doi.org/10.1074/jbc.C100714200

Campbell, W., Okada, N., & Okada, H. (2001). Carboxypeptidase R is an inactivator of complement-derived inflammatory peptides and an inhibitor of fibrinolysis. *Immunological Reviews*, *180*, 162–167. http://www.ncbi.nlm.nih.gov/pubmed/11414358

Caprioli, J., Bettinaglio, P., Zipfel, P. F., Amadei, B., Daina, E., Gamba, S., Itaslian Registry of Familial and Recurrent HUS/TTP. (2001). The molecular basis of familial hemolytic uremic syndrome: mutation analysis of factor H gene reveals a hot spot in short consensus repeat 20. *Journal of the American Society of Nephrology : JASN*, *12*(2), 297–307. http://www.ncbi.nlm.nih.gov/pubmed/11158219

Carroll, M. C., & Isenman, D. E. (2012). Regulation of Humoral Immunity by Complement. *Immunity*, 37(2):199-207. https://doi.org/10.1016/j.immuni.2012.08.002

Carpanini, S. M., Torvell, M., & Morgan, B. P. (2019). Therapeutic Inhibition of the Complement System in Diseases of the Central Nervous System. *Frontiers in Immunology*, *10*, 362. https://doi.org/10.3389/fimmu.2019.00362

Carugati, A., Pappalardo, E., Zingale, L. C., & Cicardi, M. (2001). C1-inhibitor deficiency and angioedema. *Molecular Immunology*, *38*(2–3), 161–173. https://doi.org/10.1016/s0161-5890(01)00040-2

Cashman, S. M., Ramo, K., & Kumar-Singh, R. (2011). A non membrane-targeted human soluble CD59 attenuates choroidal neovascularization in a model of age related macular degeneration. *PLoS ONE*, *6*(4). https://doi.org/10.1371/journal.pone.0019078

Chakravarti, D. N., & Muller-Eberhard, H. J. (1988). Biochemical characterization of the human complement protein C6. Association with alpha-thrombin-like enzyme and absence of serine protease activity in cytolytically active C6. *The Journal of Biological Chemistry*, *263*(34), 18306–18312. http://www.ncbi.nlm.nih.gov/pubmed/3192535

Chamberlain-Banoub, J., Neal, J. W., Mizuno, M., Harris, C. L., & Morgan, B. P. (2006). Complement membrane attack is required for endplate damage and clinical disease in passive experimental myasthenia gravis in Lewis rats. *Clinical and Experimental Immunology*, *146*(2), 278–286. https://doi.org/10.1111/j.1365-2249.2006.03198.x

Charvet, B., Reynaud, J. M., Gourru-Lesimple, G., Perron, H., Marche, P. N., & Horvat, B. (2018). Induction of Proinflammatory Multiple Sclerosis-Associated Retrovirus Envelope Protein by Human Herpesvirus-6A and CD46 Receptor Engagement. *Frontiers in Immunology*, *9*, 2803. https://doi.org/10.3389/fimmu.2018.02803

Chaudhury, C., Mehnaz, S., Robinson, J. M., Hayton, W. L., Pearl, D. K., Roopenian, D. C., & Anderson, C. L. (2003). The major histocompatibility complex-related Fc receptor for IgG (FcRn) binds albumin and prolongs its lifespan. *Journal of Experimental Medicine*, *197*(3), 315–322. https://doi.org/10.1084/jem.20021829

Chauhan, A. K., & Moore, T. L. (2011). T cell activation by terminal complex of complement and immune complexes. *Journal of Biological Chemistry*, *286*(44), 38627–38637. https://doi.org/10.1074/jbc.M111.266809

Chen, R., Ning, G., Zhao, M. L., Fleming, M. G., Diaz, L. A., Werb, Z., & Liu, Z. (2001). Mast cells play a key role in neutrophil recruitment in experimental bullous pemphigoid. *Journal of Clinical Investigation*, *108*(8), 1151–1158. https://doi.org/10.1172/JCI11494

Chen, M., Jayne, D. R. W., & Zhao, M. H. (2017). Complement in ANCA-associated vasculitis: Mechanisms and implications for management. *Nature Reviews Nephrology*, 13(6):359-367. https://doi.org/10.1038/nrneph.2017.37

Cho, Y. S., Do, M. H., Kwon, S. Y., Moon, C., Kim, K., Lee, K., Jung, C. (2016). Efficacy of CD46-targeting chimeric Ad5/35 adenoviral gene therapy for colorectal cancers. *Oncotarget*, *7*(25), 38210–38223. https://doi.org/10.18632/oncotarget.9427

Choi N. H., Mazda T., & Tomita M. (1989). A serum protein SP40,40 modulates the formation of membrane attack complex of complement on erythrocytes. *Molecular Immunology*, *26*(9), 835–840. https://doi.org/10.1016/0161-5890(89)90139-9

Choi, N. ho, Nakano, Y., Tobe, T., Mazda, T., & Tomita, M. (1990). Incorporation of SP-40,40 into the solyble membrance attack complex(SMAC, SC5b-9) of complement. *International Immunology*, *2*(5), 413–417. https://doi.org/10.1093/intimm/2.5.413

Cianflone, K. M., Sniderman, A. D., Walsh, M. J., Vu, H. T., Gagnon, J., & Rodriguez, M. A. (1989). Purification and characterization of acylation stimulating protein. *The Journal of Biological Chemistry*, *264*(1), 426–430. http://www.ncbi.nlm.nih.gov/pubmed/2909530

Cicardi, M., & Zanichelli, A. (2010). Replacement therapy with C1 esterase inhibitors for hereditary angioedema. *Drugs of Today*, 46(11):867-74 https://doi.org/10.1358/dot.2010.46.11.1534012

Clark, C., Thai, C. T., Phelan, M. M., Bella, J., Uhrín, D., Ogata, R. T., Bramham, J. (2013). 1H, 13C and 15N resonance assignments of the complement control protein modules of the complement component C7. *Biomolecular NMR Assignments*, *7*(2), 285–288. https://doi.org/10.1007/s12104-012-9429-3

Cadham, F. T. (1926). Complement in Health and in Disease. *Canadian Medical Association Journal*, *16*(4), 352–358. http://www.ncbi.nlm.nih.gov/pubmed/20315728

Colomb, M. G., Arlaud, G. J., & Villiers, C. L. (1984). Activation of C1. *Philosophical Transactions of the Royal Society of London, 306(1129):283-92.* https://doi.org/10.1098/rstb.1984.0089

Compston, D. A. S., Morgan, B. P., Oleesky, D., Fifield, R., & Campbell, A. K. (1986). Cerebrospinal fluid C9 in demyelinating disease. *Neurology*, *36*(11), 1503–1503. https://doi.org/10.1212/WNL.36.11.1503

Connell, N. T. (2019). Ravulizumab: A complementary option for PNH. *Blood*, 133(6):503-504 https://doi.org/10.1182/blood-2018-12-891499

Cooper, N. R., Jensen, F. C., Welsh, R. M., & Oldstone, M. B. A. (1976). Lysis of RNA tumor viruses by human serum: Direct antibody-independent triggering of the classical complement pathway. *Journal of Experimental Medicine*, *144*(4), 970–984. https://doi.org/10.1084/jem.144.4.970

Copland, D. A., Hussain, K., Baalasubramanian, S., Hughes, T. R., Morgan, B. P., Xu, H., Nicholson, L. B. (2010). Systemic and local anti-C5 therapy reduces the disease severity in experimental autoimmune uveoretinitis. *Clinical and Experimental Immunology*, *159*(3), 303–314. https://doi.org/10.1111/j.1365-2249.2009.04070.x

Coulthard, L. G., & Woodruff, T. M. (2015). Is the Complement Activation Product C3a a Proinflammatory Molecule? Re-evaluating the Evidence and the Myth. *The Journal of Immunology*, *194*(8), 3542–3548. https://doi.org/10.4049/jimmunol.1403068

Csuka, D., Veszeli, N., Varga, L., Prohászka, Z., & Farkas, H. (2017). The role of the complement system in hereditary angioedema. *Molecular Immunology*, 89:59-68. https://doi.org/10.1016/j.molimm.2017.05.020

Cudrici, C., Niculescu, F., Jensen, T., Zafranskaia, E., Fosbrink, M., Rus, V., Rus, H. (2006). C5b-9 Terminal Complex Protects Oligodendrocytes from Apoptotic Cell Death by

Inhibiting Caspase-8 Processing and Up-Regulating FLIP. *The Journal of Immunology*, *176*(5), 3173–3180. https://doi.org/10.4049/jimmunol.176.5.3173

Czermak, B. J., Sarma, V., Pierson, C. L., Warner, R. L., Huber-Lang, M., Bless, N. M., Ward, P. A. (1999). Protective effects of C5a blockade in sepsis. *Nature Medicine*, *5*(7), 788–792. https://doi.org/10.1038/10512

Daha, M. R., & van Kooten, C. (2016). Role of complement in IgA nephropathy. *Journal of Nephrology*, 29(1):1-4. https://doi.org/10.1007/s40620-015-0245-6

Dahl, M. R., Thiel, S., Matsushita, M., Fujita, T., Willis, A. C., Christensen, T., Jensenius, J. C. (2001). MASP-3 and its association with distinct complexes of the mannan-binding lectin complement activation pathway. *Immunity*, *15*(1), 127–135. http://www.ncbi.nlm.nih.gov/pubmed/11485744

Dalmasso, A. P. (1996). The complement system in xenotransplantation. *Immunopharmacology*, *24*(2), 149–160. http://www.ncbi.nlm.nih.gov/pubmed/1473965

Dalrymple, A., Wild, E. J., Joubert, R., Sathasivam, K., Björkqvist, M., Petersén, Å., Tabrizi, S. J. (2007). Proteomic profiling of plasma in Huntington's disease reveals neuroinflammatory activation and biomarker candidates. *Journal of Proteome Research*, *6*(7), 2833–2840. https://doi.org/10.1021/pr0700753

Davidson, A. I., Halstead, S. K., Goodfellow, J. A., Chavada, G., Mallik, A., Overell, J., Willison, H. J. (2017). Inhibition of complement in Guillain-Barré syndrome: the ICA-GBS study. *Journal of the Peripheral Nervous System*, *22*(1), 4–12. https://doi.org/10.1111/jns.12194

Deckert, M., Kubar, J., Zoccola, D., Bernard-Pomier, G., Angelisova, P., Horejsi, V., & Bernard, A. (1992). CD59 molecule: A second ligand for CD2 in T cell adhesion. *European Journal of Immunology*, *22*(11), 2943–2947. https://doi.org/10.1002/eji.1830221128

Douzi, B. (2017). Protein-Protein Interactions: Surface Plasmon Resonance. *Methods in Molecular Biology (Clifton, N.J.)*, *1615*, 257–275. https://doi.org/10.1007/978-1-4939-7033-9_21

Degn, S. E., Jensenius, J. C., & Thiel, S. (2013). Response to Comment on "Mannan-Binding Lectin-Associated Serine Protease (MASP)-1 Is Crucial for Lectin Pathway Activation in Human Serum, whereas neither MASP-1 nor MASP-3 Is Required for Alternative Pathway Function." *The Journal of Immunology*, 190(6):2477-8. https://doi.org/10.4049/jimmunol.1390003

De Jorge, E. G., Tortajada, A., García, S. P., Gastoldi, S., Merinero, H. M., García-Fernández, J., De Córdoba, S. R. (2018). Factor H competitor generated by gene conversion events associates with atypical hemolytic uremic syndrome. *Journal of the American Society of Nephrology*, *29*(1), 240–249. https://doi.org/10.1681/ASN.2017050518

De Latour, R. P., Fremeaux-Bacchi, V., Porcher, R., Xhaard, A., Rosain, J., Castaneda, D. C., Socié, G. (2015). Assessing complement blockade in patients with paroxysmal

nocturnal hemoglobinuria receiving eculizumab. *Blood*, *125*(5), 775–783. https://doi.org/10.1182/blood-2014-03-560540

Dempsey, P. W., Allison, M. E., Akkaraju, S., Goodnow, C. C., & Fearon, D. T. (1996). C3d of complement as a molecular adjuvant: bridging innate and acquired immunity. *Science (New York, N.Y.)*, *271*(5247), 348–350. https://doi.org/10.1126/science.271.5247.348

Deng, R., Jin, F., Prabhu, S., & Iyer, S. (2012). Monoclonal antibodies: What are the pharmacokinetic and pharmacodynamic considerations for drug development? *Expert Opinion on Drug Metabolism and Toxicology*, 8(2):141-60. https://doi.org/10.1517/17425255.2012.643868

Dessauer, A., & Rother, U. (1983). The fifth component of complement (C5): purification without activation. *Immunobiology*, *164*(5), 370–379. https://doi.org/10.1016/S0171-2985(83)80033-3

Dhillon, S. (2018). Eculizumab: A Review in Generalized Myasthenia Gravis. *Drugs*, *78*(3), 367–376. https://doi.org/10.1007/s40265-018-0875-9

DiScipio, R. G. (1992). Formation and structure of the C5b-7 complex of the lytic pathway of complement. *The Journal of Biological Chemistry*, *267*(24), 17087–17094. http://www.ncbi.nlm.nih.gov/pubmed/1387399

DiScipio, R. G., Chakravarti, D. N., Muller-Eberhard, H. J., & Fey, G. H. (1988). The structure of human complement component C7 and the C5b-7 complex. *The Journal of Biological Chemistry*, *263*(1), 549–560. http://www.ncbi.nlm.nih.gov/pubmed/3335508

Discipio, R. G., & Sweeney, S. P. (1994). The Fractionation of Human Plasma Proteins. II. The Purification of Human Complement Proteins C3, C3u, and C5 by Application of Affinity Chromatography. *Protein Expression and Purification*, *5*(2), 170–177. https://doi.org/10.1006/prep.1994.1027

DiScipio, R. G., Smith, C. A., Muller-Eberhard, H. J., & Hugli, T. E. (1983). The activation of human complement component C5 by a fluid phase C5 convertase. *The Journal of Biological Chemistry*, *258*(17), 10629–10636. http://www.ncbi.nlm.nih.gov/pubmed/6554279

Dodds, A. W., Ren, X. D., Willis, A. C., & Law, S. K. A. (1996). The reaction mechanism of the internal thioester in the human complement component C4. *Nature*, *379*(6561), 177–179. https://doi.org/10.1038/379177a0

Donoso, L. A., Kim, D., Frost, A., Callahan, A., & Hageman, G. (2006). The role of inflammation in the pathogenesis of age-related macular degeneration. *Survey of Ophthalmology*, *51*(2), 137–152. https://doi.org/10.1016/j.survophthal.2005.12.001

Dong, M., Xu, S., Oliveira, C. L. P., Pedersen, J. S., Thiel, S., Besenbacher, F., & Vorup-Jensen, T. (2007). Conformational Changes in Mannan-Binding Lectin Bound to Ligand Surfaces. *The Journal of Immunology*, *178*(5), 3016–3022. https://doi.org/10.4049/jimmunol.178.5.3016

Dörig, R. E., Marcil, A., Chopra, A., & Richardson, C. D. (1993). The human CD46 molecule is a receptor for measles virus (Edmonston strain). *Cell*, *75*(2), 295–305. https://doi.org/10.1016/0092-8674(93)80071-l

Doroshyenko, O., Rokitta, D., Zadoyan, G., Klement, S., Schläfke, S., Dienel, A., Fuhr, U. (2013). Drug cocktail interaction study on the effect of the orally administered lavender oil preparation silexan on cytochrome p450 enzymes in healthy volunteers. *Drug Metabolism and Disposition*, *41*(5), 987–993. https://doi.org/10.1124/dmd.112.050203

Dudkina, N. V., Spicer, B. A., Reboul, C. F., Conroy, P. J., Lukoyanova, N., Elmlund, H., Dunstone, M. A. (2016). Structure of the poly-C9 component of the complement membrane attack complex. *Nature Communications*, 7:10588. https://doi.org/10.1038/ncomms10588

Ebenbichler, C. F., Thielens, N. M., Vornhagen, R., Marschang, P., Arlaud, G. J., & Dierich, M. P. (1991). Human hnmtmodeficiency virus type 1 activates the classical pathway of complement by direct C1 binding through specific sites in the transmembrane glycoprotein gp41. *Journal of Experimental Medicine*, *174*(6), 1417–1424. https://doi.org/10.1084/jem.174.6.1417

Edwards, A. O., Ritter, R., Abel, K. J., Manning, A., Panhuysen, C., & Farrer, L. A. (2005). Complement factor H polymorphism and age-related macular degeneratioEdwards, A. O., Ritter, R., Abel, K. J., Manning, A., Panhuysen, C., & Farrer, L. A. (2005). Complement factor H polymorphism and age-related macular degeneration. Science, 308(5720), 421. *Science*, *308*(5720), 421–424. https://doi.org/10.1126/science.1110189

Endo, Y., Takahashi, M., & Fujita, T. (2006). Lectin complement system and pattern recognition. *Immunobiology*, 211(4):283-93. https://doi.org/10.1016/j.imbio.2006.01.003

Endo, Y., Matsushita, M., & Fujita, T. (2015). New Insights into the Role ofFicolins in the Lectin Pathway of Innate Immunity. *International Review of Cell and Molecular Biology*, *316*, 49–110. https://doi.org/10.1016/bs.ircmb.2015.01.003

Elvin, J. G., Couston, R. G., & Van Der Walle, C. F. (2013). Therapeutic antibodies: Market considerations, disease targets and bioprocessing. *International Journal of Pharmaceutics*, *440*(1), 83–98. https://doi.org/10.1016/j.ijpharm.2011.12.039

Ember, J. A., Sanderson, S. D., Taylor, S. M., Kawahara, M., & Hugli, T. E. (1992). Biologic activity of synthetic analogues of C5a anaphylatoxin. *Journal of Immunology*, *148*(10), 3165–3173. http://www.ncbi.nlm.nih.gov/pubmed/1578141

Espinosa, M., Ortega, R., Sanchez, M., Segarra, A., Salcedo, M. T., Gonzalez, F., Munoz, M. Í. D. (2014). Association of C4d deposition with clinical outcomes in IgA nephropathy. *Clinical Journal of the American Society of Nephrology*, *9*(5), 897–904. https://doi.org/10.2215/CJN.09710913

Falk, R. J., Dalmasso, A. P., Kim, Y., Tsai, C. H., Scheinman, J. I., Gewurz, H., & Michael, A. F. (1983). Neoantigen of the polymerized ninth component of complement. Characterization of a monoclonal antibody and immunohistochemical localization in renal disease. *Journal of Clinical Investigation*, *72*(2), 560–573. https://doi.org/10.1172/JCI111004

Falk, R. J., Podack, E., Dalmasso, A. P., & Jennette, J. C. (1987). Localization of S protein and its relationship to the membrane attack complex of complement in renal tissue. *The American Journal of Pathology*, *127*(1), 182–190. http://www.ncbi.nlm.nih.gov/pubmed/2952015

Farkas, I., Baranyi, L., Ishikawa, Y., Okada, N., Bohata, C., Budai, D., Okada, H. (2002). CD59 blocks not only the insertion of C9 into MAC but inhibits ion channel formation by homologous C5b-8 as well as C5b-9. *Journal of Physiology*, *539*(2), 537–545. https://doi.org/10.1113/jphysiol.2001.013381

Farkas, I., Baranyi, L., Takahashi, M., Fukuda, A., Liposits, Z., Yamamoto, T., & Okada, H. (1998). A neuronal C5a receptor and an associated apoptotic signal transduction pathway. *Journal of Physiology*, *507*(3), 679–687. https://doi.org/10.1111/j.1469-7793.1998.679bs.x

Farrar, C. A., Zhou, W., Lin, T., & Sacks, S. H. (2006). Local extravascular pool of C3 is a determinant of postischemic acute renal failure. *FASEB Journal*, *20*(2), 217–226. https://doi.org/10.1096/fj.05-4747com

Farrar, C. A., Tran, D., Li, K., Wu, W., Peng, Q., Schwaeble, W., Sacks, S. H. (2016). Collectin-11 detects stress-induced L-fucose pattern to trigger renal epithelial injury. *Journal of Clinical Investigation*, *126*(5), 1911–1925. https://doi.org/10.1172/JCI83000

Fearon, D. T., & Austen, K. F. (1975). Properdin: binding to C3b and stabilization of the C3b dependent C3 convertase. *Journal of Experimental Medicine*, *142*(4), 856–863. https://doi.org/10.1084/jem.142.4.856

Fearon, D. T. (1998). The complement system and adaptive immunity. *Seminars in Immunology*, *10*(5), 355–361. https://doi.org/10.1006/smim.1998.0137

Fearon, D. T., Carroll, M. C., & Carroll, M. C. (2000). Regulation of B Lymphocyte Responses to Foreign and Self-Antigens by the CD19/CD21 Complex. *Annual Review of Immunology*, *18*(1), 393–422. https://doi.org/10.1146/annurev.immunol.18.1.393

Fernie-King, B. A., Seilly, D. J., Willers, C., Würzner, R., Davies, A., & Lachmann, P. J. (2001). Streptococcal inhibitor of complement (SIC) inhibits the membrane attack complex by preventing uptake of C567 onto cell membranes. *Immunology*, *103*(3), 390–398. https://doi.org/10.1046/j.1365-2567.2001.01249.x

Ferrara, N., Damico, L., Shams, N., Lowman, H., & Kim, R. (2006). Development of ranibizumab, an anti-vascular endothelial growth factor antigen binding fragment, as therapy for neovascular age-related macular degeneration. *Retina*, 26(8):859-70. https://doi.org/10.1097/01.iae.0000242842.14624.e7

Fiane, A. E., Mollnes, T. E., Videm, V., Hovig, T., Høgåsen, K., Mellbye, O. J., Lambris, J. D. (1999). Compstatin, a peptide inhibitor of C3, prolongs survival of ex vivo perfused pig xenografts. *Xenotransplantation*, *6*(1), 52–65. http://www.ncbi.nlm.nih.gov/pubmed/10355733

Fick, R. B., Robbins, R. A., Squier, S. U., Schoderbek, W. E., & Russ, W. D. (1986). Complement activation in cystic fibrosis respiratory fluids: In vivo and in vitro generation of C5a and chemotactic activity. *Pediatric Research*, *20*(12), 1258–1268. https://doi.org/10.1203/00006450-198612000-00014

Fishelson, Z., Attali, G., & Mevorach, D. (2001). Complement and apoptosis. *Molecular Immunology*, *38*(2–3), 207–219. https://doi.org/10.1016/s0161-5890(01)00055-4

Fishelson, Z., Donin, N., Zell, S., Schultz, S., & Kirschfink, M. (2003). Obstacles to cancer immunotherapy: Expression of membrane complement regulatory proteins (mCRPs) in tumors. In *Molecular Immunology*, 40(2-4):109-23. https://doi.org/10.1016/S0161-5890(03)00112-3

Flexner, S., & Noguchi, H. (1902). Snake venom in relation to hÆmolysis, bacteriolysis, and toxicity. *Journal of Experimental Medicine*, *6*(3), 277–302. https://doi.org/10.1084/jem.6.3.277

Flückiger, R., Cocuzzi, E., Nagaraj, R. H., Shoham, M., Kern, T. S., & Medof, M. E. (2018). DAF in diabetic patients is subject to glycation/inactivation at its active site residues. *Molecular Immunology*, *93*, 246–252. https://doi.org/10.1016/j.molimm.2017.06.036

Foley, J. H., Walton, B. L., Aleman, M. M., O'Byrne, A. M., Lei, V., Harrasser, M., Conway, E. M. (2016). Complement Activation in Arterial and Venous Thrombosis is Mediated by Plasmin. *EBioMedicine*, *5*, 175–182. https://doi.org/10.1016/j.ebiom.2016.02.011

Foltyn Zadura, A., Zipfel, P. F., Bokarewa, M. I., Sturfelt, G., Jönsen, A., Nilsson, S. C., Blom, A. M. (2012). Factor H autoantibodies and deletion of Complement Factor H-Related protein-1 in rheumatic diseases in comparison to atypical hemolytic uremic syndrome. *Arthritis Research and Therapy*, 14(4):R185. https://doi.org/10.1186/ar4016

Fonsatti, E., Altomonte, M., Coral, S., De Nardo, C., Lamaj, E., Sigalotti, L., Maio, M. (2000). Emerging role of protectin (CD59) in humoral immunotherapy of solid malignancies. *La Clinica Terapeutica*, *151*(3), 187–193. http://www.ncbi.nlm.nih.gov/pubmed/10958054

Fonseca, M. I., Ager, R. R., Chu, S.-H., Yazan, O., Sanderson, S. D., LaFerla, F. M., Tenner, A. J. (2009). Treatment with a C5aR Antagonist Decreases Pathology and Enhances Behavioral Performance in Murine Models of Alzheimer's Disease. *The Journal of Immunology*, *183*(2), 1375–1383. https://doi.org/10.4049/jimmunol.0901005

Forneris, F., Ricklin, D., Wu, J., Tzekou, A., Wallace, R. S., Lambris, J. D., & Gros, P. (2010). Structures of C3b in complex with factors B and D give insight into complement convertase formation. *Science*, *330*(6012), 1816–1820. https://doi.org/10.1126/science.1195821

Fosbrink, M., Niculescu, F., Rus, V., Shin, M. L., & Rus, H. (2006). C5b-9-induced endothelial cell proliferation and migration are dependent on Akt inactivation of forkhead transcription factor FOXO1. *Journal of Biological Chemistry*, *281*(28), 19009–19018. https://doi.org/10.1074/jbc.M602055200

Frei, Y., Lambris, J. D., & Stockinger, B. (1987). Generation of a monoclonal antibody to mouse C5 application in an ELISA assay for detection of anti-C5 antibodies. *Molecular and Cellular Probes*, *1*(2), 141–149. http://www.ncbi.nlm.nih.gov/pubmed/3453897

Friedman, D. S., O'Colmain, B. J., Muñoz, B., Tomany, S. C., McCarty, C., DeJong, P. T. V. M., Congdon, N. (2004). Prevalence of Age-Related Macular Degeneration in the United States. *Archives of Ophthalmology*, *122*(4), 564–572. https://doi.org/10.1001/archopht.122.4.564

Fukuzawa, T., Sampei, Z., Haraya, K., Ruike, Y., Shida-Kawazoe, M., Shimizu, Y., Nezu, J. (2017). Long lasting neutralization of C5 by SKY59, a novel recycling antibody, is a potential therapy for complement-mediated diseases. *Scientific Reports*, 7(1):1080. https://doi.org/10.1038/s41598-017-01087-7

Furtado, P. B., Huang, C. Y., Ihyembe, D., Hammond, R. A., Marsh, H. C., & Perkins, S. J. (2008). The Partly Folded Back Solution Structure Arrangement of the 30 SCR Domains in Human Complement Receptor Type 1 (CR1) Permits Access to its C3b and C4b Ligands. *Journal of Molecular Biology*, *375*(1), 102–118. https://doi.org/10.1016/j.jmb.2007.09.085

Gaggar, A., Shayakhmetov, D., & Lieber, A. (2007). Identifying functional adenovirus-host interactions using tandem mass spectrometry. *Methods in Molecular Medicine*, *131*, 141–155. http://www.ncbi.nlm.nih.gov/pubmed/17656781

Garcia, B. L., Zwarthoff, S. A., Rooijakkers, S. H. M., & Geisbrecht, B. V. (2016). Novel Evasion Mechanisms of the Classical Complement Pathway. *The Journal of Immunology*, *197*(6), 2051–2060. https://doi.org/10.4049/jimmunol.1600863

Garred, P., Larsen, F., Madsen, H. O., & Koch, C. (2003). Mannose-binding lectin deficiency--revisited. *Molecular Immunology*, *40*(2–4), 73–84. http://www.ncbi.nlm.nih.gov/pubmed/12914814

Garred, P., Genster, N., Pilely, K., Bayarri-Olmos, R., Rosbjerg, A., Ma, Y. J., & Skjoedt, M. O. (2016). A journey through the lectin pathway of complement—MBL and beyond. *Immunological Reviews*, 274(1):74-97. https://doi.org/10.1111/imr.12468

Geleijns, K., Roos, A., Houwing-Duistermaat, J. J., van Rijs, W., Tio-Gillen, A. P., Laman, J. D., Jacobs, B. C. (2006). Mannose-Binding Lectin Contributes to the Severity of Guillain-Barré Syndrome. *The Journal of Immunology*, *177*(6), 4211–4217. https://doi.org/10.4049/jimmunol.177.6.4211

Gharavi, A. G., Kiryluk, K., Choi, M., Li, Y., Hou, P., Xie, J., Lifton, R. P. (2011). Genome-wide association study identifies susceptibility loci for IgA nephropathy. *Nature Genetics*, *43*(4), 321–329. https://doi.org/10.1038/ng.787

Gharibi, S., Moghimi, B., Haghmorad, D., Mahmoudi, M. B., Shahvazian, E., Yadegari, M., Tahoori, M. T. (2019). Altered expression patterns of complement factor H and miR-146a genes in acute-chronic phases in experimental autoimmune encephalomyelitis mouse. *Journal of Cellular Physiology*, *234*(11), 19842–19851. https://doi.org/10.1002/jcp.28583

Giles, J. L., Choy, E., van den Berg, C., Morgan, B. P., & Harris, C. L. (2015). Functional analysis of a complement polymorphism (rs17611) associated with rheumatoid arthritis. *Journal of Immunology,* *194*(7), 3029–3034. https://doi.org/10.4049/jimmunol.1402956

Gigli, I., Fujita, T., & Nussenzweig, V. (1979). Modulation of the classical pathway C3 convertase by plasma proteins C4 binding protein and C3b inactivator. *Proceedings of the National Academy of Sciences of the United States of America*, 76(12):6596-600. https://doi.org/10.1073/pnas.76.12.6596

Girardi, G., Berman, J., Redecha, P., Spruce, L., Thurman, J. M., Kraus, D., Salmon, J. E. (2003). Complement C5a receptors and neutrophils mediate fetal injury in the

antiphospholipid syndrome. *Journal of Clinical Investigation*, *112*(11), 1644–1654. https://doi.org/10.1172/JCI18817

Goicoechea De Jorge, E., Caesar, J. J. E., Malik, T. H., Patel, M., Colledge, M., Johnson, S., Lea, S. M. (2013). Dimerization of complement factor H-related proteins modulates complement activation in vivo. *Proceedings of the National Academy of Sciences of the United States of America*, *110*(12), 4685–4690. https://doi.org/10.1073/pnas.1219260110

Gotze, O., & Muller-Eberhard, H. J. (1970). Lysis of erythrocytes by complement in the absence of antibody. *J Exp Med*, *132*(5), 898–915. http://www.ncbi.nlm.nih.gov/entrez/query.fcgi?cmd=Retrieve&db=PubMed&dopt=Citation&list_uids=5470509

Gower, R. G., Busse, P. J., Aygören-Pürsün, E., Barakat, A. J., Caballero, T., Davis-Lorton, M., Maurer, M. (2011). Hereditary Angioedema Caused By C1-Esterase Inhibitor Deficiency: A Literature-Based Analysis and Clinical Commentary on Prophylaxis Treatment Strategies. *World Allergy Organization Journal*, 4(2 Suppl):S9-S21. https://doi.org/10.1097/WOX.0b013e31821359a2

Graveland, G. A., Williams, R. S., & Difiglia, M. (1985). Evidence for degenerative and regenerative changes in neostriatal spiny neurons in Huntington's disease. *Science*, *227*(4688), 770–773. https://doi.org/10.1126/science.3155875

Gregory, L. A., Thielens, N. M., Arlaud, G. J., Fontecilla-Camps, J. C., & Gaboriaud, C. (2003). X-ray structure of the Ca2+-binding interaction domain of C1s. Insights into the assembly of the C1 complex of complement. *Journal of Biological Chemistry*, *278*(34), 32157–32164. https://doi.org/10.1074/jbc.M305175200

Griffin, J. W., Li, C. Y., Ho, T. W., Tian, M., Gao, C. Y., Xue, P., Asbury, A. K. (1996). Pathology of the motor-sensory axonal guillain-barré syndrome. *Annals of Neurology*, *39*(1), 17–28. https://doi.org/10.1002/ana.410390105

Grumach, A. S., & Kirschfink, M. (2014). Are complement deficiencies really rare? Overview on prevalence, clinical importance and modern diagnostic approach. *Molecular Immunology*, 61(2):110-7. https://doi.org/10.1016/j.molimm.2014.06.030

Hadders, M., A., Bubeck, D., Roversi, P., Hakobyan, S., Forneris, F., Morgan, B. P., Gros, P. (2012). Assembly and Regulation of the Membrane Attack Complex Based on Structures of C5b6 and sC5b9. *Cell Reports*, *1*(3), 200–207. https://doi.org/10.1016/j.celrep.2012.02.003

Hafer-Macko, C. E., Sheikh, K. A., Li, C. Y., Ho, T. W., Cornblath, D. R., McKhann, G. M., Griffin, J. W. (1996). Immune attack on the Schwann cell surface in acute inflammatory demyelinating polyneuropathy. *Annals of Neurology*, *39*(5), 625–635. https://doi.org/10.1002/ana.410390512

Hageman, G. S., Anderson, D. H., Johnson, L. V., Hancox, L. S., Taiber, A. J., Hardisty, L. I., Allikmets, R. (2005). A common haplotype in the complement regulatory gene factor H (HF1/CFH) predisposes individuals to age-related macular degeneration. *Proceedings of the National Academy of Sciences of the United States of America*, *102*(20), 7227–7232. https://doi.org/10.1073/pnas.0501536102

Hahn, W. C., Menu, E., Bothwell, A. L. M., Sims, P. J., & Bierer, B. E. (1992). Overlapping but nonidentical binding sites on CD2 for CD58 and a second ligand CD59. *Science*, *256*(5065), 1805–1807. https://doi.org/10.1126/science.1377404

Haihua, C., Wei, W., Kun, H., Yuanli, L., & Fei, L. (2018). Cobra Venom Factor-induced complement depletion protects against lung ischemia reperfusion injury through alleviating blood-air barrier damage. *Scientific Reports*, 8(1):10346. https://doi.org/10.1038/s41598-018-28724-z

Haines, J. L., Hauser, M. A., Schmidt, S., Scott, W. K., Olson, L. M., Gallins, P., Pericak-Vance, M. A. (2005). Complement factor H variant increases the risk of age-related macular degeneration. *Science*, *308*(5720), 419–421. https://doi.org/10.1126/science.1110359

Hakobyan, S., Harding, K., Aiyaz, M., Hye, A., Dobson, R., Baird, A., Morgan, B. P. (2016). Complement Biomarkers as Predictors of Disease Progression in Alzheimer's Disease. *Journal of Alzheimer's Disease : JAD*, *54*(2), 707–716. https://doi.org/10.3233/JAD-160420

Hakobyan, S., Luppe, S., Evans, D. R., Harding, K., Loveless, S., Robertson, N. P., & Morgan, B. P. (2017). Plasma complement biomarkers distinguish multiple sclerosis and neuromyelitis optica spectrum disorder. *Multiple Sclerosis*, *23*(7), 946–955. https://doi.org/10.1177/1352458516669002

Hall, C., Richards, S. J., & Hillmen, P. (2002). The glycosylphosphatidylinositol anchor and paroxysmal nocturnal haemoglobinuria/aplasia model. *Acta Haematologica*, *108*(4), 219–230. https://doi.org/10.1159/000065658

Hakulinen, J., & Meri, S. (1995). Shedding and enrichment of the glycolipid-anchored complement lysis inhibitor protectin (CD59) into milk fat globules. *Immunology*, *85*(3), 495–501. http://www.ncbi.nlm.nih.gov/pubmed/7558140

Hallström, T., Uhde, M., Singh, B., Skerka, C., Riesbeck, K., & Zipfel, P. F. (2015). Pseudomonas aeruginosa uses Dihydrolipoamide dehydrogenase (Lpd) to bind to the human terminal pathway regulators vitronectin and clusterin to inhibit terminal pathway complement attack. *PLoS ONE*, 10(9):e0137630. https://doi.org/10.1371/journal.pone.0137630

Hamann, J., Vogel, B., Van Schijndel, G. M. W., & Van Lier, R. A. W. (1996). The seven-span transmembrane receptor CD97 has a cellular ligand (CD55, DAF). *Journal of Experimental Medicine*, *184*(3), 1185–1189. https://doi.org/10.1084/jem.184.3.1185

Hamann, J., Stortelers, C., Kiss-Toth, E., Vogel, B., Eichler, W., & Van Lier, R. A. W. (1998). Characterization of the CD55 (DAF)-binding site on the seven-span transmembrane receptor CD97. *European Journal of Immunology*, *28*(5), 1701–1707. https://doi.org/10.1002/(SICI)1521-4141(199805)28:05<1701::AID-IMMU1701>3.0.CO;2-2

Hamilton, K. K., Ji, Z., Rollins, S., Stewart, B. H., & Sims, P. J. (1990). Regulatory control of the terminal complement proteins at the surface of human endothelial cells: neutralization of a C5b-9 inhibitor by antibody to CD59. *Blood*, *76*(12), 2572–2577. http://www.ncbi.nlm.nih.gov/pubmed/1702330

Hammerschmidt, D. E., Hudson, L. D., Weaver, L. J., Craddock, P. R., & Jacob, H. S. (1980). Association of complement activation and elevated plasma C5a with adult respiratory distress syndrome. Pathophysiological Relevance and Possible Prognostic Value. *The Lancet*, *315*(8175), 947–949. https://doi.org/10.1016/S0140-6736(80)91403-8

Han, C., & Mayer, C. L. (2015). Prediction of Human Pharmacokineticsfor Protein-Based Biologic Therapeutics. In *Pharmaceutical Sciences Encyclopedia* (pp. 1–16). https://doi.org/10.1002/9780470571224.pse543

Hannan, J. P., Laskowski, J., Thurman, J. M., Hageman, G. S., & Holers, V. M. (2016). Mapping the complement factor H-related protein 1 (CFHR1):C3b/C3d interactions. *PLoS ONE*, 11(11): e0166200. https://doi.org/10.1371/journal.pone.0166200

Hansen, A. S., Bundgaard, B. B., Biltoft, M., Rossen, L. S., & Höllsberg, P. (2017). Divergent tropism of HHV-6AGSand HHV-6BPL1in T cells expressing different CD46 isoform patterns. *Virology*, *502*, 160–170. https://doi.org/10.1016/j.virol.2016.12.027

Harder, M. J., Kuhn, N., Schrezenmeier, H., Höchsmann, B., Von Zabern, I., Weinstock, C., Schmidt, C. Q. (2017). Incomplete inhibition by eculizumab: Mechanistic evidence for residual C5 activity during strong complement activation. *Blood*, *129*(8), 970–980. https://doi.org/10.1182/blood-2016-08-732800

Harder, M. J., Höchsmann, B., Dopler, A., Anliker, M., Weinstock, C., Skerra, A., Schmidt, C. Q. (2019). Different Levels of Incomplete Terminal Pathway Inhibition by Eculizumab and the Clinical Response of PNH Patients. *Frontiers in Immunology*, 10:1639. https://doi.org/10.3389/fimmu.2019.01639

Harris, C. L., Fraser, D. A., & Morgan, B. P. (2002). Tailoring anti-complement therapeutics. In *Biochemical Society Transactions*, 30(Pt 6):1019-26. https://doi.org/10.1042/BST0301019

Harris, C. L., Pettigrew, D. M., Lea, S. M., & Morgan, B. P. (2007). Decay-Accelerating Factor Must Bind Both Components of the Complement Alternative Pathway C3 Convertase to Mediate Efficient Decay. *The Journal of Immunology*, *178*(1), 352–359. https://doi.org/10.4049/jimmunol.178.1.352

Harris, C. L., Pouw, R. B., Kavanagh, D., Sun, R., & Ricklin, D. (2018). Developments in anti-complement therapy; from disease to clinical trial. *Molecular Immunology*, *102*, 89–119. https://doi.org/10.1016/j.molimm.2018.06.008

Harris, C. L. (2018). Expanding horizons in complement drug discovery: challenges and emerging strategies. *Seminars in Immunopathology*, 40(1):125-140.

Harris, C. L., Heurich, M., Cordoba, S. R. de, & Morgan, B. P. (2012). The complotype: Dictating risk for inflammation and infection. *Trends in Immunology*, 33(10):513-21 .https://doi.org/10.1016/j.it.2012.06.001

Harrison, R. A. (2018). The properdin pathway: an “alternative activation pathway” or a “critical amplification loop” for C3 and C5 activation? *Seminars in Immunopathology*, 40(1):15-35. https://doi.org/10.1007/s00281-017-0661-x

Hartung, H.-P., Schwenke, C., Bitter-Suermann, D., & Toyka, K. V. (1987). Guillain-barre syndrome: Activated complement components C3a and C5a in CSF. *Neurology*, *37*(6), 1006–1006. https://doi.org/10.1212/WNL.37.6.1006

He, S., Sim, R. B., & Whaley, K. (1998). Mechanism of action of anti-C1-inhibitor autoantibodies: prevention of the formation of stable C1s-C1-inh complexes. *Molecular Medicine*, *4*(2), 119–128. http://www.ncbi.nlm.nih.gov/pubmed/9508789

Heeger, P. S., & Kemper, C. (2012). Novel roles of complement in T effector cell regulation. *Immunobiology*, 217(2):216-24. https://doi.org/10.1016/j.imbio.2011.06.004

Heesterbeek, D. A., Bardoel, B. W., Parsons, E. S., Bennett, I., Ruyken, M., Doorduijn, D. J., Rooijakkers, S. H. (2019). Bacterial killing by complement requires membrane attack complex formation via surface-bound C5 convertases. *The EMBO Journal*, *38*(4). https://doi.org/10.15252/embj.201899852

Héja, D., Kocsis, A., Dobó, J., Szilágyi, K., Szász, R., Závodszky, P., Gál, P. (2012). Revised mechanism of complement lectin-pathway activation revealing the role of serine protease MASP-1 as the exclusive activator of MASP-2. *Proceedings of the National Academy of Sciences of the United States of America*, *109*(26), 10498–10503. https://doi.org/10.1073/pnas.1202588109

Heitzeneder, S., Seidel, M., Förster-Waldl, E., & Heitger, A. (2012). Mannan-binding lectin deficiency - Good news, bad news, doesn't matter? *Clinical Immunology*, 143(1):22-38.https://doi.org/10.1016/j.clim.2011.11.002

Hellstrom-Lindberg, E. (2000). Achievements in Understanding and Treatment of Myelodysplastic Syndromes. *Hematology*, *2000*(1), 110–132. https://doi.org/10.1182/asheducation-2000.1.110

Heurich, M., Martínez-Barricarte, R., Francis, N. J., Roberts, D. L., Rodríguez De Córdoba, S., Morgan, B. P., & Harris, C. L. (2011). Common polymorphisms in C3, factor B, and factor H collaborate to determine systemic complement activity and disease risk. *Proceedings of the National Academy of Sciences of the United States of America*, *108*(21), 8761–8766. https://doi.org/10.1073/pnas.1019338108

Hew, B. E., Wehrhahn, D., Fritzinger, D. C., & Vogel, C. W. (2012). Hybrid proteins of Cobra Venom Factor and cobra C3: Tools to identify functionally important regions in Cobra Venom Factor. *Toxicon*, *60*(4), 632–647. https://doi.org/10.1016/j.toxicon.2012.05.004

Hew, B. E., Fritzinger, D. C., Pangburn, M. K., & Vogel, C. W. (2019). Identification of functionally important amino acid sequences in cobra venom factor using human C3/Cobra venom factor hybrid proteins. *Toxicon*, *167*, 106–116. https://doi.org/10.1016/j.toxicon.2019.06.017

Hill, A., Ridley, S. H., Esser, D., Oldroyd, R. G., Cullen, M. J., Kareclas, P., Hillmen, P. (2006). Protection of erythrocytes from human complement-mediated lysis by membrane-targeted recombinant soluble CD59: A new approach to PNH therapy. *Blood*, *107*(5), 2131–2137. https://doi.org/10.1182/blood-2005-02-0782

Hill, A., DeZern, A. E., Kinoshita, T., & Brodsky, R. A. (2017). Paroxysmal nocturnal haemoglobinuria. *Nature Reviews Disease Primers*, *3*(1), 17028. https://doi.org/10.1038/nrdp.2017.28

Hillmen, P., Hall, C., Marsh, J. C. W., Elebute, M., Bombara, M. P., Petro, B. E., Rother, R. P. (2004). Effect of Eculizumab on Hemolysis and Transfusion Requirements in Patients with Paroxysmal Nocturnal Hemoglobinuria. *New England Journal of Medicine*, *350*(6), 552–559. https://doi.org/10.1056/NEJMoa031688

Hillmen, P., Muus, P., Röth, A., Elebute, M. O., Risitano, A. M., Schrezenmeier, H., Brodsky, R. A. (2013). Long-term safety and efficacy of sustained eculizumab treatment in patients with paroxysmal nocturnal haemoglobinuria. *British Journal of Haematology*, *162*(1), 62–73. https://doi.org/10.1111/bjh.12347

Hillmen, P., Young, N. S., Schubert, J., Brodsky, R. A., Socié, G., Muus, P., Luzzatto, L. (2006). The complement inhibitor eculizumab in paroxysmal nocturnal hemoglobinuria. *The New England Journal of Medicine*, *355*(12), 1233–1243. https://doi.org/10.1056/NEJMoa061648

Hinson, S. R., Pittock, S. J., Lucchinetti, C. F., Roemer, S. F., Fryer, J. P., Kryzer, T. J., & Lennon, V. A. (2007). Pathogenic potential of IgG binding to water channel extracellular domain in neuromyelitis optica. *Neurology*, *69*(24), 2221–2231. https://doi.org/10.1212/01.WNL.0000289761.64862.ce

Hodges, A., Strand, A. D., Aragaki, A. K., Kuhn, A., Sengstag, T., Hughes, G., Luthi-Carter, R. (2006). Regional and cellular gene expression changes in human Huntington's disease brain. *Human Molecular Genetics*, *15*(6), 965–977. https://doi.org/10.1093/hmg/ddl013

Høgåsen, A. K., Würzner, R., Abrahamsen, T. G., & Dierich, M. P. (1995). Human polymorphonuclear leukocytes store large amounts of terminal complement components C7 and C6, which may be released on stimulation. *Journal of Immunology*, *154*(9), 4734–4740. http://www.ncbi.nlm.nih.gov/pubmed/7722325

Holguin, M. H., Wilcox, L. A., Bernshaw, N. J., Rosse, W. F., & Parker, C. J. (1989). Relationship between the membrane inhibitor of reactive lysis and the erythrocyte phenotypes of paroxysmal nocturnal hemoglobinuria. *Journal of Clinical Investigation*, *84*(5), 1387–1394. https://doi.org/10.1172/JCI114311

Holguin, M. H., Fredrick, L. R., Bernshaw, N. J., Wilcox, L. A., & Parker, C. J. (1989). Isolation and characterization of a membrane protein from normal human erythrocytes that inhibits reactive lysis of the erythrocytes of paroxysmal nocturnal hemoglobinuria. *Journal of Clinical Investigation*, *84*(1), 7–17. https://doi.org/10.1172/JCI114172

Holmskov, U., Thiel, S., & Jensenius, J. C. (2003). Collectins and Ficolins: Humoral Lectins of the Innate Immune Defense . *Annual Review of Immunology*, *21*(1), 547–578. https://doi.org/10.1146/annurev.immunol.21.120601.140954

Hong, S., Beja-Glasser, V. F., Nfonoyim, B. M., Frouin, A., Li, S., Ramakrishnan, S., Stevens, B. (2016). Complement and microglia mediate early synapse loss in Alzheimer mouse models. *Science*, *352*(6286), 712–716. https://doi.org/10.1126/science.aad8373

Hosszu, K. K., Santiago-Schwarz, F., Peerschke, E. L. B., & Ghebrehiwet, B. (2010). Evidence that a C1q/C1qR system regulates monocyte-derived dendritic cell differentiation at the interface of innate and acquired immunity. *Innate Immunity*, *16*(2), 115–127. https://doi.org/10.1177/1753425909339815

Hou, L., Wang, K., Zhang, C., Sun, F., Che, Y., Zhao, X., Wang, Q. (2018). Complement receptor 3 mediates NADPH oxidase activation and dopaminergic neurodegeneration through a Src-Erk-dependent pathway. *Redox Biology*, *14*, 250–260. https://doi.org/10.1016/j.redox.2017.09.017

Hourcade, D. E. (2006). The role of properdin in the assembly of the alternative pathway C3 convertases of complement. *Journal of Biological Chemistry*, *281*(4), 2128–2132. https://doi.org/10.1074/jbc.M508928200

Hu, W. T., Watts, K. D., Tailor, P., Nguyen, T. P., Howell, J. C., Lee, R. C., Lee, E. K. (2016). CSF complement 3 and factor H are staging biomarkers in Alzheimer's disease. *Acta Neuropathologica Communications*, *4*, 14. https://doi.org/10.1186/s40478-016-0277-8

Huang, Y., Qiao, F., Abagyan, R., Hazard, S., & Tomlinson, S. (2006). Defining the CD59-C9 binding interaction. *Journal of Biological Chemistry*, *281*(37), 27398–27404. https://doi.org/10.1074/jbc.M603690200

Huber-Lang, M., Sarma, J. V., Zetoune, F. S., Rittirsch, D., Neff, T. A., McGuire, S. R., Ward, P. A. (2006). Generation of C5a in the absence of C3: A new complement activation pathway. *Nature Medicine*, *12*(6), 682–687. https://doi.org/10.1038/nm1419

Humbles, A. A., Lu, B., Nilsson, C. A., Lilly, C., Israel, E., Fujiwara, Y., Gerard, C. (2000). A role for the C3a anaphylatoxin receptor in the effector phase of asthma. *Nature*, *406*(6799), 998–1001. https://doi.org/10.1038/35023175

Huugen, D., Van Esch, A., Xiao, H., Peutz-Kootstra, C. J., Buurman, W. A., Tervaert, J. W. C., Heeringa, P. (2007). Inhibition of complement factor C5 protects against anti-myeloperoxidase antibody-mediated glomerulonephritis in mice. *Kidney International*, *71*(7), 646–654. https://doi.org/10.1038/sj.ki.5002103

Hyvärinen, S., Uchida, K., Varjosalo, M., Jokela, R., & Jokiranta, T. S. (2014). Recognition of malondialdehyde-modified proteins by the c terminus of complement factor h is mediated via the polyanion binding site and impaired by mutations found in atypical hemolytic uremic syndrome. *Journal of Biological Chemistry*, *289*(7), 4295–4306. https://doi.org/10.1074/jbc.M113.527416

Iatropoulos, P., Daina, E., Curreri, M., Piras, R., Valoti, E., Mele, C., Nastasi. (2018). Cluster analysis identifies distinct pathogenetic patterns in c3 glomerulopathies/immune complex–Mediated membranoproliferative GN. *Journal of the American Society of Nephrology*, *29*(1), 283–294. https://doi.org/10.1681/ASN.2017030258

Igawa, T., Ishii, S., Tachibana, T., Maeda, A., Higuchi, Y., Shimaoka, S., Hattori, K. (2010). Antibody recycling by engineered pH-dependent antigen binding improves the duration of antigen neutralization. *Nature Biotechnology*, *28*(11), 1203–1207. https://doi.org/10.1038/nbt.1691

Igawa, T., Mimoto, F., & Hattori, K. (2014). pH-dependent antigen-binding antibodies as a novel therapeutic modality. *Biochimica et Biophysica Acta*, *1844*(11), 1943–1950. https://doi.org/10.1016/j.bbapap.2014.08.003

Igawa, T., Haraya, K., & Hattori, K. (2016). Sweeping antibody as a novel therapeutic antibody modality capable of eliminating soluble antigens from circulation. *Immunological Reviews*, 270(1):132-51. https://doi.org/10.1111/imr.12392

Igawa, T., Maeda, A., Haraya, K., Tachibana, T., Iwayanagi, Y., Mimoto, F., Hattori, K. (2013). Engineered monoclonal antibody with novel antigen-sweeping activity in vivo. *PloS One*, *8*(5), e63236. https://doi.org/10.1371/journal.pone.0063236

Ikeda, K., Sannoh, T., Kawasaki, N., Kawasaki, T., & Yamashina, I. (1987). Serum lectin with known structure activates complement through the classical pathway. *The Journal of Biological Chemistry*, *262*(16), 7451–7454. http://www.ncbi.nlm.nih.gov/pubmed/3584121

Ingram, G., Hakobyan, S., Hirst, C. L., Harris, C. L., Loveless, S., Mitchell, J. P., Morgan, B. P. (2012). Systemic complement profiling in multiple sclerosis as a biomarker of disease state. *Multiple Sclerosis Journal*, *18*(10), 1401–1411. https://doi.org/10.1177/1352458512438238

Ingram, G., Loveless, S., Howell, O. W., Hakobyan, S., Dancey, B., Harris, C. L., Morgan, B. P. (2014). Complement activation in multiple sclerosis plaques: An immunohistochemical analysis. *Acta Neuropathologica Communications*, 2:53. https://doi.org/10.1186/2051-5960-2-53

Ingram, G., Hakobyan, S., Hirst, C. L., Harris, C. L., Pickersgill, T. P., Cossburn, M. D., Morgan, B. P. (2010). Complement regulator factor H as a serum biomarker of multiple sclerosis disease state. *Brain*, *133*(6), 1602–1611. https://doi.org/10.1093/brain/awq085

Ingram, G., Hakobyan, S., Robertson, N. P., & Morgan, B. P. (2009). Complement in multiple sclerosis: Its role in disease and potential as a biomarker. *Clinical and Experimental Immunology*. https://doi.org/10.1111/j.1365-2249.2008.03830.x

Ingram, G., Hakobyan, S., Robertson, N. P., & Morgan, B. P. (2010). Elevated plasma C4a levels in multiple sclerosis correlate with disease activity. *Journal of Neuroimmunology*, *223*(1–2), 124–127. https://doi.org/10.1016/j.jneuroim.2010.03.014

Ishii, T., & Haga, S. (1984). Immuno-electron-microscopic localization of complements in amyloid fibrils of senile plaques. *Acta Neuropathologica*, *63*(4), 296–300. https://doi.org/10.1007/BF00687336

Iwayanagi, Y., Igawa, T., Maeda, A., Haraya, K., Wada, N. A., Shibahara, N., Hattori, K. (2015). Inhibitory FcγRIIb-Mediated Soluble Antigen Clearance from Plasma by a pH-Dependent Antigen-Binding Antibody and Its Enhancement by Fc Engineering. *The Journal of Immunology*, *195*(7), 3198–3205. https://doi.org/10.4049/jimmunol.1401470

Jayne, D. R. W., Bruchfeld, A. N., Harper, L., Schaier, M., Venning, M. C., Hamilton, P., Bekker, P. (2017). Randomized trial of C5a receptor inhibitor avacopan in ANCA-associated vasculitis. *Journal of the American Society of Nephrology*, *28*(9), 2756–2767. https://doi.org/10.1681/ASN.2016111179

Jenne, D. E., & Tschopp, J. (1989). Molecular structure and functional characterization of a human complement cytolysis inhibitor found in blood and seminal plasma: Identity to sulfated glycoprotein 2, a constituent of rat testis fluid. *Proceedings of the National Academy of Sciences of the United States of America*, *86*(18), 7123–7127. https://doi.org/10.1073/pnas.86.18.7123

Jennette, J. C., Falk, R. J., Hu, P., & Xiao, H. (2013). Pathogenesis of Antineutrophil Cytoplasmic Autoantibody–Associated Small-Vessel Vasculitis. *Annual Review of Pathology: Mechanisms of Disease*, *8*(1), 139–160. https://doi.org/10.1146/annurev-pathol-011811-132453

Jiang, H., Fan, M. N., Yang, M., Lu, C., Zhang, M., Liu, X. H., & Ma, L. (2016). Association among complement factor H autoantibodies, deletions of CFHR, and the risk of atypical hemolytic uremic syndrome. *International Journal of Environmental Research and Public Health*, *13*(12). https://doi.org/10.3390/ijerph13121209

Jing, H., Babu, Y. S., Moore, D., Kilpatrick, J. M., Liu, X. Y., Volanakis, J. E., & Narayana, S. V. L. (1998). Structures of native and complexed complement factor D: Implications of the atypical His57 conformation and self-inhibitory loop in the regulation of specific serine protease activity. *Journal of Molecular Biology*, *282*(5), 1061–1081. https://doi.org/10.1006/jmbi.1998.2089

Johansson, L., Rytkönen, A., Bergman, P., Albiger, B., Källström, H., Hökfelt, T., Jonsson, A. B. (2003). CD46 in meningococcal disease. *Science*, *301*(5631), 373–375. https://doi.org/10.1126/science.1086476

Jongerius, I., Ram, S., & Rooijakkers, S. (2009). Bacterial complement escape. *Advances in Experimental Medicine and Biology*, *666*, 32–48. https://doi.org/10.1007/978-1-4419-1601-3_3

Jore, M. M., Johnson, S., Sheppard, D., Barber, N. M., Li, Y. I., Nunn, M. A., Lea, S. M. (2016). Structural basis for therapeutic inhibition of complement C5. *Nature Structural and Molecular Biology*, *23*(5), 378–386. https://doi.org/10.1038/nsmb.3196

Kaplan, M. (2002). Eculizumab (Alexion). *Current Opinion in Investigational Drugs (London, England : 2000)*, *3*(7), 1017–1023. http://www.ncbi.nlm.nih.gov/pubmed/12186261

Kassa, E., Ciulla, T. A., Hussain, R. M., & Dugel, P. U. (2019). Complement inhibition as a therapeutic strategy in retinal disorders. *Expert Opinion on Biological Therapy*, *19*(4), 335–342. https://doi.org/10.1080/14712598.2019.1575358

Kavanagh, D., & Goodship, T. H. J. (2011). Atypical hemolytic uremic syndrome, genetic basis, and clinical manifestations. *Hematology / the Education Program of the American Society of Hematology. American Society of Hematology. Education Program*, *2011*, 15–20. https://doi.org/10.1182/asheducation-2011.1.15

Kavanagh, D., & Goodship, T. (2010). Genetics and complement in atypical HUS. *Pediatric Nephrology*, 118(1):c37-42. https://doi.org/10.1007/s00467-010-1555-5

Kawai, M., Quincy, D. A., Lane, B., Mollison, K. W., Or, Y. S., Luly, J. R., & Carter, G. W. (1992). Structure-function studies in a series of carboxyl-terminal octapeptide analogues of anaphylatoxin C5a. *Journal of Medicinal Chemistry*, *35*(2), 220–223. https://doi.org/10.1021/jm00080a004

Kawai, M., Quincy, D. A., Lane, B., Mollison, K. W., Luly, J. R., & Carter, G. W. (1991). Identification and synthesis of a receptor binding site of human anaphylatoxin C5a. *Journal of Medicinal Chemistry*, *34*(7), 2068–2071. https://doi.org/10.1021/jm00111a022

Karch, C. M., & Goate, A. M. (2015). Alzheimer's disease risk genes and mechanisms of disease pathogenesis. *Biological Psychiatry*, 77(1):43-51. https://doi.org/10.1016/j.biopsych.2014.05.006

Keizer, R. J., Huitema, A. D. R., Schellens, J. H. M., & Beijnen, J. H. (2010). Clinical Pharmacokinetics of Therapeutic Monoclonal Antibodies. Clinical Pharmacokinetics, 49(8), 493–507. https://doi.org/10.2165/11531280-000000000-00000

Kemper, C., Verbsky, J. W., Price, J. D., & Atkinson, J. P. (2005). T-Cell Stimulation and Regulation: With Complements from CD46. *Immunologic Research*, *32*(1–3), 031–044. https://doi.org/10.1385/IR:32:1-3:031

Kerr, F. K., Thomas, A. R., Wijeyewickrema, L. C., Whisstock, J. C., Boyd, S. E., Kaiserman, D., Pike, R. N. (2008). Elucidation of the substrate specificity of the MASP-2 protease of the lectin complement pathway and identification of the enzyme as a major physiological target of the serpin, C1-inhibitor. *Molecular Immunology*, *45*(3), 670–677. https://doi.org/10.1016/j.molimm.2007.07.008

Kim, W. J., Mai, A., Weyand, N. J., Rendón, M. A., Van Doorslaer, K., & So, M. (2019). Neisseria gonorrhoeae evades autophagic killing by downregulating CD46-cyt1 and remodeling lysosomes. *PLoS Pathogens*, *15*(2). https://doi.org/10.1371/journal.ppat.1007495

Kinoshita, T., Medof, E., M., Silber, R., & Nussenzweig, V. (1985). Distribution of decay-accelerating factor in the peripheral blood of normal individuals and patients with paroxysmal nocturnal hemoglobinuria. *Journal of Experimental Medicine*, *162*(1), 75–92. https://doi.org/10.1084/jem.162.1.75

Kinoshita, T. (2018). Congenital Defects in the Expression of the Glycosylphosphatidylinositol-Anchored Complement Regulatory Proteins CD59 and Decay-Accelerating Factor. *Seminars in Hematology*, 55(3):136-140. https://doi.org/10.1053/j.seminhematol.2018.04.004

Kirszbaum, L., Sharpe, J. A., Murphy, B., d'Apice, A. J., Classon, B., Hudson, P., & Walker, I. D. (1989). Molecular cloning and characterization of the novel, human complement-associated protein, SP-40,40: a link between the complement and reproductive systems. *The EMBO Journal*, *8*(3), 711–718. http://www.ncbi.nlm.nih.gov/pubmed/2721499

Klein, M. A., Kaeser, P. S., Schwarz, P., Weyd, H., Xenarios, I., Zinkernagel, R. M., Aguzzi, A. (2001). Complement facilitates early prion pathogenesis. *Nature Medicine*, *7*(4), 488–492. https://doi.org/10.1038/86567

Klein, R. J., Zeiss, C., Chew, E. Y., Tsai, J.-Y., Sackler, R. S., Haynes, C., Hoh, J. (2005). Complement factor H polymorphism in age-related macular degeneration. *Science*, *308*(5720), 385–389. https://doi.org/10.1126/science.1109557

Klegeris, A., & McGeer, P. L. (2007). Complement activation by islet amyloid polypeptide (IAPP) and α-synuclein 112. *Biochemical and Biophysical Research Communications*, *357*(4), 1096–1099. https://doi.org/10.1016/j.bbrc.2007.04.055

Köhler, G., & Milstein, C. (2005). Continuous cultures of fused cells secreting antibody of predefined specificity. 1975. *Journal of Immunology*, *174*(5), 2453–2455. http://www.ncbi.nlm.nih.gov/pubmed/15728446

Kolb, W. P., Haxby, J. A., Arroyave, C. M., & Müller-Eberhard, H. J. (1973). The membrane attack mechanism of complement: Reversible interactions among the five native components in free solution. *Journal of Experimental Medicine*, *138*(2), 428–437. https://doi.org/10.1084/jem.138.2.428

Konteatis, Z. D., Siciliano, S. J., Van Riper, G., Molineaux, C. J., Pandya, S., Fischer, P., Springer, M. S. (1994). Development of C5a receptor antagonists. Differential loss of functional responses. *Journal of Immunology*, *153*(9), 4200–4205. http://www.ncbi.nlm.nih.gov/pubmed/7930622

Kopczynska, M., Zelek, W., Touchard, S., Gaughran, F., Di Forti, M., Mondelli, V., Morgan, B. P. (2019). Complement system biomarkers in first episode psychosis. *Schizophrenia Research*, *204*, 16–22. https://doi.org/10.1016/j.schres.2017.12.012

Korty, P. E., Brando, C., & Shevach, E. M. (1991). CD59 functions as a signal-transducing molecule for human T cell activation. *Journal of Immunology*, *146*(12), 4092–4098. http://www.ncbi.nlm.nih.gov/pubmed/1710238

Kremlitzka, M., Polgár, A., Fülöp, L., Kiss, E., Poór, G., & Erdei, A. (2013). Complement receptor type 1 (CR1, CD35) is a potent inhibitor of B-cell functions in rheumatoid arthritis patients. *International Immunology*, *25*(1), 25–33. https://doi.org/10.1093/intimm/dxs090

Krych-Goldberg, M., & Atkinson, J. P. (2001). Structure-function relationships of complement receptor type 1. *Immunological Reviews*, *180*, 112–122. http://www.ncbi.nlm.nih.gov/pubmed/11414353

Kusner, L. L., Yucius, K., Sengupta, M., Sprague, A. G., Desai, D., Nguyen, T., Borodovsky, A. (2019). Investigational RNAi Therapeutic Targeting C5 Is Efficacious in Pre-clinical Models of Myasthenia Gravis. *Molecular Therapy - Methods and Clinical Development*, *13*, 484–492. https://doi.org/10.1016/j.omtm.2019.04.009

Kuroda, H., & Fujihara, K. (2019). Current Status and Prospects of Complement-Targeting Therapy for Neuromyelitis Optica. *Brain and Nerve = Shinkei Kenkyu No Shinpo*, *71*(6), 573–580. https://doi.org/10.11477/mf.1416201318

Kuttner-Kondo, L. A., Mitchell, L., Hourcade, D. E., & Medof, M. E. (2001). Characterization of the Active Sites in Decay-Accelerating Factor. *The Journal of Immunology*, *167*(4), 2164–2171. https://doi.org/10.4049/jimmunol.167.4.2164

Lachmann, P. J., Lay, E., & Seilly, D. J. (2018). Experimental confirmation of the C3 tickover hypothesis by studies with an Ab (S77) that inhibits tickover in whole serum. *FASEB Journal*, *32*(1), 123–129. https://doi.org/10.1096/fj.201700734

Lambert, J. C., Heath, S., Even, G., Campion, D., Sleegers, K., Hiltunen, M., Pilotto, A. (2009). Genome-wide association study identifies variants at CLU and CR1 associated with Alzheimer's disease. *Nature Genetics*, *41*(10), 1094–1099. https://doi.org/10.1038/ng.439

Lambert, J. C., Ibrahim-Verbaas, C. A., Harold, D., Naj, A. C., Sims, R., Bellenguez, C., Seshadri, S. (2013). Meta-analysis of 74,046 individuals identifies 11 new susceptibility loci for Alzheimer's disease. *Nature Genetics*, *45*(12), 1452–1458. https://doi.org/10.1038/ng.2802

Lambris, J. D., & Holers, V. M. (2000). Therapeutic interventions in the complement system. *Humana Press*. https://www.springer.com/gp/book/9781461441175

Lambris, J. D., Lao, Z., Oglesby, T. J., Atkinson, J. P., Hack, C. E., & Becherer, J. D. (1996). Dissection of CR1, factor H, membrane cofactor protein, and factor B binding and functional sites in the third complement component. *Journal of Immunology*, *156*(12), 4821–4832. http://www.ncbi.nlm.nih.gov/pubmed/8648130

Langeggen, H., Pausa, M., Johnson, E., Casarsa, C., & Tedesco, F. (2000). The endothelium is an extrahepatic site of synthesis of the seventh component of the complement system. *Clinical and Experimental Immunology*, *121*(1), 69–76. https://doi.org/10.1046/j.1365-2249.2000.01238.x

Larsen, F., Madsen, H. O., Sim, R. B., Koch, C., & Garred, P. (2004). Disease-associated mutations in human mannose-binding lectin compromise oligomerization and activity of the final protein. *Journal of Biological Chemistry*, *279*(20), 21302–21311. https://doi.org/10.1074/jbc.M400520200

Laudisi, F., Spreafico, R., Evrard, M., Hughes, T. R., Mandriani, B., Kandasamy, M., … Mortellaro, A. (2013). Cutting Edge: The NLRP3 Inflammasome Links Complement-Mediated Inflammation and IL-1β Release. *The Journal of Immunology*, *191*(3), 1006–1010. https://doi.org/10.4049/jimmunol.1300489

Lea, S. (2002). Interactions of CD55 with non-complement ligands. In *Biochemical Society Transactions*, 30(Pt 6):1014-9. https://doi.org/10.1042/BST0301014

Le Bouguénec, C., Lalioui, L., Du Merle, L., Jouve, M., Courcoux, P., Bouzari, S., Garcia, M. I. (2001). Characterization of AfaE adhesins produced by extraintestinal and intestinal human escherichia coli isolates: PCR assays for detection of afa adhesins that do or do not recognize Dr blood group antigens. *Journal of Clinical Microbiology*, *39*(5), 1738–1745. https://doi.org/10.1128/JCM.39.5.1738-1745.2001

Le Quintrec, M., Roumenina, L., Noris, M., & Frémeaux-Bacchi, V. (2010). Atypical hemolytic uremic syndrome associated with mutations in complement regulator genes. *Seminars in Thrombosis and Hemostasis*, 36(6):641-52. https://doi.org/10.1055/s-0030-1262886

Lee, J. W., de Fontbrune, F. S., Lee, L. W. L., Pessoa, V., Gualandro, S., Füreder, W., Hill, A. (2019). Ravulizumab (ALXN1210) vs eculizumab in adult patients with PNH naive to complement inhibitors: The 301 study. *Blood*, *133*(6), 530–539. https://doi.org/10.1182/blood-2018-09-876136

Loeffler, D. A., Camp, D. M., & Conant, S. B. (2006). Complement activation in the Parkinson's disease substantia nigra: An immunocytochemical study. *Journal of Neuroinflammation*, *3*. https://doi.org/10.1186/1742-2094-3-29

Legendre, C. M., Licht, C., Muus, P., Greenbaum, L. A., Babu, S., Bedrosian C Bingham, C., Loirat, C. (2013). Terminal complement inhibitor eculizumab in atypical hemolytic-

uremic syndrome. *New England Journal of Medicine*, *368*(23), 2169–2181. https://doi.org/10.1056/NEJMoa1208981

Lehto, T., & Meri, S. (1993). Interactions of soluble CD59 with the terminal complement complexes. CD59 and C9 compete for a nascent epitope on C8. *Journal of Immunology*, 151(9), 4941–4949. http://www.ncbi.nlm.nih.gov/pubmed/7691959

Lehto, T., Morgan, B. P., & Meri, S. (1997). Binding of human and rat CD59 to the terminal complement complexes. *Immunology*, *90*(1), 121–128. https://doi.org/10.1046/j.1365-2567.1997.00120.x

Lennon, V. A., Kryzer, T. J., Pittock, S. J., Verkman, A. S., & Hinson, S. R. (2005). IgG marker of optic-spinal multiple sclerosis binds to the aquaporin-4 water channel. *Journal of Experimental Medicine*, *202*(4), 473–477. https://doi.org/10.1084/jem.20050304

Lennon, P. V. A., Wingerchuk, D. M., Kryzer, T. J., Pittock, S. J., Lucchinetti, C. F., Fujihara, K., Weinshenker, B. G. (2004). A serum autoantibody marker of neuromyelitis optica: Distinction from multiple sclerosis. *Lancet*, *364*(9451), 2106–2112. https://doi.org/10.1016/S0140-6736(04)17551-X

Levy, M., & Mealy, M. A. (2014). Purified human C1-esterase inhibitor is safe in acute relapses of neuromyelitis optica. *Neurology: Neuroimmunology and NeuroInflammation*, 1(1):e5.. https://doi.org/10.1212/NXI.0000000000000005

Lin, S. Y.-H., Cheng, C.-W., & Su, E. C.-Y. (2013). Prediction of B-cell epitopes using evolutionary information and propensity scales. *BMC Bioinformatics*, 14 Suppl 2:S10. http://www.ncbi.nlm.nih.gov/pubmed/23484214

Lin, Z., Schmidt, C. Q., Koutsogiannaki, S., Ricci, P., Risitano, A. M., Lambris, J. D., & Ricklin, D. (2015). Complement C3dg-mediated erythrophagocytosis: Implications for paroxysmal nocturnal hemoglobinuria. *Blood*, *126*(7), 891–894. https://doi.org/10.1182/blood-2015-02-625871

Lindahl, G., Sjöbring, U., & Johnsson, E. (2000). Human complement regulators: a major target for pathogenic microorganisms. *Current Opinion in Immunology*, *12*(1), 44–51. http://www.ncbi.nlm.nih.gov/pubmed/10679403

Lindorfer, M. A., Hahn, C. S., Foley, P. L., & Taylor, R. P. (2001). Heteropolymer-mediated clearance of immune complexes via erythrocyte CR1: mechanisms and applications. *Immunological Reviews*, *183*, 10–24. http://www.ncbi.nlm.nih.gov/pubmed/11782244

Linton, S. M., & Morgan, B. P. (1999). Complement activation and inhibition in experimental models of arthritis. *Molecular Immunology*, *36*(13–14), 905–914. https://doi.org/10.1016/s0161-5890(99)00113-3

Liszewski, M. K., Farries, T. C., Lublin, D. M., Rooney, I. A., & Atkinson, J. P. (1996). Control of the complement system. *Advances in Immunology*, *61*, 201–283. http://www.ncbi.nlm.nih.gov/pubmed/8834497

Loos, M. (1982). Antibody-independent activation of C1, the first component of complement. *Annales d'immunologie*, *133C*(2), 165–179. http://www.ncbi.nlm.nih.gov/pubmed/6287904

Lu, F., Liu, S., Hao, Q., Liu, L., Zhang, J., Chen, X., Huang, P. (2018). Association between Complement Factor C2/C3/CFB/CFH Polymorphisms and Age-Related Macular Degeneration: A Meta-Analysis. *Genetic Testing and Molecular Biomarkers*, *22*(9), 526–540. https://doi.org/10.1089/gtmb.2018.0110

Lubbers, R., van Essen, M. F., van Kooten, C., & Trouw, L. A. (2017). Production of complement components by cells of the immune system. *Clinical and Experimental Immunology*, 188(2):183-194. https://doi.org/10.1111/cei.12952

Lumry, W. R. (2013). Overview of epidemiology, pathophysiology, and disease progression in hereditary angioedema. The American Journal of Managed Care, 19(7 Suppl), s103-10. http://www.ncbi.nlm.nih.gov/pubmed/23844782

Lueck, K., Wasmuth, S., Williams, J., Hughes, T. R., Morgan, B. P., Lommatzsch, A., Pauleikhoff, D. (2011). Sub-lytic C5b-9 induces functional changes in retinal pigment epithelial cells consistent with age-related macular degeneration. *Eye*, *25*(8), 1074–1082. https://doi.org/10.1038/eye.2011.109

Lusthaus, M., Mazkereth, N., Donin, N., & Fishelson, Z. (2018). Receptor-interacting protein kinases 1 and 3, and mixed lineage kinase domain-like protein are activated by sublytic complement and participate in complement-dependent cytotoxicity. *Frontiers in Immunology*, 9:306. https://doi.org/10.3389/fimmu.2018.00306

Lyubchenko, T., Dal Porto, J., Cambier, J. C., & Holers, V. M. (2005). Coligation of the B Cell Receptor with Complement Receptor Type 2 (CR2/CD21) Using Its Natural Ligand C3dg: Activation without Engagement of an Inhibitory Signaling Pathway. *The Journal of Immunology*, *174*(6), 3264–3272. https://doi.org/10.4049/jimmunol.174.6.3264

Ma, Y. J., Skjoedt, M. O., & Garred, P. (2013). Collectin-11/MASP complex formation triggers activation of the lectin complement pathway - The fifth lectin pathway initiation complex. *Journal of Innate Immunity*, *5*(3), 242–250. https://doi.org/10.1159/000345356

Ma, H., Sandor, D. G., & Beck, L. H. (2013). The role of complement in membranous nephropathy. *Seminars in Nephrology*, *33*(6), 531–542. https://doi.org/10.1016/j.semnephrol.2013.08.004

Mabbott, N. A., Bruce, M. E., Botto, M., Walport, M. J., & Pepys, M. B. (2001). Temporary depletion of complement component C3 or genetic deficiency of C1q significantly delays onset of scrapie. *Nature Medicine*, *7*(4), 485–487. https://doi.org/10.1038/86562

MacLaren, R., Cui, W., & Cianflone, K. (2008). Adipokines and the immune system: an adipocentric view. *Advances in Experimental Medicine and Biology*, *632*, 1–21. https://doi.org/10.1007/978-0-387-78952-1_1

Mader, S., Gredler, V., Schanda, K., Rostasy, K., Dujmovic, I., Pfaller, K., Reindl, M. (2011). Complement activating antibodies to myelin oligodendrocyte glycoprotein in neuromyelitis optica and related disorders. *Journal of Neuroinflammation*, 8:184. https://doi.org/10.1186/1742-2094-8-184

Mandala, E., Lafaras, C., Goulis, I., Tsioni, K., Georgopoulou, V., & Ilonidis, G. (2013). Treatment of a patient with classical paroxysmal nocturnal hemoglobinuria and Budd-

Chiari syndrome, with complement inhibitor eculizumab: Case Report. *Hippokratia*, *17*(1), 81–84. http://www.ncbi.nlm.nih.gov/pubmed/23935352

Mangiarini, L., Sathasivam, K., Seller, M., Cozens, B., Harper, A., Hetherington, C., Bates, G. P. (1996). Exon I of the HD gene with an expanded CAG repeat is sufficient to cause a progressive neurological phenotype in transgenic mice. *Cell*, *87*(3), 493–506. https://doi.org/10.1016/S0092-8674(00)81369-0

Martel, C., Cointe, S., Maurice, P., Matar, S., Ghitescu, M., Théroux, P., & Bonnefoy, A. (2011). Requirements for membrane attack complex formation and anaphylatoxins binding to collagen-activated platelets. *PLoS ONE*, *6*(4). https://doi.org/10.1371/journal.pone.0018812

Martínez-Barricarte, R., Heurich, M., Valdes-Cañedo, F., Vazquez-Martul, E., Torreira, E., Montes, T., De Córdoba, S. R. (2010). Human C3 mutation reveals a mechanism of dense deposit disease pathogenesis and provides insights into complement activation and regulation. *Journal of Clinical Investigation*, *120*(10), 3702–3712. https://doi.org/10.1172/JCI43343

Masaki, T., Matsumoto, M., Nakanishi, I., Yasuda, R., & Seya, T. (1992). Factor I-dependent inactivation of human complement C4B of the classical pathway by C3B/C4B receptor (CR1, CD35) and membrane cofactor protein (MCP, CD46). *Journal of Biochemistry*, *111*(5), 573–578. https://doi.org/10.1093/oxfordjournals.jbchem.a123799

Mastellos, D., & Lambris, J. D. (2002). Complement: more than a "guard" against invading pathogens? *Trends in Immunology*, *23*(10), 485–491. http://www.ncbi.nlm.nih.gov/pubmed/12297420

Mastellos, D. C., Reis, E. S., Yancopoulou, D., Risitano, A. M., & Lambris, J. D. (2018). Expanding Complement Therapeutics for the Treatment of Paroxysmal Nocturnal Hemoglobinuria. *Seminars in Hematology*, 55(3):167-175. https://doi.org/10.1053/j.seminhematol.2018.02.002

Mastellos, D. C., Ricklin, D., & Lambris, J. D. (2019). Clinical promise of next-generation complement therapeutics. *Nature Reviews. Drug Discovery*, 18(9):707-729. https://doi.org/10.1038/s41573-019-0031-6

Matsushita, M., & Fujita, T. (1992). Activation of the classical complement pathway by marmose-binding protein in association with a novel C1s-like serine protease. *Journal of Experimental Medicine*, *176*(6), 1497–1502. https://doi.org/10.1084/jem.176.6.1497

Matsushita, M., Endo, Y., & Fujita, T. (2000). Cutting Edge: Complement-Activating Complex of Ficolin and Mannose-Binding Lectin-Associated Serine Protease. *The Journal of Immunology*, *164*(5), 2281–2284. https://doi.org/10.4049/jimmunol.164.5.2281

Matthews, K. W., Mueller-Ortiz, S. L., & Wetsel, R. A. (2004). Carboxypeptidase N: a pleiotropic regulator of inflammation. *Molecular Immunology*, *40*(11), 785–793. https://doi.org/10.1016/j.molimm.2003.10.002

Mazzone, A., & Ricevuti, G. (1995). Leukocyte CD11/CD18 integrins: biological and clinical relevance. *Haematologica*, *80*(2), 161–175. http://www.ncbi.nlm.nih.gov/pubmed/7628754

McCullough, J. W., Renner, B., & Thurman, J. M. (2013). The role of the complement system in acute kidney injury. *Seminars in Nephrology*, *33*(6), 543–556. https://doi.org/10.1016/j.semnephrol.2013.08.005

McGonigal, R., Cunningham, M. E., Yao, D., Barrie, J. A., Sankaranarayanan, S., Fewou, S. N., Willison, H. J. (2016). C1q-targeted inhibition of the classical complement pathway prevents injury in a novel mouse model of acute motor axonal neuropathy. *Acta Neuropathologica Communications*, *4*, 23. https://doi.org/10.1186/s40478-016-0291-x

McGreal, E., & Gasque, P. (2002). Structure-function studies of the receptors for complement C1q. In *Biochemical Society Transactions*, 30(Pt 6):1010-4. https://doi.org/10.1042/BST0301010

McKeage, K. (2019). Ravulizumab: First Global Approval. *Drugs*, *79*(3), 347–352. https://doi.org/10.1007/s40265-019-01068-2

Medof, E., M., Kinoshita, T., & Nussenzweig, V. (1984). Inhibition of complement activation on the surface of cells after incorporation of Decay-Accelerating Factor (DAF) into their membranes. *Journal of Experimental Medicine*, *160*(5), 1558–1578. https://doi.org/10.1084/jem.160.5.1558

Méndez, R., Leplae, R., Lensink, M. F., & Wodak, S. J. (2005). Assessment of CAPRI predictions in Rounds 3-5 shows progress in docking procedures. In *Proteins: Structure, Function and Genetics*, 1;60(2):150-69. https://doi.org/10.1002/prot.20551

Menny, A., Serna, M., Boyd, C. M., Gardner, S., Joseph, A. P., Morgan, B. P., Bubeck, D. (2018). CryoEM reveals how the complement membrane attack complex ruptures lipid bilayers. *Nature Communications*, 9(1):5316. https://doi.org/10.1038/s41467-018-07653-5

Meri, S., & Pangburn, M. K. (1990). A mechanism of activation of the alternative complement pathway by the classical pathway: protection of C3b from inactivation by covalent attachment to C4b. *European Journal of Immunology*, *20*(12), 2555–2561. https://doi.org/10.1002/eji.1830201205

Meri, S., & Pangburn, M. K. (1990). Discrimination between activators and nonactivators of the alternative pathway of complement: Regulation via a sialic acid/polyanion binding site on factor H. *Proceedings of the National Academy of Sciences of the United States of America*, *87*(10), 3982–3986. https://doi.org/10.1073/pnas.87.10.3982

Meri, S., Morgan, B. P., Davies, A., Daniels, R. H., Olavesen, M. G., Waldmann, H., & Lachmann, P. J. (1990). Human protectin (CD59), an 18,000-20,000 MW complement lysis restricting factor, inhibits C5b-8 catalysed insertion of C9 into lipid bilayers. *Immunology*, *71*(1), 1–9. http://www.ncbi.nlm.nih.gov/pubmed/1698710

Meri, S., Lehto, T., Sutton, C. W., Tyynelä, J., & Baumann, M. (1996). Structural composition and functional characterization of soluble CD59: Heterogeneity of the oligosaccharide and glycophosphoinositol (GPI) anchor revealed by laser-desorption mass spectrometric analysis. *Biochemical Journal*, *316*(3), 923–935. https://doi.org/10.1042/bj3160923

Milder, F. J., Gomes, L., Schouten, A., Janssen, B. J. C., Huizinga, E. G., Romijn, R. A., Gros, P. (2007). Factor B structure provides insights into activation of the central protease of the complement system. *Nature Structural and Molecular Biology*, *14*(3), 224–228. https://doi.org/10.1038/nsmb1210

Michailidou, I., Naessens, D. M. P., Hametner, S., Guldenaar, W., Kooi, E.-J., Geurts, J. J. G., Ramaglia, V. (2017). Complement C3 on microglial clusters in multiple sclerosis occur in chronic but not acute disease: Implication for disease pathogenesis. *Glia*, *65*(2), 264–277. https://doi.org/10.1002/glia.23090

Misawa, S., Kuwabara, S., Sato, Y., Yamaguchi, N., Nagashima, K., Katayama, K., Ogata, H. (2018). Safety and efficacy of eculizumab in Guillain-Barré syndrome: a multicentre, double-blind, randomised phase 2 trial. *The Lancet Neurology*, *17*(6), 519–529. https://doi.org/10.1016/S1474-4422(18)30114-5

Mogues, T., Ota, T., Tauber, A. I., & Sastry, K. N. (1996). Characterization of two mannose-binding protein cDNAs from rhesus monkey (Macaca mulatta): Structure and evolutionary implications. *Glycobiology*, *6*(5), 543–550. https://doi.org/10.1093/glycob/6.5.543

Mohlin, C., Sandholm, K., Ekdahl, K. N., & Nilsson, B. (2017). The link between morphology and complement in ocular disease. *Molecular Immunology*, 89:84-99. https://doi.org/10.1016/j.molimm.2017.05.028

Møller-Kristensen, M., Thiel, S., Sjöholm, A., Matsushita, M., & Jensenius, J. C. (2007). Cooperation between MASP-1 and MASP-2 in the generation of C3 convertase through the MBL pathway. *International Immunology*, *19*(2), 141–149. https://doi.org/10.1093/intimm/dxl131

Mollison, K. W., Mandecki, W., Zuiderweg, E. R. P., Fayer, L., Fey, T. A., Krause, R. A., Carter, G. W. (1989). Identification of receptor-binding residues in the inflammatory complement protein C5a site-directed mutagenesis. *Proceedings of the National Academy of Sciences of the United States of America*, *86*(1), 292–296. https://doi.org/10.1073/pnas.86.1.292

Mollnes, T. E., Lea, T., & Harboe, M. (1984). Detection and quantification of the terminal C5b-9 complex of human complement by a sensitive enzyme-linked immunosorbent assay. *Scandinavian Journal of Immunology*, *20*(2), 157–166. https://doi.org/10.1111/j.1365-3083.1984.tb00989.x

Monahan, J. B., & Sodetz, J. M. (1980). Binding of the eighth component of human complement to the soluble cytolytic complex is mediated by its beta subunit. *The Journal of Biological Chemistry*, *255*(22), 10579–10582. http://www.ncbi.nlm.nih.gov/pubmed/7430137

Morgan, B. P., van den Berg, C. W., Davies, E. V., Hallett, M. B., & Horejsi, V. (1993). Cross-linking of CD59 and of other glycosyl phosphatidylinositol-anchored molecules on neutrophils triggers cell activation via tyrosine kinase. *European Journal of Immunology*, *23*(11), 2841–2850. https://doi.org/10.1002/eji.1830231118

Morgan, B. P. (1989). Complement membrane attack on nucleated cells: Resistance, recovery and non-lethal effects. *Biochemical Journal*, 264(1):1-14. https://doi.org/10.1042/bj2640001

Morgan, B. P., & Walport, M. J. (1991). Complement deficiency and disease. *Immunology Today*, *12*(9), 301–306. https://doi.org/10.1016/0167-5699(91)90003-C

Morgan, B. P., & Meri, S. (1994). Membrane proteins that protect against complement lysis. *Springer Seminars in Immunopathology*, *15*(4), 369–396. http://www.ncbi.nlm.nih.gov/pubmed/8153873

Morgan, B. P., & Gasque, P. (1997). Extrahepatic complement biosynthesis: Where, when and why? *Clinical and Experimental Immunology*, 107(1):1-7. https://doi.org/10.1046/j.1365-2249.1997.d01-890.x

Morgan, B. P. (1999). Regulation of the complement membrane attack pathway. *Critical Reviews in Immunology*, *19*(3), 173–198. http://www.ncbi.nlm.nih.gov/pubmed/10422598

Morgan, B. P., & Harris, C. L. (1999). Complement Regulatory Proteins. *Academic Press*. https://doi.org/10.1016/B978-0-125-06965-6.X5000-4

Morgan, B. P. (2000). Complement Methods and Protocols (Vol. 150). New Jersey: *Humana Press*. https://doi.org/10.1385/159259056X

Morgan, B. P., & Harris, C. L. (2003). Complement therapeutics; history and current progress. *Molecular Immunology*, *40*(2–4), 159–170. http://www.ncbi.nlm.nih.gov/pubmed/12914822

Morgan, B. P., Chamberlain-Banoub, J., Neal, J. W., Song, W., Mizuno, M., & Harris, C. L. (2006). The membrane attack pathway of complement drives pathology in passively induced experimental autoimmune myasthenia gravis in mice. *Clinical and Experimental Immunology*, *146*(2), 294–302. https://doi.org/10.1111/j.1365-2249.2006.03205.x

Morgan, B. P. (2010). Hereditary angioedema - Therapies old and new. *New England Journal of Medicine*, *363*(6), 581–583. https://doi.org/10.1056/NEJMe1006450

Morgan, B. P., & Harris, C. L. (2015). Complement, a target for therapy in inflammatory and degenerative diseases. *Nature Reviews. Drug Discovery*, *14*(12), 857–877. https://doi.org/10.1038/nrd4657

Morgan, B. P., Walters, D., Serna, M., & Bubeck, D. (2016). Terminal complexes of the complement system: new structural insights and their relevance to function. *Immunological Reviews*, 274(1):141-151. https://doi.org/10.1111/imr.12461

Morgan, A. R., Touchard, S., O'Hagan, C., Sims, R., Majounie, E., Escott-Price, V., Morgan, B. P. (2017). The correlation between inflammatory biomarkers and polygenic risk score in Alzheimer's disease. *Journal of Alzheimer's Disease*, *56*(1), 25–36. https://doi.org/10.3233/JAD-160889

Morgan, B. P., Boyd, C., & Bubeck, D. (2017). Molecular cell biology of complement membrane attack. *Seminars in Cell and Developmental Biology*, 72:124-132. https://doi.org/10.1016/j.semcdb.2017.06.009

Morgan, B. P. (2018). Complement in the pathogenesis of Alzheimer's disease. *Seminars in Immunopathology*, *40*(1), 113–124. https://doi.org/10.1007/s00281-017-0662-9

Moxley, G., & Ruddy, S. (1985). Elevated C3 anaphylatoxin levels in synovial fluids from patients with rheumatoid arthritis. *Arthritis and Rheumatism*, *28*(10), 1089–1095. https://doi.org/10.1002/art.1780281003

Mrowietz, U., Koch, W. A., Zhu, K., Wiedow, O., Bartels, J., Christophers, E., & Schröder, J. M. (2001). Psoriasis scales contain C5a as the predominant chemotaxin for monocyte-derived dendritic cells. *Experimental Dermatology*, *10*(4), 238–245. http://www.ncbi.nlm.nih.gov/pubmed/11493312

Mukherjee, P., & Pasinetti, G. M. (2000). The role of complement anaphylatoxin C5a in neurodegeneration: implications in Alzheimer's disease. *Journal of Neuroimmunology*, *105*(2), 124–130. https://doi.org/10.1016/s0165-5728(99)00261-1

Müller-Eberhard, H. J., & Fjellström, K. E. (1971). Isolation of the anticomplementary protein from cobra venom and its mode of action on C3. *Journal of Immunology*, *107*(6), 1666–1672. http://www.ncbi.nlm.nih.gov/pubmed/5120401

Müller-Eberhard, H. J. (1984). The membrane attack complex. *Springer Seminars in Immunopathology*, *7*(2–3), 93–141. http://www.ncbi.nlm.nih.gov/pubmed/6387983

Mullins, R. F., Russell, S. R., Anderson, D. H., & Hageman, G. S. (2000). Drusen associated with aging and age-related macular degeneration contain proteins common to extracellular deposits associated with atherosclerosis, elastosis, amyloidosis, and dense deposit disease. *The FASEB Journal*, *14*(7), 835–846. https://doi.org/10.1096/fasebj.14.7.835

Murphy, B. F., Saunders, J. R., O'Bryan, M. K., Kirszbaum, L., Walker, I. D., & d'Apice, A. J. (1989). SP-40,40 is an inhibitor of C5b-6-initiated haemolysis. *International Immunology*, *1*(5), 551–554. https://doi.org/10.1093/intimm/1.5.551

Murphy, B. F., Kirszbaum, L., Walker, I. D., & d'Apice, J. F. (1988). Sp-40,40, a newly identified normal human serum protein found in the SC5b-9 complex of complement and in the immune deposits in glomerulonephritis. *Journal of Clinical Investigation*, *81*(6), 1858–1864. https://doi.org/10.1172/JCI113531

Mutti, M., Ramoni, K., Nagy, G., Nagy, E., & Szijártó, V. (2018). A New Tool for Complement Research: In vitro Reconstituted Human Classical Complement Pathway. *Frontiers in Immunology*, *9*, 2770. https://doi.org/10.3389/fimmu.2018.02770

Nagasawa, S., & Stroud, R. M. (1977). Cleavage of C2 by C1s into the antigenically distinct fragments C2a and C2b: demonstration of binding of C2b to C4b. *Proceedings of the National Academy of Sciences of the United States of America*, *74*(7), 2998–3001. https://doi.org/10.1073/pnas.74.7.2998

Nakamura, Y., & Myers, B. D. (1988). Charge selectivity of proteinuria in diabetic glomerulopathy. *Diabetes*, *37*(9), 1202–1211. https://doi.org/10.2337/diab.37.9.1202

Nan, R., Farabella, I., Schumacher, F. F., Miller, A., Gor, J., Martin, A. C. R., Perkins, S. J. (2011). Zinc binding to the Tyr402 and His402 allotypes of complement factor H: Possible implications for age-related macular degeneration. *Journal of Molecular Biology*, *408*(4), 714–735. https://doi.org/10.1016/j.jmb.2011.03.006

Naniche, D., Varior-Krishnan, G., Cervoni, F., Wild, T. F., Rossi, B., Rabourdin-Combe, C., & Gerlier, D. (1993). Human membrane cofactor protein (CD46) acts as a cellular receptor for measles virus. *Journal of Virology*, *67*(10), 6025–6032. http://www.ncbi.nlm.nih.gov/pubmed/8371352

Nelson, R. A. (1966). A new concept of immunosuppression in hypersensitivity reactions and in transplantation immunity. *Survey of Ophthalmology*, *11*(4), 498–505. http://www.ncbi.nlm.nih.gov/pubmed/5919620

Nemerow, G. R., Yamamoto, K. I., & Lint, T. F. (1979). Fernie-King. *Journal of Immunology*, 1245–1252. http://www.ncbi.nlm.nih.gov/pubmed/469249

Nesargikar, P. N., Spiller, B., & Chavez, R. (2012). The complement system: history, pathways, cascade and inhibitors. *European Journal of Microbiology & Immunology*, *2*(2), 103–111. https://doi.org/10.1556/EuJMI.2.2012.2.2

Nicholson-Weller, A., March, J. P., Rosen, C. E., Spicer, D. B., & Austen, K. F. (1985). Surface membrane expression by human blood leukocytes and platelets of decay-accelerating factor, a regulatory protein of the complement system. *Blood*, *65*(5), 1237–1244. http://www.ncbi.nlm.nih.gov/pubmed/2581636

Nicholson-Weller, A., & Wang, C. E. (1994). Structure and function of decay accelerating factor CD55. *The Journal of Laboratory and Clinical Medicine*, *123*(4), 485–491. http://www.ncbi.nlm.nih.gov/pubmed/7511675

Niculescu, F., Rus, H., van Biesen, T., & Shin, M. L. (1997). Activation of Ras and mitogen-activated protein kinase pathway by terminal complement complexes is G protein dependent. *Journal of Immunology*, *158*(9), 4405–4412. http://www.ncbi.nlm.nih.gov/pubmed/9127005

Niculescu, F., Badea, T., & Rus, H. (1999). Sublytic C5b-9 induces proliferation of human aortic smooth muscle cells: Role of mitogen activated protein kinase and phosphatidylinositol 3- kinase. *Atherosclerosis*, *142*(1), 47–56. https://doi.org/10.1016/S0021-9150(98)00185-3

Nilsson, U. R., & Mueller-Eberhard, H. J. (1965). Isolation of beta If-globulin from human serum and characterisation as the fifth component of complement. *The Journal of Experimental Medicine*, *122*, 277–298. https://doi.org/10.1084/jem.122.2.277

Ninomiya, H., & Sims, P. J. (1992). The human complement regulatory protein CD59 binds to the alpha-chain of C8 and to the “b”domain of C9. *The Journal of Biological Chemistry*, *267*(19), 13675–13680. http://www.ncbi.nlm.nih.gov/pubmed/1377690

Ninomiya, H., Stewart, B. H., Rollins, S. A., Zhao, J., Bothwell, A. L., & Sims, P. J. (1992). Contribution of the N-linked carbohydrate of erythrocyte antigen CD59 to its complement-inhibitory activity. *The Journal of Biological Chemistry*, *267*(12), 8404–8410. http://www.ncbi.nlm.nih.gov/pubmed/1373727

Nishida, N., Walz, T., & Springer, T. A. (2006). Structural transitions of complement component C3 and its activation products. *Proceedings of the National Academy of Sciences of the United States of America*, *103*(52), 19737–19742. https://doi.org/10.1073/pnas.0609791104

Nishimura, J., Yamamoto, M., Hayashi, S., Ohyashiki, K., Ando, K., Brodsky, A. L., … Kanakura, Y. (2014). Genetic variants in C5 and poor response to eculizumab. *The New England Journal of Medicine*, *370*(7), 632–639. https://doi.org/10.1056/NEJMoa1311084

Noone, D., Hebert, D., & Licht, C. (2018). Pathogenesis and treatment of ANCA-associated vasculitis-a role for complement. *Pediatric Nephrology* *33*(1), 1–11. https://doi.org/10.1007/s00467-016-3475-5

Nose, M., Katoh, M., Okada, N., Kyogoku, M., & Okada, H. (1990). Tissue distribution of HRF20, a novel factor preventing the membrane attack of homologous complement, and its predominant expression on endothelial cells in vivo. *Immunology*, *70*(2), 145–149. http://www.ncbi.nlm.nih.gov/pubmed/1695609

Nowicki, B., & Nowicki, S. (2013). DAF as a therapeutic target for steroid hormones: Implications for host-pathogen interactions. In *Advances in Experimental Medicine and Biology*, 735:83-96. https://doi.org/10.1007/978-1-4614-4118-2_5

Nowicki, B., Hart, A., Coyne, K. E., Lublin, D. M., & Nowicki, S. (1993). Short consensus repeat-3 domain of recombinant decay-accelerating factor is recognized by escherichia coli recombinant dr adhesin in a model of a cell-cell interaction. *Journal of Experimental Medicine*, *178*(6), 2115–2121. https://doi.org/10.1084/jem.178.6.2115

O'Bryan, M. K., Baker, H. W., Saunders, J. R., Kirszbaum, L., Walker, I. D., Hudson, P., Murphy, B. F. (1990). Human seminal clusterin (SP-40,40). Isolation and characterization. *The Journal of Clinical Investigation*, *85*(5), 1477–1486. https://doi.org/10.1172/JCI114594

Okada, N., Harada, R., Fujita, T., & Okada, H. (1989). A novel membrane glycoprotein capable of inhibiting membrane attack by homologous complement. *International Immunology*, *1*(2), 205–208. https://doi.org/10.1093/intimm/1.2.205

Okada, H., Nagami, Y., Takahashi, K., Okada, N., Hideshima, T., Takizawa, H., & Kondo, J. (1989). 20 KDa homologous restriction factor of complement resembles T cell activating protein. *Biochemical and Biophysical Research Communications*, *162*(3), 1553–1559. https://doi.org/10.1016/0006-291X(89)90852-8

Okinaga, S., Slattery, D., Humbles, A., Zsengeller, Z., Morteau, O., Kinrade, M. B., Gerard, C. (2003). C5L2, a nonsignaling C5A binding protein. *Biochemistry*, *42*(31), 9406–9415. https://doi.org/10.1021/bi034489v

Orren A, Wallace ME, Hobart MJ, Lachmann PJ (1989). C6 polymorphism and C6-deficiency in site strains of the mutation-prone Peru-Coppock mouse. *Complement Inflammation*, 6: 295–6 http://www.informatics.jax.org/reference/J:122430

Oroszlán, G., Kortvely, E., Szakács, D., Kocsis, A., Dammeier, S., Zeck, A., Dobó, J. (2016). MASP-1 and MASP-2 Do Not Activate Pro-Factor D in Resting Human Blood, whereas MASP-3 Is a Potential Activator: Kinetic Analysis Involving Specific MASP-1 and

MASP-2 Inhibitors. *Journal of Immunology*, *196*(2), 857–865. https://doi.org/10.4049/jimmunol.1501717

Paixão-Cavalcante, D., López-Trascasa, M., Skattum, L., Giclas, P. C., Goodship, T. H., De Córdoba, S. R., Harris, C. L. (2012). Sensitive and specific assays for C3 nephritic factors clarify mechanisms underlying complement dysregulation. *Kidney International*, *82*(10), 1084–1092. https://doi.org/10.1038/ki.2012.250

Papadopoulos, M. C., Bennett, J. L., & Verkman, A. S. (2014). Treatment of neuromyelitis optica: State-of-the-art and emerging therapies. *Nature Reviews Neurology*, 10(9):493-506. https://doi.org/10.1038/nrneurol.2014.141

Parker, C. J. (1991).Paroxymal nocturnal hemoglobinuria and glycosyl phosphatidylinositol anchored proteins that regulate complement. *Clinical & Experimental Immunology*, *86*, 36–42. https://doi.org/10.1111/j.1365-2249.1991.tb06205.x

Parsons, E. S., Stanley, G. J., Pyne, A. L. B., Hodel, A. W., Nievergelt, A. P., Menny, A., Hoogenboom, B. W. (2019). Single-molecule kinetics of pore assembly by the membrane attack complex. *Nature Communications*, 10(1):2066. https://doi.org/10.1038/s41467-019-10058-7

Patston, P. A., Schapira, M., Gettins, P., & Beechem, J. (1991). Mechanism of Serpin Action: Evidence That C1 Inhibitor Functions as a Suicide Substrate. *Biochemistry*, *30*(36), 8876–8882. https://doi.org/10.1021/bi00100a022

Pedersen, E. D., Aass, H. C. D., Rootwelt, T., Fung, M., Lambris, J. D., & Mollnes, T. E. (2007). CD59 efficiently protects human NT2-N neurons against complement-mediated damage. *Scandinavian Journal of Immunology*, *66*(2–3), 345–351. https://doi.org/10.1111/j.1365-3083.2007.01959.x

Peerschke, E. I., Reid, K. B., & Ghebrehiwet, B. (1994). Identification of a novel 33-kDa C1q-binding site on human blood platelets. *Journal of Immunology*, 5896–5901. http://www.ncbi.nlm.nih.gov/pubmed/8207215

Pérez-Caballero, D., González-Rubio, C., Esther Gallardo, M., Vera, M., López-Trascasa, M., Rodríguez de Córdoba, S., & Sánchez-Corral, P. (2001). Clustering of missense mutations in the C-terminal region of factor H in atypical hemolytic uremic syndrome. *American Journal of Human Genetics*, *68*(2), 478–484. https://doi.org/10.1086/318201

Perkins, S. J., & Goodship, T. H. J. (2002). Molecular modelling of the C-terminal domains of factor H of human complement: A correlation between haemolytic uraemic syndrome and a predicted heparin binding site. *Journal of Molecular Biology*, *316*(2), 217–224. https://doi.org/10.1006/jmbi.2001.5337

Perkins, S. J., Villiers, C. L., Arlaud, G. J., Boyd, J., Burton, D. R., Colomb, M. G., & Dwek, R. A. (1984). Neutron scattering studies of subcomponent C1q of first component C1 of human complement and its association with subunit C1r2C1s2 within C1. *Journal of Molecular Biology*, *179*(3), 547–557. https://doi.org/10.1016/0022-2836(84)90079-2

Phelan, M. M., Thai, C. T., Soares, D. C., Ogata, R. T., Barlow, P. N., & Bramham, J. (2009). Solution structure of factor I-like modules from complement C7 reveals a pair of follistatin domains in compact pseudosymmetric arrangement. *Journal of Biological Chemistry*, *284*(29), 19637–19649. https://doi.org/10.1074/jbc.M901993200

Phieler, J., Garcia-Martin, R., Lambris, J. D., & Chavakis, T. (2013). The role of the complement system in metabolic organs and metabolic diseases. *Seminars in Immunology*, *25*(1), 47–53. https://doi.org/10.1016/j.smim.2013.04.003

Pickering, R. J., Wolfson, M. R., Good, R. A., & Gewurz, H. (1969). Passive hemolysis by serum and cobra venom factor: a new mechanism inducing membrane damage by complement. *Proceedings of the National Academy of Sciences of the United States of America*, *62*(2), 521–527. https://doi.org/10.1073/pnas.62.2.521

Pickering, M. C., Botto, M., Taylor, P. R., Lachmann, P. J., & Walport, M. J. (2000). Systemic lupus erythematosus, complement deficiency, and apoptosis. *Advances in Immunology*, *76*, 227–324. http://www.ncbi.nlm.nih.gov/pubmed/11079100

Pickering, R. J. (1968). Significance of abnormalities of serum complement in human disease. *Postgraduate Medicine*, *43*(6), 39–43. https://doi.org/10.1080/00325481.1968.11693275

Pickering, M. C., D'agati, V. D., Nester, C. M., Smith, R. J., Haas, M., Appel, G. B., Cook, H. T. (2013). C3 glomerulopathy: Consensus report. In *Kidney International,* 84(6):1079-89. https://doi.org/10.1038/ki.2013.377

Pillemer, L., Blum, L., Lepow, I. H., Ross, O. A., Todd, E. W., & Wardlaw, A. C. (1954). The properdin system and immunity: I. Demonstration and isolation of a new serum protein, properdin, and its role in immune phenomena. *Science*, 120(3112):279-85. https://doi.org/10.1126/science.120.3112.279

Pittock, S. J., Berthele, A., Fujihara, K., Kim, H. J., Levy, M., Palace, J., Wingerchuk, D. M. (2019). Eculizumab in Aquaporin-4–Positive Neuromyelitis Optica Spectrum Disorder. *New England Journal of Medicine*, 381(7):614-625. https://doi.org/10.1056/nejmoa1900866

Pittock, S. J., Lennon, V. A., McKeon, A., Mandrekar, J., Weinshenker, B. G., Lucchinetti, C. F., Wingerchuk, D. M. (2013). Eculizumab in AQP4-IgG-positive relapsing neuromyelitis optica spectrum disorders: An open-label pilot study. *The Lancet Neurology*, *12*(6), 554–562. https://doi.org/10.1016/S1474-4422(13)70076-0

Podack, E. R. (1984). Molecular composition of the tubular structure of the membrane attack complex of complement. *The Journal of Biological Chemistry*, *259*(13), 8641–8647. http://www.ncbi.nlm.nih.gov/pubmed/6736043

Podack, E. R., Tschoop, J., & Muller-Eberhard, H. J. (1982). Molecular organization of C9 within the membrane attack complex of complement. Induction of circular C9 polymerization by the C5b-8 assembly. *Journal of Experimental Medicine*, *156*(1), 268–282. https://doi.org/10.1084/jem.156.1.268

Podack, E. R., & Müller-Eberhard, H. J. (1978). Binding of desoxycholate, phosphatidylcholine vesicles, lipoprotein and of the S-protein to complexes of terminal complement components. *Journal of Immunology*, *121*(3), 1025–1030. http://www.ncbi.nlm.nih.gov/pubmed/690431

Podack, E. R., & Müller-Eberhard, H. J. (1979). Isolation of human S-protein, an inhibitor of the membrane attack complex of complement. *The Journal of Biological Chemistry*, *254*(19), 9808–9814. http://www.ncbi.nlm.nih.gov/pubmed/489571

Podack, E. R., Preissner, K. T., & Müller-Eberhard, H. J. (1984). Inhibition of C9 polymerization within the SC5b-9 complex of complement by S-protein. *Acta Pathologica, Microbiologica, et Immunologica Scandinavica. Supplement*, *284*, 89–96. http://www.ncbi.nlm.nih.gov/pubmed/6587746

Podack, E. R., Kolb, W. P., & Müller-Eberhard, H. J. (1978). The C5b-6 complex: formation, isolation, and inhibition of its activity by lipoprotein and the S-protein of human serum. *Journal of Immunology*, *120*(6), 1841–1848. http://www.ncbi.nlm.nih.gov/pubmed/659879

Polley, M. J., & Müller-Eberhard, H. J. (1967). Enharncement of the hemolytic activity of the second component of human complement by oxidation. *The Journal of Experimental Medicine*, *126*(6), 1013–1025. https://doi.org/10.1084/jem.126.6.1013

Polley, M. J., & Müller-Eberhard, H. J. (1968). The second component of human complement: its isolation, fragmentation by C'1 esterase, and incorporation into C'3 convertase. *The Journal of Experimental Medicine*, *128*(3), 533–551. https://doi.org/10.1084/jem.128.3.533

Powell, R. M., Schmitt, V., Ward, T., Goodfellow, I., Evans, D. J., & Almond, J. W. (1998). Characterization of echoviruses that bind decay accelerating factor (CD55): Evidence that some haemagglutinating strains use more than one cellular receptor. *Journal of General Virology*, *79*(7), 1707–1713. https://doi.org/10.1099/0022-1317-79-7-1707

Pratt, J. R., Basheer, S. A., & Sacks, S. H. (2002). Local synthesis of complement component C3 regulates acute renal transplant rejection. *Nature Medicine*, *8*(6), 582–587. https://doi.org/10.1038/nm0602-582

Preissner, K. T., & Jenne, D. (1991). Structure of vitronectin and its biological role in haemostasis. *Thrombosis and Haemostasis*, *66*(1), 123–132. http://www.ncbi.nlm.nih.gov/pubmed/1718050

Preissner, K. T., Podack, E. R., & Müller-Eberhard, H. J. (1985). The membrane attack complex of complement: relation of C7 to the metastable membrane binding site of the intermediate complex C5b-7. *Journal of Immunology*, *135*(1), 445–451 http://www.ncbi.nlm.nih.gov/pubmed/3998468

Presanis, J. S., Kojima, M., & Sim, R. B. (2003). Biochemistry and genetics of mannan-binding lectin (MBL). *Biochemical Society Transactions*, *31*(Pt 4), 748–752. https://doi.org/10.1042/bst0310748

Preissner, K. P., Podack, E. R., & Müller-Eberhard, H. J. (1989). SC5b-7, SC5b-8 and SC5b-9 complexes of complement: ultrastructure and localization of the S-protein (vitronectin) within the macromolecules. *European Journal of Immunology*, *19*(1), 69–75. https://doi.org/10.1002/eji.1830190112

Prohászka, Z., Nilsson, B., Frazer-Abel, A., & Kirschfink, M. (2016). Complement analysis 2016: Clinical indications, laboratory diagnostics and quality control. *Immunobiology*. 221(11):1247-58. https://doi.org/10.1016/j.imbio.2016.06.008

Qiu, W., Zhang, Y., Liu, X., Zhou, J., Li, Y., Zhou, Y., Wang, Y. (2012). Sublytic C5b-9 complexes induce proliferative changes of glomerular mesangial cells in rat Thy-1

nephritis through TRAF6-mediated PI3K-dependent Akt1 activation. *Journal of Pathology*, *226*(4), 619–632. https://doi.org/10.1002/path.3011

Reader, R. H., Workman, R. G., Maddison, B. C., & Gough, K. C. (2019). Advances in the Production and Batch Reformatting of Phage Antibody Libraries. *Molecular Biotechnology*, [ahead of print]. https://doi.org/10.1007/s12033-019-00207-0

Raedler, H., Vieyra, M. B., Leisman, S., Lakhani, P., Kwan, W., Yang, M., Heeger, P. S. (2011). Anti-complement component C5 mAb synergizes with CTLA4Ig to inhibit alloreactive T cells and prolong cardiac allograft survival in mice. *American Journal of Transplantation*, *11*(7), 1397–1406. https://doi.org/10.1111/j.1600-6143.2011.03561.x

Ratnoff, , W. D., Knez, J. J., Prince, G. M., Okada, H., Lachmann, P. J., & Medof, M. E. (1992). Structural properties of the glycoplasmanylinositol anchor phospholipid of the complement membrane attack complex inhibitor CD59. *Clinical & Experimental Immunology*, *87*(3), 415–421. https://doi.org/10.1111/j.1365-2249.1992.tb03012.x

Reca, R., Mastellos, D., Majka, M., Marquez, L., Ratajczak, J., Franchini, S., Ratajczak, M. Z. (2003). Functional receptor for C3a anaphylatoxin is expressed by normal hematopoietic stem/progenitor cells, and C3a enhances their homing-related responses to SDF-1. *Blood*, *101*(10), 3784–3793. https://doi.org/10.1182/blood-2002-10-3233

Reid, K. B., & Turner, M. W. (1994). Mammalian lectins in activation and clearance mechanisms involving the complement system. *Springer Seminars in Immunopathology*, *15*(4), 307–326. http://www.ncbi.nlm.nih.gov/pubmed/8153870

Reid, K. B. M., & Day, A. J. (1989). Structure-function relationships of the complement components. *Immunology Today*, *10*(6), 177–180. https://doi.org/10.1016/0167-5699(89)90317-4

Ren, G., Huynh, C., Bijian, K., & Cybulsky, A. V. (2008). Role of apoptosis signal-regulating kinase 1 in complement-mediated glomerular epithelial cell injury. *Molecular Immunology*, *45*(8), 2236–2246. https://doi.org/10.1016/j.molimm.2007.11.013

Ricardo, A., Arata, M., DeMarco, S., Dhamnaskar, K., Hammer, R., Fridkis-Hareli, M., Treco, D. (2015). Preclinical Evaluation of RA101495, a Potent Cyclic Peptide Inhibitor of C5 for the Treatment of Paroxysmal Nocturnal Hemoglobinuria. *Blood*, *126*(23). http://www.bloodjournal.org/content/126/23/939?sso-checked=true

Richards, A., Buddles, M. R., Donne, R. L., Kaplan, B. S., Kirk, E., Venning, M. C., Goodship, T. H. J. (2001). Factor H mutations in hemolytic uremic syndrome cluster in exons 18-20, a domain important for host cell recognition. *American Journal of Human Genetics*, *68*(2), 485–490. https://doi.org/10.1086/318203

Richards, A., Kemp, E. J., Liszewski, M. K., Goodship, J. A., Lampe, A. K., Decorte, R., Goodship, T. H. J. (2003). Mutations in human complement regulator, membrane cofactor protein (CD46), predispose to development of familial hemolytic uremic syndrome. *Proceedings of the National Academy of Sciences of the United States of America*, *100*(22), 12966–12971. https://doi.org/10.1073/pnas.2135497100

Ricklin, D., Mastellos, D. C., Reis, E. S., & Lambris, J. D. (2017). The renaissance of complement therapeutics. *Nature Reviews Nephrology*, 14(1):26-47. https://doi.org/10.1038/nrneph.2017.156

Rinder, C. S., Rinder, H. M., Smith, M. J., Tracey, J. B., Fitch, J., Li, L., Smith, B. R. (1999). Selective blockade of membrane attack complex formation during simulated extracorporeal circulation inhibits platelet but not leukocyte activation. *Journal of Thoracic and Cardiovascular Surgery*, *118*(3), 460–466. https://doi.org/10.1016/S0022-5223(99)70183-2

Risitano, A. M., Notaro, R., Marando, L., Serio, B., Ranaldi, D., Seneca, E., Rotoli, B. (2009). Complement fraction 3 binding on erythrocytes as additional mechanism of disease in paroxysmal nocturnal hemoglobinuria patients treated by eculizumab. *Blood*, *113*(17), 4094–4100. https://doi.org/10.1182/blood-2008-11-189944

Rodríguez De Córdoba, S., Hidalgo, M. S., Pinto, S., & Tortajada, A. (2014). Genetics of atypical hemolytic uremic syndrome (aHUS). *Seminars in Thrombosis and Hemostasis*, *40*(4), 422–430. https://doi.org/10.1055/s-0034-1375296

Rogers, J., Schultz, J., Brachova, L., Lue, L. F., Webster, S., Bradt, B., Moss, D. E. (1992). Complement activation and beta-amyloid-mediated neurotoxicity in Alzheimer's disease. *Research in Immunology*, *143*(6), 624–630. http://www.ncbi.nlm.nih.gov/pubmed/1455054

Rogers, J., Cooper, N. R., Webster, S., Schultz, J., McGeer, P. L., Styren, S. D., Lieberburg, I. (1992). Complement activation by β-amyloid in Alzheimer disease. *Proceedings of the National Academy of Sciences of the United States of America*, *89*(21), 10016–10020. https://doi.org/10.1073/pnas.89.21.10016

Rollins , S., A., Matis, L., A., Springhorn, J., P., Setter, E., Wolff, D., W. (1995). Monoclonal antibodies directed against human C5 and C8 block complement-mediated damage of xenogeneic cells and organs. *Transplantation*, 60(11):1284-92. http://www.ncbi.nlm.nih.gov/pubmed/8525523

Rollins, S. A., & Sims, P. J. (1990). The complement-inhibitory activity of CD59 resides in its capacity to block incorporation of C9 into membrane C5b-9. *Journal of Immunology*, *144*(9), 3478–3483. http://www.ncbi.nlm.nih.gov/pubmed/1691760

Rooney, I. A., Atkinson, J. P., Krul, E. S., Schonfeld, G., Polakoski, K., Saffitz, J. E., & Morgan, B. P. (1993). Physiologic Relevance of the Membrane Attack Complex Inhibitory Protein CD59 in Human Seminal Plasma: CD59 Is Present on Extraceilular Organelles (Prostasomes), BindsCell Membranes, and Inhibits Complement-mediated Lysis. *Journal of Experimental Medicine*, *177*(5), 1409–1420. https://doi.org/10.1084/jem.177.5.1409

Rosado, C. J., Buckle, A. M., Law, R. H. P., Butcher, R. E., Kan, W. T., Bird, C. H., Whisstock, J. C. (2007). A common fold mediates vertebrate defense and bacterial attack. *Science*, *317*(5844), 1548–1551. https://doi.org/10.1126/science.1144706

Rosenling, T., Stoop, M. P., Attali, A., van Aken, H., Suidgeest, E., Christin, C., Luider, T. M. (2012). Profiling and identification of cerebrospinal fluid proteins in a rat EAE model of multiple sclerosis. *Journal of Proteome Research*, *11*(4), 2048–2060. https://doi.org/10.1021/pr201244t

Rother, R. P., Rollins, S. A., Mojcik, C. F., Brodsky, R. A., & Bell, L. (2007). Discovery and development of the complement inhibitor eculizumab. *Nature Biotechnology*, *25*(11), 1256–1264. https://doi.org/10.1038/nbt1344

Roumenina, L. T., Loirat, C., Dragon-Durey, M. A., Halbwachs-Mecarelli, L., Sautes-Fridman, C., & Fremeaux-Bacchi, V. (2011). Alternative complement pathway assessment in patients with atypical HUS. *Journal of Immunological Methods*, 365(1-2):8-26. https://doi.org/10.1016/j.jim.2010.12.020

Rudd, P. M., Paul Morgan, B., Wormald, M. R., Harvey, D. J., van den Berg, C. W., Davis, S. J., Dwek, R. A. (1998). The Glycosylation of the Complement Regulatory Protein, Human Erythrocyte CD59. *Advances in Experimental Medicine and Biology,* 435:153-62.. https://doi.org/10.1007/978-1-4615-5383-0_15

Rus, H. G., Niculescu, F., & Shin, M. L. (1996). Sublytic complement attack induces cell cycle in oligodendrocytes. *Journal of Immunology*, *156*(12), 4892–4900. http://www.ncbi.nlm.nih.gov/pubmed/8648139

Sacks, S. H. (2010). Complement fragments C3a and C5a: The salt and pepper of the immune response. *European Journal of Immunology*, 40(3):668-70.. https://doi.org/10.1002/eji.201040355

Sahashi, K., Engel, A. G., Lindstrom, J. M., Lambert, E. H., & Lennon, V. A. (1978). Ultrastructural localization of immune complexes (igg and c3) at the end-plate in experimental autoimmune myasthenia gravis. *Journal of Neuropathology and Experimental Neurology*, *37*(2), 212–223. https://doi.org/10.1097/00005072-197803000-00008

Sampei, Z., Haraya, K., Tachibana, T., Fukuzawa, T., Shida-Kawazoe, M., Gan, S. W., Nezu, J. (2018). Antibody engineering to generate SKY59, a long-acting anti-C5 recycling antibody. *PLoS ONE*, *13*(12). https://doi.org/10.1371/journal.pone.0209509

Samstad, E. O., Niyonzima, N., Nymo, S., Aune, M. H., Ryan, L., Bakke, S. S., Espevik, T. (2014). Cholesterol Crystals Induce Complement-Dependent Inflammasome Activation and Cytokine Release. *The Journal of Immunology*, *192*(6), 2837–2845. https://doi.org/10.4049/jimmunol.1302484

Santoro, F., Kennedy, P. E., Locatelli, G., Malnati, M. S., Berger, E. A., & Lusso, P. (1999). CD46 is a cellular receptor for human herpesvirus 6. *Cell*, *99*(7), 817–827. https://doi.org/10.1016/s0092-8674(00)81678-5

Saxena, A., & Wu, D. (2016). Advances in therapeutic Fc engineering - modulation of IgG-associated effector functions and serum half-life. *Frontiers in Immunology*, 7:580. https://doi.org/10.3389/fimmu.2016.00580

Schatz-Jakobsen, J. A., Zhang, Y., Johnson, K., Neill, A., Sheridan, D., & Andersen, G. R. (2016). Structural Basis for Eculizumab-Mediated Inhibition of the Complement Terminal Pathway. *The Journal of Immunology*, *197*(1), 337–344. https://doi.org/10.4049/jimmunol.1600280

Schubart, A., Anderson, K., Mainolfi, N., Sellner, H., Ehara, T., Adams, C. M., Eder, J. (2019). Small-molecule factor B inhibitor for the treatment of complement-mediated

diseases. *Proceedings of the National Academy of Sciences of the United States of America*, *116*(16), 7926–7931. https://doi.org/10.1073/pnas.1820892116

Schur, P. H., & Austen, K. F. (1968). Complement in Human Disease. *Annual Review of Medicine*, *19*(1), 1–24. https://doi.org/10.1146/annurev.me.19.020168.000245

Schutte, M., DiCamelli, R., Murphy, P., Sadove, M., & Gewurz, H. (1975). Effects of anesthesia, surgery and inflammation upon host defense mechanisms. I. Effects upon the complement system. *International Archives of Allergy and Applied Immunology*, *48*(5), 706–720. https://doi.org/10.1159/000231358

Segerman, A., Atkinson, J. P., Marttila, M., Dennerquist, V., Wadell, G., & Arnberg, N. (2003). Adenovirus Type 11 Uses CD46 as a Cellular Receptor. *Journal of Virology*, *77*(17), 9183–9191. https://doi.org/10.1128/jvi.77.17.9183-9191.2003

Servais, A., Noël, L. H., Roumenina, L. T., Le Quintrec, M., Ngo, S., Dragon-Durey, M. A., Frémeaux-Bacchi, V. (2012). Acquired and genetic complement abnormalities play a critical role in dense deposit disease and other C3 glomerulopathies. *Kidney International*, *82*(4), 454–464. https://doi.org/10.1038/ki.2012.63

Skattum, L., Van Deuren, M., Van Der Poll, T., & Truedsson, L. (2011). Complement deficiency states and associated infections. *Molecular Immunology*, 48(14):1643-55. https://doi.org/10.1016/j.molimm.2011.05.001

Skerka, C., Licht, C., Mengel, M., Uzonyi, B., Strobel, S., Zipfel, P. F., & Józsi, M. (2009). Autoimmune forms of thrombotic micorangiopathy and membranoproliferative glomerulonephritis: Indications for a disease spectrum and common pathogenic principles. *Molecular Immunology,* 46(14):2801-7. https://doi.org/10.1016/j.molimm.2009.05.018

Sethi, S., & Fervenza, F. C. (2014). Pathology of renal diseases associated with dysfunction of the alternative pathway of complement: C3 glomerulopathy and atypical hemolytic uremic syndrome (aHUS). *Seminars in Thrombosis and Hemostasis*, *40*(4), 416–421. https://doi.org/10.1055/s-0034-1375701

Sharp, T. H., Faas, F. G. A., Koster, A. J., & Gros, P. (2017). Imaging complement by phase-plate cryo-electron tomography from initiation to pore formation. *Journal of Structural Biology*, *197*(2), 155–162. https://doi.org/10.1016/j.jsb.2016.09.008

Shatursky, O., Heuck, A. P., Shepard, L. A., Rossjohn, J., Parker, M. W., Johnson, A. E., & Tweten, R. K. (1999). The mechanism of membrane insertion for a cholesterol-dependent cytolysin: A novel paradigm for pore-forming toxins. *Cell*, *99*(3), 293–299. https://doi.org/10.1016/S0092-8674(00)81660-8

Sheerin, N. S., Kavanagh, D., Goodship, T. H. J., & Johnson, S. (2016). A national specialized service in England for atypical haemolytic uraemic syndrome-the first year's experience. *QJM*, *109*(1), 27–33. https://doi.org/10.1093/qjmed/hcv082

Sheridan, D., Yu, Z. X., Zhang, Y., Patel, R., Sun, F., Lasaro, M. A., … Tamburini, P. (2018). Design and preclinical characterization of ALXN1210: A novel anti-C5 antibody with

extended duration of action. *PLoS ONE*, *13*(4). https://doi.org/10.1371/journal.pone.0195909

Shin, H. S., Gewurz, H., & Snyderman, R. (1969). Reaction of a Cobra Venom Factor with Guinea Pig Complement and Generation of an Activity Chemotactic for Polymorphonuclear Leukocytes. *Proceedings of the Society for Experimental Biology and Medicine*, *131*(1), 203–207. https://doi.org/10.3181/00379727-131-33840

Sim, R. B., Schwaeble, W., & Fujita, T. (2016). Complement research in the 18th–21st centuries: Progress comes with new technology. *Immunobiology*, 221(10):1037-45. https://doi.org/10.1016/j.imbio.2016.06.011

Sim, E., & Sim, R. B. (1981). Binding of fluid-phase complement components C3 and C3b to human lymphocytes. *Biochemical Journal*, *198*(3), 509–518. https://doi.org/10.1042/bj1980509

Sim, R. B., & DiScipio, R. G. (1982). Purification and structural studies on the complement-system control protein β1H (factor H). *Biochemical Journal*, *205*(2), 285–293. https://doi.org/10.1042/bj2050285

Sniderman, A. D., & Cianflone, K. (1994). The adipsin-ASP pathway and regulation of adipocyte function. *Annals of Medicine*, *26*(6), 388–393. http://www.ncbi.nlm.nih.gov/pubmed/7695862

Singh, A., Faber, C., Falk, M., Nissen, M. H., Hviid, T. V. F., & Sørensen, T. L. (2012). Altered expression of CD46 and CD59 on leukocytes in neovascular age-related macular degeneration. *American Journal of Ophthalmology*, *154*(1), 193–199.e2. https://doi.org/10.1016/j.ajo.2012.01.036

Singh, B., Su, Y. C., & Riesbeck, K. (2010). Vitronectin in bacterial pathogenesis: A host protein used in complement escape and cellular invasion. *Molecular Microbiology*, 78(3):545-60. https://doi.org/10.1111/j.1365-2958.2010.07373.x

Singhrao, S. K., Neal, J. W., Morgan, B. P., & Gasque, P. (1999). Increased complement biosynthesis by microglia and complement activation on neurons in Huntington's disease. *Experimental Neurology*, *159*(2), 362–376. https://doi.org/10.1006/exnr.1999.7170

Cashman, S. M., Ramo, K., & Kumar-Singh, R. (2011). A non membrane-targeted human soluble CD59 attenuates choroidal neovascularization in a model of age related macular degeneration. *PLoS ONE*, *6*(4). https://doi.org/10.1371/journal.pone.0019078

Socié, G., Caby-Tosi, M. P., Marantz, J. L., Cole, A., Bedrosian, C. L., Gasteyger, C., Haller, H. (2019). Eculizumab in paroxysmal nocturnal haemoglobinuria and atypical haemolytic uraemic syndrome: 10-year pharmacovigilance analysis. *British Journal of Haematology*, *185*(2), 297–310. https://doi.org/10.1111/bjh.15790

Sohn, J. H., Kaplan, H. J., Suk, H. J., Bora, P. S., & Bora, N. S. (2000). Chronic low level complement activation within the eye is controlled by intraocular complement regulatory proteins. *Investigative Ophthalmology & Visual Science*, *41*(11), 3492–3502. http://www.ncbi.nlm.nih.gov/pubmed/11006244

Song, H., He, C., Knaak, C., Guthridge, J. M., Holers, V. M., & Tomlinson, S. (2003). Complement receptor 2-mediated targeting of complement inhibitors to sites of complement activation. *Journal of Clinical Investigation*, *111*(12), 1875–1885. https://doi.org/10.1172/JCI17348

Soni, V., Kohli, D. V., & Jain, S. K. (2005). Transferrin coupled liposomes as drug delivery carriers for brain targeting of 5-florouracil. *Journal of Drug Targeting*, *13*(4), 245–250. https://doi.org/10.1080/10611860500107401

Spicer, B. A., Law, R. H. P., Caradoc-Davies, T. T., Ekkel, S. M., Bayly-Jones, C., Pang, S. S., Dunstone, M. A. (2018). The first transmembrane region of complement component-9 acts as a brake on its self-assembly. *Nature Communications*, *9*(1). https://doi.org/10.1038/s41467-018-05717-0

Stahel, P. F., Trentz, O., Kossmann, T., Morganti-Kossmann, M. C., Perez, D., Redaelli, C., & Gloor, B. (2001). Intrathecal levels of complement-derived soluble membrane attack complex (sc5b-9) correlate with blood-brain barrier dysfunction in patients with traumatic brain injury. *Journal of Neurotrauma*, *18*(8), 773–781. https://doi.org/10.1089/089771501316919139

Stegall, M. D., Chedid, M. F., & Cornell, L. D. (2012). The role of complement in antibody-mediated rejection in kidney transplantation. *Nature Reviews Nephrology*, 8(11):670-8. https://doi.org/10.1038/nrneph.2012.212

Stein, K. R., Gardner, T. J., Hernandez, R. E., Kraus, T. A., Duty, J. A., Ubarretxena-Belandia, I., Tortorella, D. (2019). CD46 facilitates entry and dissemination of human cytomegalovirus. *Nature Communications*, 10(1):2699. https://doi.org/10.1038/s41467-019-10587-1

Stephan, A. H., Barres, B. A., & Stevens, B. (2012). The Complement System: An Unexpected Role in Synaptic Pruning During Development and Disease. *Annual Review of Neuroscience*, *35*(1), 369–389. https://doi.org/10.1146/annurev-neuro-061010-113810

Stephan, A. H., Madison, D. V., Mateos, J. M., Fraser, D. A., Lovelett, E. A., Coutellier, L., Barres, B. A. (2013). A dramatic increase of C1q protein in the CNS during normal aging. *Journal of Neuroscience*, *33*(33), 13460–13474. https://doi.org/10.1523/JNEUROSCI.1333-13.2013

Strang, C. J., Siegel, R. C., Phillips, M. L., Poon, P. H., & Schumaker, V. N. (1982). Ultrastructure of the first component of human complement: Electron microscopy of the crosslinked complex. *Proceedings of the National Academy of Sciences of the United States of America*, *79*(2 I), 586–590. https://doi.org/10.1073/pnas.79.2.586

Strey, C. W., Markiewski, M., Mastellos, D., Tudoran, R., Spruce, L. A., Greenbaum, L. E., & Lambris, J. D. (2003). The proinflammatory mediators C3a and C5a are essential for liver regeneration. *Journal of Experimental Medicine*, *198*(6), 913–923. https://doi.org/10.1084/jem.20030374

Sugita, Y., Nakano, Y., & Tomita, M. (1988). Isolation from human erythrocytes of a new membrane protein which inhibits the formation of complement transmembrane channels. *Journal of Biochemistry*, *104*(4), 633–637. https://doi.org/10.1093/oxfordjournals.jbchem.a122524

Sugita, Y., & Masuho, Y. (1995). CD59: its role in complement regulation and potential for therapeutic use. *Immunotechnology : An International Journal of Immunological Engineering*, *1*(3–4), 157–168. http://www.ncbi.nlm.nih.gov/pubmed/9373344

Susuki, K., Rasband, M. N., Tohyama, K., Koibuchi, K., Okamoto, S., Funakoshi, K.,Yuki, N. (2007). Anti-GM1 antibodies cause complement-mediated disruption of sodium channel clusters in peripheral motor nerve fibers. *Journal of Neuroscience*, *27*(15), 3956–3967. https://doi.org/10.1523/JNEUROSCI.4401-06.2007

Suzuki, H., Yamaji, N., Egashira, A., Yasunaga, K., Sugita, Y., & Masuho, Y. (1996). Effect of the sugar chain of soluble recombinant CD59 on complement inhibitory activity. *FEBS Letters*, *399*(3), 272–276. https://doi.org/10.1016/s0014-5793(96)01340-3

Tack, B. F., Morris, S. C., Prahl, J. W., Morris, S. C., & Tack, B. F. (1979). Fifth Component of Human Complement: Purification from Plasma and Polypeptide Chain Structure. *Biochemistry*, *18*(8), 1490–1497. https://doi.org/10.1021/bi00575a016

Tacnet-Delorme, P., Chevallier, S., & Arlaud, G. J. (2001). β-Amyloid Fibrils Activate the C1 Complex of Complement Under Physiological Conditions: Evidence for a Binding Site for Aβ on the C1q Globular Regions. *The Journal of Immunology*, *167*(11), 6374–6381. https://doi.org/10.4049/jimmunol.167.11.6374

Tai, J. H., Sun, H., Liu, W., Melling, C. W. J., Hasilo, C., & White, D. J. G. (2008). Isolating human islets of langerhans causes loss of decay accelerating factor (CD55) on B-cells. *Cell Transplantation*, *17*(12), 1349–1359. https://doi.org/10.3727/096368908787648092

Takahashi, M., Ishida, Y., Iwaki, D., Kanno, K., Suzuki, T., Endo, Y., Fujita, T. (2010). Essential role of mannose-binding lectin-associated serine protease-1 in activation of the complement factor D. *The Journal of Experimental Medicine*, *207*(1), 29–37. https://doi.org/10.1084/jem.20090633

Takeda, J., Miyata, T., Kawagoe, K., Iida, Y., Endo, Y., Fujita, T., Kinoshita, T. (1993). Deficiency of the GPI anchor caused by a somatic mutation of the PIG-A gene in paroxysmal nocturnal hemoglobinuria. *Cell*, *73*(4), 703–711. https://doi.org/10.1016/0092-8674(93)90250-t

Tanuma, Y., Ohi, H., & Hatano, M. (1990). Two types of C3 nephritic factor: properdin-dependent C3NeF and properdin-independent C3NeF. *Clinical Immunology and Immunopathology*, *56*(2), 226–238. https://doi.org/10.1016/0090-1229(90)90144-f

Tatomir, A., Talpos-Caia, A., Anselmo, F., Kruszewski, A. M., Boodhoo, D., Rus, V. The complement system as a biomarker of disease activity and response to treatment in multiple sclerosis. Immunol Res. (2017) 65:1103–9. https://doi.org/10.1007/s12026-017-8961-8

Tedesco, F., Pausa, M., Nardon, E., Introna, M., Mantovani, A., & Dobrina, A. (1997). The cytolytically inactive terminal complement complex activates endothelial cells to express adhesion molecules and tissue factor procoagulant activity. *Journal of Experimental Medicine*, *185*(9), 1619–1627. https://doi.org/10.1084/jem.185.9.1619

Tegla, C. A., Cudrici, C., Patel, S., Trippe, R., Rus, V., Niculescu, F., & Rus, H. (2011). Membrane attack by complement: The assembly and biology of terminal complement

complexes. *Immunologic Research*, *51*(1), 45–60. https://doi.org/10.1007/s12026-011-8239-5

Teillet, F., Dublet, B., Andrieu, J.-P., Gaboriaud, C., Arlaud, G. J., & Thielens, N. M. (2005). The Two Major Oligomeric Forms of Human Mannan-Binding Lectin: Chemical Characterization, Carbohydrate-Binding Properties, and Interaction with MBL-Associated Serine Proteases. *The Journal of Immunology*, *174*(5), 2870–2877. https://doi.org/10.4049/jimmunol.174.5.2870

Tesar, V., & Hruskova, Z. (2018). Avacopan in the treatment of ANCA-associated vasculitis. *Expert Opinion on Investigational Drugs*, *27*(5), 491–496. https://doi.org/10.1080/13543784.2018.1472234

Thai, C.-T., & Ogata, R. T. (2004). Complement Components C5 and C7: Recombinant Factor I Modules of C7 Bind to the C345C Domain of C5. *The Journal of Immunology*, *173*(7), 4547–4552. https://doi.org/10.4049/jimmunol.173.7.4547

Thai, C.-T., & Ogata, R. T. (2005). Recombinant C345C and Factor I Modules of Complement Components C5 and C7 Inhibit C7 Incorporation into the Complement Membrane Attack Complex. *The Journal of Immunology*, *174*(10), 6227–6232. https://doi.org/10.4049/jimmunol.174.10.6227

Thakkinstian, A., Han, P., McEvoy, M., Smith, W., Hoh, J., Magnusson, K., Attia, J. (2006). Systematic review and meta-analysis of the association between complementary factor H Y402H polymorphisms and age-related macular degeneration. *Human Molecular Genetics*, 5(2):242-6. https://doi.org/10.1093/hmg/ddl220

Thai, C.-T., & Ogata, R. T. (2003). Expression and Characterization of the C345C/NTR Domains of Complement Components C3 and C5. *The Journal of Immunology*, *171*(12), 6565–6573. https://doi.org/10.4049/jimmunol.171.12.6565

The Guillain-Barré syndrome Study Group. Plasmapheresis and acute Guillain-Barré syndrome. (1985). *Neurology*, *35*(8), 1096–1104. http://www.ncbi.nlm.nih.gov/pubmed/4022342

Thiel, S., Vorup-Jensen, T., Stover, C. M., Schwaeble, W., Laursen, S. B., Poulsen, K., Jensenius, J. C. (1997). A second serine protease associated with mannan-binding lectin that activates complement. *Nature*, *386*(6624), 506–510. https://doi.org/10.1038/386506a0

Thiel, S. (2007). Complement activating soluble pattern recognition molecules with collagen-like regions, mannan-binding lectin, ficolins and associated proteins. *Molecular Immunology*, 44(16):3875-88. https://doi.org/10.1016/j.molimm.2007.06.005

Thielens, N. M., Tedesco, F., Bohlson, S. S., Gaboriaud, C., & Tenner, A. J. (2017). C1q: A fresh look upon an old molecule. *Molecular Immunology,* 89, 73–83. https://doi.org/10.1046/j.1365-2249.1997.d01-890.x

Thurman, J. M. (2015). Complement in kidney disease: Core curriculum 2015. *American Journal of Kidney Diseases*, *65*(1), 156–168. https://doi.org/10.1053/j.ajkd.2014.06.035

Thurman, J. M., Lucia, M. S., Ljubanovic, D., & Holers, V. M. (2005). Acute tubular necrosis is characterized by activation of the alternative pathway of complement. *Kidney International*, *67*(2), 524–530. https://doi.org/10.1111/j.1523-1755.2005.67109.x

Thomas, T. C., Rollins, S. A., Rother, R. P., Giannoni, M. A., Hartman, S. L., Elliott, E. A., Evans, M. J. (1996). Inhibition of complement activity by humanized anti-C5 antibody and single-chain Fv. *Molecular Immunology*, *33*(17–18), 1389–1401. http://www.ncbi.nlm.nih.gov/pubmed/9171898

Till, G. O., Johnson, K. J., Kunkel, R., & Ward, P. A. (1982). Intravascular activation of complement and acute lung injury. Dependency on neutrophils and toxic oxygen metabolites. *Journal of Clinical Investigation*, *69*(5), 1126–1135. https://doi.org/10.1172/JCI110548

Triantafilou, K., Hughes, T. R., Triantafilou, M., & Morgan, P. P. (2013). The complement membrane attack complex triggers intracellular Ca 2+ fluxes leading to NLRP3 inflammasome activation. *Journal of Cell Science*, *126*(13), 2903–2913. https://doi.org/10.1242/jcs.124388

Tschopp, J., Villiger, W., Fuchs, H., Kilchherr, E., & Engel, J. (1980). Assembly of subcomponents C1r and C1s of first component of complement: Electron microscopic and ultracentrifugal studies. *Proceedings of the National Academy of Sciences of the United States of America*, *77*(12 II), 7014–7018. https://doi.org/10.1073/pnas.77.12.7014

Tschopp, J., Chonn, A., Hertig, S., & French, L. E. (1993). Clusterin, the human apolipoprotein and complement inhibitor, binds to complement C7, C8 beta, and the b domain of C9. *Journal of Immunology*, *151*(4), 2159–2165. http://www.ncbi.nlm.nih.gov/pubmed/8345200

Tsuruta, J. K., Wong, K., Fritz, I. B., & Griswold, M. D. (1990). Structural analysis of sulphated glycoprotein 2 from amino acid sequence. Relationship to clusterin and serum protein 40,40. *Biochemical Journal*, *268*(3), 571–578. https://doi.org/10.1042/bj2680571

Väkevä, A., Lehto, T., Takala, A., & Meri, S. (2000). Detection of a soluble form of the complement membrane attack complex inhibitor CD59 in plasma after acute myocardial infarction. *Scandinavian Journal of Immunology*, *52*(4), 411–414. https://doi.org/10.1046/j.1365-3083.2000.00783.x

van Beek, J., Nicole, O., Ali, C., Ischenko, A., MacKenzie, E. T., Buisson, A., & Fontaine, M. (2001). Complement anaphylatoxin C3a is selectively protective against NMDA-induced neuronal cell death. *Neuroreport*, *12*(2), 289–293. https://doi.org/10.1097/00001756-200102120-00022

Van Den Broek, B., Van Der Flier, M., De Groot, R., De Jonge, M. I., & Langereis, J. D. (2019). Common genetic variants in the complement system and their potential link with disease susceptibility and outcome of invasive bacterial infection. *Journal of Innate Immunity*, 1-11. https://doi.org/10.1159/000500545

van Schaarenburg, R. A., Magro-Checa, C., Bakker, J. A., Teng, Y. K. O., Bajema, I. M., Huizinga, T. W., Trouw, L. A. (2016). C1q deficiency and neuropsychiatric systemic lupus erythematosus. *Frontiers in Immunology*, 7:647. https://doi.org/10.3389/fimmu.2016.00647

Veerhuis, R., van der Valk, P., Janssen, I., Zhan, S. S., Eikelenboom, P., & Van Nostrand, W. E. (1995). Complement activation in amyloid plaques in Alzheimer's disease brains does not proceed further than C3. *Virchows Archiv*, *426*(6), 603–610. https://doi.org/10.1007/BF00192116

Villiers, C. L., Arlaud, G. J., & Colomb, M. G. (1985). Domain structure and associated functions of subcomponents C1r and C1s of the first component of human complement. *Proceedings of the National Academy of Sciences of the United States of America*, *82*(13), 4477–4481. https://doi.org/10.1073/pnas.82.13.4477

Vogel, C.-W., & Fritzinger, D. (2007). Humanized Cobra Venom Factor: Experimental Therapeutics for Targeted Complement Activation and Complement Depletion. *Current Pharmaceutical Design*, *13*(28), 2916–2926. https://doi.org/10.2174/138161207782023748

Vogel, C. W., Fritzinger, D. C., Gorsuch, W. B., & Stahl, G. L. (2015). Complement depletion with humanised cobra venom factor: Efficacy in preclinical models of vascular diseases. *Thrombosis and Haemostasis*, *113*(3), 548–552. https://doi.org/10.1160/TH14-04-0300

Vogel, C. W., Finnegan, P. W., & Fritzinger, D. C. (2014). Humanized cobra venom factor: Structure, activity, and therapeutic efficacy in preclinical disease models. *Molecular Immunology*, 61(2):191-203. https://doi.org/10.1016/j.molimm.2014.06.035

Vogt, W. (2000). Cleavage of the fifth component of complement and generation of a functionally active C5b6-like complex by human leukocyte elastase. *Immunobiology*, *201*(3–4), 470–477. https://doi.org/10.1016/S0171-2985(00)80099-6

Volz, C., & Pauly, D. (2015). Antibody therapies and their challenges in the treatment of age-related macular degeneration. *European Journal of Pharmaceutics and Biopharmaceutics*, *95*, 158–172. https://doi.org/10.1016/j.ejpb.2015.02.020

Vugmeyster, Y., Xu, X., Theil, F.-P., Khawli, L. A., & Leach, M. W. (2012). Pharmacokinetics and toxicology of therapeutic proteins: Advances and challenges. *World Journal of Biological Chemistry*, *3*(4), 73–92. https://doi.org/10.4331/wjbc.v3.i4.73

Wakabayashi, K., Tanji, K., Mori, F., & Takahashi, H. (2007). The Lewy body in Parkinson's disease: molecules implicated in the formation and degradation of alpha-synuclein aggregates. *Neuropathology : Official Journal of the Japanese Society of Neuropathology*, *27*(5), 494–506. http://www.ncbi.nlm.nih.gov/pubmed/18018486

Walport, M. J., & Walport, C. M. J. (2002). Complement and systemic lupus erythematosus Complement and SLE : the clinical observations. *Arthritis Research & Therapyvolume,* 4(S279),1–28. https://doi.org/10.1186/ar586

Wang, X., Zhang, D., Sjölinder, M., Wan, Y., & Sjölinder, H. (2017). CD46 accelerates macrophage-mediated host susceptibility to meningococcal sepsis in a murine model. *European Journal of Immunology*, *47*(1), 119–130. https://doi.org/10.1002/eji.201646397

Wang, Y., Hancock, A. M., Bradner, J., Chung, K. A., Quinn, J. F., Peskind, E. R., Zhang, J. (2011). Complement 3 and factor H in human cerebrospinal fluid in Parkinson's

disease, Alzheimer's disease, and multiple-system atrophy. *American Journal of Pathology*, *178*(4), 1509–1516. https://doi.org/10.1016/j.ajpath.2011.01.006

Ware, C. F., Wetsel, R. A., & Kolb, W. P. (1981). Physicochemical characterization of fluid phase (SC5b-9) and membrane derived (MC5b-9) attack complexes of human complement purified by immunoadsorbent affinity chromatography or selective detergent extraction. *Molecular Immunology*, *18*(6), 521–531. https://doi.org/10.1016/0161-5890(81)90130-9

Ware, C. F., & Kolb, W. P. (1981). Assembly of the functional membrane attack complex of human complement: Formation of disulfide-linked C9 dimers. *Proceedings of the National Academy of Sciences of the United States of America*, *78*(10 I), 6426–6430. https://doi.org/10.1073/pnas.78.10.6426

Warwicker, P., Goodship, T. H. J., Donne, R. L., Pirson, Y., Nicholls, A., Ward, R. M., Goodship, J. A. (1998). Genetic studies into inherited and sporadic hemolytic uremic syndrome. *Kidney International*, *53*(4), 836–844. https://doi.org/10.1111/j.1523-1755.1998.00824.x

Weisman, H. F., Bartow, T., Leppo, M. K., Marsh, H. C., Carson, G. R., Concino, M. F., Fearon, D. T. (1990). Soluble human complement receptor type 1: In vivo inhibitor of complement suppressing post-ischemic myocardial inflammation and necrosis. *Science*, *249*(4965), 146–151. https://doi.org/10.1126/science.2371562

Weiss, V., Fauser, C., & Engel, J. (1986). Functional model of subcomponent C1 of human complement. *Journal of Molecular Biology*, *189*(3), 573–581. https://doi.org/10.1016/0022-2836(86)90325-6

Wetsel, R. A. (1995). Structure, function and cellular expression of complement anaphylatoxin receptors. *Current Opinion in Immunology*, *7*(1), 48–53. http://www.ncbi.nlm.nih.gov/pubmed/7772282

Wheeler, S. F., Rudd, P. M., Davis, S. J., Dwek, R. A., & Harvey, D. J. (2002). Comparison of the N-linked glycans from soluble and GPI-anchord CD59 expressed in CHO cells. *Glycobiology*, *12*(4), 261–271. https://doi.org/10.1093/glycob/12.4.261

Williams, P., Chaudhry, Y., Goodfellow, I. G., Billington, J., Powell, R., Spiller, O. B., Lea, S. (2003). Mapping CD55 function. The structure of two pathogen-binding domains at 1.7 Å. *Journal of Biological Chemistry*, *278*(12), 10691–10696. https://doi.org/10.1074/jbc.M212561200

Wong, E. K. S., Goodship, T. H. J., & Kavanagh, D. (2013). Complement therapy in atypical haemolytic uraemic syndrome (aHUS). *Molecular Immunology*, *56*(3), 199–212. https://doi.org/10.1016/j.molimm.2013.05.224

Wong, E. K. S., & Kavanagh, D. (2018). Diseases of complement dysregulation—an overview. *Seminars in Immunopathology*, 40(1):49-64. https://doi.org/10.1007/s00281-017-0663-8

Woodruff, T. M., Strachan, A. J., Dryburgh, N., Shiels, I. A., Reid, R. C., Fairlie, D. P., & Taylor, S. M. (2002). Antiarthritic activity of an orally active C5a receptor antagonist against antigen-induced monarticular arthritis in the rat. *Arthritis and Rheumatism*, *46*(9), 2476–2485. https://doi.org/10.1002/art.10449

Woodruff, T. M., Crane, J. W., Proctor, L. M., Buller, K. M., Shek, A. B., De Vos, K., Taylor, S. M. (2006). Therapeutic activity of C5a receptor antagonists in a rat model of neurodegeneration. *FASEB Journal*, *20*(9), 1407–1417. https://doi.org/10.1096/fj.05-5814com

Wren, D. R., & Noble, M. (1989). Oligodendrocytes and oligodendrocyte/type-2 astrocyte progenitor cells of adult rats are specifically susceptible to the lytic effects of complement in absence of antibody. *Proceedings of the National Academy of Sciences of the United States of America*, *86*(22), 9025–9029. https://doi.org/10.1073/pnas.86.22.9025

Wright, K. (1989). Antibodies a laboratory manual: By E Harlow and D Lane. pp 726. Cold Spring Harbor Laboratory. 1988. $50 ISBN 0-87969-314-2. *Biochemical Education*, *17*(4), 220. https://doi.org/10.1016/0307-4412(89)90165-9

Wu, J., Wu, Y. Q., Ricklin, D., Janssen, B. J. C., Lambris, J. D., & Gros, P. (2009). Structure of complement fragment C3b-factor H and implications for host protection by complement regulators. *Nature Immunology*, *10*(7), 728–733. https://doi.org/10.1038/ni.1755

Würzner, R., Joysey, V. C., & Lachmann, P. J. (1994). Complement component C7. Assessment of in vivo synthesis after liver transplantation reveals that hepatocytes do not synthesize the majority of human C7. *Journal of Immunology*, *152*(9), 4624–4629. http://www.ncbi.nlm.nih.gov/pubmed/8157976

Würzner, R., Orren, A., & Lachmann, P. J. (1992). Inherited deficiencies of the terminal components of human complement. *Immunodeficiency Reviews*, *3*(2), 123–147. http://www.ncbi.nlm.nih.gov/pubmed/1554498

Würzner, R., Schulze, M., Happe, L., Franzke, A., Bieber, F.A., Oppermann, M., Götze, O. (1991) Inhibition of terminal complement complex formation and cell lysis by monoclonal antibodies. *Complement Inflamation, 8(5-6):328-40.*328–40. http://www.ncbi.nlm.nih.gov/pubmed/1724954

Würzner, R., Fernie, B. A., Jones, A. M., Lachmann, P. J., & Hobart, M. J. (1995). Molecular basis of the complement C7 M/N polymorphism. A neutral amino acid substitution outside the epitope of the allospecific monoclonal antibody WU 4-15. *Journal of Immunology*, *154*(9), 4813–4819. http://www.ncbi.nlm.nih.gov/pubmed/7722329

Würzner, R. (2000). Modulation of complement membrane attack by local C7 synthesis. *Clinical and Experimental Immunology*, *121*(1), 8–10. https://doi.org/10.1046/j.1365-2249.2000.01263.x

Wyss-Coray, T., Yan, F., Lin, A. H. T., Lambris, J. D., Alexander, J. J., Quigg, R. J., & Masliah, E. (2002). Prominent neurodegeneration and increased plaque formation in complement-inhibited Alzheimer's mice. *Proceedings of the National Academy of Sciences of the United States of America*, *99*(16), 10837–10842. https://doi.org/10.1073/pnas.162350199

Yamaguchi, N., Misawa, S., Sato, Y., Nagashima, K., Katayama, K., Sekiguchi, Y., … Kuwabara, S. (2016). A Prospective, Multicenter, Randomized Phase II Study to Evaluate the Efficacy and Safety of Eculizumab in Patients with Guillain-Barré Syndrome (GBS): Protocol of Japanese Eculizumab Trial for GBS (JET-GBS). *JMIR Research Protocols*, *5*(4), e210. https://doi.org/10.2196/resprot.6610

Yamashina, M., Ueda, E., Kinoshita, T., Takami, T., Ojima, A., Ono, H., Kitani, T. (1990). Inherited complete deficiency of 20-kilodalton homologous restriction factor (cd59) as a cause of paroxysmal nocturnal hemoglobinuria. *New England Journal of Medicine*, *323*(17), 1184–1189. https://doi.org/10.1056/NEJM199010253231707

Yao, X., Su, T., & Verkman, A. S. (2016). Clobetasol promotes remyelination in a mouse model of neuromyelitis optica. *Acta Neuropathologica Communications*, *4*(1), 42. https://doi.org/10.1186/s40478-016-0309-4

Yasir, M., Vir Singh Sara, U., Som, I., Gaur, P., Singh, M., & Ameeduzzafar, . (2016). Nose to Brain Drug Delivery: A Novel Approach Through Solid Lipid Nanoparticles. *Current Nanomedicine*, *6*(2), 105–132. https://doi.org/10.2174/2468187306666160603120318

Yu, F., Haas, M., Glassock, R., & Zhao, M. H. (2017). Redefining lupus nephritis: Clinical implications of pathophysiologic subtypes. *Nature Reviews Nephrology*, 13(8):483-495. https://doi.org/10.1038/nrneph.2017.85

Zarbock, J., Gennaro, R., Romeo, D., Clore, G. M., & Gronenborn, A. M. (1988). A proton nuclear magnetic resonance study of the conformation of bovine anaphylatoxin C5a in solution. *FEBS Letters*, *238*(2), 289–294. https://doi.org/10.1016/0014-5793(88)80499-x

Zeerleder, S., & Levi, M. (2016). Hereditary and acquired C1-inhibitor-dependent angioedema: From pathophysiology to treatment. *Annals of Medicine*, *48*(4), 256–267. https://doi.org/10.3109/07853890.2016.1162909

Zelek, W., Fathalla, D., Orme, R. P., Morgan, A., Touchard, S., O'Hagan, C., Morgan, B. P. (2016). Complement system biomarkers in demyelinating disease. *Immunobiology*, *221*(10), 1172. https://doi.org/10.1016/j.imbio.2016.06.10

Zelek, W. M., Taylor, P. R., & Morgan, B. P. (2019). Development and characterization of novel anti-C5 monoclonal antibodies capable of inhibiting complement in multiple species. *Immunology*, *157*(4), 283–295. https://doi.org/10.1111/imm.13083

Zelek, W. M., Watkins, L. M., Howell, O. W., Evans, R., Loveless, S., Robertson, N. P., Morgan, B. P. (2019). Measurement of soluble CD59 in CSF in demyelinating disease: Evidence for an intrathecal source of soluble CD59. *Multiple Sclerosis Journal*, *25*(4), 523–531. https://doi.org/10.1177/1352458518758927

Zelek, W. M., Harris, C. L., & Morgan, B. P. (2018). Extracting the barbs from complement assays: Identification and optimisation of a safe substitute for traditional buffers. *Immunobiology*, *223*(12), 744–749. https://doi.org/10.1016/j.imbio.2018.07.016

Zelek, W. M., Stott, M., Walters, D., Harris, C. L., & Morgan, B. P. (2018). Characterizing a pH-switch anti-C5 antibody as a tool for human and mouse complement C5 purification and cross-species inhibition of classical and reactive lysis. *Immunology*, *155*(3), 396–403. https://doi.org/10.1111/imm.12982

Zhang, J., Liu, Y., Li, Y., Su, N., Zhou, Y., Xiang, J., & Sun, Y. (2018). Biological function of a gC1qR homolog (EcgC1qR) of Exopalaemon carinicauda in defending bacteria challenge. *Fish and Shellfish Immunology*, *82*, 378–385. https://doi.org/10.1016/j.fsi.2018.08.046

Zhang, H. F., Yu, J., Bajwa, E., Morrison, S. L., & Tomlinson, S. (1999). Targeting of functional antibody-CD59 fusion proteins to a cell surface. *Journal of Clinical Investigation*, *103*(1), 55–61. https://doi.org/10.1172/JCI4607

Zheng, Q., Liang, S., Xu, F., Li, G., Luo, N., Wu, S., Xu, G. (2019). C5a/C5aR1 Pathway Is Critical for the Pathogenesis of Psoriasis. *Frontiers in Immunology*, *10*. https://doi.org/10.3389/fimmu.2019.01866

Zhou, J., Fonseca, M. I., Pisalyaput, K., & Tenner, A. J. (2008). Complement C3 and C4 expression in C1q sufficient and deficient mouse models of Alzheimer's disease. *Journal of Neurochemistry*, *106*(5), 2080–2092. https://doi.org/10.1111/j.1471-4159.2008.05558.x

Zhou, Y., Gong, B., Lin, F., Rother, R. P., Medof, M. E., & Kaminski, H. J. (2007). Anti-C5 Antibody Treatment Ameliorates Weakness in Experimentally Acquired Myasthenia Gravis. *The Journal of Immunology*, *179*(12), 8562–8567. https://doi.org/10.4049/jimmunol.179.12.8562

Ziccardi, R. J. (1986). Control of C1 activation by nascent C3b and C4b: a mechanism of feedback inhibition. *Journal of Immunology*, *136*(9), 3378–3383. http://www.ncbi.nlm.nih.gov/pubmed/3485688

Zipfel, P. F., & Skerka, C. (2009, October). Complement regulators and inhibitory proteins. *Nature Reviews Immunology*, 9(10):729-40. https://doi.org/10.1038/nri2620

Zuber, J., Fakhouri, F., Roumenina, L. T., Loirat, C., & Frémeaux-Bacchi, V. (2012). Use of eculizumab for atypical haemolytic uraemic syndrome and C3 glomerulopathies. *Nature Reviews Nephrology*, 8(11):643-57. https://doi.org/10.1038/nrneph.2012.214